Multipole Moments in General Relativity
and
Dynamical Perturbations of Black-hole Magnetospheres

Thesis by

Xiao-He Zhang

In Partial Fulfillment of the Requirements

for the Degree of

Doctor of Philosophy

California Institute of Technology

Pasadena, California

1990

(Submitted June 13, 1989)

To my parents

ACKNOWLEDGEMENT

I thank my advisor, Professor Kip Thorne, for his continuous encouragement and his help. His patience as a teacher, his understanding in guiding me through various difficulties during the course of this project will certainly live in my memory in the years to come.

The friendship of all my friends, who have made my stay here not merely a scientific experience, is also acknowledged.

I thank my wife Li-Jia and my parents for their support and encouragement.

Last, but not the least, I would also like to thank Professor T. D. Lee at the University of Columbia, who initiated the CUSPEA program that makes my study here possible.

ABSTRACT

This thesis consists of two parts. In Part I, we develop a multipole moment formalism in general relativity and use it to analyze the motion and precession of compact bodies. More specifically, the generic, vacuum, dynamical gravitational field of the exterior universe in the vicinity of a freely moving body is expanded in positive powers of the distance r away from the body's spatial origin (i.e., in the distance r from its timelike-geodesic world line). The expansion coefficients, called "external multipole moments," are defined covariantly in terms of the Riemann curvature tensor and its spatial derivatives evaluated on the body's central world line. In a carefully chosen class of de Donder coordinates, the expansion of the external field involves only integral powers of r; no logarithmic terms occur. The expansion is used to derive higher-order corrections to previously known laws of motion and precession for black holes and other bodies. The resulting laws of motion and precession are expressed in terms of couplings of the time derivatives of the body's quadrupole and octopole moments to the external moments, i.e., to the external curvature and its gradient.

In part II, we study the interaction of magnetohydrodynamic (MHD) waves in a black-hole magnetosphere with the "dragging of inertial frames" effect of the hole's rotation — i.e., with the hole's "gravitomagnetic field." More specifically: we first rewrite the laws of perfect general relativistic magnetohydrodynamics (GRMHD) in 3+1 language in a general spacetime, in terms of quantities (magnetic field, flow velocity, ...) that would be measured by the "fiducial observers" whose world lines are orthogonal to (arbitrarily chosen) hypersurfaces of constant time. We then specialize to a stationary spacetime and MHD flow with one arbitrary spatial symmetry (e.g., the stationary magnetosphere of a Kerr black hole); and for this spacetime we reduce the GRMHD equations to a set of algebraic equations. The general features of the resulting stationary,

symmetric GRMHD magnetospheric solutions are discussed, including the Blandford-Znajek effect in which the gravitomagnetic field interacts with the magnetosphere to produce an outflowing jet. Then in a specific model spacetime with two spatial symmetries, which captures the key features of the Kerr geometry, we derive the GRMHD equations which govern weak, linealized perturbations of a stationary magnetosphere with outflowing jet. These perturbation equations are then Fourier analyzed in time t and in the symmetry coordinate x, and subsequently solved numerically. The numerical solutions describe the interaction of MHD waves with the gravitomagnetic field. It is found that, among other features, when an oscillatory external force is applied to the region of the magnetosphere where plasma (e^+e^-) is being created, the magnetosphere responds especially strongly at a particular, resonant, driving frequency. The resonant frequency is that for which the perturbations appear to be stationary (time independent) in the common rest frame of the freshly created plasma and the rotating magnetic field lines. The magnetosphere of a rotating black hole, when buffeted by nonaxisymmetric magnetic fields anchored in a surrounding accretion disk, might exhibit an analogous resonance. If so then the hole's outflowing jet might be modulated at resonant frequencies $\omega \simeq (m/2)\Omega_H$ where m is an integer and Ω_H is the hole's angular velocity.

Table of Contents

Chapter I

INTRODUCTION

Chapter 1. Introduction

This thesis consists of two parts: Part I, on multipole moments in general relativity, introduces the concept of "external multipole moments," and studies the laws of motion and precession of an arbitrary body in terms of couplings between the body's multipole moments and the "external moments" of the external universe. Part II studies the interaction of magnetohydrodynamic (MHD) waves with the dragging of inertial frames, and possible implications of that interaction for realistic black-hole magnetospheres.

There are two types of multipole moments: internal moments and external moments. The internal multipole moments are produced by gravitational sources internal to some region; the external multipole moments, by sources external to the region. As a familiar example, we can expand the solutions of the Laplace equation $\nabla^2\phi=0$ in Newtonian theory as

$$\phi=\sum_{l,m} I_{lm}\frac{Y^{lm}}{r^{l+1}}+\sum_{l,m} E_{lm}Y^{lm}r^{l}\ . \tag{1}$$

Up to a normalization factor, the internal multipole moments are the expansion coefficients I_{lm} in front of Y^{lm}/r^{l+1}, and the external multipole moments are the E_{lm} in front of $Y^{lm}r^{l}$.

Because of the nonlinearity of general relativity, multipole expansions of relativistic gravitational fields are rather more complicated than those of Newtonian fields. Nevertheless, such expansions are very useful in general relativistic astrophysics. Much research has been done on internal-moment expansions of the general relativistic gravitational field (spacetime metric and curvature). This research has included (i) the formulation of several different definitions of internal moments;[1,2,3,4,5] (ii) proofs that these various definitions are equivalent;[2,5,6] (iii) studies of the relationship of these moments to the properties of spacetime;[2,7,8] and (iv) studies of the roles of these moments in

gravitational radiation problems[1,9] and in the laws of motion and precession for internal bodies.[2,10,11]

By contrast, studies of general relativistic external moments have been very limited. In an appendix, Thorne and Hartle[10] present the general, linearized, stationary, external solution of the vacuum field equations for the metric and curvature of the external universe in multipole expansion form (in de Donder gauge), and propose an iterative algorithm for generating the nonlinear corrections that would convert the linearized solution and external moments into fully nonlinear ones. There was also a paper by Suen[2] which studied various aspects of the Thorne-Hartle stationary, external formalism and which thoroughly unified it with Thorne's[1] stationary internal formalism to produce a general multipole analysis of the buffer zone surrounding a stationary body in a stationary external spacetime. In both of these studies (Thorne-Hartle and Suen) the external-moment expansions were combined with internal-moment expansions to produce laws of motion and precession for the internal body; see also Chapter 3 of this thesis.

In Chapters 2 and 3 of this thesis, we extend the stationary external-moment analyses of Thorne-Hartle and Suen to fully dynamical, nonlinear situations. More specifically, in Chapter 2 we give a rather thorough treatment of the external-moment problem for fully dynamical, fully nonlinear, vacuum systems; and unlike Thorne-Hartle and Suen, we base our treatment on moments that are defined in terms of fully covariant, locally measurable quantities. This has the advantage that we do not have to know the external source distributions. More specifically, we introduce into physical spacetime a fiducial timelike-geodesic world line η about which to do our external multipole expansions; and we define the moments locally and covariantly as the symmetric and trace-free (STF) parts of the covariant gradients of the Riemann tensor on η. These moments are then functions of the proper time measured by a freely moving observer whose world line is η. In a local inertial frame of this observer, these moments take the form (Chap. 2)

$$E_{a_1a_2\cdots a_l}=\frac{1}{(l-2)!}\,(R_{0a_10a_2;a_3\cdots a_l})^{\rm STF}\,, \tag{2a}$$

$$B_{a_1a_2\cdots a_l}=\frac{3}{2(l+1)(l-2)!}\,(\varepsilon_{a_1ij}R_{ija_20;a_3\cdots a_l})^{\rm STF}\,, \tag{2b}$$

where $R_{\alpha\beta\gamma\delta}$ is the Riemann curvature tensor on η, semicolns denote covariant derivatives, Latin indicies are spatial, and 0 denotes a time index.

With these multipole moments defined, we go on in Chapter 2 to expand the external gravitational field in terms of them in a carefully chosen class of de Donder coordinates. It is a remarkable feature of our de Donder expansion that, although the spacetime is allowed to be fully dynamical and fully nonlinear, the expansion entails only integral powers of r. [See Eqs. (1.6) of Chap. 2] By contrast with the internal, dynamical expansion,[1] no $\ln r$ terms appear at any nonlinear order. (See Sec. III of Chap. 2.)

Having completed the expansion of the external gravitational field using these external multipole moments, we study in Chapter 3 the laws of motion and precession for an arbitrary object in terms of couplings of the object's internal moments to the external moments of the external universe's gravitational field.

The motion and precession of finite-sized objects is an old and important problem in general relativity. However, for objects with nonlinearly strong internal gravity, this problem has been attacked only relative recently: It has been established that an object with negligible multipole moments, whether it has strong internal gravity or not, moves on geodesics of the external spacetime and Fermi-Walker transports its spin.[12,13] There will be corrections to these simple laws of motion and precession when the arbitrary object has a finite size and small but finite multipole moments. For a binary black hole system, D'Eath has computed the leading corrections for both the black hole's motion and its precession;[14] and Damour has computed the leading corrections for the motion of binary black holes and binary neutron stars.[15] More recently, Thorne and Hartle[10]

studied the laws of motion and precession for an isolated system in an arbitrary, slowly changing background spacetime. They expressed these laws in terms of couplings of the angular momentum and quadrupole moments to the Riemann curvature of the surrounding background. In Chapter 3, all corrections to the Thorne-Hartle laws at the next higher order are derived. They are derived by expanding the Landau-Lifshitz pseudotensor (which describes the flow of gravitational energy, momentum and angular momentum) in terms of internal and external multipole moments, and then integrating the pseudotensor fluxes of four-momentum and angular momentum over a sphere that surrounds the moving, precessing object. The expansion and integration sphere are confined to a buffer region outside the object in which gravity is weak. The resulting corrections to the laws of motion and precession take the following form:

$$\left[\frac{dM}{dt}\right]_{\text{corr}} = -\frac{1}{2}\mathcal{E}_{ab}(d\,I^{ab}/dt) - \frac{2}{3}\mathcal{B}_{ab}(d\,\mathcal{S}^{ab}/dt)\,, \tag{3a}$$

$$\left[\frac{dP^i}{dt}\right]_{\text{corr}} = -\frac{1}{2}\mathcal{E}^i{}_{ab}\,I^{ab} - \frac{8}{9}\mathcal{B}^i{}_{ab}\,\mathcal{S}^{ab}$$

$$+\frac{4}{9}\varepsilon^i{}_{ab}(d\,\mathcal{E}^a{}_c/dt)\mathcal{S}^{bc} + \frac{1}{3}\varepsilon^i{}_{ab}\mathcal{B}^a{}_c(d\,I^{bc}/dt)\,, \tag{3b}$$

$$\left[\frac{d\,\mathcal{S}^i}{dt}\right]_{\text{corr}} = \frac{1}{2}\varepsilon^i{}_{ab}\,\mathcal{E}^{acd}\,I^b{}_{cd} + \varepsilon^i{}_{ab}\,\mathcal{B}^{acd}\,\mathcal{S}^b{}_{cd}\,. \tag{3c}$$

Here M, P^i, and $\mathcal{S}^i$ are the body's mass, linear momentum, and angular momentum; I_{abc} and $\mathcal{S}_{abc}$ are the body's mass octopole and current octopole moments;[1] and $\mathcal{E}_{abc}$ and $\mathcal{B}_{abc}$ are the electric-type and magnetic-type octopole moments of the external universe's curvature; i.e., they characterize the spatial gradient of that curvature.[10]

Now we turn attention to part two of this thesis: the interaction of MHD waves in relativistic magnetosphere with the dragging of inertial frames.

In recent decades, the huge energy output from active galactic nuclei (AGN's) has been firmly established, and theories using a supermassive central black hole ($\sim 10^8 M_\odot$) to explain this energy output have also been developed and have become well accepted.[16] There are also some recent observations that suggest the existence of supermassive black holes at the centers of some nearby galaxies.[17] These developments have integrated black-hole research firmly into astrophysics.

One of the most attractive models for powering jets in AGN's is the electrodynamical (or MHD) extraction of the rotational energy of a supermassive black hole.[18,19,20] All previous studies of this process have involved stationary, steady-state configurations. In the second part of this thesis, we initiate a study of dynamical features of this process; more specifically, we study the various physical properties of MHD waves in a model spacetime that captures the key features of a rotating black hole, and extrapolate our results to a rotating black hole (Kerr black hole).

Under the influence of a moving (rotating) gravitational field, inertial observers are pulled relative to distant observers in the direction of the field's motion; i.e., the inertial frames are ''dragged'' by the gravitational field. In fact, near a rotating black hole, this ''frame dragging'' effect is so extreme that no physical observer (inertial or noninertial) can remain at rest relative to distant observers. The region of space where frame dragging is this extreme is called the hole's ''ergosphere.'' It is bounded below by the hole's horizon and above by the ''static limit,'' a surface (near the horizon) where the Killing vector ($\partial/\partial t$) becomes null. Just as a moving observer in Newtonian physics views energy differently from an observer at rest, so also a ''moving (rotating) observer'' dragged by the hole's rotating gravitational field will view energy differently from a distant observer. For example, a particle near the horizon that possesses energy ε_0 and

angular momentum j as seen by a near-horizon, moving (rotating) observer will have energy $\varepsilon_\infty=\alpha(\varepsilon_0+\Omega_H j)$ as seen by an observer at infinity. The factor α is the standard gravitational redshift, while the factor $\Omega_H j$ (with Ω_H the angular velocity of the hole's horizon and of the near-horizon observer) can be thought of as energy fed into the particle by the hole's rotation: As the particle flies freely outward from near the horizon to far away, the hole's gravitomagnetic field transfers the energy $\Omega_H j$ from the hole's rotation to the particle.

Much research work has been done on the extraction of rotational energy of black holes since the pioneering work by Penrose.[21] We shall be interested here in the electromagnetic extraction of rotational energy, i.e., the Blandford-Znajek process.[18] This is the process of extracting rotational energy from a black hole by the coupling of magnetic fields threading the hole to the hole's ''gravitomagnetic field'' (its dragging of inertial frames). In their seminal paper on this subject, Blandford and Znajek[18] idealized the magnetosphere as force-free, with its plasma consisting of electron-positron pairs created by magnetic-gravitomagnetic-induced electric fields. Subsequently Macdonald and Thorne[19] analyzed this Blandford-Znajek process, using the membrane paradigm and retaining the force-free idealization near the hole. More recently, Phinney[20] has developed and applied to the Kerr geometry a (nonmembrane) formulation of general relativistic magnetohydrodynamics (GRMHD) and has used it in an improved, MHD analysis of the Blandford-Znajek process. All of this past research has dealt with equilibrium states of the magnetosphere. However, as the accretion disk orbits the central black hole, the chaotic magnetic field lines anchored on the inner edge of the disk will perturb the magnetosphere in the jet production region at the orbital frequency. The jet, a stationary outflow of plasma, will be modulated by the MHD waves generated by this dynamic perturbation. Thus, at least in principle, information about the physical conditions near the perturbation source should be revealed by a study of the dynamical

behaviors of the jet.

In this thesis, we initiate a study of MHD waves near a rotating black hole in a stationary magnetosphere consisting of a magnetized electron-positron plasma. Our primary interest is to study how the MHD waves propagate in this stationary magnetosphere under the influence of the rotating gravitational field. As our focus will be on the MHD waves, we shall assume the existence of the plasma and shall pay no particular attention in this thesis to the detailed mechanisms that create the plasma. This plasma could be, e.g., created by the huge static electric potential $[\sim 10^{20}\text{Volts}(B/10^4 G)(M/10^9 M_\odot)(a/M)]$[18,22] induced by the coupling of the external magnetic field and the gravitomagnetic field[22] in a process analogous to those in pulsar polar gap models;[23] or it could be created by the high-energy photons coming from the synchrotron radiation of, or inverse Compton scattering with, some injected high-energy protons or electrons.[24,25] Phinney has demonstrated the validity of the perfect MHD assumption for this plasma[20] and has further developed the MHD equations for this plasma with source terms.[26] We shall adopt the perfect MHD assumption but shall neglect the details of the source terms in our study of MHD waves. We shall further assume that the stationary magnetosphere has the same spatial symmetry as the gravitational background.

In Chapter 4, we rewrite the laws of perfect GRMHD in 3+1 language, a form suitable for our perturbation study and its intuitive understanding. The laws are expressed in terms of quantities (magnetic field, flow velocity, ...) that would be measured by the ''fiducial observers'' (FIDO's), whose world lines are orthogonal to the hypersurfaces of constant time. We also demonstrate that without much extra effort, Phinney's results[20] on stationary, GRMHD, black-hole magnetospheres can actually be generalized to any stationary MHD system with one spatial symmetry; and for such a system we reduce the full set of GRMHD equations to a set of algebraic relations and an (algebraic) wind

equation which, together with one nonlinear partial differential equation also contained in this set of GRMHD equations, fully determine the structure of stationary MHD flows.

Although this reformulation is motivated by the black-hole problem and meshes nicely with the membrane paradigm, the formalism is not restricted to black holes or to the membrane paradigm. In fact, it forms the basis of our study (in Chap. 5) of MHD waves in a model spacetime with the metric

$$ds^2=-dt^2+[dx+\beta(z)dt]^2+dy^2+dz^2\,, \tag{4}$$

a spacetime that is flat except for a z–dependent ''shift function'' (''gravitomagnetic potential'') $\beta=V_F\,(\tanh z-1)$ in the x–direction. (Here V_F is a constant.)

More than one decade has passed since Blandford and Znajek[18] proposed in their seminal paper the process of powering jets by the coupling of a hole's ''gravitomagnetic field'' to magnetic fields that thread the hole, and analyzed this process in the approximation that the near-hole magnetosphere is force-free. During that decade, Phinney[20] has developed a GRMHD analysis of the Blandford-Znajek process in the Kerr geometry; and by a clever use of boundary conditions, he has inferred details of the energy output while circumventing the task of solving for the global stationary configuration of the MHD jet. Mobarry and Lovelace[27], and Lovelace et al.[28] have also studied axisymmetric, stationary MHD configurations around a black hole. They were able to obtain solutions for global jet configurations by solving the relevant nonlinear, second-order, partial differential equation (PDE) numerically. However, their solutions were for a disk-accelerated jet around a Schwarzschild black hole. We need to solve a similar nonlinear, second-order PDE in the Kerr geometry to obtain global stationary MHD configurations for a jet driven by a rotating black hole. No such stationary solution is yet known — either analytic or numerical. Thus, since we wish to study dynamical features of a rotating hole's magnetosphere, we are faced with the challenges of (i) constructing

for the first time global equilibrium solutions for the magnetosphere and jet; and (ii) adding on a nontrival time evolution. The time-dependent problem will be 2+1 dimensional (2 for space, 1 for time), and will be plagued by the complexities of the Kerr geometry, the nonlinearity of the MHD equations, and the close coupling of the fluid, the magnetic field, and the gravitational field. Such a full analysis is far too difficult to attempt in a Ph.D. thesis. Instead, we seek insight into the dynamics of black-hole magnetosphere by replacing the Kerr spacetime geometry by an alternative geometry [Eq. (4)] that has one more spatial symmetry and retains the key feature of a Kerr-like gravitomagnetic field.

In Chapter 5, using the formalism developed in Chapter 4, we first build up a stationary, global solution for the flow of cold plasma [$\mu \equiv (\rho+p)/\rho_0=1$] in the model spacetime (4). This flow models the MHD winds (jets) of AGN's. The flow starts from a delta-function source in the plane $z=0$ and is accelerated by the gravitomagnetic field $\beta(z)$ to both $z=-\infty$ (the analog of the hole's horizon) and $z=+\infty$ (the analog of the hole's spatial infinity). Then for perturbations of this model magnetosphere, we derive a set of linearized MHD equations and a set of junction conditions at the $z=0$ (plasma production) plane. These two sets of equations are subsequently Fourier-analyzed in time t and the (symmetry) coordinate x, and the resulting ordinary differential equations and junction conditions are solved numerically, subject to outgoing wave conditions at both infinities. Using these numerical solutions, we study the responses of our model magnetosphere, at various frequencies ω and wave numbers k_x, to oscillatory sources of mass, energy, and momentum in the production plane, $z=0$. The magnetosphere's response is characterized by the amplitudes and energy fluxes of the waves that are excited by these ''driving'' sources near the production plane, and the amplitudes and energy fluxes that the waves acquire by the time they have propagated to $z=+\infty$ and $z=-\infty$. A variety of spectral features show up in the magnetosphere's response. The most important is a

strong resonance, when the perturbations are excited by an oscillatory force, whose angular frequency, $\omega_{\rm resonance}=k_x V_F$ is that for which the perturbations in the production plane are stationary (time-independent) in the common rest frame of the fluid and magnetic field in the production-plane — a frame that moves with a speed $dx/dt=V_F$. The resonance shows up as an especially strong response of the wave amplitude at $z=0$, and also an especially strong amplification of the waves' energy flux as they propagate to $z=\infty$.

This resonance in our model spacetime might well have an analog in the magnetosphere of a rotating black hole: Perturbations of the magnetosphere produced, e.g., by the Maxwell pressure of chaotic magnetic fields anchored in the surrounding accretion disk, might show resonances at frequencies $\omega_{\rm resonance}=m\Omega_F$, where m is an integer (the azimuthal quantum number of the perturbation), and Ω_F is the field line angular velocity. Since the field line angular velocity is likely to be about half the angular velocity $\Omega_{\rm H}$ of the hole's horizon, the result could be a modulation of the hole's outflowing jet at angular frequencies (as measured far from the hole) $\omega\simeq(m/2)\Omega_{\rm H}$.

REFERENCES

[1] K. S. Thorne, Rev. Mod. Phys., **52**, 299 (1980).

[2] W.-M. Suen, Phys. Rev. D **34**, 3617 (1986).

[3] R. Geroch, J. Math. Phys. **11**, 2580 (1970); R. O. Hansen, J. Math. Phys., **15**, 46 (1974).

[4] A. I. Janis and E. T. Newman, J. Math. Phys., **6**, 902 (1965); D. J. Lamb, J. Math. Phys. **7**, 458 (1966).

[5] W. Simon and R. Beig, J. Math. Phys., **24**, 1163 (1983); R. Beig and W. Simon, Proc. R. Soc. London ***A*** **376**, 333 (1981).

[6] Y. Gürsel, Gen. Rel. and Grav. **15**, 737 (1983).

[7] P. Kundu, J. Math. Phys. **22**, 2006 (1981).

[8] B. C. Xanthopoulos, J. Phys. ***A*** 12, 1025 (1979); R. Beig and W. Simon, Commun. Math. Phys. **78**, 75 (1980).

[9] L. Blanchet and T. Damour, Proc. Roy. Soc. (London), submitted; also L. Blanchet, *ibid.*

[10] K. S. Thorne and J. B. Hartle, Phys. Rev. D **31**, 1815 (1985).

[11] X.-H. Zhang, Phys. Rev. D **31**, 3130 (1985).

[12] P. D. D'Eath, Phys. Rev., D **11**, 1387 (1975).

[13] R. E. Kates, Phys. Rev. D **22**, 1853 (1980).

[14] P. D. D'Eath, Phys. Rev. D **12**, 2183 (1975).

[15] T. Damour, in *Gravitational Radiation*, edited by N. Deruelle and T. Piran (North-Holland, Amsterdam, 1983), p.59.

[16] M. J. Rees, Ann. Rev. Astron. Astrophys. **22**, 471 (1984)

[17] C. M. Gaskell and L.S. Sparke, Astrophys. J., **30,** 175 (1986); C. M. Gaskell and B.M. Peterson, Astrophys. J. Suppl., **65,** 1 (1987); J. L. Tonry, Astrophys. J., **322,** 632 (1987); A. Dressler and D. O. Richstone, Astrophys. J., **324,** 701 (1988); J. Kormendy, Astrophys. J., **325,** 128 (1988).

[18] R. O. Blandford and R. L. Znajek, Mon. Not. R. astr. Soc. **179,** 433 (1972).

[19] Douglas Macdonald and Kip S. Thorne, Mon. Not. R. astr. Soc. **198,** 345 (1982).

[20] E. S. Phinney, Ph.D. dissertation, Univ. of Cambridge, 1983.

[21] R. Penrose, Rev. del Nuovo Cimento, **1,** 252 (1969).

[22] K. S. Thorne, R. H. Price and D. A. Macdonald, *Black Holes: The Membrane Paradigm* (Yale University Press, New Heaven, 1986).

[23] M. Ruderman and P. G. Sutherland, Astrophys. J., **196,** 51 (1975).

[24] P. W. Guilbert, A. C. Fabian and M. J. Rees, Mon. Not. R. astr. Soc. **205,** 593 (1983).

[25] A. P. Lightman, A. A. Zdziarski and M. J. Rees, Astrophys. J., **315,** 113 (1987).

[26] E. S. Phinney, to be published, 1989.

[27] C. M. Mobarry and R. V. E. Lovelace, Astrophys. J., **309,** 455 (1986).

[28] R. V. E. Lovelace, C. Mehanian, M. Mobarry and M. E. Sulkanen, Astrophys. J., **62,** 1 (1987).

Chapter II

MULTIPOLE EXPANSIONS OF THE GENERAL RELATIVISITC GRAVITATIONAL FIELD OF THE EXTERNAL UNIVERSE

(Originally appeared in *Phys. Rev.* D34, 991(1986))

PHYSICAL REVIEW D VOLUME 34, NUMBER 4 15 AUGUST 1986

Multipole expansions of the general-relativistic gravitational field of the external universe

Xiao-He Zhang
Theoretical Astrophysics 130-33, California Institute of Technology, Pasadena, California 91125
(Received 31 October 1985)

The generic, vacuum, dynamical gravitational field in the vicinity of a freely falling observer is expanded in powers of distance away from the observer's spatial origin (i.e., in distance away from his timelike-geodesic world line). The expansion is determined fully, aside from coordinate freedom, by two families of time-dependent multipole moments—"electric-type moments" and "magnetic-type moments"—which characterize the gravitational influence of the external universe. These "external multipole moments" are defined covariantly in terms of the Riemann curvature tensor and its spatial derivatives, evaluated on the observer's world line. The properties of these moments are discussed, and an analysis is given of the structure of the gravitational field's multipole expansion for the special case of de Donder coordinates. In de Donder coordinates the expansion involves only integral powers of distance from the origin; no logarithmic terms occur in this multiparameter expansion.

I. INTRODUCTION AND SUMMARY

In theoretical physics, multipole-moment formalisms are very useful tools for dealing with fields. In a linear field theory, we can decompose the field into its multipole components and study each of them separately; and after the behavior of each multipole component is well understood, we can superimpose the components to get the full field and can use the components as aids to understand it. By contrast, in general relativity, the nonlinearity of the theory prevents us from getting a general solution of the vacuum field equations by a simple superposition of various multipole components. This limits somewhat the use of multipole moments in general relativity; but despite this, relativistic multipole formalisms are still very useful.

One reason is that exact solutions of the Einstein field equations are usually hard to interpret; and their interpretation is aided by the construction of a corresponding Newtonian solution with the same multipole moments as the exact solution. Furthermore, although the exact solution is not a simple linear superposition of multipole components, the coupling among the multipole components at each nonlinear order is definite once the coordinates have been fixed.

Another source of the usefulness of general-relativistic multipoles is the fact that, in the real universe, strongly gravitating bodies are almost always separated from each other by such great distances that their gravitational interactions are weak. This permits those interactions to be characterized by multipolar couplings, with only the lowest few multipoles and only quadratic couplings playing significant roles.

A third source of multipolar usefulness is the fact that almost all sources of gravitational radiation in the real universe are thought to have sufficiently slow internal velocities that the lowest few multipoles dominate the radiation, and the nonlinear coupling between them is of only modest consequence.

There are two types of multipole moments: internal moments and external moments. The internal multipole moments are produced by gravitational sources internal to some region; the external multipole moments by sources external to the region. In the Newtonian theory of gravity, the solutions of the Laplace equation $\nabla^2\phi=0$ can be expressed as

$$\phi=\sum_{l,m} I_{lm}\, Y^{lm}/r^{l+1}+\sum_{l,m} E_{lm}\, Y^{lm} r^{l}\,.$$

With one choice of normalization, the internal multipole moments are the expansion coefficients I_{lm} in front of Y^{lm}/r^{l+1}, and the external multipole moments are the E_{lm} in front of $Y^{lm}r^{l}$.

The gravitational interaction of a bounded system and a complicated external universe can be described in terms of couplings between the internal and external multipole moments. For example, the precession of the Earth's spin axis ("precession of the equinoxes") can be described as due to a coupling between the internal quadrupole moment of the Earth and the external quadrupole moment produced by the Sun, the Moon, and the planets—the external moment being, essentially, the "tidal gravitational field" of these "external" sources (Exercise 16.4 of Ref. 1).

In general relativity, because gravity is produced not only by mass, but also by mass motion ("mass current," "momentum density"), there are two families of multipole moments for both internal and external situations: "mass moments" and "current moments." In the internal case, in addition to the mass moments I_{lm}, which are due largely to the nonuniform distribution of mass, there are also current moments S_{lm} due to rotation, pulsation, and other mass motions. In the external case, in addition to the "electric-type moments" E_{lm}, sometimes also called "mass moments," which are essentially the tidal field and its gradients, there are also the "magnetic-type moments" B_{lm}, also called "current moments," which are produced by motions of external masses and which in turn create

velocity-dependent tidal forces on test bodies.

The linearized, stationary solution of the vacuum Einstein field equations can be expressed in terms of these multipole moments. For the sake of illustration we will suppress all normalization constants here. In an appropriate de Donder gauge, the metric has the form[2,3]

$$g_{00}=-1+\frac{2M}{r}+\sum_{l=2}^{\infty}\frac{1}{r^{l+1}}(I_{lm}Y^{lm})-\sum_{l=2}^{\infty}r^{l}(E_{lm}Y^{lm}) , \tag{1.1a}$$

$$g_{0i}=-\sum_{l=1}^{\infty}\frac{1}{r^{l+1}}(S_{lm}Y_{i}^{l,lm})-\sum_{l=2}^{\infty}r^{l}(B_{lm}Y_{i}^{l,lm}) , \tag{1.1b}$$

$$g_{ij}=\delta_{ij}\left[1+\frac{2M}{r}+\sum_{l=2}^{\infty}\frac{1}{r^{l+1}}(I_{lm}Y^{lm})-\sum_{l=2}^{\infty}r^{l}(E_{lm}Y^{lm})\right] , \tag{1.1c}$$

and the metric density, defined as $g^{\mu\nu}=\sqrt{-g}g^{\mu\nu}$, where g is the determinant of $g_{\mu\nu}$, is

$$g^{00}=-1-\frac{4M}{r}-\sum_{l=2}^{\infty}\frac{1}{r^{l+1}}(I_{lm}Y^{lm})+\sum_{l=2}^{\infty}r^{l}(E_{lm}Y^{lm}) , \tag{1.2a}$$

$$g^{0i}=-\sum_{l=1}^{\infty}\frac{1}{r^{l+1}}(S_{lm}Y_{i}^{l,lm})-\sum_{l=2}^{\infty}r^{l}(B_{lm}Y_{i}^{l,lm}) , \tag{1.2b}$$

$$g^{ij}=\delta_{ij} . \tag{1.2c}$$

Here and throughout this paper geometric units, in which $G=c=1$, are used; Y^{lm} is the spherical harmonic of order lm, and $Y_{i}^{l,lm}$ is the vectorial spherical harmonic. Aside from normalization, $\mathbf{Y}^{l,lm}=\mathbf{L}Y^{lm}$, where in three-dimensional notation $\mathbf{L}\equiv(1/i)\mathbf{r}\times\nabla$ (see Sec. III and Ref. 2).

When one studies the gravitational couplings inherent in the Einstein field equations one finds that, as in Newtonian gravity, the laws of motion and precession for an internal body are determined by couplings between the body's internal moments $\mathcal{I}_{A_l}$, $\mathcal{J}_{A_l}$ and the external moments produced by the rest of the universe, $\mathcal{E}_{A_l}$, $\mathcal{B}_{A_l}$.[3-5]

Much research has been done on internal-moment expansions. This research has included (i) the formulation of several different definitions of internal moments;[2,5-8] (ii) proofs that these various definitions are equivalent;[5,8,9] (iii) studies of the relationship of these moments to the properties of spacetime;[5,10,11] and (iv) studies of the roles of these moments in gravitational radiation problems[2,12] and in the laws of motion and precession for internal bodies.[3-5]

There are two main approaches to the definition of internal moments in fully nonlinear general relativity. In the first approach ("physical-spacetime approach") one defines the moments as expansion coefficients in physical spacetime for the metric or some other gravitational quantities.[2,7,8] In the second approach ("conformal-space approach") one performs a conformal transformation on asymptotically flat spacetime, thereby moving "infinity" into a finite location Λ; and one then defines the moments in terms of covariant derivatives of certain quantities in the conformal space at Λ.[6]

Thorne[2] is representative of the physical-spacetime approach. In Thorne's formalism, a special class of coordinates, called "asymptotically Cartesian and mass centered" (ACMC), is introduced; and the multipole moments, defined as certain expansion coefficients of the metric, are the same in all such ACMC coordinate systems. The strength of this approach lies in its usefulness in practical, astrophysically motivated calculations.[13,14]

The conformal-space approach is represented by Geroch and Hansen.[6] Their covariant definition of the multipole moments is very elegant and beautiful, because the multipole moments now become completely geometrical objects living at a specific location Λ in the conformal space. However, because the relationship between conformal space and physical spacetime is somewhat complex, this definition of the moments has not found extensive use in practical calculations.

By contrast with these extensive studies of internal moments, studies of external moments have been limited to two. The first was an appendix in Thorne and Hartle (Ref. 3), which presented the general linearized stationary solution of the vacuum field equations in multipole expansion form (in de Donder gauge), and proposed an iterative algorithm for generating the nonlinear corrections that would convert the linearized solution into a fully nonlinear one. The second was a paper by Suen[5] which studied various aspects of the Thorne-Hartle stationary, external formalism and which thoroughly unified it with Thorne's[2] stationary internal formalism to produce a general multipole analysis of the buffer zone surrounding a stationary body in a stationary external spacetime. In both of these studies (Thorne and Hartle and Suen) the external-moment expansions were combined with internal-moment expansions to produce laws of motion and precession for the internal body; see also Zhang.[4]

The purpose of this paper is to extend the stationary external-moment analyses of Thorne and Hartle and of Suen to fully dynamical situations. More specifically, we shall give a rather thorough treatment of the external-moment problem for fully dynamical, fully nonlinear, vacuum systems; and unlike Thorne and Hartle and Suen, we shall base our treatment on moments that are defined in terms of fully covariant, locally measurable quantities. This has the advantage that we do not have to know the external source distributions.

In Sec. II A we shall introduce into physical spacetime a fiducial timelike-geodesic world line λ about which to do our external multipole expansions; and we shall define the moments locally and covariantly as the symmetric and trace-free (STF) parts (equivalent to the irreducible components of a tensor) of the covariant gradients of the Riemann tensor and itself on λ. These moments will then be functions of the proper time measured by a freely falling observer who moves along λ. More specifically, in a local inertial frame of this observer these moments will take the form (Sec. II B)

$$\mathcal{E}_{A_l}=\frac{1}{(l-2)!}(R_{0a_1 0a_2;a_3\cdots a_l})^{\mathrm{STF}} , \tag{1.3a}$$

$$\mathcal{B}_{A_l}=\frac{3}{2(l+1)(l-2)!}(\epsilon_{a_1 ij}R_{ija_2 0;a_3\cdots a_l})^{\mathrm{STF}} . \tag{1.3b}$$

[Here $(\cdots)^{\mathrm{STF}}$ means to take the symmetric, trace-free parts on free indices $a_1a_2\cdots a_l$, and $\epsilon_{a_1 ij}$ is the flat

space Levi-Civita tensor.] At linear order, these moments are just the tensorial representation of E_{lm} and B_{lm} appearing in the metric (1.1) and metric density (1.2) up to normalization constants. At higher nonlinear orders, this is no longer the case. However, relations between these "true" multipole moments and those generated by the metric (density) expansion do exist and will be the subject of our study in Sec. IV.

Since these moments are not coordinate invariant in some class of simply specifiable coordinates, we cannot read them off in a straightforward way from the metric (density). The calculation of these moments in particular, and the analysis of the whole external multipole expansion formalism in general must be done in some tightly specified coordinate. The coordinate we shall use is at the same time de Donder and also "locally inertial and Cartesian" (LIC). The metric and metric density take forms similar to (1.1) and (1.2) with additional time derivative terms [Eq. (3.26)], and at higher nonlinear orders, additional r^l [$(n<l)$-pole] terms.

It is a remarkable feature of our de Donder expansion that, although the spacetime is allowed to be fully dynamical and fully nonlinear, the expansion entails only integrals of power of r. By contrast with internal, dynamical expansion,[2] no $\ln r$ terms appear at any nonlinear order; see Sec. III.

In the remainder of this paper, we shall give a more precise description of the basic ideas and some technical details of the main results. In Sec. II, the concept of the fiducial world line will be introduced, the covariant definition of external multipole moments will be given, and special coordinate systems in which to do multipole expansions will be discussed. In Sec. III we shall study the structure of our de Donder coordinate external multipole expansion of the metric density. Finally, in Sec. IV the relationship between our covariantly defined external moments $\mathscr{E}_{A_l}$, $\mathscr{B}_{A_l}$ and the "moments" obtained from the expansion coefficients of the metric density, which we will call $\mathscr{E}^{\gamma}_{A_l}$, $\mathscr{B}^{\gamma}_{A_l}$, will be derived; and various properties of the moments will be discussed.

II. CONCEPTUAL FOUNDATIONS

A. Fiducial world line and external expansion

Consider some preferred observer who wants to study spacetime in his vicinity by observing the motions of an apparatus that he carries with himself. As he moves through spacetime, his motion defines a world line. This world line will be the fiducial world line of our multipole formalism. Although in some special cases, the preferred observer might be defined by the symmetry of the spacetime, quite generally it will be chosen on the basis of the physics of the problem being studied. Our goal is to characterize, in terms of quantities defined on this fiducial world line, the gravitational field of the external universe.

In analyzing the observer's measurements we shall simplify our analysis by temporarily ignoring the gravitational influence of the apparatus. Its influence can be taken into account, after the formalism for describing the external universe is fully developed, by putting back in the gravity of the apparatus and studying the coupling between the apparatus and the external universe. The Thorne-Hartle[3]-Zhang[4] derivation of laws of motion and precession is an example of such a coupling study.

To further simplify the analysis, we shall assume in this paper that the apparatus (and, with it removed, the fiducial world line) is surrounded by a vacuum region of spacetime. This is the situation one usually encounters in practice. An example which does not have this property is a fiducial world tube in an axion filled, Friedman cosmological model (the axions will pass through the apparatus, which we have thrown away, with near impunity, so the apparatus cannot be regarded as in a local vacuum).[15]

We shall also simplify our analysis by assuming that the fiducial world line is a timelike geodesic. This is a case of common interest, e.g., in the Thorne-Hartle laws of motion and precession; but often one wants to use an accelerated world line. It would not be difficult to generalize our multipole formalism to the accelerated case. The principal effects of such acceleration have been studied already at linear, quadrupole order for a dynamical external universe by Ni and Zimmermann;[16] and at fully nonlinear, all-multipole order for a stationary external universe by Suen.[5] However, for simplicity, this paper's fully nonlinear, all-multipole, fully dynamical analysis will assume zero acceleration.

In the spirit of using locally measurable quantities to characterize the external universe, we introduce here three length scales defined on λ to characterize it in order of magnitude. They are[3]

$$\mathscr{R}=(\text{radius of curvature of spacetime on } \lambda)\ , \tag{2.1a}$$

$$\mathscr{L}=(\text{inhomogeneity scale of curvature})\ , \tag{2.1b}$$

$$\mathscr{T}=(\text{time scale for changes of curvature})\ . \tag{2.1c}$$

These length scales are defined formally, in terms of the multipole moments of Eqs. (1.3), by

$$\mathscr{R}=\mathrm{Min}\left[\frac{1}{|\mathscr{E}_{ij}|^{1/2}}\ ,\ \frac{1}{|\mathscr{B}_{ij}|^{1/2}}\right], \tag{2.1a'}$$

$$\mathscr{L}=\min_{l>2}\left[\left[\frac{|\mathscr{E}_{ij}|}{(l-2)!\,|\mathscr{E}_{A_l}|}\right]^{1/(l-2)},\left[\frac{|\mathscr{B}_{ij}|}{(l+1)(l-2)!\,|\mathscr{B}_{A_l}|}\right]^{1/(l-2)}\right], \tag{2.1b'}$$

$$\mathscr{T}=\min_{n\geq 1}\left[\left[\frac{|\mathscr{E}_{ij}|}{|d^n\mathscr{E}_{ij}/dt^n|}\right]^{1/n},\left[\frac{|\mathscr{B}_{ij}|}{|d^n\mathscr{B}_{ij}/dt^n|}\right]^{1/n}\right]. \tag{2.1c'}$$

Here time t is measured in a local inertial frame on λ (see Sec. II C). The external expansion will be a power series in the dimensionless variables $r/\mathscr{R}$, $r/\mathscr{L}$, and $r/\mathscr{T}$, where r is the spatial distance away from λ. This multiparameter expansion will be valid and will give good accuracy for the first few terms out to a distance

$r_{\max} \sim \mathrm{Min}(\mathscr{R}, \mathscr{L}, \mathscr{T})$. (Note that if a gravitational shock wave were to pass through λ, $\mathscr{L}$ and $\mathscr{T}$ would be zero at its point of passage and our formalism would be useless for studying its effects.) Of course when one restores a measuring apparatus to the world line λ, its size must be much less than $r_{\max}$ if our formalism is to be useful for studying its couplings to the external universe.[3]

Throughout the rest of this paper, our attention will focus on external fields with measuring apparatus on λ ignored; the fiducial world line λ will be a timelike geodesic inside a vacuum world tube; and we shall have the mathematical task of characterizing the external field in this world tube, out to a distance $\sim r_{\max}$, in terms of the external multipole moments defined on λ.

B. LIC coordinates and de Donder coordinates

In a covariant theory like general relativity, choosing a well-behaved coordinate system is almost as important as solving the field equations. For example, as is well known, an ill-chosen coordinate system can become singular somewhere even though nothing particularly singular happens to the spacetime there. In this subsection, we will discuss two overlapping families of coordinate systems that are well behaved in the vicinity of the fiducial world line λ and in which one might wish to perform multipole expansions.

In parallel with the ACMC coordinate systems of internal problems, we introduce for external problems the class of "locally inertial and Cartesian" (LIC) coordinate systems. A coordinate system (t, x^1, x^2, x^3) is LIC if and only if (i) its spatial origin $x^i=0$ lies on λ at all times; and (ii) the coordinate components of the metric are expandable about λ in powers of $r=[(x^1)^2+(x^2)^2+(x^3)^2]^{1/2}$, and the expansion takes the form

$$g_{\mu\nu}=\eta_{\mu\nu}+\sum_{n=2}^{\infty} r^n[(n\text{-pole})+\cdots+(0\text{-pole})] , \quad (2.2a)$$

or if expressed in terms of metric density perturbation $\bar{h}^{\mu\nu}\equiv\eta^{\mu\nu}-\mathfrak{g}^{\mu\nu}$

$$\bar{h}^{\mu\nu}=\sum_{n=2}^{\infty} r^n[(n\text{-pole})+\cdots+(0\text{-pole})] , \quad (2.2b)$$

where $\eta_{\mu\nu}$ is the flat metric (in Lorentz coordinates) and "l-pole" means a time-dependent, r-independent spherical harmonic of order l. Note that this definition guarantees that on λ the coordinate basis vectors form an orthonormal frame that is Fermi transported along λ.

It is not obvious from the outset that there exist any coordinate systems that have all these properties. However, we shall demonstrate below (Sec. III) that these properties are, in fact, satisfied by a subclass of de Donder coordinate systems.

In LIC coordinates, many calculations become greatly simplified. One example is the definition of the external moments, which reduces the precise definition (2.10), as we will give in Sec. II C, to (1.3) in LIC coordinates. But by contrast with the internal problem, where the moments read off the expansion coefficients are the same in all ACMC coordinate systems even at nonlinear orders, the external moments read off the metric or metric density are not the same in all LIC coordinate systems.

For example, consider a precisely static spacetime, so $\mathscr{B}_{ab}=0$, and examine it up to quartic order in r. More specifically, let the metric density $\mathfrak{g}^{\mu\nu}_{\mathrm{DD}}=\eta^{\mu\nu}-\bar{h}^{\mu\nu}_{\mathrm{DD}}$ in de Donder coordinates x^μ_{DD} have the form

$$\bar{h}^{00}_{\mathrm{DD}}(x^\mu_{\mathrm{DD}})=2\mathscr{E}_{ab}x^a_{\mathrm{DD}}x^b_{\mathrm{DD}} + r^4_{\mathrm{DD}}[(2\text{-pole})+(0\text{-pole})] , \quad (2.3a)$$

$$\bar{h}^{0i}_{\mathrm{DD}}(x^\mu_{\mathrm{DD}})=0 , \quad (2.3b)$$

$$\bar{h}^{ij}_{\mathrm{DD}}(x^\mu_{\mathrm{DD}})=r^4_{\mathrm{DD}}[(2\text{-pole})+(0\text{-pole})] + r^2_{\mathrm{DD}}(0\text{-pole}) , \quad (2.3c)$$

where $\mathscr{E}_{ab}$ is independent of time and the (2-pole) and (0-pole) terms are constructed from products of $\mathscr{E}_{ab}$ with itself in such a manner as to guarantee satisfaction of the vacuum Einstein equations and the de Donder gauge condition. Then to quartic order

$$g^{\mathrm{DD}}_{00}(x^\mu_{\mathrm{DD}})=-1+\mathscr{E}_{ab}x^a_{\mathrm{DD}}x^b_{\mathrm{DD}} - \tfrac{1}{2}(\mathscr{E}_{ab}\mathscr{E}_{cd})^{\mathrm{STF}}x^a_{\mathrm{DD}}x^b_{\mathrm{DD}}x^c_{\mathrm{DD}}x^d_{\mathrm{DD}} + r^4_{\mathrm{DD}}[(2\text{-pole})+(0\text{-pole})]+r^2_{\mathrm{DD}}(0\text{-pole}) , \quad (2.4a)$$

$$g^{\mathrm{DD}}_{0i}(x^\mu_{\mathrm{DD}})=0 , \quad (2.4b)$$

$$g^{\mathrm{DD}}_{ij}(x^\mu_{\mathrm{DD}})=r^4_{\mathrm{DD}}[(4\text{-pole})+(2\text{-pole})+(0\text{-pole})] + r^2_{\mathrm{DD}}[(2\text{-pole})+(0\text{-pole})] . \quad (2.4c)$$

Let us make a coordinate transformation

$$t_{\mathrm{FN}}=t_{\mathrm{DD}} , \quad (2.5a)$$

$$x^i_{\mathrm{FN}}=x^i_{\mathrm{DD}}+\tfrac{1}{6}\mathscr{E}_{ia}x^a_{\mathrm{DD}}r^2_{\mathrm{DD}}-\tfrac{1}{3}\mathscr{E}_{ab}x^a_{\mathrm{DD}}x^b_{\mathrm{DD}}x^i_{\mathrm{DD}} . \quad (2.5b)$$

(Incidentally, this transformation brings us into Fermi normal coordinate.[17]) The metric has the form

$$g^{\mathrm{FN}}_{00}(x^\mu_{\mathrm{FN}})=-1+\mathscr{E}_{ab}x^a_{\mathrm{FN}}x^b_{\mathrm{FN}} - \tfrac{5}{6}(\mathscr{E}_{ab}\mathscr{E}_{cd})^{\mathrm{STF}}x^a_{\mathrm{FN}}x^b_{\mathrm{FN}}x^c_{\mathrm{FN}}x^d_{\mathrm{FN}} + r^4_{\mathrm{FN}}[(2\text{-pole})+(0\text{-pole})]+r^2_{\mathrm{FN}}(0\text{-pole}) , \quad (2.6a)$$

$$g^{\mathrm{FN}}_{0i}(x^\mu_{\mathrm{FN}})=0 , \quad (2.6b)$$

$$g^{\mathrm{FN}}_{ij}(x^\mu_{\mathrm{FN}})=r^4_{\mathrm{FN}}[(4\text{-pole})+(2\text{-pole})+(0\text{-pole})] + r^2_{\mathrm{FN}}[(2\text{-pole})+(0\text{-pole})] \quad (2.6c)$$

corresponding to, at linear order,

$$\bar{h}^{00}_{\mathrm{FN}}(x^\mu_{\mathrm{FN}})=\tfrac{2}{3}\mathscr{E}_{ab}x^a_{\mathrm{FN}}x^b_{\mathrm{FN}}+O(r^4_{\mathrm{FN}}) , \quad (2.7a)$$

$$\bar{h}^{0i}_{\mathrm{FN}}(x^\mu_{\mathrm{FN}})=0 , \quad (2.7b)$$

$$\bar{h}^{ij}_{\mathrm{FN}}(x^\mu_{\mathrm{FN}})=r^2_{\mathrm{FN}}[(2\text{-pole})+(0\text{-pole})]+O(r^4_{\mathrm{FN}}) . \quad (2.7c)$$

Note that the $O(r^2)$ quadrupolar part of $\bar{h}^{00}_{\mathrm{DD}}$ is different from that of $\bar{h}^{00}_{\mathrm{FN}}$ (factor 2 versus $\frac{2}{3}$); this shows that, even at linear order, the quadrupole moments read off of

$\bar{h}^{\mu\nu}$ differ in the two coordinate systems. Note further that the $O(r^2)$ quadrupolar parts of $g_{00}^{\rm DD}$ and $g_{00}^{\rm FN}$ are the same, but the 4-pole parts are different (factor 0 versus factor $-\frac{5}{6}$). Thus, if one were to try to read multipole moments off g_{00} one would find different moments at the quadratically nonlinear order in the two coordinate systems. However, in a precisely fixed de Donder coordinate system this confusion of "multipole moments" obtained from metric (density) expansion will be taken away in stationary as well as in dynamic situations.

A coordinate system is de Donder if and only if its metric density satisfies the gauge condition

$$\mathfrak{g}^{\alpha\beta}{}_{,\beta}=0 . \tag{2.8}$$

In any de Donder coordinate system, the Einstein field equations and the Landau-Lifshitz pseudotensor are much simplified. This makes de Donder coordinates especially useful in practical calculations. For example, de Donder coordinates were used in the Thorne-Hartle-Zhang derivations of laws of motion and precession;[3,4] in Suen's[5] thorough treatment of stationary systems with both external and internal moments; in studies of gravitational waves from an isolated source by Blanchet and Damour[12] and others; and the proof by Thorne and Gürsel[14] that the free precession of a slowly rotating, rigid, general relativistic body is governed by the classical nonrelativistic Euler equations.

The four de Donder coordinate conditions $\mathfrak{g}^{\alpha\beta}{}_{,\beta}=0$ reduce the number of independent components of $\mathfrak{g}^{\mu\nu}$ to six (there are ten initially). Any further coordinate transformation

$$x^{\mu'}=x^{\mu}+\xi^{\mu}$$

leaves the coordinate system de Donder if (2.8) is not violated. At the linear order, this is achieved if ξ^{μ} satisfies[18]

$$\Box\xi^{\mu}=0 . \tag{2.9}$$

By an appropriate choice of ξ^{μ}, the number of dynamically independent metric coefficients is further reduced to two (e.g., the two polarizations of a gravitational wave); correspondingly, as we shall see in Secs. III and IV, the full spacetime metric near λ is rigidly fixed in terms of the time development of only two families of moments $\mathscr{I}_{A_l}$ and $\mathscr{J}_{A_l}$. Our criterion for choosing ξ^{μ} at linear order will be that in the stationary limit (i.e., at zero order in $r/\mathscr{T}$) $\bar{h}_{ij}$ should vanish. The pure time derivative terms in the linearized $\bar{h}_{ij}$ and $\bar{h}_{0i}$ of Eqs. (3.26) will then be forced to be present by the de Donder gauge condition (2.8). At higher, nonlinear orders we shall specialize our de Donder gauge to keep $\bar{h}^{\mu\nu}$ in LIC form (2.2) with "moments" $\mathscr{I}^{\gamma}_{A_l}$, $\mathscr{J}^{\gamma}_{A_l}$ always corresponding to the coefficients in front of $r^l Y^{lm}$ or $r^l Y^{l,lm}_i$, no matter what the nonlinear order is.

C. Definitions of the multipole moments

In the external problem we lose the ability of reading the moments directly off the metric (density) as one has been able to do in the internal case. However, the expansion around λ in vacuum permits us to define these moments covariantly without performing any conformal transformation. More specifically, we shall define the multipole moments of the external spacetime as STF parts of gradients of the Riemann tensor and itself, evaluated on the physical spacetime's fiducial world line λ:

$$\mathscr{I}_{\alpha_1\alpha_2\cdots\alpha_l}\equiv\frac{1}{(l-2)!}(P^{\beta_1}_{\alpha_1}P^{\beta_2}_{\alpha_2}\cdots P^{\beta_l}_{\alpha_l})^{\rm STF} \times R_{\mu\beta_1\nu\beta_2;\beta_3\cdots\beta_l}u^{\mu}u^{\nu}|_{\lambda} , \tag{2.10a}$$

$$\mathscr{J}_{\alpha_1\alpha_2\cdots\alpha_l}\equiv\frac{3}{2(l+1)(l-2)!}(P^{\beta_1}_{\alpha_1}P^{\beta_2}_{\alpha_2}\cdots P^{\beta_l}_{\alpha_l})^{\rm STF} \times\epsilon_{\mu\beta_1}{}^{\gamma\delta}R_{\gamma\delta\beta_2\nu;\beta_3\cdots\beta_l}u^{\mu}u^{\nu}|_{\lambda} . \tag{2.10b}$$

Here $P^{\mu}{}_{\nu}=g^{\mu}{}_{\nu}+u^{\mu}u_{\nu}$ is the projection tensor which projects into the local 3-space orthogonal to the 4-velocity $\mathbf{u}$; and $\mathbf{u}$ is the 4-velocity (i.e., tangent unit vector) of the fiducial world line λ, or equivalently of the preferred observer who moves along that world line.

As defined by Eqs. (2.10) the external multipole moments $\mathscr{I}_{\alpha_1\alpha_2\cdots\alpha_l}$, $\mathscr{J}_{\alpha_1\alpha_2\cdots\alpha_l}$ are symmetric, trace-free 4-tensors defined on λ and totally orthogonal to λ. If one changes from λ to some other fiducial world line, these moments will change. When one performs a $3+1$ split of spacetime from the viewpoint of the preferred observer, $\mathscr{I}_{\alpha_1\alpha_2\cdots\alpha_l}$ and $\mathscr{J}_{\alpha_1\alpha_2\cdots\alpha_l}$ become fully spatial, three-dimensional, STF tensor fields $\mathscr{I}_{a_1\cdots a_l}=\mathscr{I}_{A_l}$, $\mathscr{J}_{a_1\cdots a_l}=\mathscr{J}_{A_l}$, defined at the origin of the local 3-space of the preferred observer, and evolving with time as measured by that observer; and the definitions (2.10) reduce to those of Eqs. (1.3).

In external expansions, the expansion coefficients are expressed in terms of these multipole moments. Although these moments are defined in a coordinate-independent way, the details of the expansion still depend on the coordinate system used.

The remainder of this paper (Secs. III and IV) will deal with the expansion of the metric density, metric, and Riemann tensor in rigidly fixed de Donder coordinates—which, of course are also LIC. But in proving some of the properties of these expansions, we shall switch from Cartesian coordinates to the corresponding spherical polar coordinate system from time to time.

III. STRUCTURE OF THE EXTERNAL EXPANSION IN A RIGIDLY FIXED DE DONDER COORDINATE SYSTEM

A. Notations and mathematical formulas

In this subsection, we will explain the notations to be used in our de Donder-coordinate-system multipole expansion; and we will give some mathematical formulas which will be used in developing the expansion formalism.

The notation we shall use is that of Thorne.[2] Symmetric traceless tensors with l spatial indices ("STF-l tensors") will be denoted by capital script letters, as $\mathscr{F}_{A_l}$, which is shorthand for $(\mathscr{F}_{a_1a_2\cdots a_l})^{\rm STF}$. A product of l

spatial coordinates $x_{a_1}x_{a_2}\cdots x_{a_l}$ will be denoted X_{A_l}. The raising and lowering of these indices are effected by the Kronecker delta δ^i_j. Thus $\mathcal{F}_{A_l}X_{A_l}$ is the same as $\mathcal{F}_{a_1a_2\cdots a_l}x^{a_1}x^{a_2}\cdots x^{a_l}$. The STF harmonics and the spherical harmonics Y_{lm} (scalar), $Y_i^{l',lm}$ (vector) and $T_{ij}^{\lambda l',lm}$ (tensor) will be used extensively in this paper. The scalar spherical harmonics Y^{lm} are well known. The vector and tensor spherical harmonics are obtained by Clebsch-Gordan coupling $Y^{l'm'}$ to the basis vectors

$$\xi^0\equiv\mathbf{e}_z\ ,\quad \xi^{\pm1}\equiv\mp(\mathbf{e}_x\pm i\mathbf{e}_y)/\sqrt{2}\ , \tag{3.1}$$

and the basis tensors

$$\overleftrightarrow{t}^{\pm2}=\tfrac{1}{2}\,(\mathbf{e}_x\otimes\mathbf{e}_x-\mathbf{e}_y\otimes\mathbf{e}_y)\pm\frac{i}{2}\,(\mathbf{e}_x\otimes\mathbf{e}_y+\mathbf{e}_y\otimes\mathbf{e}_x)\ , \tag{3.2a}$$

$$\overleftrightarrow{t}^{\pm1}=\mp\tfrac{1}{2}\,(\mathbf{e}_x\otimes\mathbf{e}_z+\mathbf{e}_z\otimes\mathbf{e}_x)-\frac{i}{2}\,(\mathbf{e}_y\otimes\mathbf{e}_z+\mathbf{e}_z\otimes\mathbf{e}_y)\ , \tag{3.2b}$$

$$\overleftrightarrow{t}^{0}=6^{-1/2}(-\mathbf{e}_x\otimes\mathbf{e}_x-\mathbf{e}_y\otimes\mathbf{e}_y+2\mathbf{e}_z\otimes\mathbf{e}_z)\ , \tag{3.2c}$$

$$\overleftrightarrow{\delta}=\mathbf{e}_x\otimes\mathbf{e}_x+\mathbf{e}_y\otimes\mathbf{e}_y+\mathbf{e}_z\otimes\mathbf{e}_z\ . \tag{3.2d}$$

For a beautiful review of relations between these Clebsch-Gordan-coupled harmonics and STF harmonics and for reviews of some of their properties, see Thorne.[2] As discussed by Thorne, any STF-l tensor $\mathcal{F}_{K_l}$ can be expanded as

$$\mathcal{F}_{K_l}=\sum_m F^{lm}\mathcal{Y}^{lm}_{K_l}\ , \tag{3.3}$$

where $\mathcal{Y}^{lm}_{K_l}$ is related to Y^{lm} through

$$Y^{lm}=\mathcal{Y}^{lm}_{K_l}N_{K_l}\ . \tag{3.4}$$

Therefore we have the correspondence between $\mathcal{E}_{A_l}$ and E_{lm}, $\mathcal{B}_{A_l}$ and B_{lm}.

For the convenience of discussion below, we shall abbreviate Y^{lm}, $Y_i^{l',lm}$, and $T_{ij}^{\lambda l',lm}$ as $H^{l'lm}$. In $H^{l'lm}$, l' is the eigenvalue of the orbital angular momentum operator $L^2=-(\mathbf{r}\times\nabla)^2$

$$L^2H^{l'lm}=l'(l'+1)H^{l'lm}\ ;$$

l is the order of the irreducible representation of the rotation group generated by $H^{l'lm}$; and m is the azimuthal quantum number.[2] In our analysis, we shall often encounter the Poisson equation

$$\nabla^2 f=H^{l'lm}r^{l'+n}\ , \tag{3.5}$$

which can be inverted as

$$f=\frac{1}{(n+2)(n+2l'+3)}\,H^{l'lm}r^{l'+n+2}\quad\text{for } n\neq-2\ . \tag{3.6}$$

One can easily convince oneself that (3.6) is a solution of (3.5) by writing the Laplacian ∇^2 as $(1/r^2)\partial_r(r^2\partial_r)-L^2/r^2$.

An important lemma, which we shall use extensively, is this: *Any scalar, vector, or second-rank symmetric tensor, constructed from products of quantities with the form* $(H^{l'lm}r^{l'+2k})_{,i_1\cdots i_n}$ *(where* $k\geq0$ *and the comma denotes* $n\geq0$ *spatial derivatives) must have the form* $H^{L'LM}r^{L'+2K}$ *with* $K\geq0$. Proof: $H^{l'lm}r^{l'+2k}$ is a sum of terms[2] like $X_{B_s}\mathcal{Y}^{lm}_{C_pA_q}X_{A_q}r^{2k'}$ with the constraints

$$p+q=l\ ,\quad s+q=l'-2(k'-k)\ ,\quad k'\geq k\ . \tag{3.7}$$

When we take one spatial derivative of such a term we get

$$\partial_i(X_{B_s}\mathcal{Y}^{lm}_{C_pA_q}X_{A_q}r^{2k})=\sum_j\delta_{ib_j}X_{B_{j-1}b_{j+1}\cdots b_s}\mathcal{Y}^{lm}_{C_pA_q}X_{A_q}r^{2k}+qX_{B_s}\mathcal{Y}^{lm}_{C_piA_{q-1}}X_{A_{q-1}}r^{2k}+2kr^{2k-2}x_iX_{B_s}\mathcal{Y}^{lm}_{C_pA_q}X_{A_q}$$
$$\sim X_{B'_s}\mathcal{Y}^{lm}_{C'_pA'_q}X_{A'_q}r^{2k_1}\ , \tag{3.8}$$

where $\sim$ reads "a sum of terms of the form," and $k_1=k-\Delta k\geq0$ with $\Delta k=0$ or 1. If we take more derivatives, the range of Δk increases but k_1 remains positive. When we couple two such terms together to get scalar, vector, or tensor spherical harmonics, we obtain

$$X_{B_{s_1}}X_{B'_{s_2}}\mathcal{Y}^{l_1m_1}_{C_{p_1}A_{q_1}}\mathcal{Y}^{l_2m_2}_{C'_{p_2}A'_{q_2}}X_{A_{q_1}}X_{A'_{q_2}}r^{2k'_1+2k'_2}$$
$$\sim(\mathcal{Y}^{Lm}_{A_L}X_{A_L}r^n,\ x_i\mathcal{Y}^{Lm}_{A_L}X_{A_L}r^n,\ \mathcal{Y}^{Lm}_{iA_{L-1}}X_{A_{L-1}}r^n,\ x_ix_j\mathcal{Y}_{A_L}X_{A_L}r^n,\ x_i\mathcal{Y}^{Lm}_{jA_{L-1}}X_{A_{L-1}}r^n,\ \mathcal{Y}^{Lm}_{ijA_{L-2}}X_{A_{L-2}}r^n)\ . \tag{3.9}$$

In Eq. (3.9) the coupled terms have $s\leq2$, $l-2\leq q\leq l$ because we only want to form from them tensors of rank ≤2. Since the number of x_i's has to decrease by pairs, the following relation holds:

$$s_1+s_2+q_1+q_2=s+q+(\text{even number})\ . \tag{3.10}$$

A simple counting of powers of r on both sides of Eq. (3.9) gives

$$s_1+s_2+q_1+q_2+2k'_1+2k'_2=s+q+n\ . \tag{3.11}$$

Equations (3.10) and (3.11) can be combined to give

$$n=2k'_1+2k'_2+(\text{even number})=2K'\ ,\quad K'=0,1,2,\ldots\ .$$

If we look back at the constraints (3.7), it becomes clear that from these coupled terms we can only obtain $H^{L'LM}r^{L'+2K}$ with the condition

$$
\begin{aligned}
2K &= s+q+2K'-L' \\
&= s_1+s_2+q_1+q_2+2k_1'+2k_2'-L' \\
&= l_1'+l_2'+2k_1+2k_2-L' \geq 0 .
\end{aligned}
$$

This conclusion can also be proved more elegantly using Clebsch-Gordan coupling techniques, but we shall not do so here.

Finally, for later use we shall cite a few formulas from Mathews:[19]

$$
(f_l(kr)Y_i^{l'lm})_{,i} = \begin{cases} -k\sqrt{l/(2l+1)}\,f_l(kr)Y^{lm}\,, & l'=l-1\,, \quad (3.12a) \\ 0, & l'=l\,, \quad (3.12b) \\ -k\sqrt{(l+1)/(2l+1)}\,f_l(kr)Y^{lm}\,, & l'=l+1\,, \quad (3.12c) \end{cases}
$$

$$
(f_l(kr)T_{ij}^{2,l'lm})_{,j} = \begin{cases} -k\sqrt{(l-1)/(2l-1)}\,f_{l-1}(kr)Y_i^{l-1,lm}, & l'=l-2\,, \quad (3.13a) \\ -k\sqrt{(l-1)/2(2l+1)}\,f_l(kr)Y_i^{l,lm}, & l'=l-1\,, \quad (3.13b) \\ -k[\sqrt{(l+1)(2l+3)/6(2l+1)(2l-1)}\,f_{l-1}(kr)Y_i^{l-1,lm} & \\ \quad +\sqrt{l(2l-1)/6(2l+1)(2l+3)}\,f_{l+1}(kr)Y_i^{l+1,lm}], & l'=l\,, \quad (3.13c) \\ -k\sqrt{(l+2)/2(2l+1)}\,f_l(kr)Y_i^{l,lm}, & l'=l+1\,, \quad (3.13d) \\ -k\sqrt{(l+2)/(2l+3)}\,f_{l+1}(kr)Y_i^{l+1,lm}, & l'=l+2\,. \quad (3.13e) \end{cases}
$$

Here $f_l(kr)$ is any spherical Bessel function.

B. Algorithm for constructing the (nonlinear) metric density in a rigidly fixed de Donder coordinate system

Thorne and Hartle[3] have proposed, in their Appendix, an iterative algorithm for generating the multipolar expansion of the fully nonlinear, dynamical metric density in the vacuum region surrounding λ; but they did not analyze the mathematical details or consequences of the algorithm. In this section we shall review briefly the proposed algorithm.

In terms of the metric density $\mathfrak{g}^{\mu\nu}$ or $\bar{h}^{\mu\nu}=\eta^{\mu\nu}-\mathfrak{g}^{\mu\nu}$, the vacuum Einstein field equations in de Donder gauge read

$$\Box\bar{h}^{\mu\nu} = W^{\mu\nu}\,, \quad (3.14a)$$

$$\bar{h}^{\mu\nu}{}_{,\nu} = 0\,, \quad (3.14b)$$

where

$$W^{\mu\nu} = -16\pi(-g)t^{\mu\nu}+\bar{h}^{\mu\nu}{}_{,\alpha\beta}\bar{h}^{\alpha\beta}-\bar{h}^{\mu\alpha}{}_{,\beta}\bar{h}^{\nu\beta}{}_{,\alpha}\,; \quad (3.15)$$

$t^{\mu\nu}$ is the Landau-Lifshitz pseudotensor [Eq. (20.20) of Ref.1]

$$
\begin{aligned}
16\pi(-g)t^{\mu\nu} &= \bar{h}^{\mu\nu}{}_{,\lambda}\bar{h}^{\lambda}{}_{,\alpha}-\bar{h}^{\mu\lambda}{}_{,\lambda}\bar{h}^{\nu\alpha}{}_{,\alpha}+\tfrac{1}{2}\,g^{\mu\nu}g_{\lambda\alpha}\bar{h}^{\lambda\beta}{}_{,\rho}\bar{h}^{\rho\alpha}{}_{,\beta} \\
&\quad -(g^{\mu\lambda}g_{\alpha\beta}\bar{h}^{\nu\beta}{}_{,\rho}\bar{h}^{\alpha\rho}{}_{,\lambda}+g^{\nu\lambda}g_{\alpha\beta}\bar{h}^{\mu\beta}{}_{,\rho}\bar{h}^{\alpha\rho}{}_{,\lambda})+g_{\lambda\mu}g^{\rho\beta}\bar{h}^{\mu\lambda}{}_{,\beta}\bar{h}^{\nu\alpha}{}_{,\rho} \\
&\quad +\tfrac{1}{8}\,(2g^{\mu\lambda}g^{\nu\alpha}-g^{\mu\nu}g^{\lambda\alpha})(2g_{\beta\rho}g_{\sigma\tau}-g_{\rho\sigma}g_{\beta\tau})\bar{h}^{\beta\tau}{}_{,\lambda}\bar{h}^{\rho\sigma}{}_{,\alpha}\,. \quad (3.16)
\end{aligned}
$$

The box $\Box$ which acts on each component of $\bar{h}^{\mu\nu}$ in (3.14a) is the flat-space d'Alembertian, $\Box=\eta_{\mu\nu}(\partial/\partial x^{\mu})(\partial/\partial x^{\nu})$; and the compatibility of (3.14a) and (3.14b), i.e., the existence of a solution, is guaranteed by the identity $W^{\mu\nu}{}_{,\nu}\equiv 0$.

To solve Eqs. (3.14) one can proceed in either or both of two directions: First, one can expand $\bar{h}^{\mu\nu}$ in nonlinear orders p

$$\bar{h}^{\mu\nu} = \sum G^p\gamma_p^{\mu\nu}\,. \quad (3.17)$$

Here G is the gravitational constant which is actually equal to unity in our units, but is kept to serve the purpose of "bookkeeping." The source terms $W^{\mu\nu}$ are also expanded in this way:

$$W^{\mu\nu} = \sum_p G^p W_p^{\mu\nu}\,, \quad (3.18)$$

where $W_p^{\mu\nu}$ is constructable via Eqs. (3.15), (3.16), from products of $\gamma_{p'}^{\alpha\beta}$ with $p_1'+p_2'+\cdots=p$ and thus with each $p'\leq p-1$. One can then solve the field equations and gauge conditions (3.14) iteratively,

$$\Box\gamma_p^{\mu\nu} = W_p^{\mu\nu}\,, \quad (3.19a)$$

$$\gamma_p^{\mu\nu}{}_{,\nu} = 0\,, \quad (3.19b)$$

first for $p=1$ (where $W_p^{\mu\nu}=0$), then for $p=2,3,\ldots$. Unfortunately, Eqs. (3.19) are hard to solve in most cases.

One can also proceed in a second direction. First one makes a multiparameter expansion of the metric density

$\bar{h}^{\mu\nu}$ and the source terms $W^{\mu\nu}$ in terms of the small dimensionless variables $r/\mathscr{R}$, $r/\mathscr{L}$, $r/\mathscr{T}$; and then one decomposes each term into spherical harmonic components of order l:

$$\bar{h}^{\mu\nu}=\sum_{p,n,u,l}(\gamma^{\mu\nu})_{pnul}\ , \tag{3.20a}$$

$$(\gamma^{\mu\nu})_{pnul}\sim\left[\left[\frac{r}{\mathscr{R}}\right]^{2p}\left[\frac{r}{\mathscr{L}}\right]^{n}\left[\frac{r}{\mathscr{T}}\right]^{u}\right]_{\text{order } l}\ , \tag{3.20b}$$

$$W^{\mu\nu}=\sum W^{\mu\nu}_{pnul}\ . \tag{3.21}$$

One can verify from the definition of $\mathscr{R}$ that the p which appears here is the same as the p of the nonlinearity expansion (3.17). The field equations and gauge conditions (3.14) then take the form

$$\nabla^2\gamma^{\mu\nu}_{pnul}=W^{\mu\nu}_{pnul}+\partial_t^2\gamma^{\mu\nu}_{pn(u-2)l}\ , \tag{3.22a}$$

$$\gamma^{\mu 0}_{pn(u-1)l,0}+\gamma^{\mu i}_{pnul,i}=0\ . \tag{3.22b}$$

These equations, like (3.19), can then be solved iteratively. From Eqs. (3.5) and (3.6) one can find a particular integral of (3.22a); this is far easier than solving (3.19). One must then add to this particular integral a homogeneous solution of (3.22a), chosen so as to enforce the gauge condition (3.22b). In Secs. III D and III E, we will elucidate some of the mathematical details and consequences of this algorithm.

C. The linear part of the algorithm

The linear order ($p=1$) of the above algorithm is simplified by the fact that $W^{\mu\nu}_1=0$. The field equations and gauge conditions thus read

$$\Box\gamma^{\mu\nu}_1=0\ , \tag{3.23}$$

$$\gamma^{\mu\nu}_{1\ ,\nu}=0\ . \tag{3.24}$$

These can be solved directly without a multiparameter expansion. The desired solution, which must go as r^n with $n\geq 2$ at the origin because of our LIC coordinates, can be constructed as superpositions of "normal modes":

$$\gamma^{\mu\nu}_1\sim\sum_{l'lm}\int C_{l'lm\omega}j_{l'}(\omega r)e^{i\omega t}H^{l'lm}d\omega\quad\text{for } l\geq 2\ , \tag{3.25}$$

where $j_{l'}$ are spherical Bessel functions and $\omega\sim 1/\mathscr{T}$. The superposition coefficients $C_{l'lm\omega}$ are fixed by the demands that (i) at stationary order [i.e., at leading order $(\omega r)^{l'}$ in a power-series expansion of $j_{l'}$] $\gamma^{\mu\nu}_1=\eta^{\mu\nu}-\mathfrak{g}^{\mu\nu}$ must take on the linearized, stationary, Thorne-Hartle form (1.2), and (ii) the gauge condition (3.21) must be satisfied. A straightforward but rather tedious calculation, including a power-series expansion of $j_{l'}$, then gives (restoring all normalization constants)

$$\bar{h}^{00}=-\sum_{l=2}^{\infty}\frac{4(2l+1)!!}{l(l-1)}\sum_{k=0}^{\infty}\frac{r^{2k}}{2^k k!(2l+1+2k)!!}\,{}^{(2k)}\mathscr{G}^{\gamma}_{A_l}X_{A_l}\ , \tag{3.26a}$$

$$\bar{h}^{0i}=-\sum_{l=2}^{\infty}\frac{2(2l+1)!!}{3(l-1)}\sum_{k=0}^{\infty}\frac{r^{2k}}{2^k k!(2l+1+2k)!!}\,\epsilon_{ipq}x_p\,{}^{(2k)}\mathscr{B}^{\gamma}_{qA_{l-1}}X_{A_{l-1}}$$
$$+\sum_{l=2}^{\infty}\frac{4(2l+1)(2l+1)!!}{(l+1)l(l-1)}\sum_{k=0}^{\infty}\frac{r^{2k}}{2^k k!(2l+3+2k)!!}\left[{}^{(2k+1)}\mathscr{G}^{\gamma}_{A_l}X_{A_l}x_i-\frac{l}{2l+1}\,{}^{(2k+1)}\mathscr{G}^{\gamma}_{iA_{l-1}}X_{A_{l-1}}r^2\right]\ , \tag{3.26b}$$

$$\bar{h}^{ij}=\sum_{l=2}^{\infty}\frac{4(2l+1)(2l+1)!!}{3(l+2)(l-1)}\sum_{k=0}^{\infty}\frac{r^{2k}}{2^k k!(2l+3+2k)!!}\left[x_{(i}\epsilon_{j)pq}\,{}^{(2k+1)}\mathscr{B}^{\gamma}_{qA_{l-1}}x_pX_{A_{l-1}}-\frac{l-1}{2l+1}\,\epsilon_{pq(i}\,{}^{(2k+1)}\mathscr{B}^{\gamma}_{j)qA_{l-2}}x_pX_{A_{l-2}}r^2\right]$$
$$-\sum_{l=2}^{\infty}\frac{4(2l+3)(2l+1)(2l+1)!!}{(l+2)(l+1)l(l-1)}$$
$$\times\sum_{k=0}^{\infty}\frac{r^{2k}}{2^k k!(2l+5+2k)!!}$$
$$\times\left[{}^{(2k+2)}\mathscr{G}^{\gamma}_{A_l}X_{A_l}x_ix_j-\frac{2l}{2l+3}\,x_{(i}\,{}^{(2k+2)}\mathscr{G}^{\gamma}_{j)A_{l-1}}X_{A_{l-1}}r^2+\frac{l(l-1)}{(2l+1)(2l+3)}\,{}^{(2k+2)}\mathscr{G}^{\gamma}_{ijA_{l-2}}X_{A_{l-2}}r^4\right.$$
$$\left.+\frac{l(l-1)}{(2l+1)(2l+3)}\,{}^{(2k+2)}\mathscr{G}^{\gamma}_{ijA_{l-2}}X_{A_{l-2}}r^4-\frac{1}{2l+3}\,{}^{(2k+2)}\mathscr{G}^{\gamma}_{A_l}X_{A_l}r^2\delta_{ij}\right]\ . \tag{3.26c}$$

Here ${}^{(2k)}\mathscr{G}^{\gamma}_{A_l}$ means $(d^{2k}/dt^{2k})\mathscr{G}^{\gamma}_{A_l}(t)$, and $x_{(i}\epsilon_{j)pq}$ means to take the symmetric part on indices i,j.

It is evident that Eqs. (3.23) and (3.24) are the homogeneous part of Eqs. (3.14). To ensure that the moments $\mathscr{G}^{\gamma}_{A_l}$, $\mathscr{B}^{\gamma}_{A_l}$ read off of the final, fully nonlinear metric density $\bar{h}^{\mu\nu}$ [Eq. (3.17)] are the same as those in $\gamma^{\mu\nu}_1$ with which we start the iteration, all homogeneous parts of $\bar{h}^{\mu\nu}$ satisfying (3.23), (3.24) must be collected in $\gamma^{\mu\nu}_1$. This, then, determines $\gamma^{\mu\nu}_1$ uniquely, and becomes the starting point for the iterative solution of Eqs. (3.22) for $\gamma^{\mu\nu}_2$, $\gamma^{\mu\nu}_3$,....

D. Multipole expansion structure of $\mathfrak{g}^{\mu\nu}$ at order $p=2$

In this subsection we shall study the structure of $\gamma^{\mu\nu}_2$, i.e., of the metric density at the lowest nonlinear order

$p=2$. This study will lay a foundation for the next subsection where we shall study all higher orders, $p \geq 3$. The equations we must solve are (3.22a) and (3.22b) with $p \geq 2$. First we shall explore the structure of the source term $W_2^{\mu\nu}$ and from it shall infer the structure of a particular integral of (3.22a). Then we shall show how to construct the homogeneous solution of (3.22a) which, when added to the particular integral, produces a solution of the gauge condition (3.22b) without including terms of the form of $\gamma_1^{\mu\nu}$ [Eq. (3.26)].

In terms of the notation introduced in Sec. III A, at linear order, $\gamma_1^{\mu\nu}$ has the structure

$$\gamma_1^{\mu\nu} \sim X_{B_s}{}^{(u)} \mathcal{F}_{C_p A_q} X_{A_q} r^n \,. \tag{3.27}$$

Here $\mathcal{F}_{A_l}$ is either $\mathcal{E}_{A_l}$ or $\mathcal{B}_{A_l}$. Now $W_2^{\mu\nu}$ has the form

$$W_2^{\mu\nu} \sim \gamma^1_{\alpha\beta,\rho}\gamma^1_{\sigma\delta,\lambda} \;,\quad \gamma^1_{\alpha\beta,\rho\lambda}\gamma^1_{\sigma\delta} \,. \tag{3.28}$$

It is clear that $\gamma^1_{\alpha\beta,0}$ has the same structure ($H^{l'lm}r^{l'+2k}$) as $\gamma^1_{\alpha\beta}$. We also know (Sec. III A) that taking spatial derivatives will not change the structure of $\gamma^1_{\alpha\beta}$. Therefore, in accord with the lemma in Sec. III A

$$W_2^{\mu\nu} \sim H^{l'lm}r^{l'+2k} \,, \quad k=0,1,2,\ldots \,. \tag{3.29}$$

Using Eq. (3.6) we see that a particular integral of Eq. (3.22a) has the structure

$$p_2^{\mu\nu} \sim H^{l'lm}r^{l'+2k+2} \,, \tag{3.30}$$

aside from the possible exceptions caused by the $\partial_t^2\gamma^{\mu\nu}_{pn(u-2)l}$ term. But if we start from $\gamma^{\mu\nu}_{pn0l}$ we see that $\partial_t^2\gamma^{\mu\nu}_{pn(u-2)l}$ has the same structure as $W^{\mu\nu}_{pnul}$, i.e., no $H^{l'lm}r^{l'+2k\pm1}$ terms in it. Therefore all parts of $p_2^{\mu\nu}$ have the structure $H^{l'lm}r^{l'+2k+2}$.

The general solution of Eq. (3.22a) is a sum of this particular integral $p_2^{\mu\nu}$ and a homogeneous solution $f_2^{\mu\nu}$ of Eq. (3.22a):

$$\gamma_2^{\mu\nu}=p_2^{\mu\nu}+f_2^{\mu\nu} \,; \tag{3.31}$$

and we must choose $f_2^{\mu\nu}$ so as to guarantee that the gauge condition (3.22b) is satisfied, and that $\gamma_2^{\mu\nu}$ has no terms of the form of $\gamma_1^{\mu\nu}$. As is clear from Eqs. (3.19), (3.31), any such $f_2^{\mu\nu}$ must satisfy two relations:

$$f_2^{\mu\nu}{}_{,\nu}=-p_2^{\mu\nu}{}_{,\nu} \,, \tag{3.32}$$

$$\Box f_2^{\mu\nu}=0 \,. \tag{3.33}$$

The first of these is the desired gauge condition $\gamma_2^{\mu\nu}{}_{,\nu}=0$; the second is required by the field equation $\Box\gamma_2^{\mu\nu}=\Box(p_2^{\mu\nu}+f_2^{\mu\nu})=W_2^{\mu\nu}$ where $\Box p_2^{\mu\nu}=W_2^{\mu\nu}$. That Eqs. (3.32), (3.33) are compatible follows from $\Box(p_2^{\mu\nu}{}_{,\nu})=W_2^{\mu\nu}{}_{,\nu}=0$—where $W_2^{\mu\nu}{}_{,\nu}=0$ is the second-order part of the well-known conservation law $W^{\mu\nu}{}_{,\nu}=0$.[20] That there actually does exist a simultaneous solution to Eqs. (3.32), (3.33) we shall show below by explicit construction. That $f_2^{\mu\nu}$ can be chosen so as to keep out of $\gamma_2^{\mu\nu}$ terms of the form of $\gamma_1^{\mu\nu}$ follows from the fact that such terms satisfy the homogeneous forms of (3.32), (3.33) [cf. (3.23), (3.24)] and thus can be added to or subtracted from $f_2^{\mu\nu}$ at will.

We shall go into some detail to further illustrate the idea of adding gauge terms $f_2^{\mu\nu}$ to satisfy (3.22). For simplicity, we will use the nonlinearity expansion formalism, which easily can be converted to the multiparameter expansion formalism by expanding the spherical Bessel function $j_{l'}(\omega r)$.

We assume from the outset that $p_2^{\mu\nu}$ has been chosen so as to not include terms of the form $\gamma_1^{\mu\nu}$; this is easily done by simply removing such terms if they are present. Because $p_2^{\mu\nu}{}_{,\nu}$ satisfies $\Box p_2^{\mu\nu}{}_{,\nu}=0$, we can write it as

$$p_2^{0\nu}{}_{,\nu}=\sum_{l,m,u} {}^0P_{lm}^{(u)}(t)Y^{lm}r^{l+u}=\sum_{l,m}\int {}^0P_{lm\omega}j_l(\omega r)e^{i\omega t}d\omega Y^{lm} \,, \tag{3.34a}$$

$$\begin{aligned} p_2^{iv}{}_{,\nu}&=\sum_{l',l,m,u} {}^1P_{l'lm}^{(u)}(t)Y_i^{l',lm}r^{l'+u} \\ &=\sum_{l,m}\int {}^1P_{l-1,lm\omega}j_{l-1}(\omega r)e^{i\omega t}d\omega Y_i^{l-1,lm}+\sum_{l,m}\int {}^1P_{l,lm\omega}j_l(\omega r)e^{i\omega t}d\omega Y_i^{l,lm} \\ &\quad+\sum_{l,m}\int {}^1P_{l+1,lm\omega}j_{l+1}(\omega r)e^{i\omega t}d\omega Y_i^{l+1,lm} \,, \end{aligned} \tag{3.34b}$$

where ${}^0P_{lm}, {}^0P_{lm\omega}, {}^1P_{l'lm}, {}^1P_{l'lm\omega}$ are expansion coefficients and the superscript (u) denotes u time derivatives. It is straightforward to verify that the d'Alembertian-free functions

$$f_2^{00}=0 \,, \tag{3.35a}$$

$$f_2^{0i}=\sum_{l,m}\int {}^1F_{l+1,lm\omega}j_{l+1}(\omega r)e^{i\omega t}d\omega Y_i^{l+1,lm} \,, \tag{3.35b}$$

$$\begin{aligned} f_2^{ij}&=\sum_{l,m}\int {}^2F_{l+1,lm\omega}j_{l+1}(\omega r)e^{i\omega t}d\omega T_{ij}^{2,l+1,lm}+\sum_{l,m}\int {}^2F_{l+2,lm\omega}j_{l+2}(\omega r)e^{i\omega t}d\omega T_{ij}^{2,l+2,lm} \\ &\quad+\delta_{ij}\sum_{l,m}\int {}^2F_{l,lm\omega}j_{l(\omega r)}e^{i\omega t}d\omega Y^{lm} \end{aligned} \tag{3.35c}$$

satisfy (3.32) as desired, with $p_2^{\mu\nu}{}_{,\nu}$ in the form (3.34), if

$$ {}^1F_{l+1,lm\omega}=\frac{1}{\omega}\left[\frac{2l+1}{l+1}\right]^{1/2}{}^0P_{lm\omega}\,, \tag{3.36a} $$

$$ {}^2F_{llm\omega}=-\frac{1}{\omega}\left[\frac{2l+1}{l}\right]^{1/2}{}^1P_{l-1,lm\omega}\,, \tag{3.36b} $$

$$ {}^2F_{l+1,lm\omega}=-\frac{1}{\omega}\left[\frac{2(2l+1)}{l+2}\right]^{1/2}{}^1P_{llm\omega}\,, \tag{3.36c} $$

$$ {}^2F_{l+2,lm\omega}=\frac{1}{\omega}\left[\frac{2l+3}{l+2}\right]^{1/2}{}^1P_{l+1,lm\omega}+\frac{i}{\omega}\left[\frac{(2l+3)(2l+1)}{(l+2)(l+1)}\right]^{1/2}{}^0P_{lm\omega}-\frac{1}{\omega}\left[\frac{(l+1)(2l+3)}{l(l+2)}\right]^{1/2}{}^1P_{l-1,lm\omega}\,. \tag{3.36d} $$

Moreover, by expanding the spherical Bessel functions in (3.34) and (3.35) and by combining with (3.36), we can rewrite this d'Alembertian-free solution to (3.32) as

$$ f_2^{00}=0\,, \tag{3.37a} $$

$$ f_2^{0i}=\sum_{l,m,k}\left[\frac{2l+1}{l+1}\right]^{1/2}a_{l+1}^k\,{}^0P_{2m}^{(2k)}(t)Y_i^{l+1,lm}r^{l+1+2k}\,, \tag{3.37b} $$

$$ \begin{aligned} f_2^{ij}=&-\sum_{l,m,k}\left[\frac{2(2l+1)}{l+2}\right]^{1/2}a_{l+1}^k\,{}^1P_{llm}^{(2k)}(t)T_{ij}^{2,l+1,lm}r^{l+1+2k}\\ &+\sum_{l,m,k}a_{l+2}^k\left[\left[\frac{2l+3}{l+2}\right]^{1/2}{}^1P_{l+1,lm}^{(2k)}(t)+\left[\frac{(2l+1)(2l+3)}{(l+1)(l+2)}\right]^{1/2}{}^0P_{lm}^{(2k+1)}(t)\right.\\ &\left.+\left[\frac{(l+1)(2l+3)}{l(l+2)}\right]^{1/2}{}^1P_{l-1,lm}^{(2k+2)}(t)\right]T_{ij}^{2,l+2,lm}r^{l+2+2k}-\delta_{ij}\sum_{l,m,k}\left[\frac{2l+1}{l}\right]^{1/2}a_l^k\,{}^1P_{l-1,lm}^{(2k)}(t)Y^{lm}r^{l+2k}\,, \end{aligned} \tag{3.37c} $$

where a_l^k are the expansion coefficients of the spherical Bessel function:

$$ j_l(x)=\sum_k a_l^k x^{l+2k}\,. $$

Notice that all $l'\le l$ components in $f_2^{\mu\nu}$ have been deliberately chosen to be zero except in f_2^{ij} where we have an extra trace term ($l'=l$). This guarantees, as desired, that $\gamma_2^{\mu\nu}$ will not bring our coordinate system outside the LIC class; that $f_2^{\mu\nu}$ will not interfere with the moments $\mathscr{E}_{A_l}^{\gamma}$, $\mathscr{B}_{A_l}^{\gamma}$ read off $\bar{h}^{00}$, $\bar{h}^{0i}$ from the r^l(l-pole) terms, and (as we shall see) that $f_2^{\mu\nu}$ is unique once $p_2^{\mu\nu}$ has been chosen. It should be emphasized that $f_2^{\mu\nu}$ has the same structure as $\gamma_1^{\mu\nu}$ and $p_2^{\mu\nu}$ ($\sim H^{l'lm}r^{l'+2k}$). Therefore $\gamma_2^{\mu\nu}$, as a whole, also has this structure.

E. Multipole expansion structure of $\mathfrak{g}^{\mu\nu}$ in general

In this subsection, we shall examine the structure of $\gamma_p^{\mu\nu}$, i.e., of the metric density $\mathfrak{g}^{\mu\nu}$, at all nonlinear orders $p\ge 3$. As we saw in the previous subsection, $\gamma_2^{\mu\nu}$ has the same structure ($\sim H^{l'lm}r^{l'+2k}$, $k\ge 0$) as $\gamma_1^{\mu\nu}$. Now we shall show using induction that *for any p, $\gamma_p^{\mu\nu}$ has the same structure as $\gamma_1^{\mu\nu}$* ($\sim H^{l'lm}r^{l'+2k}$, $k\ge 0$).

We have already shown explicitly that this statement is true at $p=2$. Suppose it is also true up to order p. Then at nonlinearity order $p+1$,

$$ W_{p+1}^{\mu\nu}\sim \bar{h}_{\alpha\beta,\rho\sigma}\bar{h}_{\delta\lambda},\ \bar{h}_{\alpha\beta,\rho}\bar{h}_{\sigma\delta,\alpha},\ g_{\alpha\beta}g_{\rho\sigma}\bar{h}_{\delta\lambda,\kappa}\bar{h}_{\pi\tau,\xi},\ldots\,. $$

Since for $p'\le p$, $\gamma_{p'}^{\mu\nu}$ has the same structure as $\gamma_1^{\mu\nu}$, $g_{\alpha\beta}$ will also have this structure. The same argument leading to the conclusion about the structure of $W_2^{\mu\nu}$ (previous subsection) then reveals that

$$ W_{p+1}^{\mu\nu}\sim H^{l'lm}r^{l'+2k}\,. $$

This in turn leads to

$$ p_{p+1}^{\mu\nu}\sim H^{l'lm}r^{l'+2k+2}\,. $$

We can determine $f_{p+1}^{\mu\nu}$ from $p_{p+1}^{\mu\nu}$ in the same way as we did for the $p=2$ case; and here as there it will lead to $f_{p+1}^{\mu\nu}\sim H^{l'lm}r^{l'+2k}$. Therefore we conclude that $\gamma_{p+1}^{\mu\nu}$ has the same structure

$$ \gamma_{p+1}^{\mu\nu}\sim H^{l'lm}r^{l'+2k} \tag{3.38} $$

as was to be proved.

In terms of the external moments, each term in $\gamma_p^{\mu\nu}$ can be written in the form

$$ \gamma_{pnul}^{\mu\nu}\sim {}^{(u_1)}\mathscr{E}_{A_{l_1}}{}^{(u_2)}\mathscr{E}_{B_{l_2}}\cdots{}^{(u_i)}\mathscr{E}_{C_{l_i}}{}^{(u_1')}\mathscr{B}_{A'_{l'_1}}{}^{(u_2')}\mathscr{B}_{B'_{l'_2}}\cdots{}^{(u_j')}\mathscr{B}_{C'_{l'_j}}X_{D_{l'}}r^{2k}\,, \tag{3.39a} $$

where the superscript (u_i) means d^{u_i}/dt^{u_i}, and where

$$p=i+j\ ,\quad n=\sum_a^i l_a+\sum_b^j l'_b-2p\ ,\quad u=\sum_a^i u_a+\sum_b^j u'_b\ ,$$
$$l=\sum_a^i l_a+\sum_b^j l'_b-2k'\ \text{ with }\ k'=0,1,2,\ldots,\ l'=\sum_a^i l_a+\sum_b^j l'_b+u-2k\ . \tag{3.39b}$$

This general structure tells us two things. One is that the iterative algorithm does not suffer any breakdown at any step if we keep r small compared to $\mathscr{R}$, $\mathscr{L}$, $\mathscr{T}$. Therefore, a fully nonlinear vacuum solution can be generated from the corresponding linearized stationary solution once the gauge is fixed. The second is quite suggestive. That there is no logarithmic term in the expansion suggests that in an appropriate gauge the external expansion might be analytic. This also justifies the use of linearized theory even in a dynamic situation.

IV. EXTERNAL MULTIPOLE MOMENTS

In the Introduction, we mentioned that the curvature-defined external multipole moments $\mathscr{E}_{A_l}$, $\mathscr{B}_{A_l}$, and the moments $\mathscr{E}^{\gamma}_{A_l}$, $\mathscr{B}^{\gamma}_{A_l}$ one straightforwardly reads off the expansion are different at nonlinear orders, but are expressible in terms of each other. We shall return to this issue here and infer from these relations some general properties of the external multipole moments; and we shall give the fully explicit form of the relations between the moments at quadratic order.

A. General form of the relation between the true multipole moments and those of the iterative algorithm and some properties of the moments

Let us denote by $\mathscr{E}^{\gamma}_{A_l}$ and $\mathscr{B}^{\gamma}_{A_l}$ the moments one reads off the fully nonlinear metric density $\mathfrak{g}^{\alpha\beta}$ by the standard procedure (Sec. I) of linearized theory, or equivalently the moments that one puts into $\gamma_1^{\mu\nu}$ to start our iterative algorithm (Sec. III C); and let us denote by $\mathscr{E}_{A_l}$ and $\mathscr{B}_{A_l}$ the true multipole moments as defined covariantly by Eqs. (1.3). Our iterative algorithm will produce a $\mathfrak{g}^{\mu\nu}$ and thence a $g_{\mu\nu}$ which is a sum of terms of the form (3.39), and the Riemann tensor computed from this $g_{\mu\nu}$, when covariantly differentiated and evaluated at $x^i=0$, will produce, via definition (1.3)

$$\mathscr{E}_{A_l}=\mathscr{E}^{\gamma}_{A_l}+\sum_{\{l_i\},\{l'_j\}} e_{K,N}(\mathscr{E}^{\gamma}_{B_{l_1}}\mathscr{E}^{\gamma}_{C_{l_2}}\cdots\mathscr{E}^{\gamma}_{D_{l_k}}\mathscr{B}^{\gamma}_{E_{l'_1}}\cdots\mathscr{B}^{\gamma}_{F_{l'_n}})^{\mathrm{STF}}\ , \tag{4.1a}$$

$$\mathscr{B}_{A_l}=\mathscr{B}^{\gamma}_{A_l}+\sum_{\{l_i\},\{l'_j\}} b_{K,N}(\mathscr{E}^{\gamma}_{B_{l_1}}\mathscr{E}^{\gamma}_{C_{l_2}}\cdots\mathscr{E}^{\gamma}_{D_{l_k}}\mathscr{B}^{\gamma}_{E_{l'_1}}\cdots\mathscr{B}^{\gamma}_{F_{l'_n}})^{\mathrm{STF}}\ . \tag{4.1b}$$

Here

$$e_{K,N}=e(\{l_i\,|\,i=1,\ldots,k\}\ ,\ \{l'_j\,|\,j=1,\ldots,2n\})\ ,$$
$$b_{K,N}=b(\{l_i\,|\,i=1,\ldots,k\}\ ,\ \{l'_j\,|\,j=1,\ldots,2n+1\})\ ,$$

are numerical coefficients whose values we have not computed except at quadratic order (see Sec. IV C below); the sum is over all combinations of l_i, l'_j; and due to the fact that we evaluated (1.3) at $x^i=0$, the indices $B_{l_1},C_{l_2},\ldots,D_{l_k},E_{l'_1},\ldots,F_{l'_n}$ must be such that there are precisely l free indices $a_1a_2\cdots a_l\equiv A_l$ and no contractions between indices before we take the STF part; i.e. $\sum l_i+\sum l'_i=l$ and $B_{l_1}C_{l_2}\cdots D_{l_k}E_{l'_1}\cdots F_{l'_n}$ is a permutation of A_l.

Because γ_1^{00} and γ_1^{0i} are ordinary scalar and 3-vector fields, and because the multipole expansion of γ_1^{00} [Eq. (3.26)] is linear in $\mathscr{E}^{\gamma}_{A_l}$, while that of γ_1^{0i} [Eq. (3.26)] is linear in $\epsilon_{jpq}x_p\mathscr{B}^{\gamma}_{qA_{l-1}}$, $\mathscr{E}^{\gamma}_{A_l}$ must have electriclike parity $(-1)^l$, while $\mathscr{B}^{\gamma}_{A_l}$ (like ϵ_{jpq}) must have magneticlike parity $(-1)^{l+1}$. [Our conventions for defining parity are the same as in Thorne and Hartle;[3] see the paragraph containing their Eq. (2.3).] Similarly, because $R_{0a_10a_2;a_3\cdots a_l}$ and $R_{ija_20;a_3\cdots a_l}$ are ordinary tensor fields, the definitions (1.3) of $\mathscr{E}_{A_l}$ and $\mathscr{B}_{A_l}$ with the crucial ϵ_{a_1ij} in (1.3b) guarantee that $\mathscr{E}_{A_l}$ has electriclike parity $(-1)^l$ and $\mathscr{B}_{A_l}$ has magneticlike parity $(-1)^{l+1}$.

This set of parities implies that in each term of expression (4.1a) for $\mathscr{E}_{A_l}$, there must be an even number of $\mathscr{B}^{\gamma}_{C_l}$'s; and in each term of expression (4.1b) for $\mathscr{B}_{A_l}$ there must be an odd number of $\mathscr{B}^{\gamma}_{C_l}$'s. This explains why in $e_{K,N}$, j runs from 1 to $2n$; while in $b_{K,N}$, from 1 to $2n+1$.

The relations (4.1) can also be inverted to find out $\mathscr{E}^{\gamma}_{A_l}$ and $\mathscr{B}^{\gamma}_{A_l}$ once $\mathscr{E}_{A_l}$ and $\mathscr{B}_{A_l}$ are given. This is done step by step starting from $l=2$. For example

$$\mathscr{E}^{\gamma}_{ab}=\mathscr{E}_{ab}\ ,\quad \mathscr{E}^{\gamma}_{abc}=\mathscr{E}_{abc}\ ,$$
$$\mathscr{E}^{\gamma}_{abcd}=\mathscr{E}_{abcd}-e_{2,0}(\mathscr{E}_{ab}\mathscr{E}_{cd})^{\mathrm{STF}}$$
$$-e_{0,2}(\mathscr{B}_{ab}\mathscr{B}_{cd})^{\mathrm{STF}},\ldots,$$
$$\mathscr{B}^{\gamma}_{ab}=\mathscr{B}_{ab}\ ,\quad \mathscr{B}^{\gamma}_{abc}=\mathscr{B}_{abc}\ ,$$
$$\mathscr{B}^{\gamma}_{abcd}=\mathscr{B}_{abcd}-b_{1,1}(\mathscr{E}_{ab}\mathscr{B}_{cd})^{\mathrm{STF}}\ ,\ldots.$$

It is straightforward to verify that this inversion is unique at all orders; i.e., Eqs. (4.1) determine $\mathscr{E}^{\gamma}_{A_l}$ and $\mathscr{B}^{\gamma}_{A_l}$

uniquely in terms of $\mathscr{E}_{C_l'}$ and $\mathscr{B}_{C_l'}$. With the help of this, we can infer an important property of the external multipole moments $\mathscr{E}_{A_l}$ and $\mathscr{B}_{A_l}$.

First, it is not hard to generalize Suen's[5] Theorems 1, 2 to our case: The metric density generated from this algorithm with our specified choice of $f_p^{\mu\nu}$ is unique up to a time-independent rotation of the spatial coordinates. To prove this theorem, let us consider two de Donder coordinates related by

$$x'^{\mu}=x^{\mu}+\xi^{\mu} .$$

We make the same nonlinearity expansion

$$\xi^{\mu}=\sum_{p=0}^{\infty} G^p \xi_p^{\mu} \tag{4.2}$$

as in Suen.[5] By expanding Suen's equation relating the metric density in two coordinates

$$\mathfrak{g}'^{\mu\nu}(x'^{i})=\frac{1}{L}L^{\mu}{}_{\alpha}L^{\nu}{}_{\beta}\mathfrak{g}^{\alpha\beta}(x^{i}) ,$$

where $L^{\mu}{}_{\alpha}=(\partial x'^{\mu})/(\partial x^{\alpha})$ and $L=|\det(L^{\mu}{}_{\alpha})|$, we obtain to G^0 order

$$\xi_0^{\mu,\nu}+\xi_0^{\nu,\mu}-\eta^{\mu\nu}\xi_{0,\alpha}^{\alpha}=0 . \tag{4.3}$$

This can be readily reduced to the flat spacetime Killing equations

$$\xi_0^{\mu,\nu}+\xi_0^{\nu,\mu}=0 . \tag{4.4}$$

The solutions of Eq. (4.4) are linear combinations of the ten Killing vectors. Because the spatial origin of our coordinate is tied to λ at all times, the boost and translation generators will not contribute to ξ^{μ}. What is left are just the three spatial rotations. Having understood the effects of ξ_0^{μ}, we set it to zero to facilitate the discussion of the G^1 order part of the gauge change. At G^1 order, with ξ_0^{μ} set to zero,

$$\delta\gamma_1^{\mu\nu}\equiv\gamma_1'^{\mu\nu}-\gamma_1^{\mu\nu}=\xi_1^{\mu,\nu}+\xi_1^{\nu,\mu}-\eta^{\mu\nu}\xi_{1,\alpha}^{\alpha} ; \tag{4.5}$$

and to presume de Donder gauge ξ_1^{μ} must be d'Alembertian-free at G^1 order. For $\delta\gamma_1^{\mu\nu}$ to change $\gamma_1^{\mu\nu}$, it must have the same form as $\gamma_1^{\mu\nu}$, i.e., all $l'\le l$ terms of $\delta\gamma_1^{ij}$ and all $l'<l$ terms of $\delta\gamma_1^{0i}$ must vanish. This together with (4.5) and $\Box\xi_1^{\mu}=0$ implies that all $l\ge 2$ terms in $\delta\gamma_1^{\mu\nu}$ vanish. Furthermore, the primed coordinate system must also be LIC, which means that all $l'<2$ terms in $\delta\gamma_1^{\mu\nu}$ must vanish. This reduces ξ_1^{μ}, like ξ_0^{μ}, to only spatial rotations. To facilitate the discussion of the G^2 order part of gauge change we now set $\xi_0^{\mu}=\xi_1^{\mu}=0$; then

$$\delta\gamma_2^{\mu\nu}\equiv\gamma_2'^{\mu\nu}-\gamma_2^{\mu\nu}=\xi_2^{\mu,\nu}+\xi_2^{\nu,\mu}-\eta^{\mu\nu}\xi_{2,\alpha}^{\alpha} . \tag{4.6}$$

For $\delta\gamma_2^{\mu\nu}$ to change $\gamma_2^{\mu\nu}$, it must have the same form as $f_2^{\mu\nu}$ since $f_2^{\mu\nu}$ is the homogeneous part of the solution. The same arguments as above then lead to the conclusion that ξ_2^{μ} also only represents a spatial rotation. This can be repeated up to any p. The result is the theorem we set out to prove.

Since the multipole moments $\mathscr{E}_{A_l}^{\gamma}$, $\mathscr{B}_{A_l}^{\gamma}$ of the iterative algorithm are determined uniquely from the true external moments $\mathscr{E}_{A_l}$, $\mathscr{B}_{A_l}$, it must be true that for any set of external multipole moments $\mathscr{E}_{A_l}$ and $\mathscr{B}_{A_l}$, there corresponds a spacetime, determined uniquely inside a world tube of size $r_{\max}\sim\mathrm{Min}(\mathscr{R},\mathscr{L},\mathscr{T})$. In other words, giving a set of multipole moments on a fiducial world line λ is equivalent to specifying a spacetime inside the world tube surrounding λ.

B. Explicit quadratic-order form of the relation between the moments

Now that we have explored the general structure of the external multipole moments $\mathscr{E}_{A_l}$, $\mathscr{B}_{A_l}$, built up from the expansion coefficients $\mathscr{E}_{A_l}^{\gamma}$, $\mathscr{B}_{A_l}^{\gamma}$ of the metric density, we shall sketch a derivation of the explicit form of the expressions for $\mathscr{E}_{A_l}$, $\mathscr{B}_{A_l}$ in terms of $\mathscr{E}_{A_l}^{\gamma}$, $\mathscr{B}_{A_l}^{\gamma}$ accurate to quadratic order.

The starting point is Eqs. (1.3). The covariant derivatives in the definition (1.3) of $\mathscr{E}_{A_l}$, $\mathscr{B}_{A_l}$ can be expressed explicitly in terms of partial derivatives of the Riemann tensor $R_{\alpha\beta\gamma\delta}$ and connection coefficients $\Gamma^{\alpha}_{\beta\gamma}$; accurate to quadratic order they are

$$R_{0i0j;A_l}=R_{0i0j,A_l}+\text{terms of the form }(\Gamma R_{,\dots})_{,\dots} ; \tag{4.7a}$$

$$\epsilon_{aij}R_{ijb0;A_l}=\epsilon_{aij}R_{ijb0,A_l} + \text{terms of the form }\epsilon(\Gamma R_{,\dots})_{,\dots} . \tag{4.7b}$$

The Γ-correction terms are straightforward to evaluate to the desired quadratic order, since they involve $\Gamma^{\alpha}_{\beta\gamma}$ and $R_{\alpha\beta\gamma\delta}$ only at the linear order. Thus, we shall not discuss them in detail. The first terms in Eqs. (4.7a) and (4.7b), by contrast, involve $R_{\alpha\beta\gamma\delta}$ at quadratic order ($p=2$) and thus require some discussion. Fortunately, their evaluation is simplified by the fact that, because the external moments are evaluated at $x^i=0$, pieces of $R_{\alpha\beta\gamma\delta}$ with the form $((n<l)\text{-pole})r^l$ will not contribute to the final answer; we shall ignore such pieces in the derivations below.

The metric accurate to order $p=2$ is[20]

$$g^{\mu\nu}=\sqrt{-g}\,\mathfrak{g}^{\mu\nu}=\eta^{\mu\nu}-(\bar{h}^{\mu\nu}-\tfrac{1}{2}\bar{h}\eta^{\mu\nu})-\tfrac{1}{2}\bar{h}\bar{h}^{\mu\nu}+\tfrac{1}{8}\eta^{\mu\nu}(\bar{h}^2+2\bar{h}^{\alpha\beta}\bar{h}_{\alpha\beta}) , \tag{4.8}$$

where

$$\bar{h}^{\mu\nu}=\eta^{\mu\nu}-\mathfrak{g}^{\mu\nu} , \quad \bar{h}=\eta_{\mu\nu}\bar{h}^{\mu\nu} .$$

This can be inverted to give

$$g_{\mu\nu}=\eta_{\mu\nu}+\bar{h}_{\mu\nu}-\tfrac{1}{2}\eta_{\mu\nu}\bar{h}+\bar{h}_{\mu}{}^{\alpha}\bar{h}_{\alpha\nu}-\tfrac{1}{2}\bar{h}\bar{h}_{\mu\nu}+\tfrac{1}{8}\eta_{\mu\nu}(\bar{h}^2-2\bar{h}^{\alpha\beta}\bar{h}_{\alpha\beta}) . \tag{4.9}$$

Here $\bar{h}^{\mu\nu}$ consists of a linear part $\gamma_1^{\mu\nu}$ given by Eqs. (3.26) plus quadratic corrections $\gamma_2^{\mu\nu}=p_2^{\mu\nu}+f_2^{\mu\nu}$ [Eq. (3.31) and associated discussion]:

$$\bar{h}^{\mu\nu}=\gamma_1^{\mu\nu}+p_2^{\mu\nu}+f_2^{\mu\nu} . \tag{4.10}$$

To simplify the calculations, all $r^l((n<l)$-pole) terms will be dropped. By virtue of the forms of $\gamma_1^{\mu\nu}$ and of the $W_2^{\mu\nu}$ constructed from it, $p_2^{\mu\nu}$ can be chosen to consist solely of such terms and thus can be ignored. From this fact plus the traceless nature of γ_1^{ij} we conclude that

$$\bar{h}=-\bar{h}^{00}+\delta_{ij}f_2^{ij} .$$

Furthermore, accurate to quadratic order in p,

$$\bar{h}_{\alpha\beta}\bar{h}^{\alpha\beta}=(\bar{h}^{00})^2-2\bar{h}^{0a}\bar{h}^{0a} .$$

These relations reduce Eqs. (4.8), (4.9) to

$$g^{\mu\nu}=\eta^{\mu\nu}-\bar{h}^{\mu\nu}-\tfrac{1}{2}\,\bar{h}^{00}\eta^{\mu\nu}+\tfrac{1}{2}\,\delta^{ij}f_{ij}\eta^{\mu\nu}+\tfrac{1}{2}\,\bar{h}^{00}\bar{h}^{\mu\nu}+\tfrac{1}{8}\,\eta^{\mu\nu}[(\bar{h}^{00})^2-2\bar{h}^{0a}\bar{h}^{0a}] , \tag{4.11}$$

$$g_{\mu\nu}=\eta_{\mu\nu}+\bar{h}_{\mu\nu}+\tfrac{1}{2}\,\bar{h}^{00}\eta_{\mu\nu}-\tfrac{1}{2}\,\delta^{ij}f_{ij}\eta_{\mu\nu}+\bar{h}_{\mu}^{\alpha}\bar{h}_{\alpha\nu}+\tfrac{1}{2}\,\bar{h}^{00}\bar{h}_{\mu\nu}-\tfrac{1}{8}\,\eta_{\mu\nu}[(\bar{h}^{00})^2-2\bar{h}^{0a}\bar{h}^{0a}] . \tag{4.12}$$

The Riemann curvature tensor, as obtained from this expression for the metric, is

$$R_{0i0j}=\psi_{,ij}+3(\psi^2)_{,ij}-\tfrac{1}{4}\,(\mathbf{A}^2)_{,ij}-\tfrac{1}{4}\,H_iH_j+g_ig_j-\tfrac{1}{4}\,(\delta^{ab}f_{ab})_{,ij}+O(G^3) , \tag{4.13a}$$

$$\epsilon_a{}^{ij}R_{ijb0}=-H_{a,b}-2\psi H_{a,b}+6H_ag_b-2\epsilon_{aij}A^ig^j{}_{,b}+O(G^3) , \tag{4.13b}$$

$$R_{iajb}=\delta_{ib}g_{j,a}-\delta_{ij}g_{b,a}+\delta_{aj}g_{b,i}-\delta_{ab}g_{j,i}+O(G^2) , \tag{4.13c}$$

where

$$\psi=-\tfrac{1}{4}\,\gamma^{00}_{1(l-2)0l} , \quad A^j=-\gamma^{0j}_{1(l-2)0l} , \quad g_i=-\psi_{,i} , \quad H_i=\epsilon_i{}^{ab}A_{b,a} . \tag{4.14}$$

We need $f_2\equiv\delta_{ab}f_2^{ab}$ in order to compute $\mathscr{E}_{A_l}$. As may be seen from Eq. (3.37c), only ${}^1P_{l-1,lm}(t)$ contributes to the trace of the gauge-correcting term f_2. A simple dimensional analysis plus parity considerations tells that only p_2^{ij} contributes to ${}^1P_{l-1,lm}(t)$. It is not too hard to find p_2^{ij} from W_2^{ij}. But further simplification is still possible. Since we only want $r^l(l$-pole) terms in f_2, we may drop the time derivative and trace terms in W_2^{ij}; this results in

$$W_2^{ij}=-4g^ig^j-H^iH^j . \tag{4.15}$$

By substituting Eqs. (3.26), (4.14) into Eq. (4.15), we can easily find a particular integral p_2^{ij} for γ_2^{ij}. The gauge term determined from it [with all $r^l((n<l)$-pole) terms dropped] is

$$\begin{aligned} f_2&=\delta_{ij}f_2^{ij}\\ &=\sum_{l'=2}^{l-2}\frac{12}{(2l-1)l(l-l'-1)(l'-1)}\left[\mathscr{E}^{\gamma}_{A_{l-l'}}\mathscr{E}^{\gamma}_{A_{l'}}+\frac{(l'+1)(l-l'+1)}{9}\mathscr{B}^{\gamma}_{A_{l-l'}}\mathscr{B}^{\gamma}_{A_{l'}}\right]X_{A_l} . \end{aligned} \tag{4.16}$$

Now we can substitute Eqs. (3.26), (4.7), (4.14), (4.16) into Eqs. (1.3). After an extremely tedious but straightforward calculation, we obtain

$$\begin{aligned} \mathscr{E}_{A_l}=\mathscr{E}^{\gamma}_{A_l}&+\sum_{l'=2}^{l-2}\frac{l(l-1)}{l'(l'-1)(l-l'-1)}\left[\frac{3}{l-l'}-\frac{l'(l-2)}{l(l-1)(2l-1)}+\frac{2(l-l'-1)}{l(l'+1)}\right](\mathscr{E}^{\gamma}_{A_{l-l'}}\mathscr{E}^{\gamma}_{A_{l'}})^{\mathrm{STF}}\\ &+\sum_{l'=2}^{l-2}\frac{l(l-1)(l'+1)(l-l'+1)}{9(l'-1)(l-l'-1)}\left[\frac{1}{(l-l'+1)(l'+1)}-\frac{2}{ll'}-\frac{l-2}{l(l-1)(2l-1)}\right](\mathscr{B}^{\gamma}_{A_{l-l'}}\mathscr{B}^{\gamma}_{A_{l'}})^{\mathrm{STF}}+O(G^3) , \end{aligned} \tag{4.17a}$$

$$\begin{aligned} \mathscr{B}_{A_l}=\mathscr{B}^{\gamma}_{A_l}&+\frac{2}{l+1}\sum_{l'=2}^{l-2}\frac{1}{(l'-1)(l-l'-1)}\\ &\times\left[\frac{l-1}{l'}+\frac{l-l'+2}{l+1}+\frac{l'-1}{(l-l'-1)(l+1)}+\frac{(l+l')(l-l'+1)(l-l'-1)}{l'(l'+1)(l+1)}\right](\mathscr{B}^{\gamma}_{A_{l-l'}}\mathscr{E}^{\gamma}_{A_{l'}})^{\mathrm{STF}}\\ &+O(G^3) . \end{aligned} \tag{4.17b}$$

These, then, are the relations between the moments $\mathscr{E}^{\gamma}_{A_l}$, $\mathscr{B}^{\gamma}_{A_l}$ of the de Donder coordinate iterative algorithm (Sec. III) and the true, curvature-defined moments $\mathscr{E}_{A_l}$, $\mathscr{B}_{A_l}$.

ACKNOWLEDGMENTS

The author is grateful to Professor Kip S. Thorne for suggesting this problem to him. He thanks Professor Thorne for many helpful suggestions and stimulating discussions during the course of this work and in preparing this manuscript. He also thanks Wai-Mo Suen for many useful discussions. This work was supported in part by the National Science Foundation under Grant No. AST82-14126.

[1]C. W. Misner, K. S. Thorne, and J. A. Wheeler, *Gravitation* (Freeman, San Francisco, 1973).
[2]K. S. Thorne, Rev. Mod. Phys. **52**, 299 (1980).
[3]K. S. Thorne and J. B. Hartle, Phys. Rev. D **31**, 1815 (1985).
[4]X.-H. Zhang, Phys. Rev. D **31**, 3130 (1985).
[5]W.-M. Suen, Phys. Rev. D (to be published).
[6]R. Geroch, J. Math. Phys. **11**, 2580 (1970); R. O. Hansen, *ibid.* **15**, 46 (1974).
[7]A. I. Janis and E. T. Newman, J. Math. Phys. **6**, 902 (1965); D. J. Lamb, *ibid.* **7**, 458 (1966).
[8]W. Simon and R. Beig, J. Math. Phys. **24**, 1163 (1983); R. Beig and W. Simon, Proc. R. Soc. London **A376**, 333 (1981).
[9]Y. Gürsel, Gen. Relativ. Gravit. **15**, 737 (1983).
[10]P. Kundu, J. Math. Phys. **22**, 2006 (1981).
[11]B. C. Xanthopoulos, J. Phys. A **12**, 1025 (1979); R. Beig and W. Simon, Commun. Math. Phys. **78**, 75 (1980).
[12]L. Blanchet and T. Damour (unpublished); also L. Blanchet (unpublished).
[13]B. L. Schumaker and K. S. Thorne, Mon. Not. R. Astron. Soc. **203**, 457 (1983); L. S. Finn, Class. Quantum Gravit. **2**, 381 (1985).
[14]K. S. Thorne and Y. Gürsel, Mon. Not. R. Astron. Soc. **205**, 809 (1983).
[15]S. Weinberg, Phys. Rev. Lett. **40**, 223 (1978); F. Wilczek, *ibid.* **40**, 279 (1978); J. E. Kim, *ibid.* **43**, 103 (1979); M. Dine, W. Fischler, and M. Srednicki, Phys. Lett. **104B**, 199 (1981).
[16]W.-T. Ni and M. Zimmermann, Phys. Rev. D **17**, 1473 (1978).
[17]F. K. Manasse and C. W. Misner, J. Math. Phys. **4**, 735 (1963); see also Ref. 1, Eq. (13.73).
[18]See, for example, Sec. 7.4 in S. Weinberg, *Gravitation and Cosmology* (Wiley, New York, 1972), but notice that the d'Alembertian there lives in curved space $\Box^2 \equiv g^{\mu\nu}\nabla_\mu\nabla_\nu$ while in this paper $\Box \equiv \eta^{\mu\nu}\partial_\mu\partial_\nu$.
[19]J. Mathews, *Tensor Spherical Harmonics* (California Institute of Technology, Pasadena, Calif., 1981).
[20]K. S. Thorne and S. J. Kovács, Astrophys. J. **200**, 245 (1975).

Chapter III

HIGHER-ORDER CORRECTIONS TO THE LAWS OF MOTION AND PRECESSION FOR BLACK HOLES AND OTHER BODIES

(Originally appeared in *Phys. Rev.* D31, 3130(1985))

PHYSICAL REVIEW D VOLUME 31, NUMBER 12 15 JUNE 1985

Higher-order corrections to the laws of motion and precession for black holes and other bodies

Xiao-He Zhang
Theoretical Astrophysics 130-33, California Institute of Technology, Pasadena, California 91125
(Received 2 January 1985)

In a recent paper, Thorne and Hartle have derived laws of motion and precession for black holes and other bodies. Using two different methods, higher-order corrections to those laws are derived here: a time change of the body's mass-energy due to coupling of the time derivatives of the body's quadrupole moments to the external curvature; a force due to coupling of the time derivatives of the body's quadrupole moments to the external curvature and coupling of the body's quadrupole moments to the gradient of the external curvature; and a torque due to coupling of the body's octopole moments to the gradient of the external curvature.

I. INTRODUCTION AND SUMMARY

Recently, Thorne and Hartle[1] have derived laws of motion and precession for black holes and other bodies. Their analysis characterizes the body of interest by three parameters: $M=$(mass), $L=$(size), and $T=$(time scale for changes of multipole moments); and it characterizes the external universe, through which the body moves, by three other parameters: $\mathscr{R}=$(radius of curvature along body's world line), $\mathscr{L}=$(inhomogeneity scale of curvature), and $\mathscr{T}=$(time scale for changes in curvature). Their analysis relies on the approximations that the body's moments change slowly and the body is well isolated:

$$T\gg L\gtrsim M\ ,\quad \mathscr{R}\gg L\ ,\quad \mathscr{L}\gg L\ ,\quad \mathscr{T}\gg L\ , \tag{1}$$

and on the assumption that there is negligible gravitating matter in a "buffer region" $L\ll r\ll\mathscr{L}$ surrounding the body. The external universe's curvature in the buffer region is then nearly constant and satisfies the vacuum Einstein equation. Thorne and Hartle set up in this buffer region a coordinate system which is as nearly Lorentz as the spacetime curvature permits, and in which the body is at rest at time $t=0$; and in this "local asymptotic rest frame of the body" they compute the effects of the external universe on the body's motion.

The resulting Thorne-Hartle laws of motion and precession, written in terms of components in the body's local asymptotic rest frame, take the following form to leading order in the small dimensionless parameters L/T, $L/\mathscr{R}$, $L/\mathscr{L}$, and $L/\mathscr{T}$, and a similar set of parameters with L replaced by M:

$$\frac{dM}{dt}\ll\frac{ML}{\mathscr{R}^2}\ , \tag{2a}$$

$$\frac{dP^i}{dt}=-\mathscr{S}^a\mathscr{B}_a{}^i=O\left[\frac{ML}{\mathscr{R}^2}\right]\ , \tag{2b}$$

$$\frac{d\mathscr{S}^i}{dt}=-\epsilon^i{}_{ab}\mathscr{I}^a{}_c\mathscr{E}^{cb}-\tfrac{4}{3}\epsilon^i{}_{ab}\mathscr{S}^a{}_c\mathscr{B}^{bc}=O\left[\frac{ML^2}{\mathscr{R}^2}\right] \tag{2c}$$

[Eqs. (1.9) of Thorne and Hartle,[1] denoted henceforth as Eqs. (TH,1.9)]. Here P^j, $\mathscr{S}^j$, $\mathscr{I}^{jk}$, and $\mathscr{S}^{jk}$ are the body's momentum, spin, and mass and current quadrupole moments; $\epsilon^i{}_{ab}$ is the flat-space Levi-Cività tensor (used to form vector cross products); and $\mathscr{E}^{jk}$ and $\mathscr{B}^{jk}$ are the electric and magnetic parts of the Riemann curvature tensor of the external universe. Summation over repeated indices (which are always spatial, $i=1,2,3$) is assumed; and indices on the multipole moments are raised and lowered with the three-dimensional flat metric (Kronecker delta). Thorne and Hartle also discuss at some length the procedure for converting these laws of motion into equations of motion for any given situation satisfying Eqs. (1).

The purpose of this paper is to derive all corrections to the laws of motion and precession (2) with magnitudes

$$\left[\frac{dM}{dt}\right]_{\rm corr}\gtrsim\frac{ML^2}{\mathscr{R}^2(\mathscr{L}\text{ or }\mathscr{T}\text{ or }T)}\ ,$$
$$\left[\frac{dP^i}{dt}\right]_{\rm corr}\gtrsim\frac{ML^2}{\mathscr{R}^2(\mathscr{L}\text{ or }\mathscr{T}\text{ or }T)}\ , \tag{3}$$
$$\left[\frac{d\mathscr{S}^i}{dt}\right]_{\rm corr}\gtrsim\frac{ML^3}{\mathscr{R}^2(\mathscr{L}\text{ or }\mathscr{T}\text{ or }T)}\ .$$

Those corrections turn out to be

$$\left[\frac{dM}{dt}\right]_{\rm corr}=-\tfrac{1}{2}\mathscr{E}_{ab}\dot{\mathscr{I}}^{ab}-\tfrac{2}{3}\mathscr{B}_{ab}\dot{\mathscr{S}}^{ab}\ , \tag{4a}$$

$$\left[\frac{dP^i}{dt}\right]_{\rm corr}=-\tfrac{1}{2}\mathscr{E}^i{}_{ab}\mathscr{I}^{ab}-\tfrac{8}{9}\mathscr{B}^i{}_{ab}\mathscr{S}^{ab}$$
$$+\tfrac{4}{9}\epsilon^i{}_{ab}\dot{\mathscr{E}}^a{}_c\mathscr{S}^{bc}+\tfrac{1}{3}\epsilon^i{}_{ab}\mathscr{B}^a{}_c\dot{\mathscr{I}}^{bc}\ , \tag{4b}$$

$$\left[\frac{d\mathscr{S}^i}{dt}\right]_{\rm corr}=\tfrac{1}{2}\epsilon^i{}_{ab}\mathscr{E}^{acd}\mathscr{I}^b{}_{cd}+\epsilon^i{}_{ab}\mathscr{B}^{acd}\mathscr{S}^b{}_{cd}\ . \tag{4c}$$

Here overdots denote time derivatives. $\dot{\mathscr{I}}^{ab}\equiv d\mathscr{I}^{ab}/dt$; $\mathscr{I}_{abc}$ and $\mathscr{S}_{abc}$ are the body's mass octopole and current octopole moments;[2] and $\mathscr{E}_{abc}$ and $\mathscr{B}_{abc}$ are the electric-type and magnetic-type octopole moments of the external universe's curvature, i.e., they characterize the spatial gra-

dient of that curvature.[1,3] Thorne and Hartle[1] discuss, but do not derive, the most important of the above corrections [both terms in (4a), which are the leading nonzero contributions to dM/dt; and the first term in (4b), which in many realistic situations will dominate over the lower-order term (2b) and thus will be the leading contribution to dP^i/dt].

The interpretation of the laws of motion (2) and (4) involves a number of subtleties which are discussed by Thorne and Hartle. One of these subtleties is crucial for our derivation, so we review it here: The nonlinear interaction of the body's curvature and the external curvature cause the body's mass M, momentum P^i, and spin $\mathcal{S}^i$ to be slightly ambiguous, i.e., to be uncertain by amounts

$$\Delta M \sim ML^2/\mathcal{R}^2 , \quad \Delta P^i \sim ML^2/\mathcal{R}^2 , \quad \Delta \mathcal{S}^i \sim M^3L/\mathcal{R}^2 \tag{5}$$

[Eq. (TH,1.8)]. This means that we can obtain physically meaningful changes of M, P^i, and $\mathcal{S}^i$ by integrating the laws of motion (2) and (4) only if we integrate over a time long enough that the changes exceed the uncertainties (5). Correspondingly, dM/dt, dP^i/dt, and $d\mathcal{S}^i/dt$ are actually ambiguous. Any set of formulas that give the same time-integrated changes to within the uncertainties of Eq. (5) are just as good as Eqs. (2) and (4). This means, in particular, that one can add to dM/dt [Eqs. (2a) and (4a)] any multiple of $(d/dt)(\mathcal{E}_{ab}\mathcal{S}^{ab})$ or $(d/dt)(\mathcal{B}_{ab}\mathcal{S}^{ab})$, and can add to dP^i/dt [Eqs. (2b) and (4b)] any multiple of $(d/dt)(\epsilon^i{}_{ab}\mathcal{E}^a{}_c\mathcal{S}^{bc})$ or $(d/dt)(\epsilon^i{}_{ab}\mathcal{B}^a{}_c\mathcal{S}^{bc})$—or equivalently, one can replace the terms in Eqs. (4a) and (4b) involving time derivatives by averages, $\langle\ \rangle$, of those terms over a few internal time scales, (few)$\times T$ [cf. Eq. (TH,1.15)].

The remainder of this paper consists of two derivations of the corrections (4) to the laws of motion and precession. The first derivation, based on the techniques of Thorne and Hartle,[1] is given in Sec. II. This derivation is valid for any body, including a black hole, that satisfies the constraints of Eqs. (1). The second derivation, given in Sec. III, is restricted to the special case of an arbitrary body with absolutely negligible self-gravity. It serves as a check of the first derivation and provides additional insight into the physical origins of the energy changes (4a), forces (4b), and torques (4c).

II. DERIVATION FOR AN ARBITRARY BODY

We begin our derivation from the standard formulas

$$\dot{M} = -\oint (-g)t^{0j}d^2S_j , \tag{6a}$$

$$\dot{P}^i = -\oint (-g)t^{ij}d^2S_j , \tag{6b}$$

$$\dot{\mathcal{S}}^i = -\oint (-g)\epsilon^i{}_{jk}x^j t^{kl}d^2S_l , \tag{6c}$$

where $t^{\mu\nu}$ is the Landau-Lifshitz pseudotensor and the surface integral is over a closed two-surface in the buffer region. (See Thorne and Hartle[1] for a discussion of the applicability of these formulas to this problem.) In these formulas, one could equally well use some other energy-momentum pseudotensor, provided it participates in conservation laws of the type discussed in Sec. 20.3 of MTW.[4] In that case, the time changes could be different from those in Eqs. (4), but the differences could only be as great as the uncertainties discussed in Sec. I.

Since we are only interested in the nonlinear couplings between the external universe and the body moving through it, the metric we will use is the sum of that for a single body and that for the external universe, with the spatial origin attached at time $t=0$ to the world line of the center of the body. To further simplify the calculation, we notice that only those coupling terms with the same temporal and spatial transformation properties as the left-hand side of Eqs. (6) can appear and survive the surface integral. Take $\dot{M}$ as an example. Under time reversal, $\dot{M}\to -\dot{M}$; under a spatial reflection, $\dot{M}\to\dot{M}$. At the order $ML^2/\mathcal{R}^2T$ and $ML^2/\mathcal{R}^2\mathcal{T}$ [no scalar can be constructed if T (or $\mathcal{T}$) is replaced by $\mathcal{L}$ or $\mathcal{R}$], the transformation properties of the only possible terms are

	$\dot{M}$	$\mathcal{E}_{ab}\dot{\mathcal{S}}^{ab}$ or $\dot{\mathcal{E}}_{ab}\mathcal{S}^{ab}$	$\mathcal{B}_{ab}\dot{\mathcal{S}}^{ab}$ or $\dot{\mathcal{B}}_{ab}\mathcal{S}^{ab}$	$\mathcal{B}_{ab}\dot{\mathcal{S}}^{ab}$ or $\dot{\mathcal{B}}_{ab}\mathcal{S}^{ab}$	$\mathcal{E}_{ab}\dot{\mathcal{S}}^{ab}$ or $\dot{\mathcal{E}}_{ab}\mathcal{S}^{ab}$
time reversal	−	−	−	+	+
spatial reflection	+	+	+	−	−

Therefore only $\mathcal{E}_{ab}\dot{\mathcal{S}}^{ab}$, $\dot{\mathcal{E}}_{ab}\mathcal{S}^{ab}$, $\mathcal{B}_{ab}\dot{\mathcal{S}}^{ab}$, and $\dot{\mathcal{B}}_{ab}\mathcal{S}^{ab}$ will appear in the final answer (for a more detailed discussion, see Thorne and Hartle,[1] Sec. III E):

$$\begin{aligned}\dot{M} &= \mu_1\mathcal{E}_{ab}\dot{\mathcal{S}}^{ab} + \mu_2\dot{\mathcal{E}}_{ab}\mathcal{S}^{ab} + \mu_3\mathcal{B}_{ab}\dot{\mathcal{S}}^{ab} + \mu_4\dot{\mathcal{B}}_{ab}\mathcal{S}^{ab} \\ &= (\mu_1-\mu_2)\mathcal{E}_{ab}\dot{\mathcal{S}}^{ab} + (\mu_3-\mu_4)\mathcal{B}_{ab}\dot{\mathcal{S}}^{ab} + (\text{negligible total time derivatives}) .\end{aligned} \tag{7a}$$

Similarly,

$$\dot{P}^i = \mu_5\mathcal{E}^i{}_{ab}\mathcal{S}^{ab} + \mu_6\mathcal{B}^i{}_{ab}\dot{\mathcal{S}}^{ab} + (\mu_7-\mu_8)\epsilon^i{}_{ab}\mathcal{E}^a{}_c\dot{\mathcal{S}}^{bc} + (\mu_9-\mu_{10})\epsilon^i{}_{ab}\mathcal{B}^a{}_c\dot{\mathcal{S}}^{bc} , \tag{7b}$$

$$\dot{\mathcal{S}}^i = \mu_{11}\epsilon^i{}_{ab}\mathcal{E}^{acd}\mathcal{S}^b{}_{cd} + \mu_{12}\epsilon^i{}_{ab}\mathcal{B}^{acd}\mathcal{S}^b{}_{cd} . \tag{7c}$$

Our task now reduces to the calculation of these μ's. The linearized, truncated, and trace-reversed metric perturbation needed for this calculation is (see Thorne[2] for the metric of the central body; see Zhang[3] for the metric of the external universe)

$$\bar{h}^{00}\equiv -4\psi=6\frac{\mathscr{I}_{ab}x^a x^b}{r^5}+10\frac{\mathscr{I}_{abc}x^a x^b x^c}{r^7}-2\mathscr{E}_{ab}x^a x^b-\tfrac{2}{3}\mathscr{E}_{abc}x^a x^b x^c\ , \tag{8a}$$

$$\bar{h}^{0j}\equiv -A^j=4\frac{\epsilon^j{}_{pq}x^q\mathscr{S}^p{}_l x^l}{r^5}+\frac{15}{2}\frac{\epsilon^j{}_{pq}x^q\mathscr{S}^p{}_{bc}x^b x^c}{r^7}+2\frac{\dot{\mathscr{I}}^j{}_a x^a}{r^3}$$
$$+\tfrac{2}{3}\epsilon^j{}_{pq}x^q\mathscr{B}^p{}_l x^l+\tfrac{1}{3}\epsilon^j{}_{pq}x^q\mathscr{B}^p{}_{bc}x^b x^c+\tfrac{10}{21}(\dot{\mathscr{E}}_{ab}x^a x^b x^j-\tfrac{2}{5}r^2\dot{\mathscr{E}}^j{}_a x^a)\ , \tag{8b}$$

$$\bar{h}^{ij}=\frac{8}{3}\frac{\epsilon_{pq}{}^{(i}\dot{\mathscr{S}}^{j)p}x^q}{r^3}+\tfrac{5}{21}(x^{(i}\epsilon^{j)}{}_{pq}\dot{\mathscr{B}}^q{}_l x^p x^l-\tfrac{1}{5}r^2\epsilon_{pq}{}^{(i}\dot{\mathscr{B}}^{j)q}x^p)\ . \tag{8c}$$

Inserting Eqs. (8) into MTW (Ref. 4) Eq. (20.22) with $\bar{g}^{\mu\nu}=\eta^{\mu\nu}-\bar{h}^{\mu\nu}$, and keeping only those terms that will contribute to the final answer, we obtain

$$16\pi(-g)t^{0k}=-A^k{}_{,j}\dot{A}^j-12\dot{\psi}g^k+4\epsilon^k{}_{ab}H^a g^b$$
$$-2A_{a,b}\bar{h}^{a[k,b]}\ , \tag{9a}$$

$$16\pi(-g)t^{ij}=4g^i g^j+H^i H^j-8\dot{A}^{(i}g^{j)}$$
$$+\tfrac{1}{2}\delta^{ij}(8\mathbf{g}\cdot\dot{\mathbf{A}}-4\mathbf{g}^2-\mathbf{H}^2)\ , \tag{9b}$$

where $\mathbf{g}$ is the gravitational acceleration and $\mathbf{H}$ is the gravitational analog of the magnetic field (three-dimensional notation is used here):

$$\mathbf{g}=-\nabla\psi\ ,\quad \mathbf{H}=\nabla\times\mathbf{A}\ . \tag{10}$$

In Eq. (9b) the $\mathbf{A}$ terms are needed only for the calculation of $\dot{P}^i$.

Now we can insert the necessary parts of Eqs. (8) into Eqs. (9a) and (9b) separately, and perform the surface integrations in Eqs. (6). The results, after dropping negligible total time derivative terms, are Eqs. (4) above. Because in this derivation we only need the metric in the buffer region where it is linearized, the results are valid for any body, including a black hole, provided that the conditions of Eq. (1) are satisfied.

III. DERIVATION FOR A TEST BODY

In this section, another derivation of Eqs. (4) will be presented. The basic idea is local energy-momentum conservation. The purpose of doing this is twofold. First, it can serve as a check of the previous derivation. Second, in the derivation of Sec. II the physical meanings were almost buried in the complicated, though straightforward, algebra; and the physics may be much clearer in this calculation.

Our derivation will be restricted to a body that has totally negligible self-gravity and is made of "normal" material, for which $|T^{ab}|\ll T^{00}$ in the body's center-of-mass frame. The mass, momentum, and spin of this body are

$$M=\int T^{00}(-g)d^3x\ , \tag{11a}$$

$$P^i=\int T^{0i}(-g)d^3x\ , \tag{11b}$$

$$\mathscr{S}^i=\int\epsilon^i{}_{pq}x^p T^{0q}(-g)d^3x\ , \tag{11c}$$

where $T^{\mu\nu}$ is the energy-momentum tensor for the body alone, and g is the determinant of the metric for the external universe alone. The factor $(-g)$ could equally well be $(-g)^n$ for any n of order unity; by changing the power of $(-g)$ one changes M, P^i, and $\mathscr{S}^i$ by amounts of order their uncertainties [Eqs. (5)]. As in Sec. II our calculation is performed in a coordinate system that is as nearly Lorentz and mass centered as possible, and in which the body is momentarily (at $t=0$) at rest: $P^i=0$ and $\mathscr{S}^i$ = (mass dipole moment) $=0$ at $t=0$.

By taking the time derivatives of Eqs. (11) and using the fact that $T^{\mu\nu}=0$ outside the body, we obtain

$$\dot{M}=\int[T^{0\nu}(-g)]_{,\nu}d^3x\ ,\quad \dot{P}^i=\int[T^{i\nu}(-g)]_{,\nu}d^3x\ ,$$
$$\dot{\mathscr{S}}^i=\int\epsilon^i{}_{pq}x^p[T^{\nu q}(-g)]_{,\nu}d^3x\ .$$

By combining with the local law of energy-momentum conservation

$$T^{\mu\nu}{}_{;\nu}=\frac{1}{\sqrt{-g}}(T^{\mu\nu}\sqrt{-g}\,)_{,\nu}+\Gamma^\mu_{\nu\alpha}T^{\nu\alpha}=0$$

or equivalently,

$$[T^{\mu\nu}(-g)]_{,\nu}=-\Gamma^\mu_{\alpha\beta}T^{\alpha\beta}+2(\psi T^{\mu\alpha})_{,\alpha}$$

and removing negligible time derivatives, vanishing surface integrals, and other terms that are negligible, we bring these equations into the form

$$\dot{M}=\int(g_a-\dot{A}_a)T^{0a}d^3x\ , \tag{12a}$$

$$\dot{P}^i=\int[(g^i-\dot{A}^i)T^{00}+\epsilon^i{}_{ab}T^{0a}H^b+g^i T^a{}_a]d^3x\ , \tag{12b}$$

$$\dot{\mathscr{S}}^i=\int\epsilon^i{}_{ab}x^a[(g^b-\dot{A}^b)T^{00}+\epsilon^b{}_{pq}T^{0p}H^q]d^3x\ . \tag{12c}$$

The $g^i T^a{}_a$ term in Eq. (12b) is not discarded because the $g^i T^{00}$ integral, which one might have thought to be dominant, gives as its formally leading piece $\mathscr{E}^i{}_a\mathscr{S}^a$, which vanishes in our mass-centered coordinates ($\mathscr{S}^a=0$).

The physical meanings are rather clear here. Take $\dot{M}$

as an example. In the Newtonian limit, $T^{0i}=\rho v^i$, Eq. (12a) reduces to

$$\dot{M}=\int (g_a-\dot{A}_a)\rho v^a d^3x=\int F_a v^a d^3x \ ,$$

where $F_a=\rho(g_a-\dot{A}_a)$ is the gravitational force per unit volume exerted on the body by the external universe. Thus in the Newtonian limit, the total mass-energy of an object changes because the external universe does "$\mathbf{F}\cdot\mathbf{v}$" work on various parts of it. This is just what we would naively expect. We can understand $\dot{P}^i$ and $\dot{\mathscr{S}}^i$ in a similar fashion.

In order to express the $\dot{M}$, $\dot{P}^i$, and $\dot{\mathscr{S}}^i$ of Eqs. (12) in terms of the multipole moments of the body and the universe, we can express g_i, A_i, and H_i in terms of the external universe's moments [Eqs. (8) and (10)] and then perform the integrations using the definitions of the body's multipole moments[2]

$$\mathscr{I}_{A_l}\equiv\left[\int T^{00}x_{a_1}x_{a_2}\cdots x_{a_l}d^3x\right]^{\rm STF} ,$$

$$\mathscr{S}_{A_l}\equiv\left[\int \epsilon_{a_1pq}x^p T^{0q}x_{a_2}x_{a_3}\cdots x_{a_l}d^3x\right]^{\rm STF} .$$

Here $(\cdots)^{\rm STF}$ means take the symmetric, trace-free part. The result is the laws of motion (2) and (4). Because the actual calculation is not so straightforward as in the last section, we give a few of its details in an appendix.

ACKNOWLEDGMENTS

I am grateful to Professor K. S. Thorne for suggesting this problem to me. His suggestions and many helpful discussions with him were crucial in the calculations of Sec. III and the preparation of this paper. It is also a pleasure to thank W.-M. Suen and other members of the Paradigm Society at Caltech for some useful discussions. This work was supported in part by the National Science Foundation Grant No. AST82-14126.

APPENDIX

In this appendix we will carry out the calculations leading to Eqs. (4) from Eqs. (12). First we define a few quantities that will be used later:

$$I_{A_l}\equiv\int T^{00}x_{A_l}d^3x \ , \tag{A1a}$$

$$J^a{}_{A_l}\equiv\int T^{0a}x_{A_l}d^3x \ , \tag{A1b}$$

$$K^{ab}{}_{A_l}\equiv\int T^{ab}x_{A_l}d^3x \ , \tag{A1c}$$

where $x_{A_l}\equiv x_{a_1}x_{a_2}\cdots x_{a_l}$. From these definitions, the finiteness of the body, and the law of energy-momentum conservation $T^{\alpha\beta}{}_{,\beta}=0$ (with gravitational effects here neglected), we can find a few very useful relations:

$$J^{ab}=\tfrac{1}{2}\dot{I}^{ab}+J^{[ab]} \ , \tag{A2a}$$

$$J^{abc}=\tfrac{1}{3}\dot{I}^{abc}+\tfrac{2}{3}J^{[ab]c}+\tfrac{2}{3}J^{[ac]b} \ , \tag{A2b}$$

$$K^{cca}=\dot{J}^{cca}-\tfrac{1}{2}\dot{J}^{acc} \ . \tag{A2c}$$

Here square brackets denote antisymmetrization, and indices are raised and lowered with the three-dimensional flat metric (Kronecker delta).

Using Eqs. (A1) and (A2) we can rewrite Eqs. (12) as follows:

$$\dot{M}=\tfrac{1}{2}\dot{\mathscr{E}}_{ab}I^{ab}+\tfrac{2}{3}\dot{\mathscr{B}}_{ab}\mathscr{S}^{ab} \ ,$$

$$\begin{aligned}\dot{P}^i&=-\tfrac{1}{2}\mathscr{E}^i{}_{ab}\dot{I}^{ab}+\tfrac{2}{3}\epsilon^i{}_{pq}\dot{\mathscr{B}}^p{}_l I^{ql}-2\epsilon^i{}_{jk}\mathscr{B}^k{}_a J^{ja}-\tfrac{4}{3}\epsilon^i{}_{jk}\mathscr{B}^k{}_{ab}J^{jab}+\tfrac{4}{3}\delta^{ij}_{pq}\dot{\mathscr{E}}^q{}_a J_j{}^{pa}-\mathscr{E}^i{}_a K^{jja}\\&=-\tfrac{1}{2}\mathscr{E}^i{}_{ab}\dot{I}^{ab}+\tfrac{2}{3}\epsilon^i{}_{pq}\dot{\mathscr{B}}^p{}_l I^{ql}-2\epsilon^i{}_{jk}\mathscr{B}^k{}_a J^{[ja]}-\epsilon^i{}_{jk}\mathscr{B}^k{}_a\dot{I}^{ja}\\&\quad-\tfrac{4}{9}\epsilon^i{}_{jk}\dot{\mathscr{B}}^k{}_{ab}\dot{I}^{jab}-\tfrac{16}{9}\epsilon^i{}_{jk}\mathscr{B}^k{}_{ab}J^{[ja]b}+\tfrac{8}{9}\dot{\mathscr{E}}_{ab}J^{[bi]a}+\tfrac{4}{9}\dot{\mathscr{E}}^i{}_a J^{[ba]}{}_b+\tfrac{4}{9}\dot{\mathscr{E}}_{ab}\dot{I}^{abi}-\tfrac{5}{18}\dot{\mathscr{E}}^i{}_a\dot{I}^{abb} \ ,\end{aligned}$$

and

$$\begin{aligned}\dot{\mathscr{S}}^i&=-\tfrac{1}{2}\epsilon^i{}_{pq}\mathscr{E}^q{}_{ab}I^{pab}+\mathscr{B}_{abc}(J^{abci}+\tfrac{1}{3}J^{iabc})-\tfrac{2}{3}\mathscr{B}^i{}_{ab}(J^{ccab}+J^{abcc})-\tfrac{4}{3}\mathscr{B}_{abc}J^{iabc}+\tfrac{4}{3}\mathscr{B}^i{}_{ab}J^{ccab}\\&=-\tfrac{1}{2}\epsilon^i{}_{pq}\mathscr{E}^q{}_{ab}I^{pab}-2\mathscr{B}_{abc}J^{[ia]bc}-\tfrac{4}{3}\mathscr{B}^i{}_{ab}J^{[ac]b}{}_c \ .\end{aligned}$$

In writing these three equations in terms of multipole moments, we notice that

$$\mathscr{I}_{A_l}=(I_{A_l})^{\rm STF} \ ,$$

$$\epsilon^i{}_{pq}\dot{\mathscr{E}}^{pa}\mathscr{S}^q{}_a=-\epsilon^i{}_{pq}\dot{\mathscr{E}}^{pa}(\epsilon^q{}_{mn}J^{mn}{}_a+\epsilon_{[a\,|\,mn}J^{mn\,|\,q]})=-2\dot{\mathscr{E}}_{pa}J^{[ip]a}-\dot{\mathscr{E}}^i{}_a J^{[ab]}{}_b \ ,$$

where $\epsilon_{[a\,|\,mn}J^{mn\,|\,q]}$ means that we are only antisymmetrizing indices a, q; and

$$\begin{aligned}\epsilon^i{}_{jk}\mathscr{S}^j{}_{ab}\mathscr{B}^{kab}&=\tfrac{1}{3}\epsilon^i{}_{jk}\mathscr{B}^k{}_{ab}(\epsilon^a{}_{pq}J^{qpbj}+\epsilon^b{}_{pq}J^{qpaj}+\epsilon^j{}_{pq}J^{qpab})\\&=\tfrac{1}{3}\epsilon^i{}_{jk}\mathscr{B}^k{}_{ab}(2\epsilon^{[a}{}_{pq}J^{\,|qpb\,|j]}+2\epsilon^{[b}{}_{pq}J^{\,|qpa\,|j]}+3\epsilon^i{}_{pq}J^{qpab})\\&=\tfrac{4}{3}\mathscr{B}^i{}_{ab}J^{[ad]b}{}_d+2\mathscr{B}_{abc}J^{[ia]bc} \ .\end{aligned}$$

Using these relations, we can further simplify Eqs. (12) into

$$\dot{M} = -\tfrac{1}{2}\mathscr{E}_{ab}\dot{\mathscr{I}}^{ab} - \tfrac{2}{3}\mathscr{B}_{ab}\dot{\mathscr{S}}^{ab}\,, \tag{A3a}$$

$$\dot{P}^i = -\tfrac{1}{2}\mathscr{E}^i{}_{ab}\dot{\mathscr{I}}^{ab} - \tfrac{8}{9}\mathscr{B}^i{}_{ab}\mathscr{S}^{ab} + \tfrac{1}{3}\epsilon^i{}_{ab}\mathscr{B}^a{}_c\dot{\mathscr{I}}^{bc} + \tfrac{4}{9}\epsilon^i{}_{ab}\dot{\mathscr{E}}^a{}_c\mathscr{S}^{bc} - \tfrac{4}{9}\epsilon^i{}_{pq}\mathscr{B}^q{}_{ab}\dot{\mathscr{I}}^{pab} - \tfrac{8}{15}\dot{\mathscr{E}}^i{}_a\dot{I}^{abb} + \tfrac{4}{9}\dot{\mathscr{E}}_{ab}\dot{I}^{abi}\,, \tag{A3b}$$

$$\dot{\mathscr{S}}^i = -\tfrac{1}{2}\epsilon^i{}_{pq}\mathscr{E}^q{}_{ab}\mathscr{I}^{pab} - \epsilon^i{}_{pq}\mathscr{B}^q{}_{ab}\mathscr{S}^{pab}\,. \tag{A3c}$$

The last three terms in Eq. (A3b) are part of the next-higher-order contributions [$\sim(ML^3/\mathscr{R}^2T)(1/\mathscr{T}$ or $1/\mathscr{L})$] and thus can be dropped. After this, Eqs. (A3) are the same as Eqs. (4).

---

[1]K. S. Thorne and J. B. Hartle, Phys. Rev. D **31**, 1815 (1985).
[2]K. S. Thorne, Rev. Mod. Phys. **52**, 299 (1980).
[3]X.-H. Zhang (unpublished).
[4]C. W. Misner, K. S. Thorne, and J. A. Wheeler, *Gravitation* (Freeman, San Francisco, 1973); cited in text as MTW.

Chapter IV

3+1 FORMULATION OF GENERAL-RELATIVISTIC PERFECT MAGNETOHYDRODYNAMICS

(Originally appeared in *Phys. Rev.* D39, 2933(1989))

3+1 formulation of general-relativistic perfect magnetohydrodynamics

Xiao-He Zhang

Theoretical Astrophysics 130-33

California Institute of Technology

Pasadena, California 91125

ABSTRACT

The laws of perfect general-relativistic magnetohydrodynamics (GRMHD) are rewritten in 3+1 language in a general spacetime. The laws are expressed in terms of quantities (magnetic field, flow velocity, ...) that would be measured by the "fiducial observers," whose world lines are orthogonal to the hypersurfaces of constant time. This 3+1 formalism of GRMHD should be of interest in numerical relativity, numerical astrophysics, and the membrane paradigm for black holes. The GRMHD equations are also specialized to a stationary spacetime and a stationary MHD flow with one arbitrary spatial symmetry (e.g., a stationary MHD magnetosphere for a rotating Kerr black hole); and the general features of stationary, symmetric GRMHD solutions are discussed.

I. INTRODUCTION

In astrophysics one often encounters magnetic fields. When interstellar clouds condense into stars, when stars collapse to neutron stars, and when accreting material falls into black holes, they all carry magnetic flux with them into a much smaller region, thereby producing a relatively large-scale, ordered magnetic field. Meanwhile other processes, e.g., the dynamo effect, also extract energy from the fluid's motion and further intensify the already existing magnetic field. In order to understand many interesting phenomena in our universe, we need a well-developed theory of magnetized plasmas. However, the full plasma theory is difficult to handle even in some of the most simple situations, and there are many situations where, as a first approximation to plasma theory, a theory of magnetohydrodynamics (MHD) can be rather accurate and reveal much interesting physics. For example, to study magnetic phenomena inside our sun, Newtonian MHD is sufficient.[1] To study magnetospheres and interiors of a neutron star, special-relativistic MHD gives one a good understanding,[2] but general-relativistic MHD is desirable.[3] However, to study the innermost regions of accretion disks and jets of magnetized, accreting black holes, the strength of gravity demands a general-relativistic MHD treatment.

There have been many efforts to develop a fully general-relativistic magnetohydrodynamic (GRMHD) theory and to apply it to interesting astrophysical situations (Refs. 3–8 and references cited therein). Thus, GRMHD is already a rather mature subject. However, it is found in research that some versions of the theory are more helpful in intuitive thinking than others, or are more convenient to use for some problems. A 3+1 formulation is particularly useful for numerical calculations,[6,9] and it shows promise for intuitive understanding in black-hole situations (the "membrane paradigm,"[10] a 3+1 version of black-hole theory based on a special family of fiducial observers). There has

been one previous 3+1 formulation of GRMHD: that of Sloan and Smarr.[6] However, that formalism expressed the theory in terms of a set of variables (energy density, energy flux, stress tensor) that are not optimal for intuitive understanding. The objective of this paper is to re-express GRMHD in a more intuitively useful form: a form based on fluid and field quantities that are measured by a preferred family of fiducial observers (FIDO's) directly (the FIDO-measured magnetic field $\vec{B}$, fluid velocity $\vec{V}$, and the mass density ρ and pressure p as seen in fluid's rest frame). Expressed in this way the 3+1 equations of GRMHD are Eqs. (2.5) or (2.13), (2.6), (2.12), (2.22), (2.24), and (2.26) below.

The work reported here has been particularly motivated by the "Blandford-Znajek effect;" i.e., the extraction of rotational energy from a black hole by the coupling of magnetic fields threading the hole to the hole's gravitomagnetic field (its "dragging of inertial frames"). In their seminal paper on this subject, Blandford and Znajek[11] idealized the magnetosphere as force-free, with its plasma consisting of electron-positron pairs created by magnetic-gravitomagnetic-induced electric fields. Macdonald and Thorne[12] analyzed this Blandford-Znajek process using the membrane paradigm and retaining the force-free idealization near the hole. More recently, Phinney[7] has developed and applied to the Kerr geometry a (non-3+1) formulation of GRMHD theory and has used it in an improved, MHD analysis of the Blandford-Znajek process. All of this past research has dealt with equilibrium states of the magnetosphere. A natural extension of these studies would be an investigation of the magnetosphere's dynamical properties, or as a first step, the behavior of MHD waves propagating in it. The author is carrying out an initial study of such waves in a black-hole magnetosphere. As a foundation for that study, a 3+1 version of GRMHD is developed and presented in this paper.

Although the formulation presented in this paper was motivated by the black-hole problem and meshes nicely with the membrane paradigm, the formalism is not restricted

to black holes or the membrane paradigm. It is presented initially (Sec. II) in a much more general form than that. However, in the Kerr geometry we have a set of preferred FIDO's [the zero angular momentum observers[13] (ZAMO's)]; and our general formalism can be easily specialized to the Kerr geometry with the ZAMO's playing the role of the FIDO's. The result is the membrane paradigm version of GRMHD.

In Sec. II of this paper the full and general set of GRMHD equations is given in terms of quantities measured by the FIDO's. In Sec. III we demonstrate that without much extra effort, Phinney's results[7] on stationary, GRMHD, black-hole magnetospheres can actually be generalized to any stationary MHD system with one spatial symmetry; and for such a system we reduce the full set of GRMHD equations to a set of algebraic relations and an (algebraic) wind equation which, along with one nonlinear partial differential equation also contained in this set of GRMHD equations, fully determine the structure of MHD flows. In a subsequent paper we will use those equations to build equilibrium models, which we will then perturb in order to get insight into dynamical black-hole magnetospheres.

II. GENERAL-RELATIVISTIC MAGNETOHYDRODYNAMIC EQUATIONS

A. Notation

For the concept of a 3+1 split of spacetime into space plus time and the concept of the FIDO's, associated with such a split, readers are referred to York,[14] to the membrane paradigm book,[10] and to references cited therein. Here only the basic points will be summarized. The foundation for the 3+1 split is a particular choice of time coordinate t (i.e., a particular ''foliation'' of spacetime into ''universal time'' t and ''absolute space,'' the hypersurfaces of constant t). With a specific choice of time t and spatial coordinate x^i,

the spacetime line element takes the form

$$ds^2=-\alpha^2 dt^2+\gamma_{ij}(dx^i+\beta^i dt)(dx^j+\beta^j dt), \tag{2.1}$$

and the FIDO's (whose world lines are orthogonal to the hypersurfaces of constant t) have four-velocities,

$$\boldsymbol{n}=\frac{1}{\alpha}\left(\frac{\partial}{\partial t}-\beta^i\frac{\partial}{\partial x^i}\right). \tag{2.2}$$

The FIDO's proper time τ is related to the "universal time" t by $d\tau=\alpha dt$. The rate of change of any scalar physical quantity as seen by a FIDO is

$$\frac{df}{d\tau}\equiv\boldsymbol{n}\cdot{}^{(4)}\nabla f=\frac{1}{\alpha}\left(\frac{\partial}{\partial t}-\vec{\beta}\cdot\vec{\nabla}\right)f, \tag{2.3a}$$

and the FIDO-measured rate of change of any three-dimensional vector $\vec{S}$ or tensor $\overleftrightarrow{D}$ that lies in absolute space (i.e., orthogonal to $\boldsymbol{n}$) is defined by

$$\frac{d\vec{S}}{d\tau}\equiv\frac{1}{\alpha}\left[\pounds_t\vec{S}-(\vec{\beta}\cdot\vec{\nabla})\vec{S}\right],\quad \frac{d\overleftrightarrow{D}}{d\tau}\equiv\frac{1}{\alpha}\left[\pounds_t\overleftrightarrow{D}-(\vec{\beta}\cdot\vec{\nabla})\overleftrightarrow{D}\right]. \tag{2.3b}$$

Here, ${}^{(4)}\nabla$ denotes the gradient in four-dimensional spacetime, $\vec{\nabla}$ is the gradient in three-dimensional space, and $\pounds_t$ is the Lie derivative along $\partial/\partial t$, so $\pounds_t\vec{S}$ is the three-vector whose components in the coordinate system (2.1) are $\partial S^j/\partial t$.

In this paper geometrized units, with $G=c=1$, will be used. Vectors and tensors living in four-dimensional spacetime will be denoted by boldface italic letters, such as the FIDO's four-velocity $\boldsymbol{n}$; vectors living in three-dimensional absolute space will be denoted by boldface roman or Greek letters, such as the shift function $\vec{\beta}$; three-dimensional tensors are distinguished from vectors by a dyad over the letter, such as the

three-dimensional metric $\overleftrightarrow{\gamma}$. All vector-analysis notations such as the gradient, curl, and vector cross product will be those of the three-dimensional absolute space whose three-metric is $\overleftrightarrow{\gamma}$, unless specified otherwise. The determinant of the three-metric is denoted as g:

$$g \equiv \det | \gamma_{ij} | . \tag{2.4}$$

Latin letters $i, j, k, \ldots$ represent indices in absolute space and thus run from 1 to 3; Greek letters $\alpha, \beta, \gamma, \ldots$ represent indices in spacetime and thus run from 0 to 3. Summation on repeated indices is assumed.

B. Evolution of the magnetic field

In an MHD fluid, the motion of the fluid will change the magnetic field; and the magnetic field, in turn, will change the state of the fluid's flow through its Lorentz and Coulomb forces.

The FIDO-measured magnetic field $\vec{B}$ is governed by half of Maxwell's equations [Eqs. (3.4), (2.16), (2.17) of Ref. 15, together with (2.3b) above; see also Ref. 6]:

$$\frac{d\vec{B}}{d\tau} + \frac{1}{\alpha}\vec{B}\cdot\vec{\nabla}\vec{\beta} + \theta\vec{B} = -\frac{1}{\alpha}\vec{\nabla}\times(\alpha\vec{E}), \tag{2.5}$$

$$\vec{\nabla}\cdot\vec{B} = 0. \tag{2.6}$$

Here, θ is the expansion rate of the FIDO's four-velocity, i.e., three times the direction-averaged ''Hubble expansion rate'' of absolute space as seen by them,

$$\theta \equiv {}^{(4)}\nabla\cdot\boldsymbol{n}, \tag{2.7}$$

and is expressible in terms of $g = \det | \gamma_{ij} |$, the ''lapse function'' α, and ''shift function'' (or

''gravitomagnetic potential'') $\vec{\beta}$ by

$$\theta=\frac{1}{\alpha}\left(\frac{g_{,t}}{2g}-\vec{\nabla}\cdot\vec{\beta}\right). \tag{2.7'}$$

The FIDO-measured electric field $\vec{E}$, electric current $\vec{j}$, and electric-charge density ρ_e are treated as auxiliary quantities in the GRMHD formalism. For imperfect MHD (MHD with finite electrical conductivity), they can be found from the other half of Maxwell's equations [Eqs. (3.4), (2.16), (2.17) of Ref. 15 together with (2.3b) above; see also Ref. 6];

$$\frac{d\vec{E}}{d\tau}+\frac{1}{\alpha}\vec{E}\cdot\vec{\nabla}\vec{\beta}+\theta\vec{E}=\frac{1}{\alpha}\vec{\nabla}\times(\alpha\vec{B})-4\pi\vec{j}, \tag{2.8}$$

$$\vec{\nabla}\cdot\vec{E}=4\pi\rho_e, \tag{2.9}$$

and from Ohm's law (the spatial part of the 3+1 version of $J^\mu+u^\mu u^\nu J_\nu=\sigma F^{\mu\nu}u_\nu$, where u_ν is the fluid four-velocity):

$$\vec{j}+\gamma^2(\vec{V}\cdot\vec{j})\vec{V}-\rho_e\gamma^2\vec{V}=\sigma\gamma(\vec{E}+\vec{V}\times\vec{B}). \tag{2.10}$$

Here $\vec{V}$ is the FIDO-measured fluid velocity, γ is the fluid's Lorentz factor as seen by the FIDO's,

$$\gamma\equiv(1-\vec{V}^2)^{-1/2}, \tag{2.11}$$

and σ is the electric conductivity as measured in the fluid rest frame, not in the FIDO's frame.

In this paper we will restrict attention to perfect MHD, i.e., to MHD with perfectly conducting ($\sigma\to\infty$) fluids; this is an excellent idealization for most astrophysical situations. For a detailed discussion of its validity in the context of active galactic nuclei

(AGN's), see Sec.V3 of Phinney.[7] Under the perfect MHD assumption there can be no electric field in the fluid's rest frame, i.e.,

$$\vec{E}+\vec{V}\times\vec{B}=0. \tag{2.12}$$

This equation can be formally derived from $u^{\mu}F_{\mu\nu}=0$ or can be inferred from (2.10) with $\sigma\to\infty$. Note that for perfect MHD, $\vec{E}$ can be computed from $\vec{V}$ and $\vec{B}$, using Eq. (2.12); then $\vec{j}$ and ρ_e can be computed from (2.8) and (2.9). In the following, Eqs. (2.8) and (2.9) will not be used again except to calculate the auxiliary quantities $\vec{j}$ and ρ_e when needed.

For perfect MHD the magnetic-field evolution equation (2.5) can be simplified by substituting $-\vec{V}\times\vec{B}$ for $\vec{E}$ and making use of Eq. (2.6). The result is

$$\frac{D\vec{B}}{D\tau}+\frac{1}{\alpha}\vec{B}\cdot\vec{\nabla}(\vec{\beta}-\alpha\vec{V})+\left(\theta+\frac{\vec{\nabla}\cdot(\alpha\vec{V})}{\alpha}\right)\vec{B}=0, \tag{2.13}$$

where

$$\frac{D}{D\tau}\equiv\frac{d}{d\tau}+\vec{V}\cdot\vec{\nabla}=\frac{1}{\alpha}\left(\frac{\partial}{\partial t}+(\alpha\vec{V}-\vec{\beta})\cdot\vec{\nabla}\right) \tag{2.14}$$

is the time derivative moving with the fluid. As Evans and Hawley[9] have pointed out, with a little bit of manipulation this evolution law can be reduced to a form more suitable for numerical calculations:

$$\frac{1}{\sqrt{g}}\frac{\partial\sqrt{g}\vec{B}}{\partial t}-\vec{\nabla}\times[(\alpha\vec{V}-\vec{\beta})\times\vec{B}]=0. \tag{2.13'}$$

Because the evolution law (2.13) represents only half of the dynamic Maxwell equations [Eq. (2.5) but not (2.8)], a natural question arising at this stage is: Should one impose the constraint (2.6) ($\vec{\nabla}\cdot\vec{B}=0$) at all times or just on the initial data? The answer is

what we would guess intuitively: As in everyday physics we need to impose it only on the initial data. The proof is very straightforward; we will sketch it here to conclude this section. First we move $d/d\tau$ inside $\vec{\nabla}$ in $(d/d\tau)(\vec{\nabla}\cdot\vec{B})$, taking care to include curvature terms when we change the orders of differentiation; then we use (2.5) to eliminate $d\vec{B}/d\tau$. The end result is

$$\frac{d}{d\tau}\vec{\nabla}\cdot\vec{B}=-\theta\,\vec{\nabla}\cdot\vec{B}, \tag{2.15}$$

which says explicitly that once $\vec{\nabla}\cdot\vec{B}=0$ is imposed on the initial data, it will continue to hold at later times as the magnetic field is evolved, using (2.5) [or its consequence, (2.13) or (2.13′)].

C. Motion of the fluid

The total energy-momentum tensor of an MHD system must obey the conservation laws,

$$^{(4)}\nabla\cdot(\boldsymbol{T}_{\text{fluid}}+\boldsymbol{T}_{\text{EM}})=0. \tag{2.16}$$

Here $\boldsymbol{T}_{\text{fluid}}$ is the four-dimensional energy-momentum tensor of the fluid and $\boldsymbol{T}_{\text{EM}}$ is that of the electromagnetic field. Each of these $\boldsymbol{T}$'s is broken into the FIDO-measured energy density ε, energy flux or momentum density $\vec{S}$, and stress tensor $\overleftrightarrow{W}$.[6,15] For the electromagnetic field alone we have [Eq. (3.10) of Ref. 15]

$$\varepsilon_{\text{EM}}=\frac{1}{8\pi}(\vec{E}^2+\vec{B}^2), \tag{2.17a}$$

$$\vec{S}_{\text{EM}}=\frac{1}{4\pi}(\vec{E}\times\vec{B}), \tag{2.17b}$$

$$\overleftrightarrow{W}_{\text{EM}}=\frac{1}{4\pi}\left[-(\vec{E}\otimes\vec{E}+\vec{B}\otimes\vec{B})+\frac{1}{2}(\vec{E}^2+\vec{B}^2)\overleftrightarrow{\gamma}\right]. \tag{2.17c}$$

For the perfect fluid we have [Eq. (3.11) of Ref. 15]:

$$\varepsilon=(\rho+p\vec{V}^2)\gamma^2, \tag{2.18a}$$

$$\vec{S}=(\rho+p)\gamma^2\vec{V}, \tag{2.18b}$$

$$\overleftrightarrow{W}=(\rho+p)\gamma^2\vec{V}\otimes\vec{V}+p\overleftrightarrow{\gamma}, \tag{2.18c}$$

where ρ is the mass density and p is the presure as seen in the fluid's rest frame, $\gamma=(1-\vec{V}^2)^{-1/2}$ is the fluid's Lorentz factor [Eq. (2.11)], and $\otimes$ denotes the tensor product.

The conservation law (2.16) can be viewed in two equivalent ways. One is to treat its two parts separately and to regard the electromagnetic part as an external force acting on the fluid, an approach used by Sloan and Smarr.[6] We shall also adopt this approach in deriving our dynamic GRMHD equations. The other approach is to treat the total energy-momentum tensor as a whole.[3,7] This is found to be more useful in deriving conservation laws when symmetry exists and will be used in Sec. III below to deduce properties of equilibrium solutions.

When we project (2.16) along a FIDO's world line, we get the local energy conservation law as seen by the FIDO; when we project (2.16) into absolute space; i.e., orthogonal to the FIDO's world line, what we get is a force balance equation as seen by the FIDO's. The two resulting equations are[6,10,15]

$$\frac{d\varepsilon}{d\tau}+\theta\varepsilon+\frac{1}{2\alpha}W^{ij}\pounds_t\gamma_{ij}=-\frac{1}{\alpha^2}\vec{\nabla}\cdot(\alpha^2\vec{S})+\frac{1}{\alpha}(\vec{\nabla}\vec{\beta}):\overleftrightarrow{W}+\vec{E}\cdot\vec{j}, \tag{2.19}$$

$$\frac{dS_i}{d\tau}+\theta S_i+(\pounds_t\gamma_{ij})S^j=-\varepsilon a_i-W_{ij}a^j$$

$$+\frac{1}{\alpha}\beta_{j\,|i}S^j-W_i{}^j{}_{|j}+\rho_e E_i$$

$$+(\vec{j}\times\vec{B})_i . \tag{2.20}$$

Here, ε, S_i, and W_{ij} are the FIDO-measured energy density, energy flux, and stress in the fluid alone [Eq. (2.18)];

$$\vec{a}\equiv(\vec{\nabla}\alpha)/\alpha \tag{2.21}$$

is the negative of the FIDO-measured gravitational acceleration; and the covariant derivative in three-dimensional absolute space is denoted by a slash $_{|i}$. The auxiliary quantities $\rho_e, \vec{j}, \vec{E}$ are to be found from Eqs. (2.8), (2.9), and (2.12). If we replace $\varepsilon, \vec{S}, \overleftrightarrow{W}$ in (2.19) and (2.20) by the appropriate expressions for a fluid with dissipation and retain a finite conductivity σ, what we get are the "imperfect" general GRMHD equations.[8] However, since we will concentrate on perfect MHD in this paper, we shall replace $\varepsilon, \vec{S}, \overleftrightarrow{W}$ by their perfect-fluid expressions in (2.18). When this is done, the FIDO-measured law of force balance (2.20) becomes

$$\left[\left(\rho_0\gamma^2\mu+\frac{\vec{B}^2}{4\pi}\right)\gamma_{ij}+\rho_0\gamma^4\mu V_i V_j-\frac{1}{4\pi}B_iB_j\right]\frac{DV^j}{D\tau}+\rho_0\gamma^2\mu V_i\frac{D\mu}{D\tau}-\left(\frac{\vec{B}^2}{4\pi}\gamma_{ij}-\frac{1}{4\pi}B_iB_j\right)(V^j{}_{|k}V^k)$$

$$=-\rho_0\gamma^2\mu\left(a_i-\frac{1}{\alpha}\beta_{j\,|i}V^j-(\angle_i\gamma_{ij})V^j\right)-p_{|i}+\frac{1}{4\pi}(\vec{V}\times\vec{B})_i\vec{\nabla}\cdot(\vec{V}\times\vec{B})-\frac{1}{8\pi\alpha^2}(\alpha\vec{B})^2{}_{|i}+\frac{1}{4\pi\alpha}(\alpha B_i)_{|j}B^j$$

$$+\frac{1}{4\pi\alpha}\left[\vec{B}\times\left\{\vec{V}\times[\vec{\nabla}\times(\alpha\vec{V}\times\vec{B})-(\vec{B}\cdot\vec{\nabla})\vec{\beta}]-(\vec{V}\times\vec{B})\cdot\vec{\nabla}\vec{\beta}\right\}\right]_i . \tag{2.22}$$

Here a subscript i on a vector quantity means the i component of that vector:

$$\mu\equiv\frac{\rho+p}{\rho_0} \tag{2.23}$$

is the specific enthalpy of the fluid [and also the inertial mass per unit rest mass; cf.

Exercise 5.4 of Misner, Thorne, and Wheeler[16] (MTW)]; and ρ_0 is the fluid's rest mass density. In deriving the above equation, the local law of conservation of rest mass [3+1 version of $(\rho_0 u^\mu)_{;\mu}=0$]

$$\frac{D\rho_0}{D\tau}+\rho_0\gamma^2\vec{V}\cdot\frac{D\vec{V}}{D\tau}+\frac{\rho}{\alpha}\left(\frac{1}{2g}g_{,t}+\vec{\nabla}\cdot(\alpha\vec{V}-\vec{\beta})\right)=0 \tag{2.24}$$

was used.

Here we deliberately will not make the law of energy conservation (2.19) explicit because in perfect MHD, a combination of (2.19) and (2.20) is easier to use. We shall turn to this in some detail in the next subsection.

Because of the underlying plasma processes, where the fluid particles are locked onto magnetic field lines, it is easier for fluid to move along magnetic field lines than across them. If we think of the coefficient of $DV^j/d\tau$ on the left-hand side (LHS) of (2.22) as an "effective inertia," we can clearly see this anisotropy in the fluid's inertia caused by the magnetic field. The quartic term in γ on the LHS is a relativistic correction: fluid is harder to accelerate at higher speed. The second term on the LHS of (2.22) represents the force needed for a moving fluid when its specific enthalpy is changing. The last term on the LHS is a correction to the first inertial term. On the right-hand side (RHS) of (2.22), the first term in the large parentheses is the standard gravitational acceleration (because of failure of the FIDO's to fall freely); the second term in that set of parentheses is the gravitomagnetic acceleration; and the third term comes from the coupling of the motion of the fluid to nonstatic spatial curvature. The second term on the RHS is the familiar pressure gradient. The third and fourth terms on the RHS are just the Coulomb and Lorentz forces. The curl of the $\alpha\vec{V}\times\vec{B}$ term is the coupling of the induced electric field to the fluid velocity and the magnetic field. The rest of the term comes from

the coupling of the magnetic field to the gravitomagnetic field, a force underlying the Blandford-Znajek effect.

D. Thermodynamic variables

In perfect MHD there is no Ohmic dissipation nor viscous loss, so entropy is strictly conserved locally. Therefore, we can write the first law of thermodynamics as

$$d\rho=\frac{\rho+p}{\rho_0}d\rho_0 \tag{2.25}$$

as seen in the fluid's rest frame, or

$$\frac{D\rho}{D\tau}=\mu\frac{D\rho_0}{D\tau}. \tag{2.25'}$$

We can also derive Eq. (2.25) from the law of energy conservation as seen by the fluid $T^{\alpha\beta}{}_{;\alpha}u_\beta=0$ plus the frozen-in condition and the conservation of rest mass, or equivalently from a linear combination of (2.19) and (2.20) plus (2.6) and (2.24). Notice that in Eq. (2.25) only the fluid's variables appear; and energy conservation has the same form as for an ordinary fluid with no magnetic field. This comes from the perfect MHD assumption that in the fluid's rest frame there is no electric field and therefore no exchange of energy between the fluid and magnetic field. In our MHD equations we choose to use (2.25) instead of (2.19). Of course, our MHD equations are not complete without an equation of state

$$F(\rho_0,p,s)=0, \tag{2.26}$$

where s is the specific entropy. In this paper we assume, for simplicity, that the system of equations for perfect MHD is closed by a barotropic equation of state (i.e., s is

constant throughout the fluid and, of course, constant in time)

$$p=p(\rho_0), \tag{2.26'}$$

and, correspondingly, ρ can be computed once and for all from [cf. Eq. (2.25)]

$$\rho=\rho(\rho_0)=\rho_0\int\frac{p}{\rho_0^2}d\rho_0 \ . \tag{2.27}$$

To summarize, in our 3+1 equations for perfect MHD, the basic variables are the FIDO-measured magnetic field $\vec{B}$ and fluid velocity $\vec{V}$, and the rest-mass density ρ_0 as measured in the fluid's rest frame. The total density of mass-energy ρ and pressure p (in the fluid rest frame) are computed from ρ_0 via Eqs. (2.26′) and (2.27); the FIDO-measured electric field $\vec{E}$ is computed from $\vec{V}$ and $\vec{B}$ via Eq. (2.12); the FIDO-measured current density $\vec{j}$ and charge density ρ_e are computed from Eqs. (2.8) and (2.9); the magnetic field $\vec{B}$ is evolved via Eq. (2.13); and the fluid velocity $\vec{V}$ is evolved via Eq. (2.22). These are the perfect GRMHD equations in their most general form. Using these equations, we can study stationary configurations, dynamic evolution of conducting fluid with appropriate boundary conditions, or a small perturbation to an equilibrium state.

III. GRMHD IN A STATIONARY, SYMMETRIC BACKGROUND

In this section we restrict attention to a stationary spacetime with one spatial symmetry and demand that the MHD flow have the same symmetries. More specifically, we assume that spacetime has a timelike Killing vector field (KVF) $\boldsymbol{k}=\partial/\partial t$ and a spacelike KVF $\vec{m}=\partial/\partial\xi$ which commute with each other, and we insist that all fluid and electromagnetic quantities have vanishing Lie derivatives along $\boldsymbol{k}$ and $\vec{m}$. Moreover, we also insist (as is the case for a rotating, Kerr black hole) that the gravitomagnetic potential point along the symmetry direction $\vec{m}$,

$$\vec{\beta}\equiv\beta\vec{m}. \tag{3.1}$$

These restrictions guarantee that (i) our metric (2.1) will be independent of t and ξ; (ii) $\vec{\beta}$ and $\vec{m}$ will both lie in the hypersurfaces of constant time; i.e., they are three-vectors in absolute space; (iii) the congruence of FIDO world lines will not expand,

$$\theta=0; \tag{3.2}$$

and (iv) the gravitational acceleration will have vanishing projection along $\vec{\beta}$:

$$\vec{a}\cdot\vec{\beta}=0. \tag{3.3}$$

We shall see how 3+1 electrodynamics can be simplified under these conditions (Sec.III A) and how the conservation laws associated with these KVF's can be used to simplify the analysis of equilibrium configurations (Secs.III B and III C). This discussion is a 3+1 treatment of Phinney,[7] and an extension to MHD of Macdonald and Thorne[12] (but with the spacetime slightly more general than in those cases).

A. Electrodynamics

To study electrodynamics in a stationary, symmetric spacetime, we first introduce, as auxiliary quantities used in intermediate steps, some special components of the four-vector potential. They are[15]

$$\vec{A}\equiv\overleftrightarrow{\gamma}\cdot(\text{four-vector potential})$$

$$=(\text{three-vector potential living in three-dimensional absolute space}), \tag{3.4}$$

$$A_0\equiv\vec{k}\cdot(\text{four-vector potential})$$

$$=(\text{time component of four-vector potential}), \tag{3.5}$$

$A_\xi \equiv \vec{m}\cdot$(four-vector potential)

$=\vec{m}\cdot$(three-vector potential)

$=$(ξ-component of three-vector of four-vector potential). (3.6)

Using these potentials, we can write the electric and magnetic fields as [Eqs. (5.9) and (5.10) of Ref. 15],

$$\vec{E}=\frac{1}{\alpha}(\vec{\nabla}A_0-\beta\vec{\nabla}A_\xi), \tag{3.7}$$

$$\vec{B}=\vec{\nabla}\times\vec{A}. \tag{3.8}$$

Because A_ξ will play an important role in determining the structure of stationary MHD flows, let us examine the physical content of A_ξ first. Consider a curve C in absolute space with tangent vector $\vec{m}$ (i.e., an ''integral curve'' of $\vec{m}$) and a magnetic flux tube bounded by C (see Fig. 1). The magnetic flux Ψ inside such a flux tube is related to A_ξ in the following way:

$$\Psi(\vec{x})=\iint_S \vec{B}\cdot d\vec{S}=\oint_C A_\xi d\xi \ . \tag{3.9}$$

Here Ψ, regarded as a scalar field in absolute space, has the above value at any point $\vec{x}$ that lies on curve C. Because $\vec{m}\equiv\partial/\partial\xi$ is assumed to be a KVF, A_ξ is independent of ξ; so we can consider A_ξ as the flux per unit ξ length of C within the flux tube. In an axisymmetric spacetime, ξ is equal to the angle ϕ around the axis of symmetry, the line integral (3.9) runs from 0 to 2π, and $\Psi(\vec{x})$ is the flux inside the circle that passes through $\vec{x}$ and is generated by $\partial/\partial\xi$. In a translation symmetric spacetime, ξ runs from $-\infty$ to $+\infty$, and for finiteness we make use of the ξ symmetry and restrict the line integral (3.9) to a small, fixed interval [say $\xi_0(\vec{x})<\xi<\xi_0(\vec{x})+\delta L$ for some small δL], and regard $\Psi(\vec{x})$ as the flux in a

tube bounded by (i) the integral curve of $\vec{m}$ through $\vec{x}$; (ii) a curve at $\xi=\xi_0(\vec{x})$; (iii) a curve at $\xi=\xi_0(\vec{x})+\delta L$, and (iv) some fixed fiducial integral curve of $\vec{m}$.

Before we try to relate A_ξ to $\vec{B}$ and $\vec{E}$, let us first decompose, for later convenience, any vector $\vec{U}$ in absolute space into its ξ component U^ξ and the part $\vec{U}^P$ perpendicular to $\vec{m}=\partial/\partial\xi$:

$$\vec{U}=\vec{U}^P+U^\xi\vec{m}. \tag{3.10}$$

(The superscript P stands for ''Poloidal'' — a terminology adapted from the axisymmetric case where ξ is the angle around the symmetry axis.) Then it turns out that (see below)

$$\vec{V}^P \| \vec{B}^P. \tag{3.11}$$

Here $\vec{V}^P$ and $\vec{B}^P$ are the ''poloidal'' parts of the fluid velocity and magnetic field, respectively. Thus, the poloidal magnetic field lines coincide with the fluid's poloidal stream lines on surfaces orthogonal to $\vec{m}$. This can be derived by taking a scalar product of (3.7) with $\vec{m}$ and then using the ξ symmetry and the frozen-in condition (2.6) to conclude that

$$\vec{m}\cdot(\vec{V}\times\vec{B})=0, \tag{3.12}$$

or

$$\vec{m}\cdot(\vec{V}^P\times\vec{B}^P)=0, \tag{3.13}$$

which says that $\vec{m}$, $\vec{V}^P$, and $\vec{B}^P$ are not linearly independent; hence the statement in (3.11). Because $\vec{V}^P$ and $\vec{B}^P$ are parallel, we can define a proportionality coefficient k to relate them. By a careful choice, it is defined as[3.7]

$$\vec{V}^P \equiv \frac{k}{4\pi\alpha\rho_0\gamma}\vec{B}^P. \tag{3.14}$$

With this choice we can show, using (2.6) and (2.24), that

$$\vec{B}^P \cdot \vec{\nabla} k = 0. \tag{3.15}$$

The proof involves combining the stationary, symmetric versions of the law of mass conservation (2.24)

$$\vec{\nabla} \cdot (\alpha \rho_0 \gamma \vec{V}^P) = 0 \tag{3.16}$$

and the law of flux conservation $\vec{\nabla} \cdot \vec{B}^P = 0$. Therefore, k will be constant on magnetic surfaces, or flux tubes, though typically it will vary from one magnetic surface to another.

Now we wish to find a relation between $\vec{B}$ and A_ξ. The argument here is that of Thorne and Macdonald.[15] Consider an integral curve C' of $\vec{m}$ which differs slightly from C. The flux per unit length of C, between C and C', is

$$dA_\xi = (\vec{\nabla} A_\xi) \cdot d\vec{x} = \vec{B} \cdot (\vec{m} \times d\vec{x}) = (\vec{m} \times \vec{B}) \cdot d\vec{x}, \tag{3.17}$$

where $d\vec{x}$ is any vector reaching from C to C'. Because C' is arbitrary, $d\vec{x}$ is also arbitrary, and we thus have

$$\vec{\nabla} A_\xi = \vec{m} \times \vec{B} = \vec{m} \times \vec{B}^P. \tag{3.18}$$

By taking a cross product with $\vec{m}$, we can invert (3.18) to obtain

$$\vec{B}^P = -\frac{\vec{m} \times \vec{\nabla} A_\xi}{\gamma_{\xi\xi}}. \tag{3.19}$$

Here, $\gamma_{\xi\xi} = \vec{m} \cdot \vec{m}$ is the ''$\xi\xi$ component'' of the three-metric. From (3.19) we can deduce that

$$\vec{B}^P \cdot \vec{\nabla} A_\xi = 0. \tag{3.20}$$

This guarantees that A_ξ, as is k, is a constant on magnetic surfaces and that k can be regarded as a function of A_ξ:

$$k=k(A_\xi). \tag{3.21}$$

The coefficient k is called the stream function[7] because it is constant along a ''stream line,'' i.e., along an integral curve of $\vec{V}=\vec{V}^P+V^\xi\vec{m}$. As we shall see in Sec. III C, stream functions play an important role in determining the structure of stationary flows.

We can also express $\vec{E}$ in terms of the gradient of A_ξ. The frozen-in condition (2.12) implies that $\vec{E}$ is orthogonal to $\vec{B}$; and thus (2.12) plus Eqs. (3.7) and (3.20) and ξ symmetry implies

$$\vec{B}^P\cdot\vec{\nabla}A_0=0, \tag{3.22}$$

which in turn implies that

$$A_0=A_0(A_\xi). \tag{3.23}$$

Since $\vec{\nabla}^P A_0$ and $\vec{\nabla}^P A_\xi$ are both poloidal (by ξ symmetry) and are both orthogonal to $\vec{B}^P$, they must be parallel to each other:

$$\vec{\nabla}A_0=-V^F\vec{\nabla}A_\xi, \tag{3.24}$$

for some scalar field V^F. Correspondingly, Eq. (3.7) implies

$$\vec{E}=-\frac{1}{\alpha}(\beta+V^F)\vec{\nabla}A_\xi=-\frac{1}{\alpha}(V^F\vec{m}+\vec{\beta})\times\vec{B}. \tag{3.25}$$

By taking derivatives along $\vec{B}^P$ of both sides of (3.24) and using (3.20) and (3.22), we conclude that V^F must be a function of A_ξ; i.e., $\vec{B}^P\cdot\vec{\nabla}V^F=0$, and V^F is also a stream function. We can think of V^F as the coordinate speed of the magnetic field, because observers

who move with $d\xi/dt=V^F$ [i.e., at velocity $(V^F\vec{m}+\vec{\beta})/\alpha$ as measured by FIDO's] see an electric field

$$\vec{E}'\propto\left[\vec{E}+\left(\frac{V^F\vec{m}+\vec{\beta}}{\alpha}\right)\times\vec{B}\right]=0 \tag{3.26}$$

that vanishes; i.e., they regard the magnetic field as at rest with respect to themselves. A comparison of Eqs. (2.12) and (3.26) gives us an algebraic relation

$$V^{\xi}=\frac{kB^{\xi}}{4\pi\alpha\rho_0\gamma}+\frac{V^F+\beta}{\alpha}, \tag{3.27}$$

which relates V^{ξ} to B^{ξ}.

B. MHD flow

For the stationary and symmetric MHD flow, since the FIDO's move along symmetry directions, $d(\text{everything})/d\tau=0$. FIDO's do not see any changes in the MHD flow around themselves. Moreover, associated with the two KVF's, we have two conserved fluxes [Eqs. (3.65b) and (3.69b) of Ref. 10],

$$\vec{S}_{p_\xi}\equiv\overleftrightarrow{W}\cdot\vec{m},\ \vec{S}_{E_-}\equiv\alpha\vec{S}-\vec{\beta}\cdot\overleftrightarrow{W}, \tag{3.28}$$

whose products with the lapse function α are divergence-free under stationary, symmetric assumptions:

$$\vec{\nabla}\cdot(\alpha\vec{S}_{p_\xi})=0,\ \vec{\nabla}\cdot(\alpha\vec{S}_{E_-})=0 \tag{3.29}$$

[Eqs. (3.67) and (3.71) of Ref. 10]. Here, $\vec{S}_{p_\xi}$ is the flux of the ξ component of momentum, and $\vec{S}_{E_-}$ is the flux of energy at infinity, or "red-shifted energy." Because of the symmetry, the ξ components of these fluxes give identically zero contribution to the

conservation laws (3.29). Thus, the poloidal parts of the fluxes also satisfy the conservation laws (3.29), and we shall concentrate attention on them. Using expressions (3.14) and(3.25) for $\vec{E}$ and $\vec{B}$, we find

$$\vec{S}^P_{P_\xi}=(\mu\gamma V_\xi-\alpha B_\xi/k)\rho_0\gamma\vec{V}^P, \tag{3.30}$$

$$\vec{S}^P_{E_\infty}=[\gamma\mu(\alpha-\beta V_\xi)-V^F\alpha B_\xi/k]\rho_0\gamma\vec{V}^P, \tag{3.31}$$

which allows us to introduce two more stream functions:[7]

$$l\equiv\gamma\mu V_\xi-\alpha B_\xi/k,\ l=l(A_\xi), \tag{3.32}$$

$$e\equiv\gamma\mu(\alpha+\beta V_\xi)-V^F\alpha B_\xi/k,\ e=e(A_\xi). \tag{3.33}$$

That l and e are indeed stream functions (i.e., are constant along $\vec{B}^P$ and thus are expressible as functions of A_ξ) can be verified directly from (3.16) and (3.29)–(3.33). We can rewrite Eqs. (3.30) and (3.31), using l and e, as

$$\vec{S}^P_{P_\xi}=l(A_\xi)\rho_0\gamma\vec{V}^P, \tag{3.30′}$$

$$\vec{S}^P_{E_\infty}=e(A_\xi)\rho_0\gamma\vec{V}^P. \tag{3.31′}$$

As pointed out by Phinney[7] and also quite obvious here, l and e can be interpreted as the covariant ξ component of momentum (henceforth, the ''generalized momentum'') and the energy at infinity carried by unit rest mass of fluid. Sometimes, especially when seeking solutions to the ''wind equation'' [Eq. (3.46) below], a combination of e and l, the field-rest-frame specific energy f, is more useful in determining the flow structure. It is defined as

$$f\equiv e-V^F l=\gamma\mu(\alpha-CV_\xi), \tag{3.34}$$

where

$$C \equiv \beta + V^F . \tag{3.35}$$

Using Eqs. (3.29)–(3.31) we can also write the extraction rate of ξ component of momentum, $\dot{L}$, and that of energy at infinity, $\dot{M}$, in terms of stream functions l, e, and k. Consider two flux tubes S_1 and S_2, which are bounded separately by integral curves C_1 and C_2 of $\vec{m}$ on a two-dimensional surface $S_{\rm up}$ with its normal orthogonal to $\vec{m}$ (see Fig. 2). Let us assume that $S_{\rm up}$ is located in a nearly flat region, so the total fluxes of generalized momentum and energy at infinity across it between S_1 and S_2 can be regarded as the rates of extraction of these quantities from the strong gravity region; e.g., leaving a surface $S_{\rm down}$ whose normal is also orthogonal to $\vec{m}$ inside that region. Using Eq. (3.29) we see that

$$\dot{L} \equiv \int_{S_{\rm up}} \alpha \vec{S}_{P_\xi} \cdot d\vec{S} = \int_{S_{\rm up}} \alpha \vec{S}^P_{P_\xi} \cdot d\vec{S}$$

$$= -\int_{S_{\rm down}} \alpha \vec{S}^P_{P_\xi} \cdot d\vec{S}, \tag{3.36}$$

$$\dot{M} \equiv \int_{S_{\rm up}} \alpha \vec{S}_{E_-} \cdot d\vec{S} = \int_{S_{\rm up}} \alpha \vec{S}^P_{E_-} \cdot d\vec{S}$$

$$= -\int_{S_{\rm down}} \alpha \vec{S}^P_{E_-} \cdot d\vec{S}. \tag{3.37}$$

Thus, in stationary perfect GRMHD, the flux tubes act as wires in a dc circuit, guiding energy and momentum from one place to another without dissipation.[12] To study how the energy is converted into photons that observers can see requires an analysis that goes beyond perfect MHD.[14] Of course, this does not render perfect GRMHD uninteresting: perfect GRMHD is still a good approximation in which we can understand how the energy is transported from the strong gravity region to the dissipation region, where

gravity is usually weak and non-general-relativistic analysis would be adequate. To express $\dot{L}$ and $\dot{M}$ in terms of stream functions, we rewrite $\vec{S}^P_{P_t}$ and $\vec{S}^P_{E_\infty}$ using (3.30′) and (3.31′), and we also make use of Eqs. (3.14), (3.18), and (3.19) to obtain

$$\dot{L}=\int_{S_{up}} \alpha l \rho_0 \gamma \vec{V}^P \cdot d\vec{S}=\int_{S_{up}} \frac{lk}{4\pi} \vec{B}^P \cdot d\vec{S}$$

$$=-\frac{1}{4\pi}\int_{S_{up}} \frac{lk(\vec{m}\times d\vec{S})\cdot\vec{\nabla}A_\xi}{\gamma_{\xi\xi}}.$$

On S_{up},

$$d\vec{S}=d\vec{x}^P\times(\vec{m}d\xi);$$

therefore,

$$\dot{L}=-\frac{1}{4\pi}\int_{A_\xi^{(1)}}^{A_\xi^{(2)}} lk\, dA_\xi \int_{\mathcal{L}} d\xi, \tag{3.38}$$

where $A_\xi^{(1)}$ is the value of A_ξ on flux tube S_1, $A_\xi^{(2)}$ is the value of A_ξ on flux tube S_2. Also to include the case where $\int_{\mathcal{L}} d\xi \to \infty$, we use the extraction rate per unit ξ length C of momentum between flux tubes S_1 and S_2, $\dot{\mathcal{L}}$. Then

$$\dot{\mathcal{L}}=-\frac{1}{4\pi}\int_{A_\xi^{(1)}}^{A_\xi^{(2)}} lk\, dA_\xi. \tag{3.39}$$

Similarly, for the extraction rate per unit length of energy at infinity, we have

$$\dot{\mathcal{M}}=-\frac{1}{4\pi}\int_{A_\xi^{(1)}}^{A_\xi^{(2)}} ek\, dA_\xi. \tag{3.40}$$

For a Kerr black hole we shrink S_1 to the hole's symmetry axis and let S_2 approach the equatorial plane. Then Eqs. (3.39) and (3.40) become (7.5) of Ref. 7 modulo a factor of

4π (2π from the length $\int d\phi$, 2 from the reflection symmetry about the equatorial plane assumed for the MHD flow).

C. The wind equation and its solutions

For our stationary, symmetric system, we have just seen how most of the GRMHD equations can be integrated once, giving us one algebraic relation and five stream functions A_0, V^F, k, l, and e or f, whose values are determined by boundary conditions. From these and one other algebraic constraint

$$\gamma^2(1-\vec{V}^2)=1\,, \tag{3.41}$$

we can find out all the components of $\vec{V}$ and $\vec{B}$, once we have solved for A_ξ. To solve for A_ξ, we can express $\vec{V}$, $\vec{B}$, ρ_0, ..., in terms of stream functions and metric coefficients, and then substitute them into the remaining unintegrated force-balance equation. The result will be a second-order, nonlinear, partial differential equation. In general, we do not have analytic solutions to this equation. In the following, as did Phinney[7] (on whose work our 3+1 analysis is modeled), we will assume that this equation has already been solved for A_ξ and will leave the actual solution to numerical work; and following Phinney we shall concentrate on (3.41) and examine what constraint it puts on the stream functions in addition to those demanded by boundary conditions.

More specifically, what we shall do is express $\vec{V}$ and γ completely in terms of stream functions and metric coefficients, and then insert them into (3.41) to get a so-called ''wind equation'' for $V^P \equiv |\vec{V}^P|$. Actually, it turns out that using the components of four-velocity,

$$V_\xi \equiv \gamma V_\xi, \tag{3.42a}$$

$$V^P \equiv \gamma \vec{V}^P, \tag{3.42b}$$

makes the calculation simpler than working with V_ξ and $\vec{V}^P$ themselves. To derive the wind equation, we first use the definitions for l and f [Eqs. (3.32) and (3.34)] to eliminate B^ξ and γ from Eq. (3.27) and get an expression for V_ξ:

$$V_\xi = \frac{\alpha k l\, V^P - C f\, \gamma_{\xi\xi} B^P/\mu}{\alpha k \mu\, V^P + \gamma_{\xi\xi} B^P C^2 - \alpha^2 B^P}. \tag{3.43}$$

Here and below, we are to regard $\vec{B}^P$ as a function of the "known" quantity A_ξ, given by Eq. (3.19). By substituting (3.43) into (3.34), we get an expression for γ also in terms of known quantities and V^P:

$$\gamma = \frac{(f + Cl) k \mu\, V^P - \alpha f B^P}{\mu(\alpha k \mu\, V^P + \gamma_{\xi\xi} B^P C^2 - \alpha^2 B^P)}. \tag{3.44}$$

In terms of V_ξ and V^P, (3.41) is

$$\gamma^2 - V_\xi^2/\gamma_{\xi\xi} - (V^P)^2 = 1, \tag{3.45}$$

which can be manipulated into the form

$$D \equiv K \frac{(V^P - F_1)(V^P - F_2)}{(V^P - F_3)^2} - (V^P)^2 - 1 = 0. \tag{3.46}$$

Here,

$$K = \frac{(f + Cl)^2 k^2 \gamma_{\xi\xi} - \alpha^2 k^2 l^2}{\alpha^2 k^2 \mu^2 \gamma_{\xi\xi}}, \tag{3.47a}$$

$$F_1 = \frac{\sqrt{\gamma_{\xi\xi}}(\alpha + \sqrt{\gamma_{\xi\xi}} C f)}{\mu k [(f + Cl)\sqrt{\gamma_{\xi\xi}} + \alpha l]} B^P, \tag{3.47b}$$

$$F_2=\frac{\sqrt{\gamma_{\xi\xi}}(\alpha-\sqrt{\gamma_{\xi\xi}}Cf)}{\mu k[(f+Cl)\sqrt{\gamma_{\xi\xi}}-\alpha l]}B^P, \tag{3.47c}$$

$$F_3=\frac{\alpha^2-C^2\gamma_{\xi\xi}}{\alpha k\mu}B^P. \tag{3.47d}$$

Equation (3.46), with (3.47) substituted in, is the "wind equation" from which we can determine the structure of MHD flows.[7,17]

For the special case of an "isothermal equation of state,"

$$\mu=\frac{\rho+p}{\rho_0}=\text{const}, \tag{3.48}$$

all quantities in the wind equation except V^P can be regarded as known from the solution for A_ξ and from boundary conditions. Thus, the wind equation (3.46) can be solved for V^P, and the remaining flow structure can be computed algebraically from Eqs. (3.14), (3.27), (3.43), and (3.44). Thus, the flow structure is completely determined from (3.46). But for more realistic equations of state

$$\mu=\mu(\rho_0), \tag{3.49}$$

we must use (3.49) to eliminate μ from Eqs. (3.43)–(3.45); and it then may be easiest to use (3.45) directly as our wind equation. For ease of discussion below, we will assume an isothermal equation of state. This type of equation of state is also of interest because it includes the cold-flow limit, $p=0$.

For continuous flows (no shocks) the solutions to the wind equation (3.45) should extend smoothly from the region of interest to spatial infinity. However, for an arbitrary set of stream functions, D will generally become singular at critical surfaces where the flow speed equals one of the perturbation propagation speeds inside the stationary flow.

Either we have no solutions beyond these critical surfaces, or if energy and momentum conservation permit, we have shocks. To avoid such situations we have to constrain the stream functions in such a way that either these critical surfaces are pushed to or beyond spatial infinity, or the solutions pass through the critical surfaces smoothly.[7,17] To make our discussion more concrete, let us assume that we have parameterized the stream lines by a parameter y^P, which can be regarded as the coordinate length along the stream lines. Then the constraint equations for smooth passage through a critical surface as found by Kennel, Fujimura, and Okamoto[17] for special relativistic flow, which are also true general relativistically, are (see also Chap. V of Ref. 7)

$$\left.\frac{\partial D}{\partial V^P}\right|_{V=V_c^r,\, y^r=y_c^r}=0, \tag{3.50a}$$

$$\left.\frac{\partial D}{\partial y^P}\right|_{V=V_c^r,\, y^r=y_c^r}=0, \tag{3.50b}$$

where V_c^P is the flow speed on one of the critical surfaces, and y_c^P denotes one of the locations of the critical surfaces. Solutions with shocks will introduce many interesting processes into our problem. However, to handle shocks well, more careful analysis is required. In particular, to determine the structures of shocks, a detailed analysis of full plasma theory is required (see, for example, Ref. 18). Such an analysis is far beyond the scope of this paper.

IV. CONCLUSION

In this paper the GRMHD equations were rewritten in 3+1 language in a general spacetime. They were expressed as (i) evolution equations for the FIDO-measured magnetic field $\vec{B}$ and flow velocity $\vec{V}$ [Eqs. (2.13) and (2.22)], and the fluid's rest mass

density ρ_0 [Eq. (2.24)]; (ii) the frozen-in condition of perfect MHD [Eq.(2.12)]; and (iii) algebraic constraining equations on the magnetic field [Eq. (2.6)] and thermodynamic variables [the equation of state (2.26′) or (2.27)]. Then for a stationary, symmetric flow in a stationary, symmetric spacetime these equations were reduced to a wind equation (3.46) from which one determines $\mathcal{V}^P$ (given A_ξ as known), and the algebraic relations (3.14), (3.27), (3.43), and (3.44) from which one computes ρ_0, $\vec{V}^P$, V^ξ, and B^ξ for an isothermal equation of state. With A_ξ given or calculated from a nonlinear partial differential equation derived from (2.22), $\vec{B}^P$ is calculated using (3.19).

In a future paper the author will use this formalism to build stationary, symmetric MHD model magnetospheres, and will linearize the evolution equations to study dynamic perturbations of those magnetospheres so as to gain insight into the dynamical effects of the coupling of the magnetic field to the gravitomagnetic field.

ACKNOWLEDGMENTS

The author would like to thank Kip Thorne for many useful discussions and helpful suggestions during the course of this work and in writing this paper. He has also benefited from discussions with Sterl Phinney. Partial support of this work by NSF Grant No. AST85-14911 is also acknowledged.

[1] E. R. Priest, *Solar Magneto-Hydrodynamics* (Reidel, Holland, 1982); E. N. Parker, Astrophys. J. **122,** 293(1955).

[2] P. Goldreich and W. H. Julian, Astrophys. J. **157,** 869(1969).

[3] Jacob D. Bekenstein and Eliezer Oron, Phys. Rev. D **18,** 1809(1978); **19,** 2827(1979).

[4] A. Lichnerowicz, *Relativistic Hydrodynamics and Magnetohydrodynamics* (Benjamin, New York, 1967).

[5] T. Damour, Ann. N.Y. Acad. Sci. **262,** 113(1975).

[6] J. H. Sloan and L. Smarr, in *Numerical Astrophysics,* edited by J. M. Centrella, J. M. Le Blanc, and D. L. Bowers (Jones and Bartlett, Boston, 1985).

[7] E. S. Phinney, Ph.D. dissertation, University of Cambridge, 1983.

[8] E. S. Phinney (unpublished).

[9] C. Evans and J. Hawley, Astrophys. J., **332,** 659(1988).

[10] K. S. Thorne, R. H. Price, and D. A. Macdonald, *Black Holes: The Membrane Paradigm* (Yale University Press, New Haven, CT, 1986).

[11] R. D. Blandford and R. L. Znajek, Mon. Not. R. Astron. Soc. **179,** 433(1972).

[12] Douglas Macdonald and Kip S. Thorne, Mon. Not. R. Astron. Soc. **198,** 345(1982).

[13] J. M. Bardeen, in *Black Holes,* edited by C. Dewitt and B. S. Dewitt (Gordon and Breach, New York, 1973).

[14] James W. York, Jr., in *Sources of Gravitational Radiation,* edited by Larry L. Smarr (Cambridge University Press, England, 1979).

[15] Kip S. Thorne and Douglas Macdonald, Mon. Not. R. Astron. Soc. **198,** 339(1982).

[16] C. W. Misner, K. S. Thorne, and J. A. Wheeler, *Gravitation* (Freeman, San Francisco, 1973).

[17] C. F. Kennel, F. S. Fujimura, and I. Okamoto, Geophys. Astrophys. F Dyn. **26,** 147(1983).

[18] D. P. Cox, Astrophys. J. **178,** 143(1972); J. C. Raymond, Astrophys. J. Suppl. **39,** 1(1979).

FIG. 1. Magnetic flux inside flux tube bounded by C is $\Psi(\vec{x})=\oint_C A_\xi d\xi = A_\xi \oint_C d\xi$. (a) When Ψ and $\oint_C d\xi$ are finite, A_ξ is clearly the flux per unit length of C within the tube; (b) when $\oint_C d\xi$ is not finite; e.g., if $\vec{m}$ is a translational symmetry and C extends to infinity, Ψ is infinite unless A_ξ vanishes. For any finite A_ξ, we use the ξ symmetry and consider only a small portion δL of curve C. Then $\delta\Psi=A_\xi \delta L$ and we can still think of A_ξ as the flux per unit length of C within the flux tube.

FIG. 2. (a) The generalized momentum and energy are transported from one region to another between flux tubes S_1 and S_2. On a two-dimensional surface S_{up}, whose normal is orthogonal to $\vec{m}$, these flux tubes are bounded by integral curves C_1 and C_2 of $\vec{m}$. S_{down} is another two-dimensional surface whose normal is also orthogonal to $\vec{m}$. (b) When the length of integral curves of $\vec{m}$ is unbounded, e.g., when $\vec{m}$ corresponds to a translation, we consider a portion of flux sheets S_1 and S_2 of width δL and the generalized momentum and energy at infinity transported within δL between integral curves C_1 and C_2.

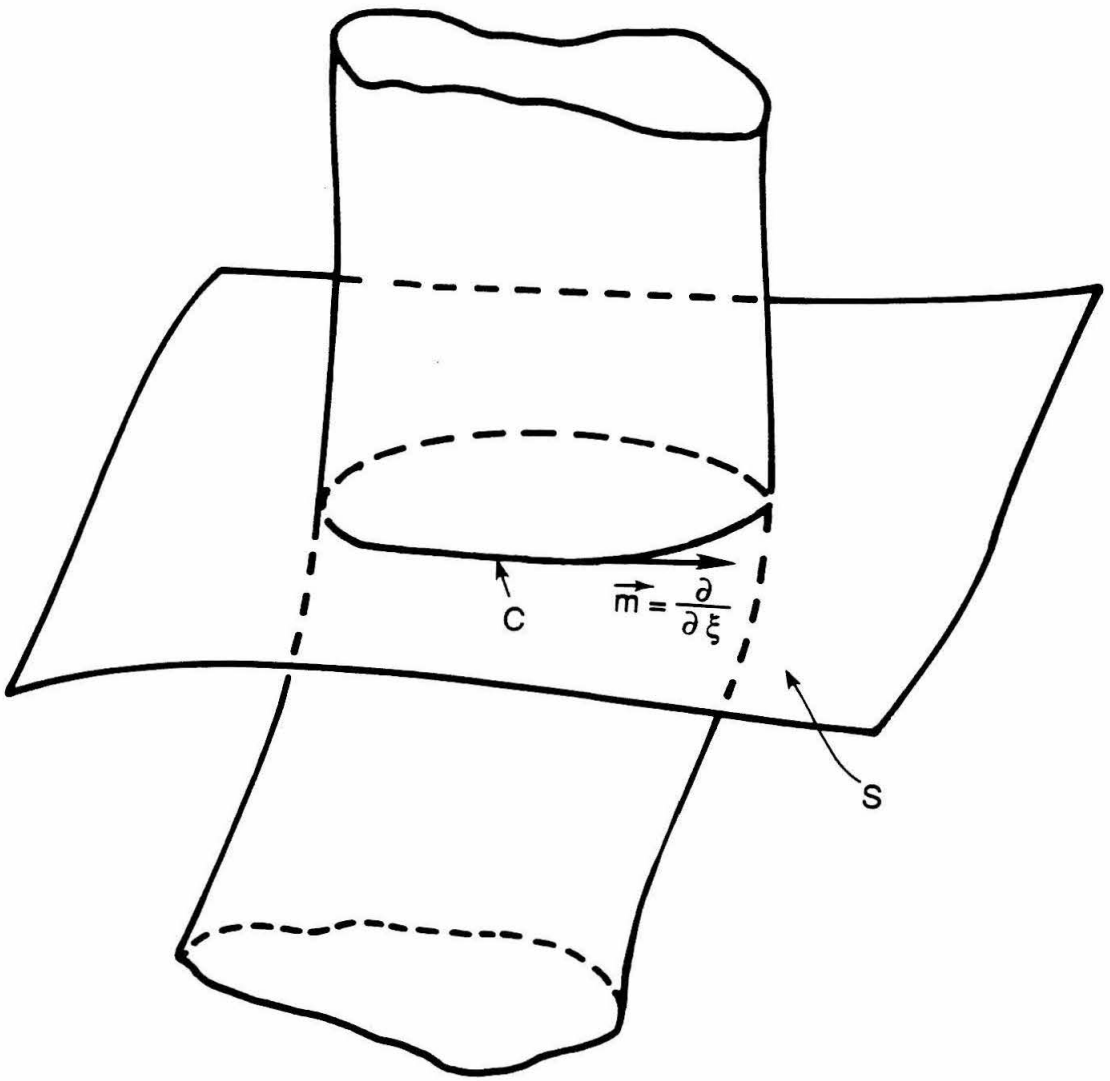

Fig. 1 a)

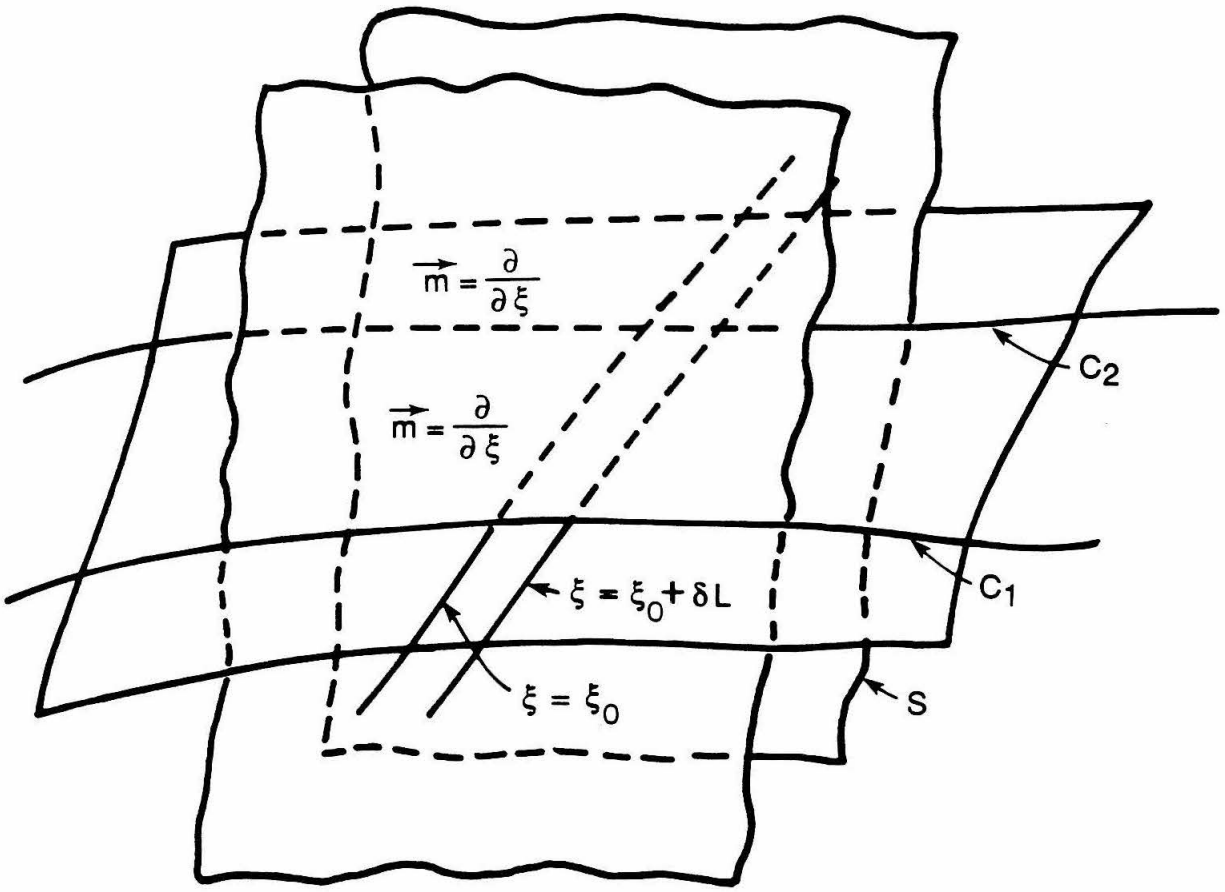
$\vec{m} = \frac{\partial}{\partial \xi}$
$\vec{m} = \frac{\partial}{\partial \xi}$
C_2
C_1
$\xi = \xi_0 + \delta L$
$\xi = \xi_0$
S

Fig. 1 b)

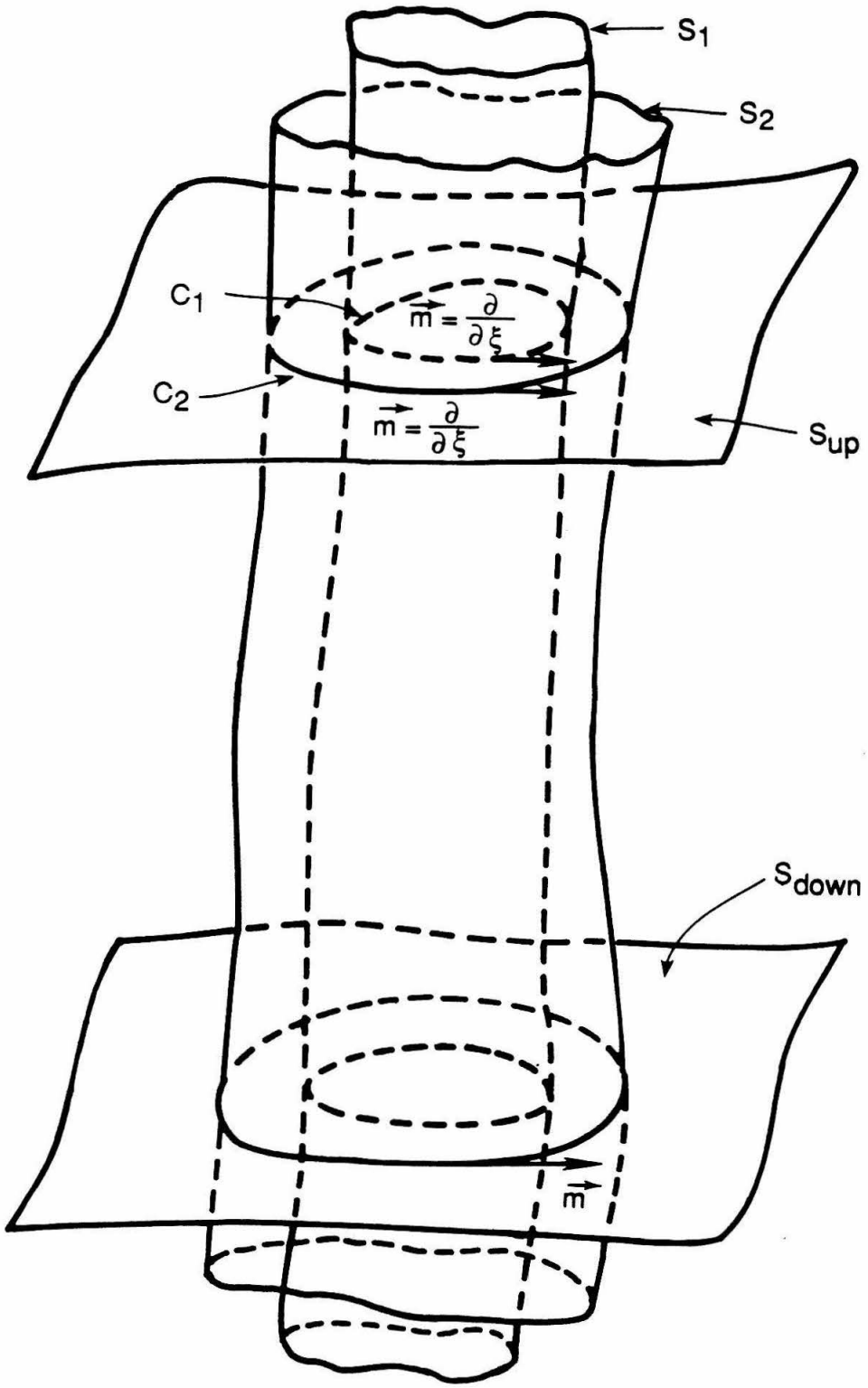
S_1
S_2
C_1
$\vec{m} = \frac{\partial}{\partial \xi}$
C_2
$\vec{m} = \frac{\partial}{\partial \xi}$
S_{up}
S_{down}
$\vec{m}$

Fig. 2 a)

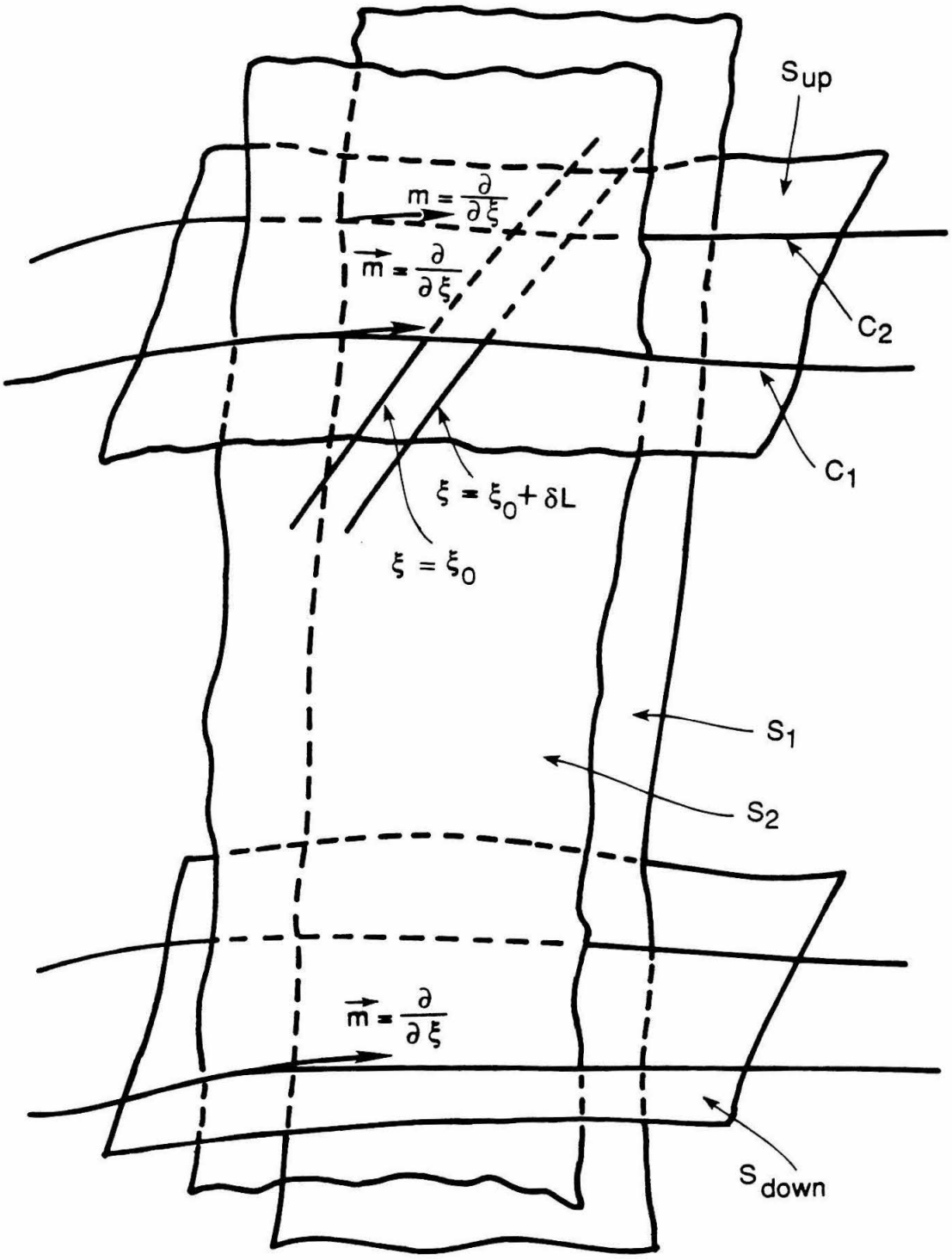
S_{up}
$\vec{m} = \frac{\partial}{\partial \xi}$
$\vec{m} = \frac{\partial}{\partial \xi}$
C_2
C_1
$\xi = \xi_0 + \delta L$
$\xi = \xi_0$
S_1
S_2
$\vec{m} = \frac{\partial}{\partial \xi}$
S_{down}

Fig. 2 b)

Chapter V

THE INTERACTION OF MAGNETOHYDRODYNAMIC WAVES WITH GRAVITOMAGNETIC FIELDS, AND THEIR POSSIBLE ROLES IN BLACK-HOLE MAGNETOSPHERE

(To be submitted to *Phys. Rev.*)

The interactions of magnetohydrodynamic waves with gravitomagnetic fields, and their possible roles in black-hole magnetospheres

ABSTRACT

The magnetospheres of rotating, magnetized black holes are thought to generate some of the jets observed in quasars and active galactic nuclei. Previous research on such magnetospheres has focussed on stationary configurations. This paper is an initial, exploratory study of dynamical magnetospheres. Because a dynamical study in a rotating hole's Kerr spacetime would be exceedingly difficult, this paper introduces a class of simpler, plane-symmetric or cylindrically symmetric model spacetimes in which to explore the dynamics. These model spacetimes preserve the key physical features of the Kerr geometry: they have a Kerr-like gravitomagnetic potential (shift function), a Kerr-like horizon, and a Kerr-like asymptotically flat region far from the horizon. This first exploratory study is restricted to the simplest of these spacetimes, one with the planar metric $ds^2=-dt^2+(dx+\beta dt)^2+dy^2+dz^2$, gravitomagnetic potential $\beta=V_F(\tanh z-1)$, and horizon lateral velocity $dx/dt=2V_F$. In this spacetime the asymptotically flat region is at $z\gg 1$, and the horizon has been pushed off to $z=-\infty$. Kerr-like models of stationary magnetospheres are built in this spacetime as exact solutions to the fully nonlinear equations of general relativistic magnetohydrodynamics (GRMHD). In these

solutions the magnetic field, under the influence of the horizon's lateral motion, is driven to move laterally with velocity $dx/dt=V_F$; and plasma particles (e^+e^- pairs) are created at $z=0$, and are then driven up to relativistic velocities by magnetic-gravitomagnetic coupling, as they flow off to ''infinity'' ($z=+\infty$) and down toward the ''horizon'' ($z=-\infty$). Weak perturbations of these analytic magnetospheres are studied using a linearization of the GRMHD perturbation equations. The linearized perturbation equations are Fourier-analyzed in t and x [$\exp(-i\,\omega t+ik_x x)$] and are solved numerically to obtain the z dependence of the perturbations. The numerical solutions describe the response of the magnetosphere to oscillatory driving forces in the plasma-injection plane, $z=0$. This models the response of a Kerr hole's magnetosphere to oscillatory driving forces near the plasma-production region — forces that might arise when lumpy magnetic fields, anchored in an accretion disk, orbit the hole, pressing inward on the magnetosphere. In our model spacetime the magnetosphere responds resonantly at frequencies (as measured at infinity) $\omega=k_x V_F$, i.e., at frequencies for which the perturbations are stationary as seen in the field lines' rest frame. The analog for a Kerr magnetosphere would be resonant responses at $\omega=m\,\Omega_F$, where m is the azimuthal quantum number of the perturbation and Ω_F is the field-line angular velocity (roughly equal to half the horizon angular velocity). Such resonances, if they occur in real black-hole magnetospheres, would show up as a modulation of the jet's outflowing energy flux.

I. INTRODUCTION

In recent decades, the huge energy output (up to $\sim 10^{48}$ ergs/sec) from active galactic nuclei (AGN's) has been firmly established, and theories using a supermassive central black hole ($\sim 10^8 M_\odot$) to explain this energy output have been developed and become well accepted.[2] There are also some recent observations that suggest the existence of supermassive black holes at the centers of some nearby galaxies.[3]

One of the most attractive models for powering jets in AGN's is electrodynamical (or MHD) extraction of the rotational energy of a magnetized, supermassive black hole,[4,5,6] the ''Blandford-Znajek effect.'' In this model the hole is threaded by a magnetic field, which is held on it by the Maxwell pressure of surrounding fields that are anchored in an accretion disk. (If the disk were suddenly removed, the field threading the hole would fly away.) The rotation of the hole (as embodied in the hole's ''gravitomagnetic potential'' or ''shift function'' $\vec{\beta}$) interacts with the threading magnetic field $\vec{B}$ to produce an intense electric field $\vec{E}$, which in turn accelerates charged particles to high speeds, causing them to radiate or Compton scatter. The resulting high-energy photons then interact with the charged particles or the $\vec{B}$-field to produce a rich plasma of electron-positron pairs.[7,8,9] In this way, the hole's magnetosphere is kept filled with plasma. The plasma is created near the hole (at something like 2 black-hole radii). The rotation of the hole and its magnetic field lines (i.e., the ''gravitomagnetic-magnetic coupling''), then drives some of the plasma to flow into the horizon and some off toward infinity, forming an MHD wind, which becomes the observed jet when far from the hole.

All previous studies of this model have focused on stationary, steady-state magnetospheres. This has been justified by the fact that the hole's horizon ''cleans'' the field lines that thread it,[5,10] leaving them (approximately) smooth and axisymmetric. More specifically: The horizon-threading $\vec{B}$-field was originally, long ago, embedded in the accretion disk. Differential rotation of the disk amplified the field and then reconnection

made it tangled and chaotic. This chaotic field was then carried onto the horizon by the disk's accreting plasma, and the horizon then quickly "cleaned" the field; i.e., it got rid of all closed loops and helped the remaining field to distribute itself in a smooth, approximately axisymmetric way, over the horizon.

Despite this cleaning process, the hole's $\vec{B}$-field should not be precisely axisymmetric. Nonaxisymmetric perturbations will be produced by the external agent that holds the field on the hole — the chaotic, disk-anchored $\vec{B}$-field that presses in on the smoother, hole-threading field. As lumps of disk-anchored field orbit the hole, their Maxwell pressure will buffet the hole-threading field, thereby creating (near the plasma-production region) oscillatory perturbations of the magnetosphere. These perturbations presumably will give rise to MHD waves, some of which propagate into the horizon and others off toward infinity, along with the accelerated plasma. The result should be an oscillatory modulation of the energy carried by the magnetosphere's wind and jet.

This scenario for nonaxisymmetric effects in a black-hole magnetosphere is totally speculative, since nobody has yet attempted an analysis of dynamical, nonaxisymmetric perturbations. The purpose of this paper is to carry out a first, exploratory analysis of such perturbations.

Even in the stationary, axisymmetric case, the modeling of a black-hole magnetosphere is very difficult: Blandford and Znajek[4] simplified their original analysis by focusing attention, primarily, on the near-horizon region, which they assumed to be force-free, axisymmetric, and stationary. Macdonald[11] succeeded in solving numerically the two-dimensional, partial-differential stream equation for the structure of the force-free region; but his analysis and that of Blandford and Znajek had to assume somewhat arbitrary boundary conditions at the outer edge of the force-free region, where plasma inertia begins to be important. In order to obtain an unified, global treatment of the entire stationary magnetosphere (the inner force-free region, the wind region, the jet

region), Phinney[6] assumed that the plasma would everywhere be so highly conducting that perfect MHD describes it well; and then, with the aid of a clever analysis of the magnetosphere's boundary conditions (and avoiding the task of actually solving the MHD version of the stream equation), he was able to infer a variety of properties of the outflowing MHD wind and jet.

To solve the MHD stream equation in the Kerr spacetime of a rotating hole is so difficult that nobody has yet tackled it, so far as we know — except in the case of a non-rotating hole.[12,13] To solve for the dynamical behavior of a perturbed magnetosphere in the Kerr spacetime would be even more difficult.

The difficulties are so great that we have chosen a different route: We have altered the spacetime in which the magnetosphere lives so as to simplify the analysis. The main source of difficulty with the Kerr spacetime is its low symmetry: it is stationary (independent of time t) and axisymmetric (independent of angle ϕ); but that is all: it has nontrivial dependences on radius r and polar angle θ. To make the analysis tractable, we add one more symmetry — and demand that it be a symmetry not only of the spacetime, but also of the equilibrium magnetosphere — and we do so while preserving the key features of the Kerr metric: its horizon, its asymptotically flat distant region, and its gravitomagnetic potential. The resulting, altered spacetimes and their horizons are all cylindrical or planar; see Sec. II for full details.

These model spacetimes should be useful not only for getting insight into dynamical perturbations of a black-hole magnetosphere (the goal of this paper), but also for studying the details of how such a magnetosphere, when first formed, settles down into its equilibrium configuration. That settling down and the resulting equilibrium are a subject of current controversy: one issue is whether the equilibrium state will be that of Blandford and Znajek, which can extract the hole's rotational energy via electrodynamic process.[14,15]

In this paper we study magnetospheric dynamics in the simplest of the model spacetimes: one with the planar metric

$$ds^2=-dt^2+(dx+\beta dt)^2+dy^2+dz^2\,, \tag{1.1}$$

which has a gravitomagnetic potential (shift function) $\vec{\beta}=\beta\partial/\partial x$ where

$$\beta=V_F(\tanh z-1)\,. \tag{1.2}$$

(We shall henceforth refer to the scalar field β as the shift function.) In this spacetime the asymptotically flat region is at $z\gg 1$, and the horizon has been pushed off to $z=-\infty$; i.e., it has been converted into a second asymptotically flat region. Our reason for getting rid of the horizon is our desire to study, as cleanly and simply as possible, the interaction of the gravitomagnetic potential β with the magnetosphere. We strongly suspect (but only future calculations will show for sure) that the horizon is rather unimportant: The key gravitational influences on the magnetosphere are all due to the the gravitomagnetic potential. The z direction in this spacetime is the analog of the radial, r direction in Kerr; the x direction is the analog of Kerr's axial, ϕ direction; the y direction is the analog of Kerr's poloidal θ direction; and t is the analog of the Kerr metric's time coordinate t. The Kerr metric depends nontrivially on both r and θ, whereas the metric (1.1) depends nontrivially on only z. In our model spacetime (1.1) the ''horizon,'' $z=-\infty$, moves in the x direction with speed $dx/dt=2V_F$ relative to ''infinity,'' $z=+\infty$. This is analogous to the rotational motion of a Kerr hole's horizon with angular velocity $d\phi/dt=\Omega_H$ relative to infinity, $r=+\infty$.

In Secs. III and IV we build models for stationary magnetospheres in this model spacetime. Our models are exact, analytic solutions to the general relativistic magnetohydrodynamic (GRMHD) equations, with the plasma assumed for simplicity to be ''cold'' (negligible particle pressure). The magnetosphere's magnetic field lines extend

out of the ''horizon'' ($z=-\infty$) and off to ''infinity'' ($z=+\infty$). The plasma is created in the central plane $z=0$ [analog of the plasma creation region $r\sim 2$(black-hole radii) in Kerr]; and some of the plasma then flows down to the ''horizon,'' while the rest flows off to ''infinity.'' The perfect conductivity of the flowing plasma forces the field lines to move rigidly in the x-direction with a velocity equal to half the horizon's velocity, $dx/dt=V_{\rm F}$. The outflowing plasma is accelerated along the $\vec{B}$-field lines by the joint action of the field line motion and the gravitomagnetic potential — i.e., by ''magnetic-gravitomagnetic coupling.'' The asymptotic velocity of the plasma as it approaches $z=\pm\infty$ is always less than or equal to the speed of fast magnetosonic waves.

In Secs. V and VI we analyze weak, linearized perturbations of our stationary magnetospheric models — with the perturbations confined, for simplicity, to the x-z plane (no dependence on y). Section V derives a set of linearized GRMHD equations for the perturbations [Eqs. (5.6)] and a set of junction conditions at the $z=0$ (plasma production) plane [Eqs. (5.7)]. These two sets of equations are then Fourier-analyzed in time and space, so that all perturbation quantities oscillate as $\exp(-i\omega t+ik_x x)$ with ω the angular frequency and k_x the lateral wave number.

The resulting ordinary differential equations (5.13) are solved numerically in Sec. VI to determine the z-dependence of the magnetosphere's response to oscillatory driving ''forces'' that are applied in the plasma production plane, $z=0$. In general, the magnetosphere responds with oscillations of its magnetic field and plasma. The oscillations develop into a superposition of downgoing and upgoing plasma waves as they propagate into the regions $z\lesssim -1$ and $z\gtrsim +1$. At $z\ll -1$ and $z\gg +1$, where the equilibrium magnetosphere is homogeneous, the waves can be resolved into MHD modes: a fast magnetosonic mode (which typically carries most of the energy), and two slow magnetosonic modes, which are frozen into the plasma because of the assumption of vanishing plasma pressure. These waves modulate the energy flux carried by the magnetosphere's wind.

Our numerical solutions are restricted to just one equilibrium magnetosphere (an equilibrium shown in Fig. 3), but they cover a wide range of angular frequencies ω and lateral wave numbers k_x, and a complete set of driving ''forces'' that act in the plasma-production plane, $z=0$. Each driving ''force'' is characterized by the amplitude f_x of the sinusoidal oscillations of x-momentum injected into the magnetosphere, the amplitudes $f_E^{\pm}$ of energy injected upward and downward, and the amplitudes $N^{\pm}$ of plasma rest mass injected upward and downward. The results of the numerical integrations are shown in a huge number of figures: Figs. 5—19; and the numerical methods used are discussed in an appendix.

Most interesting are injections of x-momentum (i.e., f_x driving ''forces''), since they correspond most closely to the buffeting pressure of lumpy external $\vec{B}$-fields that push in on a black-hole magnetosphere. For these ''forces'' the most interesting feature of the numerical solutions is a resonance that shows up in the magnetosphere's response. This resonance occurs when the angular frequency, as measured in the common rest frame of the magnetic field and newly injected plasma, vanishes:

$$\omega_F \equiv \omega - k_x V_F = 0 \,. \tag{1.3}$$

For a black hole with perturbations $\propto \exp(-i\,\omega t + im\,\phi)$, the analogous resonance would be at

$$\omega_F \equiv \omega - m\,\Omega_F = 0 \,, \tag{1.4}$$

where Ω_F is the field-line angular velocity, and is roughly equal to half the horizon's angular velocity Ω_H. Correspondingly, if our simple magnetospheric model is a reasonable guide (and it might not be!), then the buffeting of the magnetosphere by surrounding, lumpy, accretion-disk $\vec{B}$-fields might produce modulations of the energy flux in the wind and jet at characteristic frequencies $\omega \approx (m/2)\Omega_H$.

For our simple planar model the resonance shows up both as peaks in the response of the magnetosphere near $z=0$ to the driving force (sharp ridges along the lines $\omega=2k_x$ in Figs. 15), and as peaks in the amplification of the perturbations as they propagate from $z=0$ to $z\gg1$ (sharp ridge in Fig. 12a). On resonance, where the magnetosphere's response is strongest, the fractional modulation of the upward energy flux, as measured at $z=0$ in the rest frame of the magnetic field and the newly injected plasma, is

$$\frac{\delta S_z(z=0)}{S_z(z=0)}\simeq 1.15\frac{\delta T_{xz}}{T_{xz}} . \tag{1.5a}$$

Here $\delta T_{xz}/T_{xz}$ is the driving force's fractional modulation of the magnetosphere's momentum flux (stress tensor) at $z=0$. (The quantity f_x is δT_{xz} divided by the upward flux of rest mass in the equilibrium magnetosphere.) During upflow from $z=0$ to $z=+\infty$, the gravitomagnetic-magnetic interaction amplifies the energy flux of the unperturbed magnetosphere by a factor of 80, while amplifying the perturbations by only a factor of 19:

$$\frac{S_z(z\gg1)}{S_z(z=0)}\simeq 80 , \quad \frac{\delta S_z(z\gg1)}{\delta S_z(z=0)}\simeq 19 . \tag{1.5b}$$

(If off-resonance, this ''amplification factor'' for perturbations is usually in the range 0.2 to 3.) Correspondingly, on resonance the distant wind's energy flux is modulated by a factor $1.15\times(19/80)\simeq 0.3$:

$$\frac{\delta S_z(z\gg1)}{S_z(z>>1)}\simeq 0.3\frac{\delta T_{xz}(z=0)}{T_{xz}(z=0)} . \tag{1.5c}$$

Thus, on resonance the fractional oscillatory response of the distant wind is roughly equal in magnitude to the fractional oscillatory driving force, while off resonance the response will be far smaller.

For a Kerr hole's magnetosphere, the maximum possible value of the driving force of the buffeting $\vec{B}$-fields is $\delta T_{ij}/T_{ij} \simeq 1$, and it may well be that typical magnetospheres are buffeted with $\delta T_{ij} \ll 1$. Thus, if our simple model is a reasonable guide, then the resonant modulation of the wind might not be large enough for detection.

These implications of our calculations for black-hole magnetospheres are discussed more fully in Sec. VII, and possible directions for further research are discussed in Sec. VIII.

II. MODEL SPACETIMES IN WHICH TO STUDY INTERACTIONS OF PLASMA WITH RELATIVISTIC GRAVITY

As was discussed in the introduction, the dynamics of a black-hole magnetosphere is very complicated to analyze if one insists on using, as the hole's spacetime geometry, the (realistic) Kerr solution to the Einstein field equations. One of the major sources of difficulty is that the analysis must be 2+1 dimensional (two space dimensions plus one time dimension). Another source of difficulty is the inherent complexity of the MHD equations.

When dealing with vacuum electrodynamics around a black hole, the second difficulty is eased considerably: the vacuum Maxwell equations are far less complex than the MHD equations. Nevertheless, little progress was made on vacuum electrodynamics until Teukolsky[16] eased the first difficulty as well, by showing how to separate variables in the vacuum Maxwell equations and thereby converted the analysis from 2+1 dimensions to 1+1.

Since, even in flat spacetime, the MHD equations are inherently far more complex than vacuum Maxwell equations, it seems unlikely that the ''complexity'' difficulty will ever be eased much for MHD around black holes. It also seems unlikely that the MHD equations will ever be converted into a form, in the Kerr spacetime, that permits reduction from 2+1 dimensions to 1+1. In view of this fact, it may be that the most reasonable method to get insight into the dynamics of MHD black-hole magnetospheres is to switch from the realistic Kerr metric to more idealized spacetime metrics that admit a 1+1 analysis, but still preserve the key features of a rotating black hole.

The key features of a rotating black hole are nicely isolated from each other by a ''3+1 split'' of the spacetime metric:[17,18]

$$ds^2=-\alpha^2 dt^2+\gamma_{ij}(dx^i+\beta^i dt)(dx^j dt+\beta^j dt). \tag{2.1}$$

The quantities α (''lapse function''), β^i (''shift function'' or ''gravitomagnetic potential''), and γ_{ij} (''spatial metric'') can be thought of as 3-dimensional scalar, vector, and tensor fields that reside in 3-dimensional space (with spatial coordinates x^i) and evolve with the passage of time t. The lapse function α embodies the Newtonian-type gravitational acceleration of the black hole, the gravitational redshift of the ticking rates of clocks, and also the existence and structure of the black-hole horizon (the location at which α goes to zero). The shift function β^i embodies the dragging of inertial frames that is due to rotation of the hole, the storage of rotational energy in the hole's external gravitational field, and it is also the entity by which the rotational energy can be coupled out into electromagnetic fields and particles, thereby driving MHD winds and perhaps amplifying MHD waves. The spatial metric γ_{ij} embodies the geometry of space, both near the hole and far away, and thereby, for example, it produces a significant portion of the deflection of light rays by the hole's gravitational field.

It seems evident that for black-hole magnetospheres the most important of the above phenomena are (i) the storage and release of the hole's rotational energy, as embodied in β^i; and (ii) the hole's Newton-type gravitational attraction and especially its horizon, as embodied in α. Far less important should be the spatial geometry, γ_{ij}.

In order to produce a reasonably simple 1+1 dimensional magnetosphere without losing the key features of a real black hole, then, it seems reasonable to use an idealized, model spacetime in which (i) the spatial metric γ_{ij} is flat; (ii) there is a nonzero shift function β^i — which is inhomogeneous, so its curl, the "gravitomagnetic field"[10] is nonvanishing; (iii) there is a nonzero lapse function α which goes to zero linearly with proper distance from a horizon; and (iv) the shift and lapse functions are invariant under time translations and under displacements along two of the symmetry directions of the flat space (i.e., the full spacetime possesses one temporal and two spatial Killing vector fields). (Here implied is the assumption that the stationary MHD magnetosphere, whose dynamics one wishes to study, has the same symmetry as the gravitational background.) It is this last requirement that will permit the existence of 1+1 dimensional, dynamical MHD magnetospheres. We should also require that far from the horizon the lapse function α and the shift function β^i asymptote to unity and zero, respectively, so the spacetime becomes flat; and, by analogy with a Kerr black hole, α should increase monotonically and the absolute value of β^i should decrease monotonically as one goes outward from the horizon to "infinity."

There are just two types of spacetimes with these properties. In one α and β^i are invariant under rotational ($\partial/\partial\phi$) and translational ($\partial/\partial z$) symmetries; i.e., the spacetime is cylindrical:

$$ds^2=-\alpha^2(r)dt^2+dr^2+dz^2+r^2[d\phi^2+\beta(r)dt]^2 . \qquad (2.2)$$

In the other, α and β^i are invariant under two translation symmetries ($\partial/\partial x$ and $\partial/\partial y$);

i.e., the spacetime is planar:

$$ds^2=-\alpha^2(z)dt^2+[dx+\beta(z)dt]^2+dy^2+dz^2. \tag{2.3}$$

In the cylindrical spacetime (2.2) α vanishes at a cylindrical horizon $r=r_H$, and it increases monotonically from 0 to 1 as r goes from r_H to ∞; and β takes on a maximum absolute value, β_H (the cylindrical horizon's angular velocity) at $r=r_H$, and it decreases monotonically to zero as r increases to ∞. In the planar spacetime (2.3) α vanishes at a horizon which we can place at $z=0$, and it increases monotonically to unity as z increases from 0 to ∞; and the absolute value of β takes on a maximum value, β_H (the horizon's linear velocity relative to infinity) at $z=0$, and it decreases monotonically to zero at $z\rightarrow\infty$. Note that the cylindrical spacetime (2.2) and its stationary MHD magnetosphere have the nice feature that as in flat spacetime, so also here, magnetic field lines that thread the horizon will diverge from each other as they reach out to infinity (circumference increases in proportion to radius r). By contrast, the planar spacetime (2.3) and its stationary MHD magnetosphere have the nice computational features that (i) all aspects of the magnetosphere should become asymptotically z-independent at large z, and (ii) the nondivergence of magnetic field lines at infinity turns out to push a stationary magnetosphere's fast magnetosonic point off to $z\rightarrow\infty$, thereby saving us from struggling with the computational complexities of smooth transitions through that sonic point.

In this paper we are not even so ambitious as to study MHD magnetospheres in these two model spacetimes. Rather, as a first step in seeking insight into the dynamical MHD interaction of plasmas with rotating-black-hole-type gravity, we shall isolate out just one aspect of the gravitational interaction and study it by itself. Our chosen aspect, of course, will be the shift function β with its storage and release of the spacetime's rotational (or translational) energy. We shall isolate it by working with a modified version of the planar spacetime (2.3) in which the lapse function α is unity everywhere (no horizon;

no redshifts)

$$ds^2=-dt^2+[dx+\beta(z)dt]^2+dy^2+dz^2\ , \tag{2.4}$$

while the value of the shift function β decreases monotonically from 0 at $z\to\infty$ to some constant value (denoted below as $-2V_F$) at $z\to-\infty$. The specific form we shall use for β is

$$\beta(z)=V_F(\tanh z-1)\ . \tag{2.5}$$

As we shall see, in this very simple spacetime, as in the Kerr spacetime of a real black hole, the shift function β drives an MHD wind which can extract translational energy (rotational energy for Kerr) from the spacetime's gravitational field. Stationary MHD winds in this spacetime are very similar to those in the Kerr metric; and in this spacetime, by contrast with Kerr, it is a manageable problem to study dynamical perturbations of such a wind — the principal objective of this paper.

We should mention that the spacetimes (2.1)—(2.4) are not empty (as can be seen by a straightforward calculation of their Ricci tensor). This is not important for our analyses, however. Because these spacetimes are merely testbeds for studying various aspects of the interaction of relativistic gravity with plasmas, we are free to (and shall) assume that there is no direct, nongravitational interaction between the plasmas we study and the ''materials'' whose stress-energy produce the spacetime curvature.

We regard this paper as just a first step in trying to understand dynamical magnetospheres of black holes. The next, very important step will be to restore a horizon-producing lapse function to the spacetime, i.e., to study MHD in the spacetimes (2.2) and (2.3) rather than (2.4). We shall comment further on this next step in the conclusion of this paper, Sec. VIII below.

III. MHD IN A PLANAR SPACETIME WITH SHIFT BUT NO LAPSE

It is reasonable to expect that in any spacetime with three killing vector fields (one timelike and two spacelike), and for a magnetized dissipation-free plasma, there are MHD equilibrium states whose structure can be analyzed purely algebraically (no differential equations to solve!). In this section we shall exhibit an explicit example of this: the algebraic structure of plane-symmetric, stationary flows of a zero-temperature MHD fluid in our model spacetime (2.4). The flows we shall construct will be used in subsequent sections as stationary model "magnetospheres" whose dynamical perturbations are to be studied.

Before proceeding further, let us introduce a few definitions. We will use a 3+1 notation consistent with that of the membrane paradigm,[10] even though we have not included a horizon here. All vector-analysis notations such as the gradient, curl, and vector cross product will be those of the 3-dimensional absolute space whose 3-metric is δ_{ij}, the Kroneck delta (see Sec. II A of Ref. 1). All quantities will be those measured by FIDO's (fiducial observers), whose 4-velocity is

$$\vec{n}=\frac{\partial}{\partial t}-\beta\frac{\partial}{\partial x} \tag{3.1}$$

in our model spacetime (2.4). The FIDO-measured fluid velocity of our plasma is described by a spatial vector field lying in the $x-z$ plane:

$$\vec{V}=V(z)\vec{e}_x+u(z)\vec{e}_z\ . \tag{3.2}$$

This fluid velocity is related to the components U^{μ} of the fluid 4-velocity in the coordinate system (2.4) by

$$U^0=\gamma\ ,\quad U^x=\gamma(V-\beta)\ ,\quad U^y=0\ ,\quad U^z=\gamma u\ , \tag{3.3}$$

where γ is the Lorentz factor,

$$\gamma \equiv \frac{1}{\sqrt{1-u^2-V^2}}; \tag{3.4}$$

i.e., the $\vec{V}$ of (3.2) is the standard 3+1 embodiment of the 4-velocity (3.3). For further details on 3+1 splits of 4-dimensional quantities see York,[18] Ref. 10, and the references cited therein. The FIDO-measured magnetic field is also assumed to lie in the $x-z$ plane:

$$\vec{B} = B\,[\lambda(z)\vec{e}_x + \vec{e}_z]. \tag{3.5}$$

Here B, the z-component of $\vec{B}$, is a constant as guaranteed by the vanishing divergence of the magnetic field [Eq. (2.6) of Ref. 1; see also Eq. (5.8b) of Ref. 19]. The electric field $\vec{E}$ generated by the fluid's motion relative to the FIDO's will be in the y-direction,

$$\vec{E} = -\vec{V} \times \vec{B} = E_y \vec{e}_y. \tag{3.6}$$

The magnetic field $\vec{B}$ and the electric field $\vec{E}$ are related to the electromagnetic field tensor $F_{\mu\nu}$ and its dual ${}^*F^{\mu\nu}$ via

$$E^i = -F_\mu{}^i n^\mu, \tag{3.7}$$

$$B^i = {}^*F_\mu{}^i n^\mu. \tag{3.8}$$

We shall assume for simplicity that the plasma has vanishing thermal pressure and vanishing thermal energy density; i.e., we shall restrict ourselves to a ''cold plasma,'' for which the total density of mass-energy ρ and the rest-mass density ρ_0 are the same:

$$p = 0\,, \quad \rho = \rho_0\,, \tag{3.9}$$

and

$$\mu \equiv \frac{p+\rho}{\rho_0} = 1. \tag{3.10}$$

This assumption has been used previously, for example, by Michel[20] and by Okamoto[21] in their studies of relativistic stellar winds. In our study it will allow much of the stationary solution to be analyzed analytically, given some additional symmetry requirements.

In our geometry (2.4), the "poloidal" direction, the direction orthogonal to $\vec{\beta}$, is $\vec{e}_z$; so u, B are our V^P, B^P as defined in Ref. 1 [Eq. (3.10) of Ref. 1], and V, λ are our V^T, B^T, the projections of the velocity and magnetic field onto the symmetry direction $\partial/\partial x$. Once we have made this identification, it is very easy to specialize Eqs. (3.27), (3.32), and (3.34) of Ref. 1 to our model and obtain a set of constraints (first integrals) that a stationary MHD configuration must satisfy: From Eq. (3.27) of Ref. 1, we have

$$V = C + \lambda u \ . \tag{3.11}$$

Here,

$$C \equiv \beta + V_F \ , \tag{3.12}$$

and V_F is an integration constant (or "stream-function" in the terminology of Phinney[6]), the transverse speed of the frozen-in magnetic field as measured by FIDO's at $z \to \infty$. Notice that the quantity C is nothing but the shift function β, with a constant added onto it; thus, we shall call it the "renormalized shift." Throughout our analysis we shall use C rather than β to embody the spacetime's gravitomagnetic field. In this section we shall not assume the specific form (2.5) for $\beta(z)$, but rather shall allow $\beta(z)$ to be arbitrary (except for the constraint $\beta \to 0$ as $z \to \infty$). Later, in Sec. IV, we shall specialize to the specific form (2.5) with the V_F that appears there set equal to the V_F of (3.12). From Eq. (3.32) of Ref. 1, a result of momentum conservation, we have

$$l=\gamma V-\lambda/s. \tag{3.13}$$

Here l is the (constant, i.e., z–independent) x-component of the magnetosphere's linear momentum, p_x, per unit mass and s is a ratio measuring the relative strength of the magnetic field and the plasma inertia:

$$s\equiv\frac{4\pi\rho\gamma u}{B^2}. \tag{3.14}$$

Because of the conservation of the rest mass,

$$\rho\gamma u=\text{const}, \tag{3.15}$$

and the vanishing divergence of $\vec{B}$ (B=const), s is another constant. From Eq. (3.34) of Ref. 1, a result of the conservation of energy and momentum, we have

$$f=\gamma(1-CV). \tag{3.16}$$

Here f is also a constant, representing the specific energy measured by an ''imaginary'' observer who is comoving with the frozen-in magnetic field. The observer is ''imaginary'' because on one side of the light planes ($|C|\geq 1$), the field moves faster than the speed of the light. Notice that the constants V_F, l, s, f are all dimensionless.

Equations (3.4), (3.11), (3.13) and (3.16) can be combined into a single quartic equation for one of the stationary, dimensionless quantities u, V or λ; we shall choose the combination γu. This quartic equation will be solved to obtain a stationary configuration: the quantity γu as a function of the renormalized shift C and the constant parameters s, l, f (which are regarded as specified beforehand); and then via Eqs. (3.11), (3.17) and (3.18), the quantities u, V, λ. In this procedure the z-dependence of the equilibrium configuration will arise solely through the renormalized shift function $C(z)$.

More specifically, we first use (3.11) and (3.16) to eliminate V and λ from (3.13) and obtain an expression for γ in terms of γu, C and the (specified) constant parameters s, l and f,

$$\gamma=\frac{(Cl+f)\gamma u-f/s}{\gamma u-(1-C^2)/s}. \tag{3.17}$$

In turn, Eq. (3.17) is substituted into (3.16), resulting in a similar expression for γV,

$$\gamma V=\frac{\gamma ul-fC/s}{\gamma u-(1-C^2)/s}. \tag{3.18}$$

The quartic equation for $\gamma u(C,s,l,f)$, obtained by combining (3.4), (3.17) and (3.18), is the following ''wind equation'' [see Eqs. (3.46) and (3.47) of Ref. 1; also Eqs. (IV,8.5), (V,5.1) of Phinney[6] and Eq. (3.12) of Kennel et al.[22]]:

$$D\equiv K\frac{(\gamma u-F_1)(\gamma u-F_2)}{(\gamma u-F_3)^2}-(\gamma u)^2-1=0. \tag{3.19a}$$

Here,

$$K\equiv(f+Cl)^2-l^2, \tag{3.19b}$$

$$F_1\equiv\frac{1-C}{f+Cl-l}\frac{f}{s}, \tag{3.19c}$$

$$F_2\equiv\frac{1+C}{f+Cl+l}\frac{f}{s} \tag{3.19d}$$

$$F_3\equiv\frac{1-C^2}{s}. \tag{3.19e}$$

As we can see, the wind equation (3.19) is quartic in γu, so it generally has 0, 2 or 4 real solutions. It has an apparent singular point at $\gamma u=F_3$, or

$$s\gamma u+C^2-1=0. \tag{3.20}$$

This is the Alfven point, i.e., the point at which the phase velocity of short-wavelength, small-amplitude Alfven waves is the same as the fluid speed.[6,22] However, it turns out that the MHD wind can always pass through this "critical point" smoothly (see Phinney[6] for a detailed discussion). There is another singular point hidden in the denominator of the derivative of γu with respect to C. By rewriting (3.4) [or (3.19a)] as

$$D=\gamma^2-\gamma^2V^2-\gamma^2u^2-1=\gamma^2-\left(\frac{f-\gamma}{C}\right)^2-\gamma^2u^2-1=0$$

and differentiating it with respect to C, we obtain

$$\frac{\partial\ln(\gamma u)}{\partial\ln C}=\frac{\gamma u\left(\frac{\partial D}{\partial C}\right)_{\gamma u}}{C\left(\frac{\partial D}{\partial\gamma u}\right)_C}=\frac{(\gamma V)^2(s\gamma u+C^2-1)+\lambda\gamma u\,(sl\gamma u-2\gamma C)}{(\gamma u)^2(s\gamma u+C^2-1-\lambda^2)}. \tag{3.21}$$

Because of the assumption of zero thermal pressure, no slow magnetosonic waves are present in our model and the factor $(\gamma u)^2$ in the denominator is just a reminder that there is no slow magnetosonic critical point for our plasma flow to cross. The point where the other factor vanishes,

$$s\gamma u+C^2-1-\lambda^2=0, \tag{3.22}$$

is the fast magnetosonic point.[6,22] It will look familiar if we rewrite $s\gamma u$ as $4\pi\rho\gamma^2u^2/B^2$. This point is also where the two positive solutions for γu meet and terminate. (See, for example, Sec. 7.5 of Ref. 22.)

Shown in Fig. 1 are solutions of (3.19) for a particular set of parameters s, l and f. By making a one-to-one monotonic map of the "normalized shift" C to the z coordinate

[such as Eqs. (2.5) and (3.12)], we can re-express these solutions as functions of height z: $\gamma u = \gamma u(z)$. The solution of interest to us is the "wind" branch (b) along which γu increases monotonically from much less than the Alfven speed, through the Alfven speed, and up toward the fast magnetosonic speed. If $V_F \equiv C_\infty$ is equal to C_0, then the wind speed approaches the fast magnetosonic speed as $z \to \infty$ [curve (b) of Fig. 2]. If $V_F < C_0$, then the wind asymptotes to a speed less than fast magnetosonic speed [curve (c) of Fig. 2a). If $V_F > C_0$, then the MHD outflow terminates before it reaches spatial infinity, resulting in a nonphysical solution [curve (a) of Fig. 2].

By using the schematic method employed in Kennel et al,[22] we can convince ourselves that Figs. 1 and Fig. 2 are quite generic; they depict schematically solutions of (3.19) for a general set of s, l, f (and V_F). In other words, for all s, l, f, we always have as in Fig. 1 a positive, increasing (with C) "wind" branch that meets with another positive branch from below at the fast magnetosonic point C_0 and terminates there. The Alfven point, where these two positive branches intersect, is inside the "light plane," i.e., the plane where the electromagnetic field moves at the speed of light ($C=1$). The other positive branch always changes sign at the "light plane." We also have a negative branch that approaches to a large negative value very quickly.

We shall not present here an analysis of our model similar to the analysis in Ref. 22. Instead, we shall look at the wind equation and the constraints it places on stationary configurations in regions of the flow where C is very small and where it is very large. The resulting equations are not very useful as approximations in their own right. But they do give us some hint on how the characteristics of the wind solutions change with the flow constants s, l, f (and V_F).

Focus attention, first, on the region of the flow (near $z=0$ in the models of Sec. IV) where $C \ll 1$. We shall assume that the flux of conserved x–momentum ($\vec{S}^{P}_{P_\xi}$ of Ref. 1)

is mostly in the electromagnetic field, $l \gg 1$. We shall also assume that $(sl)^2 \gg 1$. The role of this product sl will become evident later at the end of this section. Since we are interested in the "wind" branch where γu increases with C, we shall regard this as the region in which the flow "starts." Restrict attention to flows for which, at $C=0$, the plasma velocity is small and thus γ is near unity. Since $\gamma=f$ when $C=0$ [Eq. (3.16)], such flows must have

$$\Delta f \equiv f-1 \ll 1 , \tag{3.23}$$

and at $C=0$,

$$(\gamma u)^2=u^2 \lesssim 2\Delta f \ll 1. \tag{3.24}$$

Thus, Δf determines how fast the flow starts out at $C=0$. In the region of small C we shall denote $C \equiv \varepsilon$. The region of interest will be

$$C \equiv \varepsilon \lesssim \sqrt{\Delta f} \ll 1 \ll l. \tag{3.25}$$

In this region we would expect that

$$u, V \sim \varepsilon \lesssim \sqrt{\Delta f} \ll 1 \ll l. \tag{3.26}$$

Indeed, this is the case: We rewrite (3.16) as

$$\Delta f = \frac{1}{2}u^2 + \frac{1}{2}V^2 - \varepsilon V. \tag{3.27}$$

Combining this with (3.11) and (3.13) we immediately have

$$u = \left[\frac{2\Delta f + \varepsilon^2}{1+s^2 l^2} \right]^{1/2}, \tag{3.28a}$$

and

$$V=\varepsilon-sl\left[\frac{2\Delta f+\varepsilon^2}{1+s^2l^2}\right]^{1/2}, \tag{3.28b}$$

$$\lambda=-sl+s\left[\varepsilon-sl\left[\frac{2\Delta f+\varepsilon^2}{1+s^2l^2}\right]^{1/2}\right]. \tag{3.28c}$$

Notice that for $sl>0$, V starts out negative (because of the strong dragging of inertial frames there) and then changes sign at $\varepsilon\sim\sqrt{\Delta f}$. As ε gets larger, moving into the region $1\gg\varepsilon^2\gg\Delta f$,

$$u\simeq\frac{\varepsilon}{\sqrt{1+s^2l^2}}, \tag{3.28'a}$$

$$V\simeq\frac{\varepsilon}{2s^2l^2}, \tag{3.28'b}$$

$$\lambda\simeq-sl+\frac{\varepsilon}{2sl^2}. \tag{3.28'c}$$

We see that when the product sl is large, the fluid will be difficult to accelerate and when l is also large, the frozen-in magnetic field lines can hardly be bent as C (i.e., β) changes.

Turn, next, to the region of the flow in which $C\gg1$. In this region the wind equation (3.19) shows that this same product, sl, together with V_F ($\equiv C_\infty$), determines whether a particular stationary solution can reach spatial infinity. At

$$C\gg1,$$

the wind equation can be approximated as

$$(Cl)^2\left[(\gamma u)^2-\frac{f^2}{(sl)^2}\right]\simeq[(\gamma u)^2+1]\left[\gamma u+\frac{C^2}{s}\right]^2. \tag{3.29}$$

By definition,

$$s\gamma u=\frac{4\pi\rho\gamma^2u^2}{B^2}>0;$$

therefore,

$$\left[\gamma u+\frac{C^2}{s}\right]^2>\left[\frac{C^2}{s}\right]^2.$$

Using this inequality, we can reduce (3.29) to the form

$$[(sl)^2-C^2](\gamma u)^2\geq C^2.$$

Hence, the following inequality holds,

$$(sl)^2\geq C^2, \tag{3.30}$$

which means that the product sl must be large enough in order for the wind equation to have any positive solutions at C. For a wind with fixed V_F to reach spatial infinity in a given gravitational background, either we should have s large enough so the fluid initially (at $C\ll 1$) will have enough inertia that its speed cannot be accelerated beyond the fast magnetosonic speed; or we should have l big enough so the magnetized fluid will have enough x–momentum stored in the magnetic field to be converted into the (particle) energy (via the shift function) to make its mass inertia become large at $C\gg 1$.

IV. STATIONARY MHD "MAGNETOSPHERE"

It is generally believed that in or near the ergosphere of a rotating, magnetized black hole, electron-positron pairs are created by high-energy photons, electrons or protons with the help of the magnetic field or its coupling to the gravitomagnetic field of the rotating hole.[4,6,7,8,10] Part of the resulting electron-positron-pair plasma flows into the horizon, and part is driven out to infinity as a steady MHD wind.[4,6,9] When this MHD wind is dynamically perturbed, e.g., by the pressure of chaotic magnetic fields anchored in the hole's accretion disk, there will result MHD waves that ride on top of and modulate the wind's steady flow. In Secs. V and VI we shall study such MHD waves. But first, in this section, we shall prepare for that study by building explicit models for the stationary, MHD background flow. Throughout, we shall restrict attention to the planar model spacetime (2.4).

To model the background flow, we use the stationary solutions derived in the previous section and assume the following to join solutions in the positive z half plane with those in the negative z half plane:

$$\vec{V}(-z)=-\vec{V}(z),\ \rho(-z)=\rho(z)\,, \tag{4.1}$$

$$\vec{B}(-z)=\vec{B}(z), \tag{4.2}$$

$$\beta'(-z)=\beta'(z)\ \text{ and } \beta(z)\ \text{is continuous across } z=0. \tag{4.3}$$

It is not hard to verify the following transformation rules for the flow constants on both sides of the $z=0$ plane under the above assumptions:

$$s^{+}=-s^{-}, \tag{4.4a}$$

$$l^{+}=-l^{-}, \tag{4.4b}$$

$$f^{+}=f^{-}. \tag{4.4c}$$

Here the superscripts "+" indicate that those flow constants are in the $z>0$ half plane, while the superscripts "−" indicate those in the $z<0$ half plane. In the following, we will drop the superscripts "+" and "−" for the flow constants and refer to them using their values in the $z>0$ half plane, unless explicitly specified otherwise.

The MHD flow is intended to model a wind flowing out of the ergosphere of a Kerr black hole and also an accretion flow down to the horizon, both originated in the ergosphere, so we will choose

$$C=0 \ , \ \text{at} \ \ z=0 \, . \tag{4.5}$$

In other words, we assume in our model the pair production region to be delta-function sources and put this production plane at the origin, $z=0$. Thus, the MHD plasma will emerge from $z=0$ and will flow from there in both directions, to $z\rightarrow-\infty$ and to $z\rightarrow+\infty$. In our planar model, the magnetic field lines do not diverge from each other at infinity, so no steady, continuous solution exists beyond the fast magnetosonic critical point (see Sec. III; see also Ref. 22). This means that in order for our wind to reach infinity, we must choose parameters $s, l, V_{\rm F}$ such that the flow speed never exceeds, and at most approaches, that of the fast magnetosonic waves at the spatial infinity. In other words, the chosen parameters s, l are such that the maximumly allowed "normalized shift" C_0 determined from s and l for the wind branch will be no larger than $V_{\rm F}$, the asymptotic value of C (see Fig. 2). We would like our plasma-production region ($C=z=0$) to resemble the ergosphere of a black hole, in that no object there can remain at rest relative to "infinity"; i.e., the "dragging of inertial frames" is so strong that $|\beta|\geq 1$ there. These considerations will considerably restrict our choice of V_F.

Under the condition $C(z=0)=0$, we have, for the Lorentz factor of our stationary flow, $\gamma=f$ at the origin, where the flow starts. We shall not choose $f=1$ because that would force u to vanish at $z=0$ and (since $\rho\gamma u=$const) would also force the plasma density ρ to be infinite there — and that, in turn, would prevent MHD waves from propagating across the plasma production region $z=0$. Instead, we will choose

$$\Delta f \equiv f-1 \ll 1 \tag{3.23}$$

so that the wind can start at a small but finite speed. Because of our assumption (4.1), the flow velocity is not continuous across $z=0$. The jumps in the flow velocity and in other MHD quantities at $z=0$ must satisfy a set of junction conditions that depend on the details of the delta-function source of plasma. The junction conditions at the interface are actually just a special form of the MHD equations there. They can be derived from the MHD equations or from combinations of them, using the standard pill box or tiny integration-loop method. From the conservation of the magnetic flux [Eq. (2.6) of Ref. 1], this method gives

$$[B_z]=0. \tag{4.6}$$

Here and below square brackets denote the jump: $[B_z]\equiv B_z$(just above $z=0$) $-\,B_z$(just below $z=0$). From Ampere's law [Eq. (2.5) of Ref. 1], we obtain

$$[E_y]\equiv[B_z V_x - B_x V_z]=0. \tag{4.7}$$

From the conservation of the rest mass (or baryon number) [Eq. (2.24) of Ref. 1], we obtain

$$[\rho\gamma V_z]=\dot{M}\ . \tag{4.8}$$

From the conservation of energy measured locally by FIDO's at the origin (i.e., the

conservation of the projection of 4-momentum on the Killing vector $\partial/\partial t - V_F \partial/\partial x$), we obtain

$$[\rho\gamma^2 V_z] + \frac{1}{4\pi}(V_z B_x - V_x B_z)[B_x] = \dot{E}. \tag{4.9}$$

From the conservation of the x–component of momentum, we obtain

$$[\rho\gamma^2 V_x V_z] - \frac{B_z}{4\pi}[B_x] = \dot{P}. \tag{4.10}$$

In the above equations, we have used the following definitions for our delta-function sources at $z=0$:

$\dot{M} \equiv$ (rest-mass injection rate at $z=0$ per unit area, per unit FIDO time); (4.11a)

$\dot{E} \equiv$ (injection rate at $z=0$ per unit area, per unit FIDO time

of energy measured by FIDO's); (4.11b)

$\dot{P} \equiv$ (injection rate at $z=0$ of x–momentum per unit area, per unit FIDO time). (4.11c)

Note: Because the lapse function is unity everywhere, proper time as measured by the FIDO's (''FIDO time'') is everywhere equal to coordinate time t. We can also combine $\dot{M}$ and $\dot{E}$ to get $\dot{E}_K \equiv \dot{E} - \dot{M}$, the injection rate of the kinetic energy measured locally by the FIDO's and obtain a junction condition involving $\dot{E}_K$:

$$[\rho\gamma(\gamma-1)V_z] + \frac{1}{4\pi}(V_z B_x - V_x B_z)[B_x] = \dot{E}_K. \tag{4.9′}$$

By specializing to our stationary configuration [Eq. (3.6) and our assumption on the pair-production plane (4.5)], we obtain

$$E_y(z=0)=C(z=0)B=0\,. \tag{4.12}$$

This, combined with the junction condition (4.6) and the definition of V_F (3.12), implies

$$B[V_F]=B[C]=[E_y]=0. \tag{4.13}$$

Therefore, the continuity of the electric field (produced by the fluid's motion under our perfect MHD assumption) forces V_F to be the same on both sides of the interface. Since we assume for the stationary configuration that $V_z^+=-V_z^-$, the stationary flow carries away the mass injected at the interface equally to both sides,

$$\dot{M}=[\rho\gamma u]=2\rho\gamma u^+=-2\rho\gamma u^-. \tag{4.14}$$

Since we have also chosen $\lambda^+=\lambda^-$, no net force in the x–direction acts on the exiting stationary flow; i.e.,

$$\dot{P}=[\rho\gamma^2 uV]-\frac{B^2}{4\pi}[\lambda]=0; \tag{4.15}$$

and the injected energy

$$\dot{E}=[\rho\gamma^2 u]+\frac{B^2}{4\pi}(\lambda u-V)[\lambda]=\rho f^2[u], \tag{4.16a}$$

or

$$\dot{E}_K=\rho f(f-1)[u] \tag{4.16b}$$

is completely in the fluid's motion and is carried away equally to both sides. The Poynting flux, however, is guaranteed to be continuous by the vanishing of the electric field [Eqs. (4.5)] at the interface.

Figure 3 shows a schematic representation of this background, equilibrium flow, upon which we shall study MHD perturbations. The downward "wind" solution (i.e., downward flowing stationary solution) on the $z<0$ side is constructed from the "wind" branch of Fig. 1 on the $z>0$ side, using the symmetries (4.1)—(4.3). In this figure, and henceforth, we specialize to the specific shift function (2.5):

$$\beta(z)=V_{\rm F}\,(\tanh z-1)\ ;\qquad C(z)=V_{\rm F}\tanh z. \tag{2.5}$$

The parameters s, l, f and $V_{\rm F}$ are such that the asymptotic speeds of the background flow at the two infinities are less than the fast magnetosonic speed, and the flow starts at a finite speed at $z=0$. Because of the monotonic, one-to-one nature of map (2.5) from the shift function to the z-coordinate, and because of the general form of γu as functions of the "normalized shift" C (fig. 1), this particular stationary background flow does not cross any magnetosonic points. (Note that because of the assumption of zero thermal pressure, the slow magnetosonic speed degenerates to the flow speed.) This will save us from the trouble of passing waves through their sonic points when we later study the dynamic perturbations numerically in Sec. VI.

As a last point, we wish to mention here that although our chosen spacetime has no horizon (thereby permitting a study of shift-function effects in isolation), we can think of the region $z\to-\infty$ as analogous to a horizon. This viewpoint is justified by the fact that a black-hole horizon behaves very much like an "infinity" (as one sees from analyses using the Regge-Wheeler[23] "tortoise coordinate,"[24] and as Punsley and Coroniti[14] emphasize in their approach to black-hole magnetospheres). If the flow is chosen to asymptotically approach the fast-magnetosonic speed, then this viewpoint is reinforced by the fact that no information can propagate in from $z=-\infty$ via any kind of MHD wave. It will be instructive, in future research, to test this viewpoint that $z\to-\infty$ is analogous to a horizon by comparing MHD flows in the horizon-endowed model spacetime (2.3) with

those in our horizon-free spacetime (2.4).

V. MHD WAVES IN THE "MAGNETOSPHERE": ANALYTIC ANALYSIS

We turn, now, to perturbations of the steady "magnetospheres" constructed in Sec. IV. For ease of analysis we shall assume that the amplitude of the perturbations is small, and we shall linearize in that amplitude. In this section we shall develop the linearized, analytic theory of the perturbations, and then in Sec. VI we shall describe numerical solutions to the perturbation equations.

This section is divided into subsections. In Subsection A we present the perturbation equations in the time domain, and we present the junction conditions which the perturbations must satisfy at the location, $z=0$, of the background flow's discontinuity. In Subsection B, we specialize to monochromatic perturbations, i.e., to perturbations with dependences $e^{-i\omega t}e^{ik_x x}$ on t and x. In Subsection C we derive and discuss a complete set of solutions to the perturbation equations at spatial infinity, where the background flow and the shift function are constant. These "solutions at infinity" will be used in Sec. VI as checks on the asymptotic forms of our numerical solutions for MHD waves in the magnetosphere.

A. Perturbation Equations and Junction Conditions

For simplicity we shall confine attention to magnetospheres in which the perturbed flow, like the steady background flow, has its magnetic field and velocity entirely in the x-z plane and is symmetric in the y-direction (no dependence of perturbed quantities on y). However, the waves can propagate in any direction in the x-z plane and thus must depend on x and z as well as on time t. We shall characterize the perturbed MHD flow

by its velocity $\vec{V}$ and magnetic field $\vec{B}$ as measured by the FIDO's, and the fluid's density ρ as measured in the fluid's rest frame. More specifically, $\vec{V}$ is related to the components of the FIDO's four-velocity by the standard relation (3.3); $\vec{B}$ is related to the components of the Maxwell tensor by the standard relations (3.8); and ρ is the density of rest mass and also the density of total fluid mass-energy as measured in the fluid's local rest frame. The unperturbed quantities will be denoted by a superscript "0" when otherwise there would be ambiguities. The first-order perturbations in these quantities we shall denote by $\delta\vec{V}$, $\delta\vec{B}$, and $\delta\rho$.

We shall use the following dimensionless notation for the perturbation quantities: For the magnetic-field perturbation $\delta\vec{B}$ and density perturbation $\delta\rho$, we define b_x, b_z and $\tilde{\rho}$ by

$$\vec{b} \equiv \delta\vec{B}/B = b_x(t,x,z)\vec{e}_x + b_z(t,x,z)\vec{e}_z , \tag{5.1}$$

$$\tilde{\rho} \equiv \delta\rho/\rho = \tilde{\rho}(t,x,z). \tag{5.2}$$

The velocity perturbation $\delta\vec{V}$ is already dimensionless in our geometric units where $G \equiv c \equiv 1$, so we define v_x and v_z by

$$\vec{v} \equiv \delta\vec{V} = v_x(t,x,z)\vec{e}_x + v_z(t,x,z)\vec{e}_z . \tag{5.3}$$

The general relativistic MHD equations in a general, well-behaved background spacetime were written down in Ref. 1 [Eqs. (2.5), (2.13), (2.22) and (2.24)]. Because our specific spacetime has such a simple metric, (2.4), all the gravitational quantities in those equations are zero except the derivative of β. Our simple equation of state $\mu=1$ [Eq. (3.10)], and the assumption of confining $\vec{B}$ and $\vec{V}$ to the $x-z$ plane also simplify the MHD equations considerably. For example, the full equation describing force balance becomes

$$[(\rho\gamma^2+\frac{\vec{B}^2}{4\pi})\delta_{ij}+\rho\gamma^4 V_i V_j-\frac{1}{4\pi}B_i B_j](\frac{\partial}{\partial t}-\vec{\beta}\cdot\vec{\nabla})V^j+\frac{1}{4\pi}(\vec{B}\times\{\vec{V}\times[(\frac{\partial}{\partial t}-\vec{\beta}\cdot\vec{\nabla})\vec{B}]\})_i$$

$$+\rho\gamma^2 V_{i,j}V^j+\rho\gamma^4 V_i V_{j,k}V^j V^k$$

$$=\rho\gamma^2\beta_{j,i}V^j+\frac{1}{4\pi}(B_{i,j}B^j-B_{j,i}B^j). \tag{5.4}$$

By invoking the above facts, substituting

$$\vec{B}=\vec{B}^0+\delta\vec{B},\ \vec{V}=\vec{V}^0+\delta\vec{V},\ \rho=\rho^0+\delta\rho,$$

and

$$\gamma=\frac{1}{\sqrt{1-u^2-V^2}}+\frac{\vec{V}^0\cdot\delta\vec{V}}{(1-u^2-V^2)^{3/2}}$$

into the general relativistic MHD equations [Eqs. (2.5), (2.13), (2.24) of Ref. 1 and Eq. (5.4) above], and keeping only terms linear in the perturbations, we obtain the following form of the perturbed MHD equations in terms of the dimensioned perturbations $\delta\vec{V}$, $\delta\vec{B}$, $\delta\rho$,

$$(\frac{\partial}{\partial t}-\vec{\beta}\cdot\vec{\nabla})\delta\vec{B}=\vec{\nabla}\times(\vec{v}\times\vec{B})+\vec{\nabla}\times(\vec{V}\times\delta\vec{B})-\delta\vec{B}\cdot\vec{\nabla}\vec{\beta}, \tag{5.5a}$$

$$\vec{\nabla}\cdot(\delta\vec{B})=0, \tag{5.5b}$$

$$[(\rho\gamma^2+\frac{\vec{B}^2}{4\pi})\delta_{ij}+\rho\gamma^4 V_i V_j-\frac{1}{4\pi}B_i B_j](\frac{\partial}{\partial t}-\vec{\beta}\cdot\vec{\nabla})v^j+\frac{1}{4\pi}\left[\vec{B}\times\{\vec{V}\times[(\frac{\partial}{\partial t}-\vec{\beta}\cdot\vec{\nabla})\delta\vec{B}]\}\right]_i$$

$$+\rho\gamma^2 v_{i,j}V^j+\rho\gamma^4 V_i v_{j,k}V^j V^k-\frac{1}{4\pi}(\delta B_{i,j}-\delta B_{j,i})B^j$$

$$=\gamma^2[\delta\rho V^j+2\rho\gamma^2(\vec{V}\cdot\vec{v})V^j+\rho v^j]\beta_{j,i}-\rho\gamma^4(v_i V^j+V_i v^j)V_{k,j}V^k+\frac{1}{4\pi}(B_{i,j}-B_{j,i})\delta B^j$$

$$-\gamma^2[\delta\rho V^j+2\rho\gamma^2V^j(\vec{V}\cdot\vec{v})+\rho v^j]V_{i,j}-\gamma^4V_i[\delta\rho V^j+4\rho\gamma^2V^j(\vec{V}\cdot\vec{v})+\rho v^j]V_{j,k}V^k, \quad (5.5c)$$

$$(\frac{\partial}{\partial t}-\vec{\beta}\cdot\vec{\nabla}+\vec{V}\cdot\vec{\nabla})\delta\rho-\frac{\delta\rho}{\rho}\vec{V}\cdot\vec{\nabla}\rho+\rho\gamma^2\vec{V}\cdot[(\frac{\partial}{\partial t}-\vec{\beta}\cdot\vec{\nabla}+\vec{V}\cdot\vec{\nabla})\vec{v}]+\rho\vec{\nabla}\cdot\vec{v}$$

$$=-2\rho\gamma^2(\vec{V}\cdot\vec{v})\vec{V}\cdot\vec{\nabla}(\ln\gamma)-\rho\gamma^2(\vec{V}\cdot\vec{\nabla}\vec{V})\cdot\vec{v}+\rho\vec{v}\cdot\vec{\nabla}(\ln u). \quad (5.5d)$$

In deriving (5.5d), we also need Eq. (3.15) ($\rho\gamma u$=const) to eliminate derivatives of ρ. Rewritten explicitly in component form and using the dimensionless version of the perturbation variables (b_x, b_z, v_x, v_z, $\tilde{\rho}$), these perturbation equations take the form

$$\frac{db_x}{d\tau}+Vb_{x,x}+ub_{x,z}=-u'b_x+(V-\beta)'b_z+v_{x,z}-\lambda v_{z,z}-\lambda' v_z, \quad (5.6a)$$

$$\frac{db_z}{d\tau}+Vb_{z,x}+ub_{z,z}=\lambda v_{z,x}-v_{x,x}, \quad (5.6b)$$

$$b_{x,x}+b_{z,z}=0, \quad (5.6c)$$

$$\left[\frac{B^2}{4\pi}+\rho\gamma^2(1+\gamma^2V^2)\right]\frac{dv_x}{d\tau}+(\rho\gamma^4uV-\frac{\lambda B^2}{4\pi})\frac{dv_z}{d\tau}$$

$$+\left[\rho\gamma^2(1+\gamma^2V^2)-\frac{B^2}{4\pi}\right](Vv_{x,x}+uv_{x,z})+(\rho\gamma^4uV+\frac{\lambda B^2}{4\pi})(Vv_{z,x}+uv_{z,z})$$

$$-\frac{B^2}{2\pi}uVb_{z,z}+\frac{B^2}{4\pi}[(1-V^2)b_{z,x}-(1-u^2)b_{x,z}]$$

$$=-\frac{B^2}{4\pi}uu'b_x+\frac{B^2}{4\pi}[\lambda'+u(V-\beta)']b_z-\rho\gamma^2u[(1+\gamma^2V^2)V'+\gamma^2uVu']\tilde{\rho}$$

$$-\rho\gamma^4u[(1+4\gamma^2V^2)uu'+4(1+\gamma^2V^2)VV']v_x$$

$$-\left[\frac{B^2}{4\pi}u\lambda'+\rho\gamma^2[(1+2\gamma^2u^2)(1+2\gamma^2V^2)-\gamma^2V^2]V'+2\rho\gamma^4(1+2\gamma^2u^2)uVu'\right]v_z, \qquad (5.6d)$$

$$\left[\frac{\lambda^2B^2}{4\pi}+\rho\gamma^2(1+\gamma^2u^2)\right]\frac{dv_z}{d\tau}+(\rho\gamma^4uV-\frac{\lambda B^2}{4\pi})\frac{dv_x}{d\tau}$$

$$+\left[\rho\gamma^2(1+\gamma^2u^2)-\frac{\lambda^2B^2}{4\pi}\right](Vv_{z,x}+uv_{z,z})+(\rho\gamma^4uV+\frac{\lambda B^2}{4\pi})(Vv_{x,x}+uv_{x,z})$$

$$+\frac{\lambda B^2}{2\pi}uVb_{z,z}-\frac{\lambda B^2}{4\pi}[(1-V^2)b_{z,x}-(1-u^2)b_{x,z}]$$

$$=-\frac{B^2}{4\pi}(\lambda'-\lambda uu')b_x-\frac{\lambda B^2}{4\pi}u(V-\beta)'b_z-\rho\gamma^2[(1+\gamma^2u^2)uu'+\gamma^2u^2VV'-V\beta']\tilde{\rho}$$

$$-\rho\gamma^2[\gamma^2u^2(1+4\gamma^2V^2)V'-(1+2\gamma^2V^2)\beta'+2\gamma^2uV(1+2\gamma^2u^2)u']v_x$$

$$-[\rho\gamma^2(1+\gamma^2u^2)(1+4\gamma^2u^2)u'+2\rho\gamma^4(1+2\gamma^2u^2)uVV'-2\rho\gamma^4uV\beta'-\frac{\lambda B^2}{4\pi}u\lambda']v_z, \qquad (5.6e)$$

$$\frac{d\tilde{\rho}}{d\tau}+V\tilde{\rho}_{,x}+u\tilde{\rho}_{,z}+\gamma^2V\frac{dv_x}{d\tau}+\gamma^2u\frac{dv_z}{d\tau}+(1+\gamma^2V^2)v_{x,x}+(1+\gamma^2u^2)v_{z,z}+\gamma^2uV(v_{x,x}+v_{z,x})$$

$$=-\gamma^2u[(1+2\gamma^2V^2)V'+2\gamma^2uVu']v_x+[(1-2\gamma^2u^2)(1+\gamma^2u^2)u'/u-2\gamma^4u^2VV']v_z. \qquad (5.6f)$$

In these equations, a comma (‘‘,’’) denotes a partial derivative, a prime (‘‘′’’) denotes a derivative with respect to z, and $(d/d\tau)\equiv(\partial/\partial t-\beta\partial/\partial x)$ is the time derivative in the FIDO's frame. These equations are to be solved together with the following set of junction conditions at $z=0$, where the background flow is discontinuous:

$$[b_z]=0, \qquad (5.7a)$$

$$[v_x]-\lambda[v_z]-u\{b_x\}+2\lambda u b_z=0, \tag{5.7b}$$

$$\{\tilde{\rho}\}+\lambda f^2 u[v_x]+\frac{1+f^2u^2}{u}[v_z]=N, \tag{5.7c}$$

$$\{\tilde{\rho}\}+\frac{f^2(2f-1)\lambda u}{f-1}[v_x]+\frac{(f-1)(1+f^2u^2)+f^3u^2}{(f-1)u}[v_z]=f_E, \tag{5.7d}$$

$$\lambda f u[\tilde{\rho}]+f(1+2f^2\lambda^2u^2)[v_x]+\lambda f(1+2f^2u^2)[v_z]-\frac{1}{s}[b_x]=f_x. \tag{5.7e}$$

Here, for an arbitrary function F(z), we use the notation

$$[F]\equiv F(z=0^+)-F(z=0^-), \tag{5.8a}$$

$$\{F\}\equiv F(z=0^+)+F(z=0^-). \tag{5.8b}$$

[The junction conditions (5.7) can be obtained by applying the standard pill box or integration loop method to the perturbation equations (5.5); or, equally well, they can be inferred from the nonlinear junction conditions (4.6)—(4.11) by linearization and by insertion of Eqs. (3.11), (3.15) and (3.16).] In the junction conditions (5.7) there appear several (normalized) delta-function sources of perturbations. Defined in terms of quantities evaluated at $z=0$, these sources are the following: N is the fractional perturbation of the rate of rest mass injection

$$N\equiv\delta\dot{M}/\rho\gamma u; \tag{5.9}$$

f_E is the fractional perturbation of the rate of injection of kinetic energy

$$f_E\equiv\delta\dot{E}_K/\rho\gamma u(f-1); \tag{5.10}$$

and f_x is the perturbation of the rate of injection of x–component of momentum (i.e., the force in the x–direction exerted on the magnetosphere by the perturbations of the

injection process), divided by the rate of injection of rest mass

$$f_x \equiv \delta\dot{P}/\rho\gamma u. \tag{5.11}$$

B. Fourier-analyzed perturbation equations and junction conditions

Because both our stationary background and the background flow are symmetrical in time and in the x–direction ($\partial/\partial t$ and $\partial/\partial x$ are two KVF's), we can Fourier-analyze the magnetospheric perturbations in t and x without loss of generality; i.e., we can restrict attention to perturbations with sinusoidal dependences of t and x: $e^{-i(\omega t - k_x x)}$ for all perturbation quantities. Moreover, because of the constraint (5.6c), Eqs. (5.6a) and (5.6b) are not independent. In the following, we choose to eliminate b_x and use the resulting Eqs. (5.13a-d) below as our *independent* MHD perturbation equations. We eliminate b_x and $b_{x,z}$ from these perturbation equations by means of

$$b_x = \frac{1}{u}\left[v_x - \lambda v_z - \left(\frac{\omega}{k_x} + \beta - V\right) b_z \right] , \tag{5.12}$$

which is a combination of the Fourier-analyzed Eqs. (5.6a) and (5.6c). By substituting (5.12) into (5.6b), (5.6d), (5.6e) and (5.6f), our Fourier-analyzed MHD equations take the following form:

$$b_z' = ik_x(\lambda v_z - v_x) + i(\omega + \beta k_x - V) b_z , \tag{5.13a}$$

$$\left[\rho\gamma^2(1+\gamma^2V^2) - \frac{B^2}{4\pi}\right] u v_x' + \left(\rho\gamma^4 uV + \frac{\lambda B^2}{4\pi}\right) u v_z'$$

$$- \frac{B^2}{2\pi} uV b_z' - \frac{B^2}{4\pi}(1-u^2)\left[\left[\frac{v_x - \lambda v_z}{u}\right]' - \left[\left(\frac{\omega}{k_x} + \beta - V\right)\frac{b_z}{u}\right]'\right]$$

$$=-\frac{B^2}{4\pi}u'\left(v_x-\lambda v_z-(\frac{\omega}{k_x}+\beta-V)b_z\right)+\frac{B^2}{4\pi}[\lambda'+u(V-\beta)']b_z-ik_x\frac{B^2}{4\pi}(1-V^2)b_z$$

$$-\rho\gamma^2u[(1+\gamma^2V^2)V'+\gamma^2uVu']\tilde{\rho}-\rho\gamma^4u[(1+4\gamma^2V^2)uu'+4(1+\gamma^2V^2)VV']v_x$$

$$-\left(\frac{B^2}{4\pi}u\lambda'+\rho\gamma^2[(1+2\gamma^2u^2)(1+2\gamma^2V^2)-\gamma^2V^2]V'+2\rho\gamma^4(1+2\gamma^2u^2)uVu'\right)v_z$$

$$+i(\omega+\beta k_x)\left[\frac{B^2}{4\pi}+\rho\gamma^2(1+\gamma^2V^2)\right]v_x+i(\omega+\beta k_x)(\rho\gamma^4uV-\frac{\lambda B^2}{4\pi})v_z$$

$$-ik_x\left[\rho\gamma^2(1+\gamma^2V^2)-\frac{B^2}{4\pi}\right]Vv_x-ik_x(\rho\gamma^4uV+\frac{\lambda B^2}{4\pi})Vv_z, \qquad (5.13b)$$

$$\left[\rho\gamma^2(1+\gamma^2u^2)-\frac{\lambda^2B^2}{4\pi}\right]uv_z'+(\rho\gamma^4uV+\frac{\lambda B^2}{4\pi})uv_x'$$

$$+\frac{\lambda B^2}{2\pi}uVb_z'+\frac{\lambda B^2}{4\pi}(1-u^2)\left[\left(\frac{v_x-\lambda v_z}{u}\right)'-\left((\frac{\omega}{k_x}+\beta-V)\frac{b_z}{u}\right)'\right]$$

$$=-\frac{B^2}{4\pi}(\lambda'-\lambda uu')\left[\left(\frac{v_x-\lambda v_z}{u}\right)-\left((\frac{\omega}{k_x}+\beta-V)\frac{b_z}{u}\right)\right]-\frac{\lambda B^2}{4\pi}u(V-\beta)'b_z-ik_x\frac{B^2}{4\pi}(1-V^2)b_z$$

$$-\rho\gamma^2[(1+\gamma^2u^2)uu'+\gamma^2u^2VV'-V\beta']\tilde{\rho}$$

$$-\rho\gamma^2[\gamma^2u^2(1+4\gamma^2V^2)V'-(1+2\gamma^2V^2)\beta'+2\gamma^2uV(1+2\gamma^2u^2)u']v_x$$

$$-[\rho\gamma^2(1+\gamma^2u^2)(1+4\gamma^2u^2)u'+2\rho\gamma^4(1+2\gamma^2u^2)uVV'-2\rho\gamma^4uV\beta'-\frac{\lambda B^2}{4\pi}u\lambda']v_z$$

$$+i(\omega+\beta k_x)\left[\frac{\lambda^2 B^2}{4\pi}+\rho\gamma^2(1+\gamma^2V^2)\right]v_z+i(\omega+\beta k_x)(\rho\gamma^4 uV-\frac{\lambda B^2}{4\pi})v_x$$

$$-ik_x\left[\rho\gamma^2(1+\gamma^2u^2)-\frac{\lambda^2B^2}{4\pi}\right]Vv_z-ik_x(\rho\gamma^4uV+\frac{\lambda B^2}{4\pi})Vv_x, \qquad (5.13c)$$

$$u\tilde{\rho}'+(1+\gamma^2u^2)v_z'$$

$$=-\gamma^2u[(1+\gamma^2V^2)V'+2\gamma^2uVu']v_x+[(1-2\gamma^2u^2)(1+\gamma^2u^2)u'/u-2\gamma^4u^2VV']v_z$$

$$+i(\omega+\beta k_x-k_xV)\tilde{\rho}-i(\omega+\beta k_x)\gamma^2(Vv_x+uv_z)-ik_x(1+\gamma^2V^2+\gamma^2uV)v_x-ik_x\gamma^2uVv_z. \qquad (5.13d)$$

[Here a prime (‘‘′’’) denotes derivatives with respect to z. Note that this is the only kind of derivative present, since all stationary and Fourier-analyzed perturbation quantities depend only on the z coordinate.] The accompanying junction conditions [Eqs. (5.7a)-(5.7e)], in this sinusoidal situation and by virtue of Eq. (5.12), take the form

$$[b_z]=0, \qquad (5.14a)$$

$$\{\tilde{\rho}\}+\lambda f^2u[v_x]+\frac{1+f^2u^2}{u}[v_z]=N, \qquad (5.14b)$$

$$\{\tilde{\rho}\}+\frac{f^2(2f-1)\lambda u}{f-1}[v_x]+\frac{(f-1)(1+f^2u^2)+f^3u^2}{(f-1)u}[v_z]=f_E, \qquad (5.14c)$$

$$\lambda fu[\tilde{\rho}]+f(1+2f^2\lambda^2u^2)[v_x]+\lambda f(1+2f^2u^2)[v_z]$$

$$-\frac{1}{su}\{v_x\}+\frac{\lambda}{su}\{v_z\}-\frac{2}{su}(\frac{\omega}{k_x}-V_F)b_z=f_x. \qquad (5.14d)$$

To recapitulate, we will study the MHD perturbations on background flows having reflection symmetries (4.1)-(4.3); the perturbations will be characterized by

dimensionless quantities $\vec{v}$, $\vec{b}$, and $\tilde{\rho}$ [Eqs. (5.1)-(5.3)]; the MHD equations describing the time-dependent perturbations are Eqs. (5.5) or (5.6), together with a set of junction conditions [Eqs. (5.7a)-(5.7e)]; and the Fourier-analyzed perturbations are described by Eqs. (5.13a)-(5.13d), together with the Fourier-analyzed junction conditions (5.14a)-(5.14d).

C. General solution of the perturbation equations at infinity

In the regions $z \gg 1$ and $z \ll -1$, where the background functions β, u, V, and λ are constant (independent of z), the Fourier-analyzed MHD equations (5.13) can be solved analytically. These analytic solutions have been used to check the numerical code described in the next section; they also are useful in understanding the results of the numerical calculations, since the numerical solutions must asymptote to them at large $|z|$. These analytic solutions also exhibit explicitly the effects of β (i.e., of transforming to coordinates that slide with velocity $dx/dt = -\beta$) on the perturbation modes.

It is very tedious though maybe straightforward to derive the analytic solutions directly from the perturbation equations (5.13); and we did not do so. Rather, we derived them by first writing down the general solutions in the rest frame of the fluid, and by then performing a Lorentz boost to the FIDO's rest frame.

In the fluid's rest frame (denoted by primes) with a uniform magnetic field along the z'–direction, and the velocity and the magnetic field restricted to the x'–z' plane, the Fourier components of the magnetosonic modes satisfy

$$v_x' : v_z' : b_x' : b_z' : \tilde{\rho} = 1 : 0 : (-\frac{k_z'}{\omega'}) : (\frac{k_x'}{\omega'}) : (\frac{k_x'}{\omega'}); \qquad (5.15)$$

and the frequency ω' and wave vector (k_x', k_z') are related by the dispersion relation

$$(\omega')^2=\frac{\vec{B}'^2}{4\pi\rho+\vec{B}'^2}[(k_x')^2+(k_z')^2] \ . \tag{5.16}$$

There are also two ''convective modes'' (zero-temperature limit of the slow magnetosonic modes) that have zero frequency in the fluid's frame:

$$\vec{b}'=v_x'=0, \quad v_z' \text{ arbitrary function of } x', z' \ , \quad \text{and } \tilde{\rho}=-t'\vec{\nabla}'\cdot\vec{v}' \ ; \tag{5.17}$$

and

$$\vec{v}'=\vec{b}'=0, \quad \tilde{\rho} \text{ arbitrary function of } x', z'. \tag{5.18}$$

The Lorentz boost from the fluid's rest frame to the FIDO's rest frame, in 3+1 form with the fluid-frame quantities expressed in terms of the FIDO-frame quantities, has the following form: (see, for example, Jackson[25]):

$$\vec{B}'=\frac{\vec{B}}{\gamma}+\frac{\gamma\vec{B}\cdot\vec{V}}{\gamma+1}\vec{V} \ , \tag{5.19a}$$

$$\delta\vec{B}'=\frac{\delta\vec{B}}{\gamma}+\gamma(\vec{B}\cdot\vec{V}\vec{v}-\vec{V}\cdot\vec{v}\vec{B})+\frac{\gamma\delta\vec{B}\cdot\vec{V}}{\gamma+1}\vec{V} \ , \tag{5.19b}$$

$$\vec{v}'=\frac{\gamma^3\vec{V}}{\gamma+1}\vec{V}\cdot\vec{v}+\gamma\vec{v} \ , \tag{5.19c}$$

$$\omega'=\gamma(\omega+\beta k_x-k_x V-k_z u) \ , \tag{5.19d}$$

$$\vec{k}'=\vec{k}-[\omega+\beta k_x-\frac{\gamma}{\gamma+1}(k_x V+k_z u)]\vec{V} \ . \tag{5.19e}$$

This boost brings the fluid-frame MHD solutions into the following FIDO-frame form: For the fast magnetosonic modes, the solution [Eq. (5.15)] becomes

$$b_x=-\frac{(1+\lambda^2-C^2)k_z}{\omega+\beta k_x-k_x V-k_z u}Ae^{-i(\omega t-k_x x-k_z z)}, \tag{5.20a}$$

$$b_z=\frac{(1+\lambda^2-C^2)k_x}{\omega+\beta k_x-k_x V-k_z u}Ae^{-i(\omega t-k_x x-k_z z)}, \tag{5.20b}$$

$$v_x=(1-Cv)Ae^{-i(\omega t-k_x x-k_z z)}, \tag{5.20c}$$

$$v_z=(\lambda+Cu)Ae^{-i(\omega t-k_x x-k_z z)}, \tag{5.20d}$$

$$\tilde{\rho}=\frac{k_x-(\omega+\beta k_x)V-\lambda[k_z-(\omega+\beta k_x)u]}{\omega+\beta k_x-k_x V-k_z u}Ae^{-i(\omega t-k_x x-k_z z)}, \tag{5.20e}$$

where A is a constant wave amplitude. The dispersion relation (5.16) for these modes takes the following form:

$$(\omega+\beta k_x-k_x V-k_z u)^2-(1+\lambda^2-C^2)\frac{u}{s\gamma}[k_x^2+k_z^2-(\omega+\beta k_x)^2]=0. \tag{5.21}$$

The dispersion relation (5.21) can be regarded as a quadratic equation for k_z in terms of known quantities (ω, k_x, ...). For some ranges of ω and k_x there will be no real solutions; i.e., fast magnetosonic waves will not be able to propagate to infinity. For other ranges there will be two real solutions, one describing outward-propagating magnetosonic waves; the other, inward-propagating.

The two convective modes both have dispersion relations

$$\omega+\beta k_x-k_x V-k_z u=0 \tag{5.22}$$

corresponding to $\omega'=0$. One convective mode [Eq. (5.17)] involves frozen-in velocity perturbations, which can be thought of as put into the fluid at $z=0$. These velocity perturbations produce a density perturbation that grows linearly with time in the fluid frame, and linearly with z in the FIDO frame:

$$\vec{b}=0, \tag{5.23a}$$

$$v_x=\lambda A e^{-i(\omega t-k_x x-k_z z)}, \tag{5.23b}$$

$$v_z=A e^{-i(\omega t-k_x x-k_z z)}, \tag{5.23c}$$

$$\tilde{\rho}=i\frac{\lambda k_x+k_z}{\beta k_x-k_x V-k_z u}k_z z A e^{-i(\omega t-k_x x-k_z z)}. \tag{5.23d}$$

The other convective mode involves a frozen-in density perturbation and no velocity perturbation:

$$\vec{b}=0,\ \vec{v}=0,\ \tilde{\rho}=A e^{-i(\omega t-k_x x-k_z z)}. \tag{5.24}$$

For the stationary "magnetosphere" of Sec. IV, the periodic perturbations at the interface $z=0$ will produce waves that propagate out to $|z|\gg 1$, where they become a mixture of above fast magnetosonic and "convective" modes.

VI. Interaction of MHD waves with the shift function: numerical results

In this section we shall present the results of our numerical solutions of the Fourier-analyzed MHD perturbation equations [Eqs. (5.13)]. These equations are ordinary differential equations (ODE's) with z as the independent variable. They have been solved in the stationary background of Sec. IV (Fig. 4 and related discussions), subject to the following boundary conditions at spatial infinity ($z\to\pm\infty$) and at the interface ($z=0$). At spatial infinity (numerically, very large $|z|$ where the background flow has constant values) we require that:

There are no ingoing waves at both $z\to+\infty$ and $z\to-\infty$. (6.1)

At the interface, we require that [see also Eqs. (5.14a)—(5.14d)]:

$$b_z^+ = b_z^- \,, \tag{6.2a}$$

$$f_{\rm E}^{\pm} = \tilde{\rho}^{\pm} \pm \frac{f^2(2f-1)\lambda u}{f-1} v_x^{\pm} \pm \frac{(f-1)(1+f^2u^2)+f^3u^2}{(f-1)u} v_z^{\pm} \quad , \tag{6.2b}$$

$$N^{\pm} = \tilde{\rho}^{\pm} \pm \lambda f^2 u v_x^{\pm} \pm \frac{1+f^2u^2}{u} v_z^{\pm} \quad , \tag{6.2c}$$

$$f_x = \lambda f u [\tilde{\rho}] + f(1+2f^2\lambda^2u^2)[v_x] + \lambda f(1+2f^2u^2)[v_z] - \frac{1}{su}\{v_x\} + \frac{\lambda}{su}\{v_z\} - \frac{2}{su}\left(\frac{\omega}{k_x} - V_{\rm F}\right) b_z \,. \tag{6.2d}$$

Here, $f_{\rm E}^{\pm}$, $N^{\pm}$ and f_x are dimensionless perturbations to the stationary delta-function sources of kinetic energy, rest mass, and x-momentum at the interface, with frequency ω, and wave number k_x; see Sec. V, Eqs. (5.9)—(5.11). What we shall study are MHD perturbations that are driven at $z=0$ by $f_{\rm E}^{\pm}$, $N^{\pm}$, and f_x and propagate toward $z=\pm\infty$. We shall study how these perturbations interact with the shift function and the stationary background flow as they propagate.

Each perturbation solution has specific values of ω and k_x; i.e., it can be thought of as lying at a particular point in the ω-k_x plane. We have restricted our numerical calculation to those regions of the ω-k_x plane where (i) $\omega>0$ (an arbitrary convention), (ii) $k_x>0$ (this is the only region in which superradiance can occur for our model spacetime), and (iii) all k_z's are real at $z\to\pm\infty$, i.e. (outgoing) fast magnetosonic waves can propagate at both $z\to\infty$ and $z\to-\infty$. By imposing (iii) above in the dispersion relation (5.21), we infer that the boundaries of this region are aslo, besides $\omega=0$ and $k_x=0$,

$$\omega = -\beta(z)k_x + \frac{V}{1-u^2+\frac{u}{s\gamma}(1+\lambda^2-C^2)}k_x$$

$$\pm\frac{k_x}{1-u^2+\frac{u}{s\gamma}(1+\lambda^2-C^2)}\sqrt{V^2-u^2+\frac{u}{s\gamma}(1+\lambda^2-C^2)+u^2[u-\frac{1}{s\gamma}(1+\lambda^2-C^2)]^2} \quad (6.3)$$

For our chosen stationary background,

$$u(\pm\infty)=\pm 0.49\ ,\quad V(\pm\infty)=\pm 0.06\ ,\quad \gamma(\pm\infty)=1.15\ ,\quad \lambda(\pm\infty)=-3.99\ ,$$

$$C(+\infty)=2.0\ ,\quad C(-\infty)=-2.0\ ,$$

$$\beta(+\infty)=0\ ,\quad \beta(-\infty)=-4.0\ ,$$

these boundaries are $\omega=0$, $\omega=4.99k_x$, $\omega=3.01k_x$, $\omega=0.99k_x$, and $k_x=0$. By examining the dispersion relation (5.21) more closely, we can identify that

$$\omega\geq 0.99k_x$$

corresponds to k_z real at $z=+\infty$; and

$$\omega\geq 4.99k_x$$

or

$$\omega\leq 3.01k_x$$

corresponds to k_z real at $z=-\infty$. Therefore, if we restrict attention to $0.01\leq\omega\leq 9.99$, then

$$0.01\leq 0.99k_x\leq\omega\leq 3.01k_x\ ,\quad 4.99k_x\leq\omega\leq 9.99 \quad (6.4)$$

are the regions of the ω-k_x plane that we shall study.

For each point in the ω-k_x region (6.4), there are 5 independent solutions with outgoing waves at $z\rightarrow\pm\infty$, corresponding to 5 independent values of the sources $f_{\mathrm{E}}^{\pm}, N^{\pm}, f_x$. These 5 solutions have been constructed by the following procedure: (i) Integrate the

ODE's (5.13) outward from $z=0$ to $z=+\infty$ starting, in turn, with only one of b_z, v_x, v_z, $\tilde{\rho}$ nonzero; thereby obtain four independent solutions at $z>0$. (ii) Similarly integrate (5.13) from $z=0$ to $z=-\infty$ starting, in turn, with only one of b_z, v_x, v_z, $\tilde{\rho}$ nonzero; thereby obtain four independent solutions at $z<0$. (iii) For each of the five choices of $\{f_{\mathrm{E}}^{\pm}, N^{\pm}, f_x\}$, impose the eight boundary conditions (6.1), (6.2) on the eight numerical solutions (4 at $z>0$, 4 at $z<0$) to get a unique solution that satisfies the ODE's and the boundary conditions.

The ODE's (5.13) comprise a coupled fourth-order ODE system. For most choices of ω, k_x this system is stiff near the interface; i.e., there is one heavily damped solution and three growing solutions. This stiffness can be quantified as follows: at a fixed z, write the ODE's (5.13) in the form

$$y_i' = Q_i{}^j y_j \ , \tag{6.5}$$

where $y_1=b_z$, $y_2=v_x$, $y_3=v_z$ $y_4=\tilde{\rho}$. Then the matrix $Q_i{}^j$ (at fixed z) has 4 eigenvectors

$$Y_i = A_i{}^j y_j \tag{6.6a}$$

and four corresponding eigenvalues $k_{z,i}$; i.e.,

$$Y_i' = k_{z,i} Y_i \qquad \text{(no summation)}. \tag{6.6b}$$

These Y_i's are locally sinusoidal solutions with local wave numbers $k_{z,i}$. Shown in Fig. 4 are the four local wave numbers $k_{z,i}$ as functions of height z for a typical set of (ω, k_x). [Note the near-degeneracy even at $|z| \ll 1$ of two of the eigenvalues, which asymptote to the degenerate convective modes (5.23), (5.24) at $|z| \gg 1$.] At large $|z|$, these $k_{z,i}$'s are all constant, and therefore the locally sinusoidal solutions are globally (at $|z| \gg 1$) sinusoidal. At $|z| \ll 1$, the imaginary parts of the local k_z's are usually big, and the real

parts change rapidly with z. One of the four $\mathrm{Im}(k_z)$'s is positive for $z>0$ and one is negative for $z<0$; this is the strongly damped solution, which produces the stiffness of the equations. A numerical solution to the ODE's, starting from a given value at $z=0$, will be altered strongly, because of the large and rapidly changing $k_{z,i}$'s, as it tries to propagate to the uniform region ($z=\pm\infty$). The imaginary part of k_z is produced by β', the spatial derivative of the shift function and the spatial derivatives of MHD variables — which are also caused by β'. Therefore, starting from a given initial condition at $z=0$, how the numerical solution evolves to its sinusoidal form at large $|z|$, and what sinusoidal form the solution evolves to are completely determined by β', once the frequency ω and the wave number k_x are fixed.

The ODE system (5.13) for our Fourier analyzed MHD perturbations has been solved using the well-known ODE solver, the LSODE package.[26] This is a variable-step, variable-order code using linear multistep methods. For stiff systems such as ours, it uses Backward Differentiation Formulas (BDF) with maximum order 5. To ensure the correct coding of our MHD perturbation equations [Eqs. (5.13)], we have used the symbolic manipulating program SMP[27] to eliminate algebraic coding errors. We have also checked our numerical solutions in the uniform region against the analytic solutions presented in Sec.V [Eqs. (5.20)—(5.24)]. In the nonuniform region, we have spot-checked the code to be sure that the numerical solutions satisfy the first-order perturbed differential-energy-conservation law. Details of our numerical methods and checks, and of the numerical accuracy, are discussed in the appendix.

In Fig. 5 is shown a typical one of our numerical solutions. This solution has $\omega=6.5$ and $k_x=3.25$, and its driving "force" is $f_x=10^{-6}$, $f_{\mathrm{E}}^{+}=f_{\mathrm{E}}^{-}=N^{+}=N^{-}=0$. Notice this solution's rapid, nonsinusoidal changes near $z=0$, and the manner in which it finally settles down to a sinusoidal form in the region $|z|\gg 1$. By studying how these perturbations settle into their asymptotic forms and what asymptotic forms they settle into, we

shall be able to infer the effects of the shift function on the MHD perturbations. By studying perturbations at different frequency ω and wave number k_x, we will be able to infer the response of the MHD system to perturbations in the ω-k_x plane.

As an aid to understanding our perturbation solutions, we shall mostly examine the perturbation variables $\vec{v}$, $\vec{b}$ and $\tilde{\rho}$, but also the z-component of the first-order perturbation of the energy flux as measured by FIDO's. The exact, nonlinear energy flux measured by the FIDO's is

$$\vec{S}=\rho\gamma^2\vec{V}+\frac{1}{4\pi}(\vec{V}\times\vec{B})\times\vec{B}\ ; \tag{6.7}$$

and the first-order perturbation of its z-component is

$$\delta S^z=\rho\gamma u\,[\tilde{\rho}\,\gamma+2\gamma^3(Vv_x+uv_z)+\gamma v_z/u-\lambda(Vb_z-ub_x-\lambda v_z+v_x)/s-Cb_x/s]\ . \tag{6.8}$$

This first-order energy flux is a modulation of the stationary flux and has zero time-averaged value. A nonzero time-averaged energy flux carried by the perturbations shows up only at second (quadratic) order. This second-order flux will not be of interest to us: We wish to understand the modulation of the outpouring energy by the perturbations; and the modulation is embedded in the first-order δS_z.

In the following, we shall describe our solutions for the outflowing waves generated by various delta-function sources in terms of the following quantities: (i) the perturbations b_z, v_x, v_z, $\tilde{\rho}$ excited at the interface; (ii) the ratios of the asymptotic values of b_z, v_x, v_z, $\tilde{\rho}$ to their values at the interface; (iii) the ratio of the first-order energy flux δS_z evaluated at $z\to\pm\infty$ to that at the interface. These quantities will be plotted as functions of frequency ω at fixed wave number k_x, functions of wave number k_x at fixed frequency ω, and functions of (ω, k_x) in three-dimensional plots. The ratios of quantities at $z=\pm\infty$ to those at $z=0$ reflect how strongly (the curl of) the shift function interacts with the

MHD perturbations; and the size of the perturbation variables at the interface represents how easily a perturbation to the stationary flow can be excited by the ''driving force'' at the interface. Variations of these quantities in the ω-k_x plane characterize the response of our MHD system to the ''driving force'' at different frequencies ω and wave numbers k_x. This study will give us insight into understanding some general features of interactions of MHD perturbations with the shift function, and will help us to identify some interesting directions for future research.

Shown in Figs. 6—8 are perturbations on both sides of the interface excited by three types of delta-function sources: $\{f_x=10^{-6}, f_E^{\pm}=N^{\pm}=0\}$, $\{f_E^{+}=f_E^{-}=10^{-6}, f_x=N^{\pm}=0\}$, and $\{N^{+}=N^{-}=10^{-6}, f_x=f_E^{\pm}=0\}$. Shown in Figs. 9—14 are the ratios of the first-order FIDO-measured energy fluxes evaluated at $z=\pm 7.35$ and $z=0$, as functions of ω and k_x. (Since the lengthscale of the background is ~1, $z=\pm 7.35$ is far enough into the uniform region to be representative of conditions at $z=\pm\infty$. See Figs. 3, 4 and 5.) In the three dimensional plots, the vertical direction represents the quantities being plotted, and the flat floor is the region outside (6.4), where we have not constructed solutions. We also show perturbations excited at the origin that are due to $f_x=10^{-6}$ alone (Figs. 15); perturbations to the magnetic field that are due to $f_E^{+}=f_E^{-}=10^{-6}$ alone (Figs. 16) and perturbations that are due to $N^{+}=N^{-}=10^{-6}$ alone (Figs. 17). Perturbations in fluid variables that are due to $f_E^{+}=f_E^{-}=10^{-6}$ alone do not show much variation in the ω-k_x plane and are not shown here.

In these figures, we see four distinct classes of responses in the ω-k_x plane. There are resonance near the line

$$\omega+\beta(0)k_x\equiv\omega-V_F k_x=0\ , \tag{6.9}$$

which manifest themselves as ridges or neighboring ridges and valleys; there are ridges

along lines parallel to (6.9); there are undulations along lines parallel to (6.7); and there are single shallow valleys along (6.9). All these appear only in the ''superradiant'' region, the region in the ω-k_x plane where the FIDO-measured wave frequency

$$\omega_0 \equiv \omega + \beta(z) k_x \tag{6.10}$$

has opposite signs for FIDO's at $z \rightarrow -\infty$ from those at $z \rightarrow \infty$. We have seen no distinctive features in that part of the nonsuperradiant region which we have explored: $0 < 4.99 k_x \leq \omega \leq 9.99$.

Of these features, the most interesting seems to be the resonance along $\omega - V_F k_x = 0$. The key feature of $\omega - V_F k_x$ is not its role as the FIDO-measured angular frequency at the interface, but rather its role as the angular frequency in the field lines' rest frame at the point $z=0$, where the driving ''forces'' act. We shall emphasize this by denoting $\omega - V_F k_x \equiv \omega_F$ (F for ''field lines''). *The resonance occurs, then, at $\omega_F = 0$, i.e., for those values of ω and k_x, which produce vanishing angular velocity in the field lines' rest frame at the point where the driving ''forces'' act.* Evidently, it is easier to drive perturbations, with a fixed rate of injection of linear momentum $f_x \rho \gamma u$ or a fixed rate of injection of kinetic energy $f_E \rho \gamma u (f - 1)$, when one does so near zero frequency in the field's rest frame, $\omega_F \approx 0$, than when one does so well away from zero frequency, $|\omega_F| \geq 1$. As Figs. 18 show, not only are the perturbation quantities b_z, v_x, v_z and $\tilde{\rho}$ especially easily excited at $\omega_F \approx 0$, it is also especially easy for these perturbations to propagate to $z = \infty$, carrying with them a modulation of the magnetosphere's outflowing energy.

By contrast with this resonant ease of excitation for perturbations driven by f_x and $f_E^+ = f_E^-$, there is at $\omega_F = 0$ a resonant resistance to perturbations driven solely by modulations of the rest-mass injection rate, $N^+ = N^- = 0$ (see the resonant valley in Fig. 14). The physical reason for this is not clear.

The case of injection of linear momentum corresponds most closely to buffeting of a black-hole magnetosphere, in the plasma-creation region, by lumpy accretion-disk $\vec{B}$-fields. For this case the strength of the driving force can be characterized by its amplitude of injected momentum per unit area, i.e., the amplitude $\delta T_{xz}=\rho\gamma u f_x$ of the oscillatory discontinuity in the stress. When divided by the equilibrium magnetosphere's conserved stress $T_{xz}=\rho\gamma u l$ [See Eqs. (3.28), (3.30′) of Ref. 1], this injected momentum-per-unit area gives a dimensionless driving force

$$\frac{\delta T_{xz}}{T_{xz}}=\frac{f_x}{l}=\frac{f_x}{40} \tag{6.11}$$

that is a better measure of the strength of the force than f_x alone. Here, $l=40$ is the value of l used throughout our numerical calculations. Since our numerical calculations also use $f_x=10^{-6}$, the value of this dimensionless driving force is $\delta T_{xz}/T_{xz}=2.5\times10^{-8}$. This driving force produces a magnetospheric response in the plasma production plane, which can be characterized by the amplitude $\delta S_x(z=0)$ of the modulations of the FIDO-measured upward energy flux. From Fig. 19 we read off the value $\delta S_z(z=0)\simeq 2.9\times10^{-8}\rho\gamma u$. For comparison, in the unperturbed magnetosphere the upward energy flux at $z=0$ is $S_z=\rho\gamma u f=1.01\rho\gamma u$ [see Eqs. (3.28), (3.31′) of Ref. 1]. By combining these numbers with Eq. (6.11), we obtain

$$\frac{\delta S_z(z=0)}{S_z(z=0)}\simeq 1.15\frac{\delta T_{xz}}{T_{xz}}\ . \tag{6.12}$$

In words: the driving force produces a fractional modulation of the magnetosphere's energy flux, at $z=0$ and on resonance, that is nearly the same as the dimensionless measure $\delta T_{xz}/T_{xz}$ of the force.

As the magnetospheric perturbations propagate outward to $z \gg 1$, they get amplified by an amount (Fig. 9a)

$$\frac{\delta S_z(z \gg 1)}{\delta S_z(z=0)} \simeq 19 , \tag{6.13}$$

on resonance. Off resonance, this ''amplification factor'' is usually in the range 0.2 to 3. For comparison, the amplification of the upward energy flux in the unperturbed magnetosphere is, since $S_z = \rho\gamma u(f + Cl)$ at all heights,

$$\frac{S_z(z \gg 1)}{S_z(z=0)} = \frac{f + V_F l}{f} \simeq 80 ; \tag{6.14}$$

this is four times larger than the amplification (6.13) of the perturbation. By combining Eqs. (6.12) and (6.14) we see that on resonance the fractional modulation of the distant wind's energy flux is about one-third the dimensionless measure of the driving force:

$$\frac{\delta S_z(z \gg 1)}{S_z(z \gg 1)} \simeq 0.3 \frac{\delta T_{xz}}{T_{xz}} . \tag{6.15}$$

Thus, the wind's response on resonance is strong, but not terribly strong.

VII. Implications for Kerr black holes

In the numerical results presented in Sec. VI we saw resonances near $\omega_F \equiv \omega - V_F k_x = 0$ in the ω–k_x plane — i.e., for values of ω and k_x that produce a near-vanishing angular frequency in the rest frame of the field lines in the driving region. It is reasonable to speculate that a similar behavior will occur in the magnetosphere of a Kerr black hole.

In the magnetosphere of a Kerr hole the field-line angular velocities Ω_F are constant along each field line, but may differ from one field line to another. However, from detailed studies of magnetospheres,[6,12,13] it seems likely that the variations are not great and that Ω_F is approximately equal to one-half the angular velocity of rotation of the hole's horizon, $\Omega_F \simeq \Omega_H/2$.

For a Kerr hole the angular quantum number m (which takes on integral values) is the analog of our planar magnetosphere's k_x, and the perturbation angular frequency ω as measured at infinity is the analog of our planar ω. The perturbation angular frequency ω_F as measured at any radius in the rest frame of the field lines (but using as the ''clock'' the ''universal time'' t of the membrane paradigm — i.e., the Killing-vector defined time t, i.e., the Boyer-Lindquist time coordinate t, i.e., proper time as measured at infinity) is given by $\omega_F = \omega - m\Omega_F$. This is the analog of our planar relation $\omega_F = \omega - k_x V_F$. Thus, if our planar results can be extrapolated to a Kerr black hole, then *perturbations of a Kerr hole's magnetosphere with angular quantum number m may be especially easy to excite at angular frequencies, as measured at infinity, given by*

$$\omega \simeq m\Omega_F \simeq \frac{m}{2}\Omega_H = \frac{m}{4M}\frac{a}{1+\sqrt{1-a^2}} . \tag{7.1}$$

Here, M is the hole's mass and a is its dimensionless angular momentum parameter (its angular momentum divided by its squared mass).

A likely driving force for perturbations of a Kerr hole is the Maxwell pressure of nonaxisymmetrically distributed magnetic field lines anchored in the innermost region of the accretion disk — i.e., chaotic clumps of field lines anchored in the disk. Such a clump will orbit the hole with an angular velocity approximately equal to the ''Keplerian'' (geodesic) angular velocity at the radius of the lump of plasma that anchors it; and as it orbits, its Maxwell pressure will buffet the field lines that thread the hole,

thereby driving magnetospheric perturbations.

In order for such a clump of field lines to drive magnetospheric perturbations on resonance, the Keplerian angular velocity [e.g., Eq. (5.4.3) of Ref. 28]

$$\Omega_K = \frac{M^{1/2}}{r_L^{3/2} + aM^{3/2}} \tag{7.2}$$

of its anchoring lump (which orbits at radius r_L) must be approximately equal to the field-line angular velocity (7.1). This implies for a rapidly rotating hole $a \simeq 1$ that

$$r_L \simeq \frac{(4-m)^{2/3}}{m^{1/3}} M = (2.08,\ 1.26,\ 0.69)\, M \quad .$$

Here, 2.08 corresponds to $m=1$, 1.26 corresponds to $m=2$, and 0.69 corresponds to $m=3$. For an extreme Kerr black hole, the last stable circular orbit for a corotating particle is at $r=M$. Therefore, for a Keplerian orbit, only a very few angular quantum numbers can be responsible for this kind of resonant excitation. On the other hand, the disk's pressure gradient may well force clumps that are anchored near its inner edge to orbit at an angular velocity much slower than Keplerian. In this case, resonant excitations can occur for more angular quantum numbers m than the Keplerian orbit would predict.

It is far from certain that the resonance seen at $\omega_F = 0$ in our planar magnetosphere will also show up in the magnetosphere of a Kerr hole. Only a detailed study of the dynamics of Kerr-hole magnetospheres can reveal for sure. If the resonance does show up and is much more easily excited than in our model magnetosphere [Eq. (6.15)], then observations of temporal modulations of the innermost regions of jets in Active Galactic Nuclei might someday reveal the angular velocities of the central hole's magnetic field lines.

VIII. Conclusions and future research

The numerical calculations presented here have raised more questions than have been answered. However, they do point out some interesting directions for future research. Of those features we see in Sec.VI, the most striking is the resonance near $\omega_F \equiv \omega - V_F k_x = 0$. It would be useful to understand more deeply this resonance in terms of the structures of the gravitational and MHD background. To help us understand this resonance, it would also be useful to perform a more detailed calculation to locate the precise sites of this resonance in the ω-k_x plane (in particular, to determine if a finite flow speed at $z=0$ will shift the location of the resonance line). In Sec. VII, we speculated about the implications of this resonance for the magnetosphere of a Kerr black hole. The need for perturbation computations in the Kerr geometry, or at the least in the planar model spacetime (2.3) with a horizon, is obvious. Even in the planar spacetime (2.4) of this paper, additional studies would be useful: Perturbations with $\delta B_y \neq 0$ would correspond more closely than those of this paper ($\delta B_y = 0$) to a Kerr magnetosphere perturbed by clumpy fields in a surrounding disk, and the influence of a nonzero y-component of the wave vector deserves study.

We have also seen undulations in the ratios of energy fluxes at large $|z|$ to those at the interface, and in some cases undulations in ratios of perturbations of fluid variables evaluated at these two locations. It would be worthwhile to understand the origin of these undulations and how to relate their amplitudes and periods to the gravitational and MHD background parameters.

We also note that the region in the ω-k_x plane where we have seen interesting features is the ''superradiant'' region. It would be interesting to study in this region whether the (quadratic) time-averaged energy flux of the perturbations exhibits superradiance analogous to that for vacuum electromagnetic (and other) waves.

Finally, we note that the study of fully dynamical ''magnetospheres'' in the planar spacetime (2.2) with a horizon might provide insight into the issue of whether and how a black-hole magnetosphere, if strongly perturbed, settles down into an energy-extracting, Blandford-Znajek-type[4] equilibrium state. (Punsley and Coroniti[14] argue that it does not do so.) This, of course, require a nonlinear analysis.

ACKNOWLEDGEMENTS

The author is indebted to Kip Thorne, who suggested this problem and has given considerable help in the course of this work and in the writing of this manuscript. The author would like to thank Paul Coppi for help in some of the graphic presentations of the numerical results. He has also benefited from discussions with Charles Evans in dealing with numerical difficulties. This work was supported in part by NSF grants AST85-14911 and AST88-17792.

APPENDIX

In this appendix, we discuss in some detail our numerical implementation of the MHD perturbation equations [Eqs. (5.13)], and their solutions. We discuss various checks performed on the coding process, on the numerical code and on the solutions it produces. We also identify the regions where the numerical solutions presented in Sec. VI are not reliable because of the numerical method employed.

The ODE system (5.13) is solved using the standard ODE solver, the LSODE package.[26] This package uses Backward Differentiation Formulas (BDF) methods when the equations are stiff, which is the case for our ODE system near $z=0$, i.e., in the region where the background interacts strongly with the MHD perturbation (the process we wish to study). Thus, we used the BDF option in our code. The maximum order that we used in computing derivatives was the default value of 5. The stationary background quantities appear in coefficients of the ODE system. They were provided to the ODE solver at 402 points with uniform separations Δz in the region $-7.35 \leq z \leq 7.35$. The values of the ODE coefficients between these points were obtained by parabolic interpolation. The numerical solutions were output at the 402 uniformly spaced points.

At each step, the (relative) tolerance we provided to LSODE was 2×10^{-6}. However, because of the accumulation of errors and because of the internal steps used by the ODE solver in each zone, the actual global error may not be as good as this, as indicated by a test done with constant-coefficient ODE's. In this test, we construct a constant-coefficient ODE system by replacing the coefficients in Eqs. (5.13) at all other locations by their values at $z=0$. We chose the values at $z=0$ in this test because the imaginary parts of wave numbers there are the largest; i.e., the ODE system is the stiffest there and therefore this is the most difficult region for the solver to handle. We integrated the resulting ODE system starting from, in turn, only one of $\{b_z, v_x, v_z, \tilde{\rho}\}$ nonzero; and we then compared our numerical solutions with the analytic solutions for this constant ODE

system. It was found that if we require

$$\frac{|\phi_{\text{numerical}}-\phi_{\text{analytic}}|}{(|\phi_{\text{numerical}}|+|\phi_{\text{analytic}}|)/2} \leq 0.1\% \quad , \tag{A.1}$$

then we can always integrate the ODE's out to $z \simeq 2$ or even farther (Table I). This is such a high z that for the ODE's of our real problem, the equations have ceased to be stiff for most choices of (ω, k_x). [See Fig. 4] However, because of (i) the stiffness of the problem at small z, near $\omega \simeq 0.99 k_x$; (ii) the single precision used in the numerical integration; and (iii) our lack of any way to separate globally and cleanly the growing and decaying solutions in the changing β region, the fastest decaying solutions can be completely lost to numerical truncation error even though the numerical solution and the analytic solution agree to the last digit. This loss of one solution will occur if near $z=0$, $-\text{Im}(k_z)$ of the fastest decaying mode does not approach zero rapidly enough as z moves away from the interface. More specifically, if, roughly, we have at $z=\delta L$,

$$-\text{Im}(k_z)\, \delta L \sim 10 \quad , \tag{A.2}$$

for the fastest decaying mode, then the single precision we used will not be adequate to preserve the decaying component of the numerical solution. As an example, in Fig. 20, we plot the local wave numbers k_z at frequency $\omega=6.5$ and wave number $k_x=6$. It is seen that $-\text{Im}(k_z)$ for the fastest decaying mode is still quite significant near $z \simeq 2$. truncation. This produces wild fluctuations in quantities like $|\delta S_z(+7.35)/\delta S_z(0)|$, shown in Fig. 9(a). If we were to use double precision (and higher accuracy) in our computation, this fluctuating region would be pushed to larger k_x, i.e., to near the boundary $\omega \simeq 9.99 k_x$. In Fig. 21 is shown one such result computed at $\omega=6.5$, using double precision and (relative) tolerance of 2×10^{-7} at each step. Note that the fluctuation region begins only after $k_x \simeq 5.5$ as opposed to $k_x \simeq 4$ in Fig. 9(a), where single precision and larger tolerance

2×10^{-6} were used. This test can also serve as a global error estimate, where we use a smaller tolerance, i.e., a smaller step size in the integration, and the result in the nonfluctuating region stay the same.

To ensure the correct coding for our computation, we have made a few other numerical and algebraic checks: The simplest was a comparison of our numerical solutions in the uniform region (region of constant background variables) with the analytic solutions presented in Sec. V. To be more precise, one must be able to decompose the numerical solutions into individual wave modes; and each mode should evolve (with coordinate z) according to Eqs. (5.20)—(5.24). From test results shown in Table I, we know that the ODE solver as implemented will give correct numerical solutions for constant coefficient ODE's. Therefore, the key point here is that in the uniform region, our code should produce numerical solutions for each wave mode, which have the correct ratios of the amplitude of the perturbation quantities [Eqs. (5.20), (5.23), (5.24)] and the correct dispersion relations [Eqs. (5.21), (5.22)]. Shown in Table II are the results for such a comparison between the numerical and the analytic solutions of the magnetosonic modes for typical values of (ω,k_x). The agreement is good. They also agree quite well in tests taken at other values of (ω, k_x).

We also have to be sure that the code is implemented correctly in the nonuniform region, where the background is changing. To test the code, we have checked to see that our numerical solutions satisfy the differential energy conservation law,

$$\frac{d\varepsilon}{d\tau}+\vec{\nabla}\cdot\delta\vec{S}=\beta'\delta T_{xz} \quad . \tag{A.3}$$

Here,

$$\varepsilon=\rho\gamma u\left[\frac{1}{s}\left[\lambda b_x+b_z+C\left(Vb_z-ub_x+v_x-\lambda v_z\right)\right]+2\gamma^3(v_xV/u+v_z)+\tilde{\rho}\gamma/u\right] \quad , \tag{A.4a}$$

$$\delta S^x=\rho\gamma u\left[2\gamma^3 V(v_x V/u+v_z)+\tilde{\rho}\gamma v/u+\gamma v_x/u+\frac{1}{s}(Vb_z-ub_x-\lambda v_z+v_x)+\frac{C}{s}b_z\right] \quad \text{(A.4b)}$$

$$\delta S_z=\rho\gamma u\left[\tilde{\rho}\gamma+2\gamma^3(Vv_x+uv_z)+\gamma v_z/u-\frac{\lambda}{s}(Vb_z-ub_x-\lambda v_z+v_x)-\frac{C}{s}b_x\right] , \quad \text{(A.4c)}$$

$$\delta T_{xz}=\rho\gamma u\left[\tilde{\rho}\gamma V+(1+2\gamma^2V^2)\gamma v_x+(1+2\gamma^2u^2)\gamma V v_z/u-\frac{1}{s}(b_x+\lambda b_z)\right] \quad \text{(A.4d)}$$

are the FIDO-measured, first-order (i.e., linear in perturbation quantities) energy density, energy flux and x-z component of stress, In Table III is shown the result of such a test. There the relative error is defined as

$$(err\,\%)\equiv\frac{|-i[\omega+\beta(z)k_x]\varepsilon+ik_x\delta S^x+\delta S_z'-\beta'\delta T_{xz}|}{(|[\omega+\beta(z)k_x]\varepsilon|+|k_x\delta S^x|+|\delta S_z'|+|\beta'\delta T_{xz}|)/4} .$$

In these tests, the zone size was $\Delta z=0.002$, and the largest value of the wave number was $|k_z|\lesssim 100$. Therefore, we would expect that the error should be no larger than

$$\left[\frac{1}{k_z\Delta z}\right]^2\simeq 4\% ,$$

which is the case in these tests as shown in Table III.

Finally, as another powerful check, we have subjected the code to scrutiny by a symbolic manipulation program, SMP.[27] This check is a purely symbolic algebraic check, and the program SMP does not have any known bugs in this area. Because of the complexity of the MHD perturbation equations [Eqs. (5.13)], this check has been done in the following steps. We first coded Eq. (5.5) in the SMP format and decomposed it into its component form, consisting of terms involving MHD perturbations and their time and spatial derivatives. We also did the same for (A.3). The conservation of energy (A.3) is

guaranteed by the equations of motion [Eqs. (5.6) or (5.13)]. By expressing the time derivatives of the perturbations in terms of the perturbations themselves and their spatial derivatives, and by substituting these expressions for the time derivatives into (A.3), we should have (A.3) now identically zero. This is what we have done successfully using SMP. Now we have a correct form of (5.6) in the SMP format. We ''translated'' it into Fortran format to be used in our code. We also translated the resulting Fortran code back to SMP format and compared it with the original SMP version of the MHD equations term by term, to eliminate any possible errors in this ''translation'' process (one big source of errors is the correct positioning of parentheses). Our final Fortran code of the MHD equations was the Fourier-analyzed form of this SMP checked version, i.e., with the time derivatives in our intermediate code replaced by $-i\omega$ and derivatives with respect to x replaced by ik_x.

To conclude, the coding of the MHD perturbation equations and their numerical solutions have been subjected to extensive checks and tests, both numerically and algebraically. These tests and checks make it very likely that there are no programming errors left. The single precision used in the computation, and the stiffness of the problem near the boundary of the integration region in the ω-k_x plane, render the solutions presented in Sec. VI not reliable in that part of the integration region. However, to show the general trend in the ω-k_x plane of various quantities, results in this unreliable region were still kept.

REFERENCES

[1] X.-H. Zhang, Phys. Rev. D**39**, 2933 (1989).

[2] M. J. Rees, Ann. Rev. Astron. Astrophys. **22,** 471 (1984).

[3] C. M. Gaskell and L.S. Sparke, Astrophys. J., **30,** 175 (1986); C. M. Gaskell and B.M. Peterson, Astrophys. J. Suppl., **65,** 1 (1987); J. L. Tonry, Astrophys. J., **322,** 632(1987); A. Dressler and D. O. Richstone, Astrophys. J., **324,** 701(1988); J. Kormendy, Astrophys. J., **325,** 128 (1988).

[4] R. O. Blandford and R. L. Znajek, Mon. Not. R. astr. Soc. **179,** 433 (1972).

[5] Douglas Macdonald and Kip S. Thorne, Mon. Not. R. astr. Soc. **198,** 345 (1982).

[6] E. S. Phinney, Ph.D. dissertation, Univ. of Cambridge, 1983.

[7] P. W. Guilbert, A. C. Fabian and M. J. Rees, Mon. Not. R. astr. Soc. **205,** 593 (1983).

[8] M. Ruderman and P. G. Sutherland, Astrophys. J., **196,** 51 (1975).

[9] A. P. Lightman, A. A. Zdziarski and M. J. Rees, Astrophys. J., **315,** 113 (1987).

[10] K. S. Thorne, R. H. Price and D. A. Macdonald, *Black Holes: The Membrane Paradigm* (Yale University Press, New Heaven, 1986).

[11] D. A. Macdonald, Mon. Not. R. astr. Soc. **211,** 313 (1984).

[12] C. M. Mobarry and R. V. E. Lovelace, Astrophys. J., **309,** 455 (1986).

[13] R. V. E. Lovelace, C. Mehanian, M. Mobarry and M. E. Sulkanen, Astrophys. J., **62,** 1 (1987).

[14] B. Punsley and F. V. Coroniti, UCLA preprints PPG-1208, PPG-1209.

[15] R. D. Blandford, to be published.

[16] S. A. Teukolsky, Phys. Rev. Lett., **29,** 1114 (1972).

[17] S. Arnowitt, S. Deser, and C. W. Misner, in *Gravitation,* p.227, edited by L. Witten (Wiley, New York, 1962).

[18] James W. York, Jr., in *Sources of Gravitational Radiation,* edited by Larry L. Smarr (Cambridge University Press, Cambridge, 1979).

[19] Kip S. Thorne and Douglas Macdonald, Mon. Not. R. astr. Soc. **198,** 339 (1982).

[20] C. Michel, Astrophys. J., **157,** 1183 (1969).

[21] I. Okamoto, Mon. Not. R. astr. Soc. **185** , 69 (1978).

[22] C. F. Kennel, F. S. Fujimura and I. Okamoto, Geophys. & Astrophys. F. Dyn. **26,** 147 (1983).

[23] T. Regge and J. A. Wheeler, Phys. Rev., **108,** 1063 (1957).

[24] J. A. Wheeler, Phys. Rev., **97,** 511 (1955).

[25] J. D. Jackson, *Classical Electrodynamics* (Wiley, New York, 1975).

[26] Alan C. Hindmarsh, in *Scientific Computing,* edited by R. S. Stepleman et al. (North-Holland, 1983), p.55.

[27] SMP Customer Support, Inference Corp., 5300 W. Century Blvd., LA, CA 90045.

[28] Novikov and Thorne, in *Black Holes,* edited by C. DeWitt and B. S. DeWitt (Gordan and Breach, 1973), p.343.

Table I. Comparison of numerical solution and analytic solution. This is to test the implementation of the LSODE solver. The z-coordinate z_0 shown in the table is the place where the two solutions begin to differ by more than 0.1%, i.e., when

$$\frac{|\phi_{\text{numerical}}-\phi_{\text{analytic}}|}{(|\phi_{\text{numerical}}|+|\phi_{\text{analytic}}|)/2} \geq 0.1\% \ .$$

The integration starts from $z=0$, with only one of b_z, v_x, v_z, $\tilde{\rho}$ nonzero. This test is done for a constant matrix $Q_i{}^j$ [Eq. (6.5)] with eigenvalues $k_{z,i}$: (–0.891791,1.81247), (0.929320,–1.34887), (28.8836,–0.447894) and (29.0075,0.992878). Here in $k_{z,i}=(a,b)$, a is the real part, b is the imaginary part.

	$b_z(z=0)\neq 0$	$v_x(z=0)\neq 0$	$v_z(z=0)\neq 0$	$\tilde{\rho}(z=0)\neq 0$
z_0	1.64	20.0	16.78	4.2

Table II. Comparison of numerical and analytic MHD wave solutions in the uniform region. Compared here are the wave numbers $k_{z,i}$ and the four components of the eigenvectors Y_i of the magnetosonic modes [see Eq. (6.6)]. This is to check the coding of MHD perturbation equations. Here complex numbers are written in the form (a,b) with a being the real part, and b the imaginary part. The two solutions are compared at ω=5, k_x=3 and β=–4, i.e., at z=–∞.

	numerical	analytic	numerical	analytic
wave number $k_{z,i}$	–6.46604	–6.46832	6.34466	6.34691
eigenvectors Y_i	0.626141	0.62608	0.902400	0.902377
	–0.141465	–0.141472	–0.0764952	–0.0765017
	–0.485317	–0.485341	–0.262427	–0.262450
	–0.593635	–0.593678	0.333097	0.333141

Table III. Test on numerical solutions of conservation of FIDO measured energy. Shown in the table are relative errors at several z's. Here the relative error is defined as

$$(\text{err}\%) \equiv \frac{|-i[\omega+\beta(z)k_x]\varepsilon+ik_x\delta S_x+\delta S_z'-\beta'\delta T^{xz}|}{(|[\omega+\beta(z)k_x]\varepsilon|+|k_x\delta S^x|+|\delta S_z'|+|\beta'\delta T^{xz}|)/4}$$

Shown in the table are results for four initial conditions starting, in turn, from one of b_z, v_x, v_z, $\tilde{\rho}$ nonzero.

	$z=0$	$z=0.4$	$z=1$	$z=3$
$b_z(z=0)\neq 0$	0.2	1.4	<0.1	0.1
$v_x(z=0)\neq 0$	0.2	1.6	0.4	0.1
$v_z(z=0)\neq 0$	0.2	0.7	0.4	<0.1
$\tilde{\rho}(z=0)\neq 0$	0.1	0.6	0.5	<0.1

FIGURE CAPTIONS:

Fig. 1 Solutions $\gamma u(C)$ to Eq. (3.19) for s=0.1, l=40, f=1.01. The "light plane" where C=1 is outside the Alfven point C_A, the location where the two positive branches cross each other. The fast magnetosonic point where the positive branches meet and terminate in this cold plasma model is located at C_0=3.94. (a) Diagram showing both sonic points; (b) Diagram showing details near the Alfven point C_A=0.988.

Fig. 2 The same stationary solution as in Fig. 1, drawn as a function of the coordinate z, with β (or C) the monotonic increasing function of z given by Eqs. (2.5) and (3.12). The solution is shown for three different values of $C_\infty \equiv V_F$, the value of C at $z \to \infty$. Curves (c) and (c′) correspond to $C_\infty > C_0$, which permits the stationary "wind" solution [curve (c)] to reach spatial infinity at a flow speed smaller than the fast magnetosonic speed there. Curves (b) and (b′) correspond to $C_\infty = C_0$, the critical value of C_∞ that enables the (continuously increasing) "wind" branch of the solution [curve (b) to approach the fast magnetosonic speed at spatial infinity. Curve (a) corresponds to $C_\infty < C_0$, an unphysical case in which the wind branch terminates at finite z. (a) Stationary solutions in the range $0 \leq z < 7.5$; (b) Stationary solutions near the Alfven point.

Fig. 3 A stationary gravitational and MHD background, with reflection symmetries (4.1)-(4.3), for the parameter set s=0.1, l=40, f=1.01 and V_F=2.

Fig. 4 Local wave numbers k_z of MHD perturbations as functions of z for the stationary background shown in Fig. 3. The perturbations have frequency ω=6.5 and wave number

k_x=3.

Fig. 5 A typical numerical solution of MHD perturbation equations (5.13). Only the four independent perturbation variables b_z, v_x, v_z, $\tilde{\rho}$ are plotted. The perturbations are excited by $f_x=10^{-6}$ alone at the interface $z=0$ (i.e., $f_{\rm E}^{\pm}=N^{\pm}=0$), and there are no ingoing waves at large $|z|$. The perturbations in the MHD background flow interact with the background strongly near $z=0$, and do not have a simple wave form. At large $|z|$, the perturbations are a superposition of outgoing sinusoidal waves.

Fig. 6 Perturbations excited by $f_x=10^{-6}$ alone (i.e., $f_{\rm E}^{\pm}=N^{\pm}=0$) at the interface. Note the resonance at $\omega+\beta(0)k_x=0$ [$\beta(0)=-2$]. Solid curves represent perturbations excited on the positive z side of the interface. Dashed curves represent perturbations on the negative side of the interface. (a) Perturbations at fixed frequency $\omega=6.5$; (b) Perturbations at fixed wave number $k_x=2.57$.

Fig. 7 Same quantities as plotted in Fig. 6, but for perturbations excited by $f_{\rm E}^{+}=f_{\rm E}^{-}=10^{-6}$ alone at the interface.

Fig. 8 Same quantities as plotted in Fig. 6, but for perturbations excited by $N^{+}=N^{-}=10^{-6}$ alone at the interface.

Fig. 9 The ratio $|\delta S_z(\pm 7.35)/\delta S_z(0)|$ for perturbations excited by $f_x=10^{-6}$ alone at the interface $z=0$. Here $\delta S_z(z)$ is the first-order perturbation of the z-component of the FIDO-measured energy flux [Eq. (6.6)]. The region where curves break is the region where MHD waves cannot propagate freely at $z\rightarrow-\infty$ and where numerical computations

have not been done. Solid curves correspond to perturbations on the $z>0$ side; dashed curves correspond to perturbations on the $z<0$ side. (a) The perturbations are excited at the fixed frequency ω=6.5; (b) The perturbations are excited at the fixed wave number k_x=2.57.

Fig. 10 Same quantities as plotted in Fig. 9, but for perturbations excited by $f_{\mathrm{E}}^{+}=f_{\mathrm{E}}^{-}=10^{-6}$ alone at the interface.

Fig. 11 Same quantities as plotted in Fig. 9, but for perturbations excited by $N^{+}=N^{-}=10^{-6}$ alone at the interface.

Fig. 12 The ratio $|\delta S_z(\pm 7.35)/\delta S_z(0)|$ for perturbations excited by $f_x=10^{-6}$ alone at the interface $z=0$. Here the ratio is plotted in the logarithmic scale. The flat floor is the region where MHD waves cannot propagate freely at $z\rightarrow-\infty$ and where the computation is not done. They have been assigned value one in these three-dimensional plots. (a) The ratio $|\delta S_z(7.35)/\delta S_z(0)|$ for perturbations on the $z>0$ side; (b) The ratio $|\delta S_z(-7.35)/\delta S_z(0)|$ for perturbations on the $z<0$ side.

Fig. 13 Same quantities as plotted in Fig. 12, but for perturbations excited by $f_{\mathrm{E}}^{+}=f_{\mathrm{E}}^{-}=10^{-6}$ alone at the interface.

Fig. 14 Same quantities as plotted in Fig. 12, but for perturbations excited by $N^{+}=N^{-}=10^{-6}$ alone at the interface.

Fig. 15 Perturbations excited on both sides of the interface by a delta-function source $f_x=10^{-6}$ there alone. The vertical direction is plotted on a logarithmic scale. (a)-(d): perturbations excited on the $z<0$ side; (e)-(g): perturbations excited on the $z>0$ side.

Fig. 16 Perturbations to the magnetic field b_z excited on both sides of the interface by a delta-function source $f_{\mathrm{E}}^{+}=f_{\mathrm{E}}^{-}=10^{-6}$ alone at the interface. Perturbations to the fluid variables do not show much variation and thus are not given here. (a) perturbations excited on the $z<0$ side; (b) perturbations excited on the $z>0$ side.

Fig. 17 Same quantities as plotted in Fig. 15. Perturbations are excited by $N^{+}=N^{-}=10^{-6}$ alone at the interface.

Fig. 18 Amplification factors (ratios of amplitudes of perturbations evaluated at large $|z|$ and at $z=0$) for perturbations excited by $f_x=10^{-6}$ alone at $z=0$. Here the ratio is plotted in the logarithmic scale. The flat floor is the region where MHD waves cannot propagate freely at $z\rightarrow-\infty$ Note the undulation in these quantities for perturbation in fluid variables. (a)-(d): perturbations excited on the $z<0$ side; (e)-(h): perturbations excited on the $z>0$ side.

Fig. 19 Energy flux at the interface, excited by $f_x=10^{-6}$ at $z=0$ alone. Note that when excited by only f_x, $\delta S_z(0)$ is continous at the interface.

Fig. 20 Local wave numbers k_z of MHD perturbations as functions of z for the stationary background shown in Fig. 3. The perturbations have frequency $\omega=6.5$ and wave number $k_x=6$.

Fig. 21 The ratio $|\delta S_z(\pm 7.35)/\delta S_z(0)|$ for perturbations excited by $f_x=10^{-6}$ alone at the interface $z=0$. The region where curves break is the region where MHD waves cannot propagate freely at $z \rightarrow -\infty$ and where numerical computations have not been done. Solid curves correspond to perturbations on the $z>0$ side; dashed curves correspond to perturbations on the $z<0$ side. This is computed with the double precision. The local tolerance used in the LSODE solver is 2×10^{-7}. Note that on the $z>0$ side, fluctuation begins at roughly $k_x \gtrsim 5.5$ as opposed to $k_x \simeq 4$ in Fig. 9, where single precision and local tolerance of 2×10^{-6} were used in that computation.

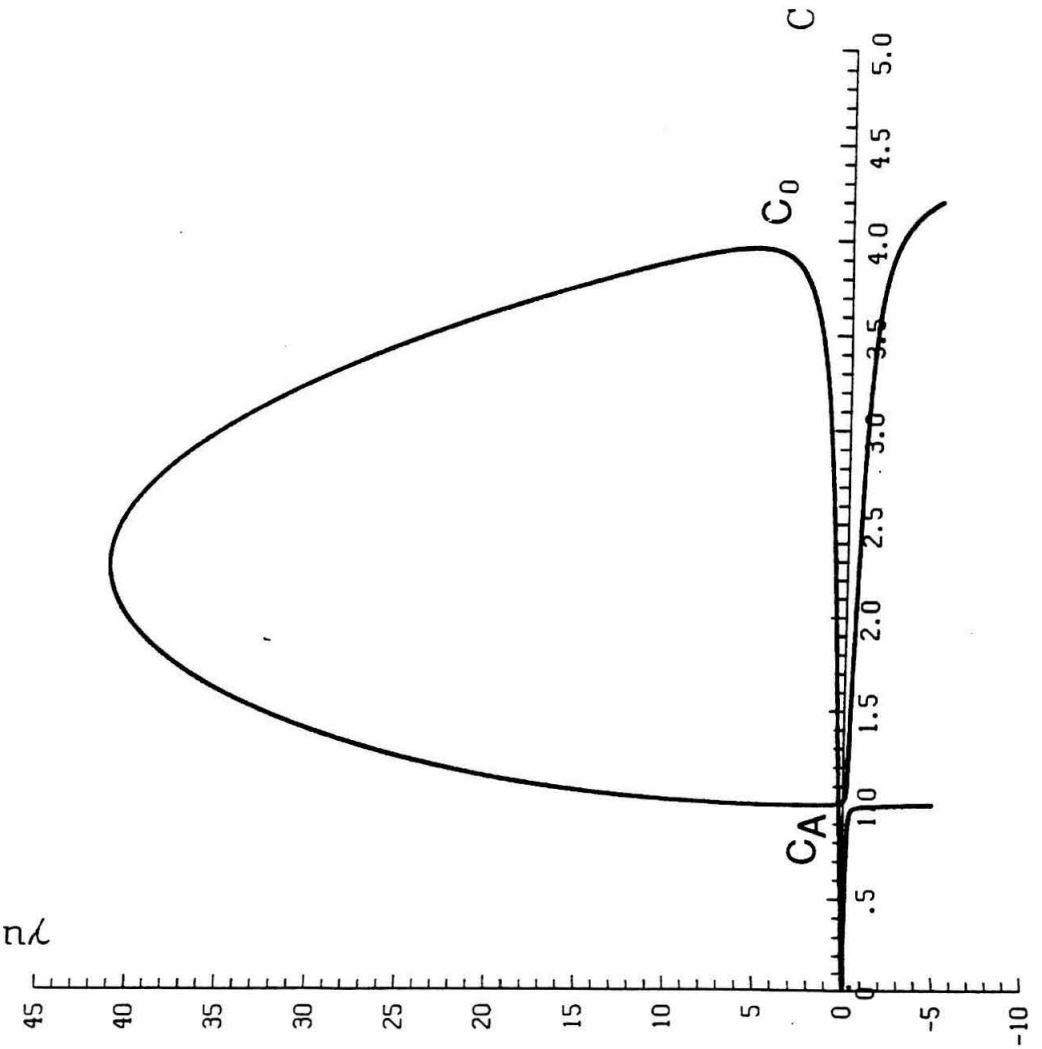

Fig.1(a)

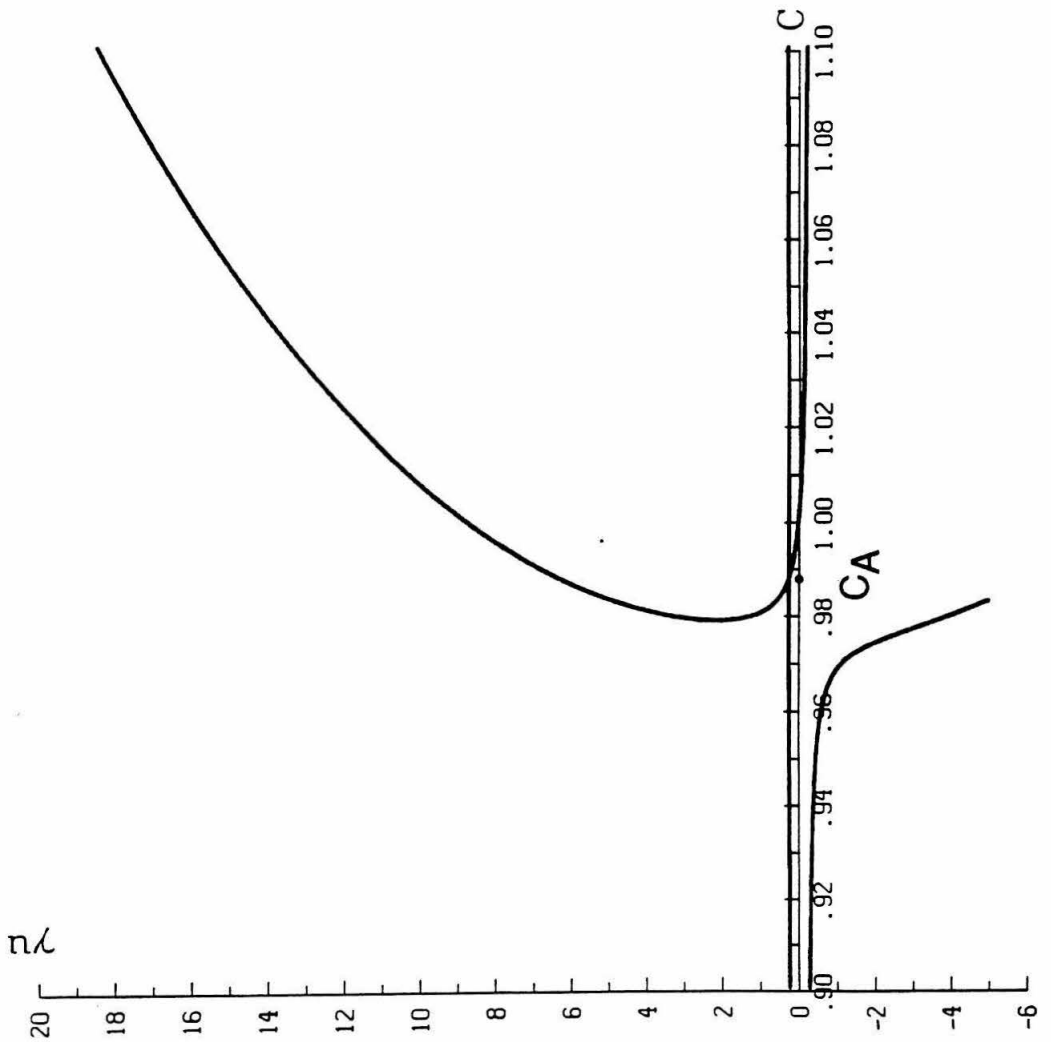
γu
20
18
16
14
12
10
8
6
4
2
0
-2
-4
-6
.90
.92
.94
.96
.98
1.00
1.02
1.04
1.06
1.08
1.10
C
C_A

Fig.1(b)

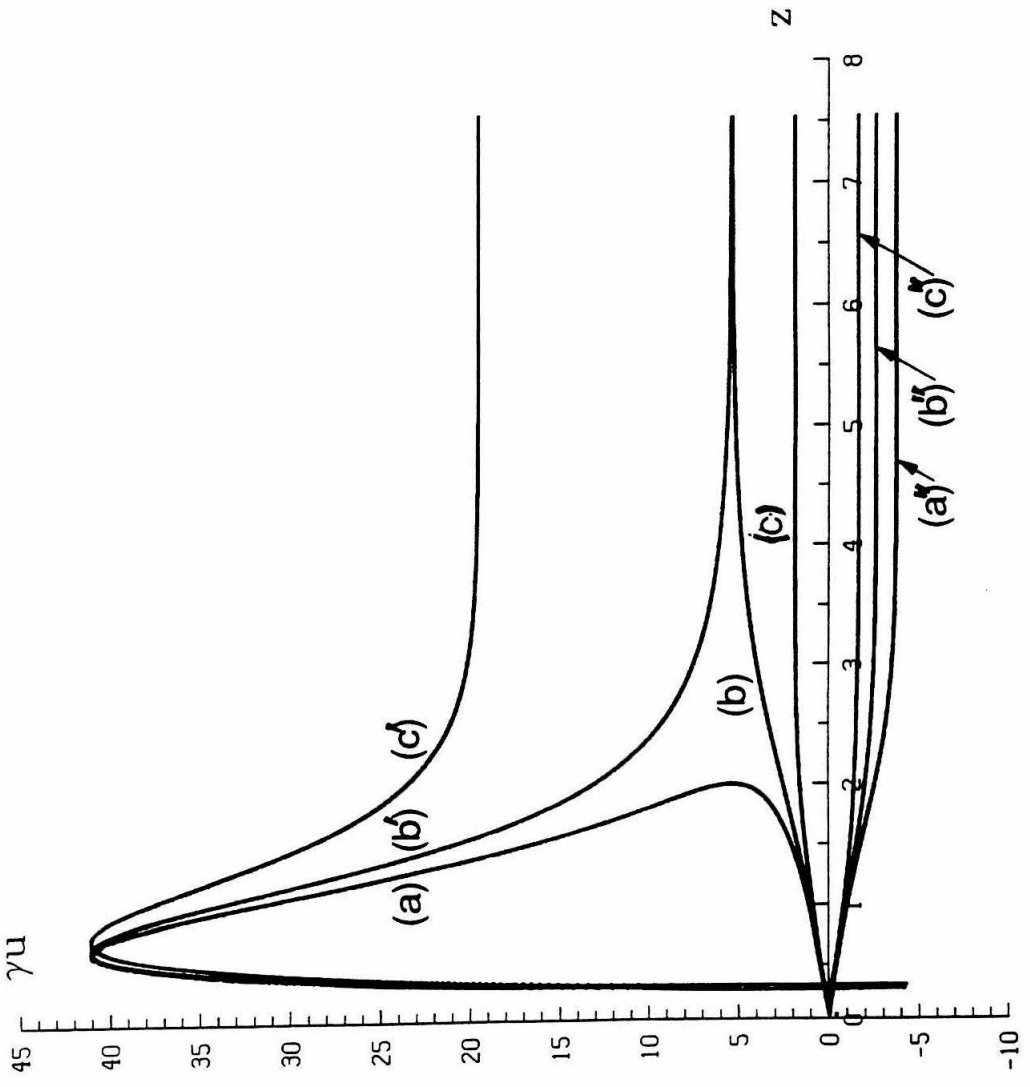

Fig.2(a)

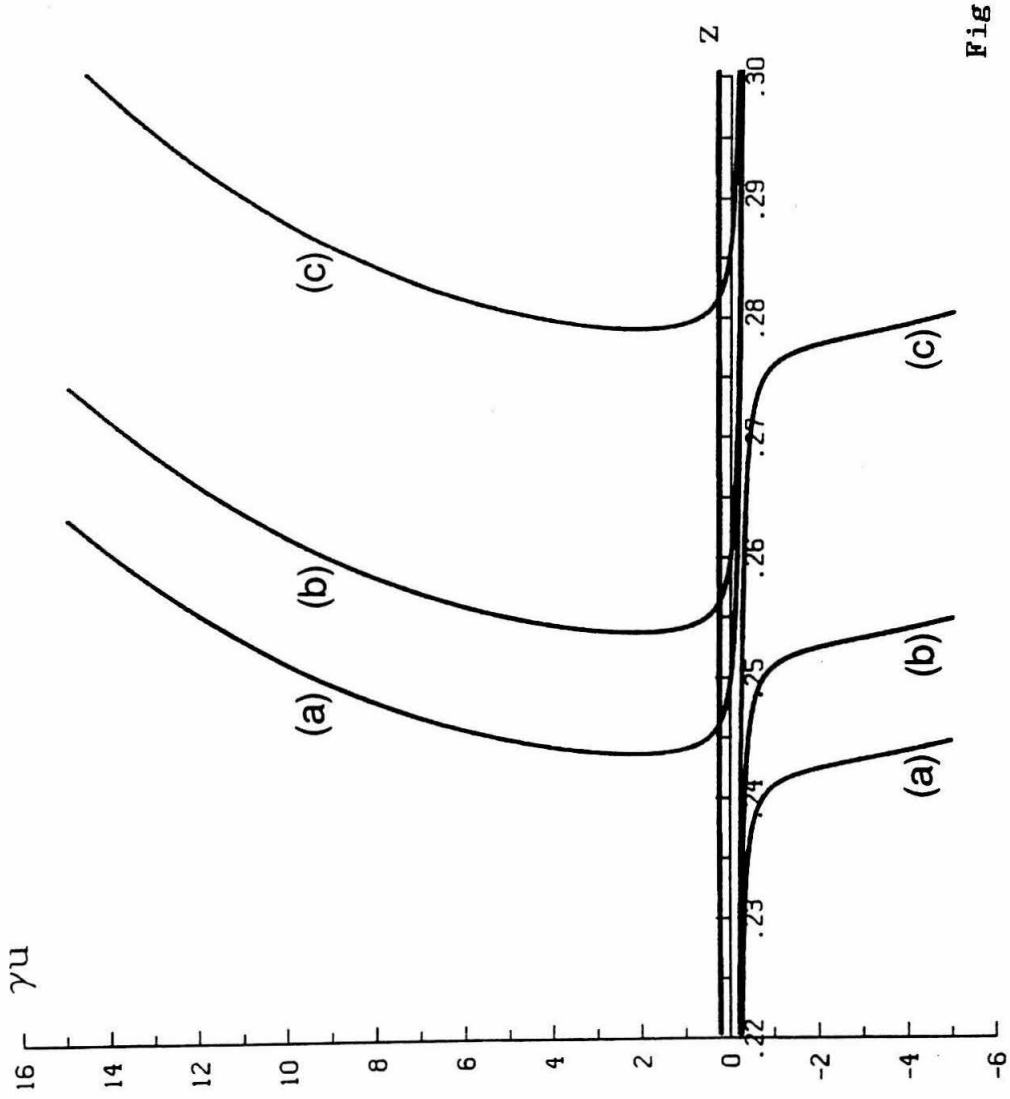

Fig.2(b)

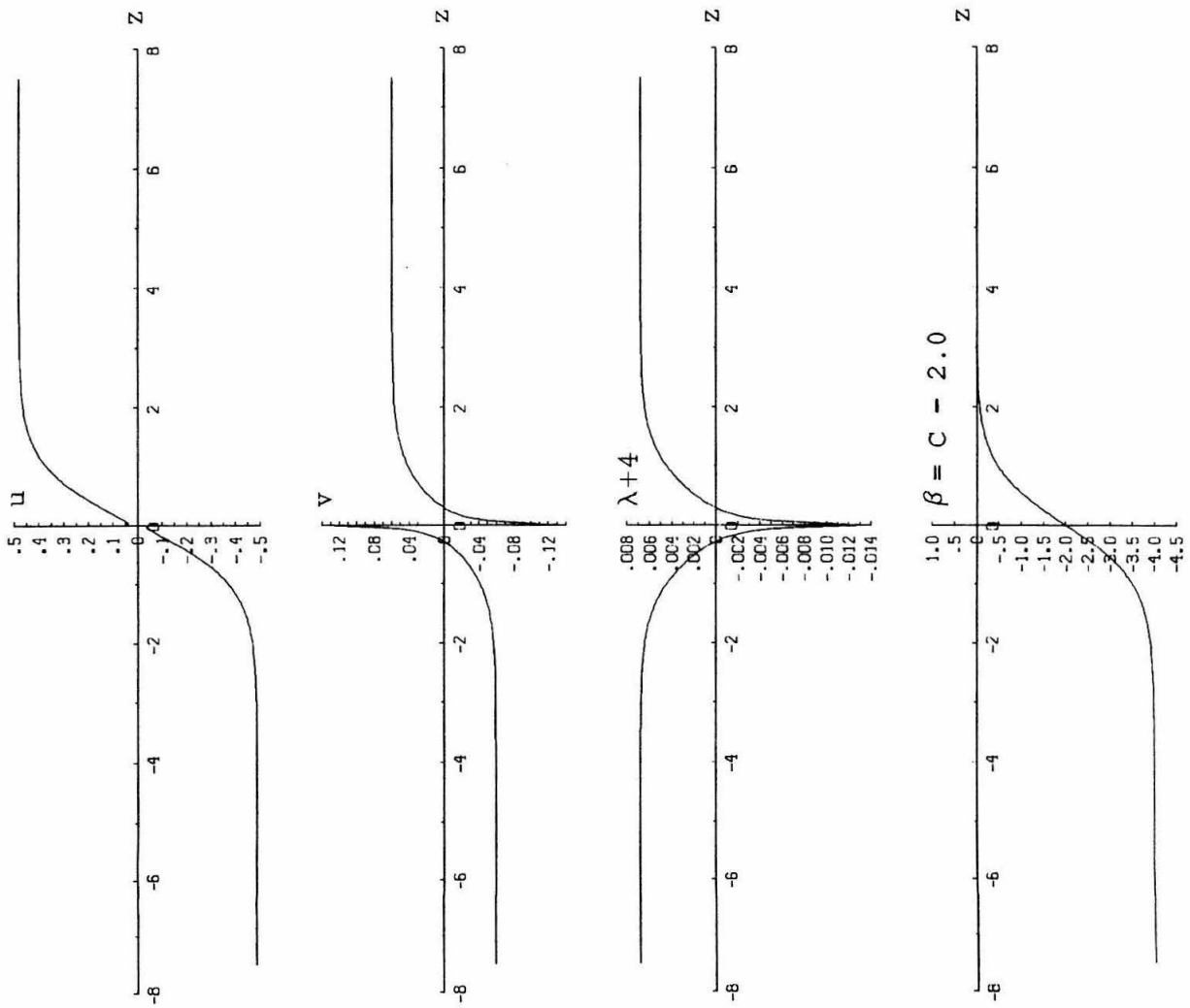

Fig. 3

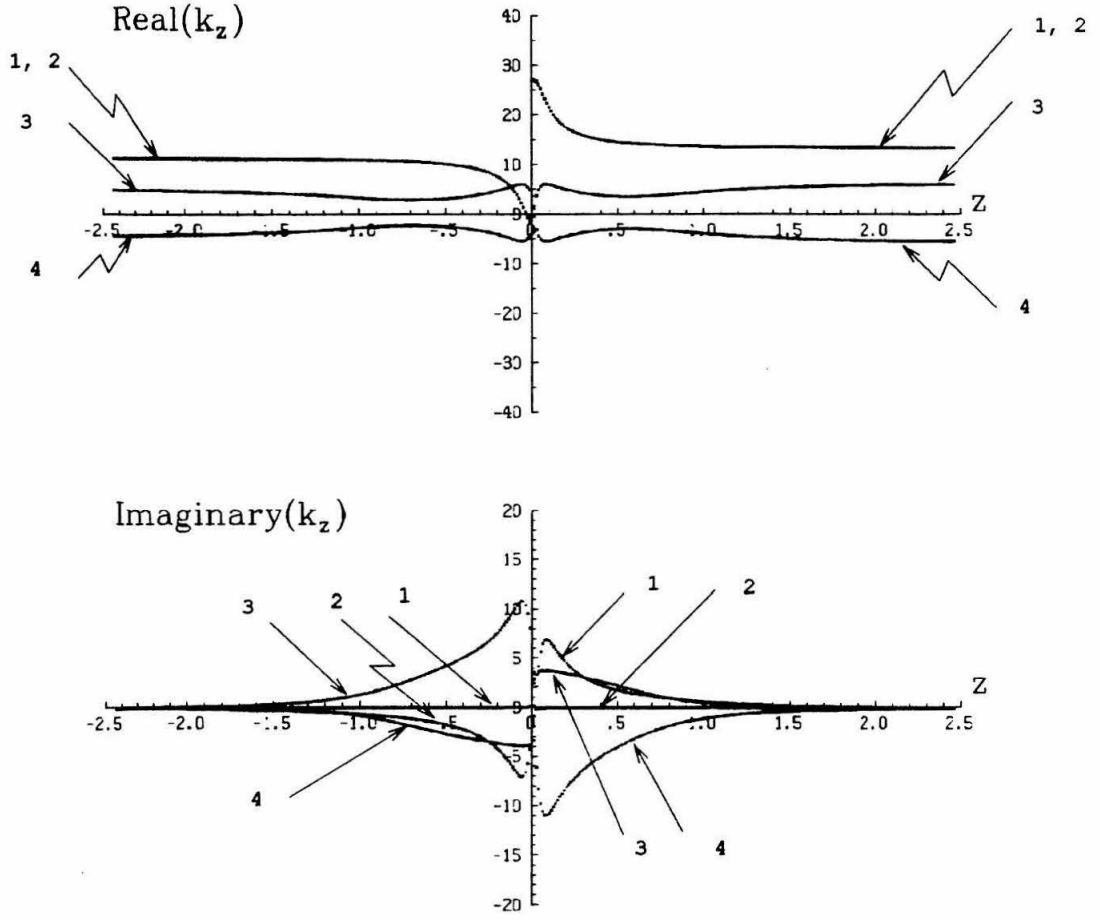

Fig. 4

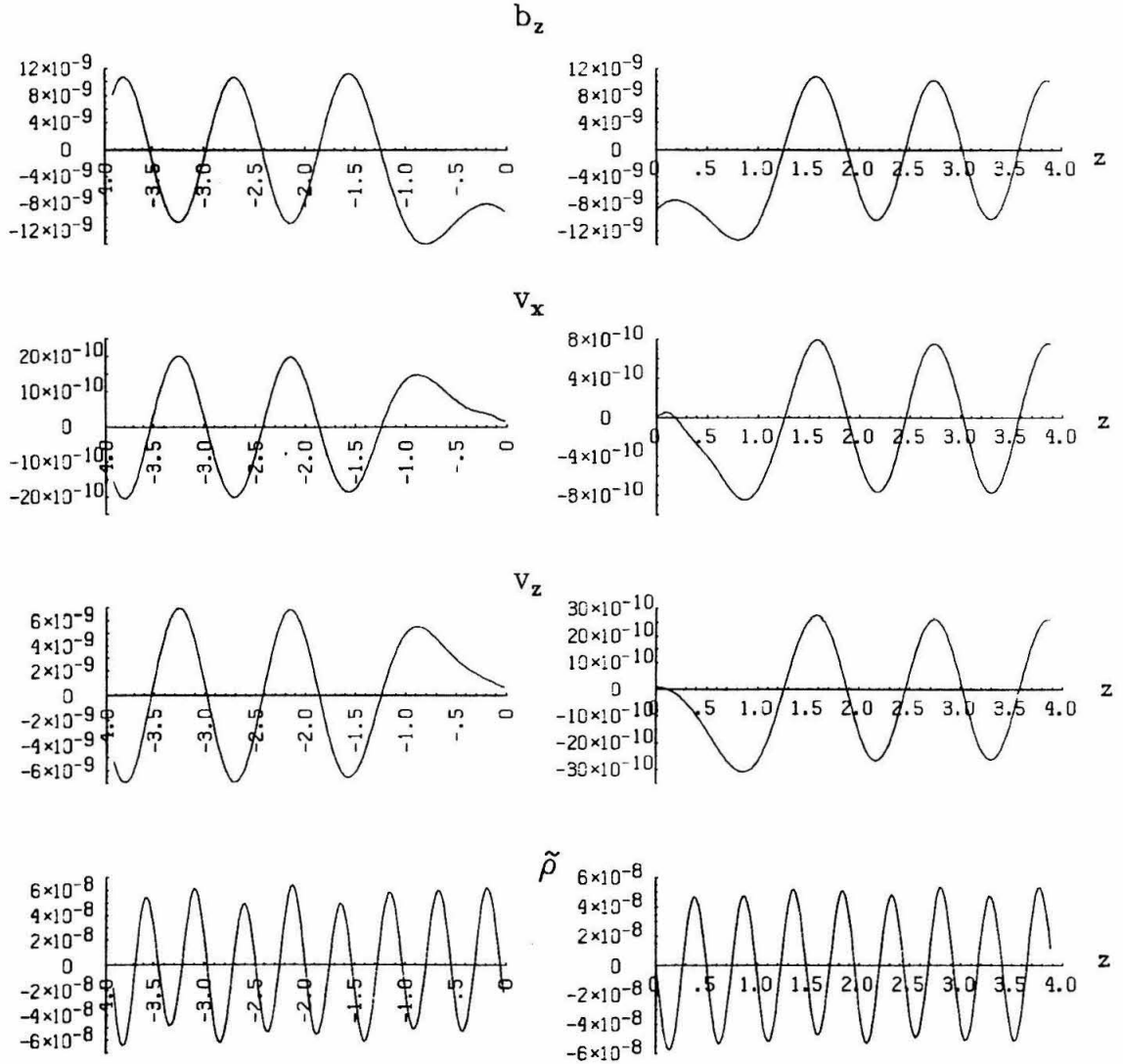
b_z
12×10⁻⁹
8×10⁻⁹
4×10⁻⁹
0
-4×10⁻⁹
-8×10⁻⁹
-12×10⁻⁹
-4.0 -3.5 -3.0 -2.5 -2.0 -1.5 -1.0 -.5 0
0 .5 1.0 1.5 2.0 2.5 3.0 3.5 4.0 z
v_x
20×10⁻¹⁰
10×10⁻¹⁰
-10×10⁻¹⁰
-20×10⁻¹⁰
8×10⁻¹⁰
4×10⁻¹⁰
-4×10⁻¹⁰
-8×10⁻¹⁰
v_z
6×10⁻⁹
4×10⁻⁹
2×10⁻⁹
-2×10⁻⁹
-4×10⁻⁹
-6×10⁻⁹
30×10⁻¹⁰
20×10⁻¹⁰
10×10⁻¹⁰
-10×10⁻¹⁰
-20×10⁻¹⁰
-30×10⁻¹⁰
$\tilde{\rho}$
6×10⁻⁸
4×10⁻⁸
2×10⁻⁸
-2×10⁻⁸
-4×10⁻⁸
-6×10⁻⁸

Fig. 5

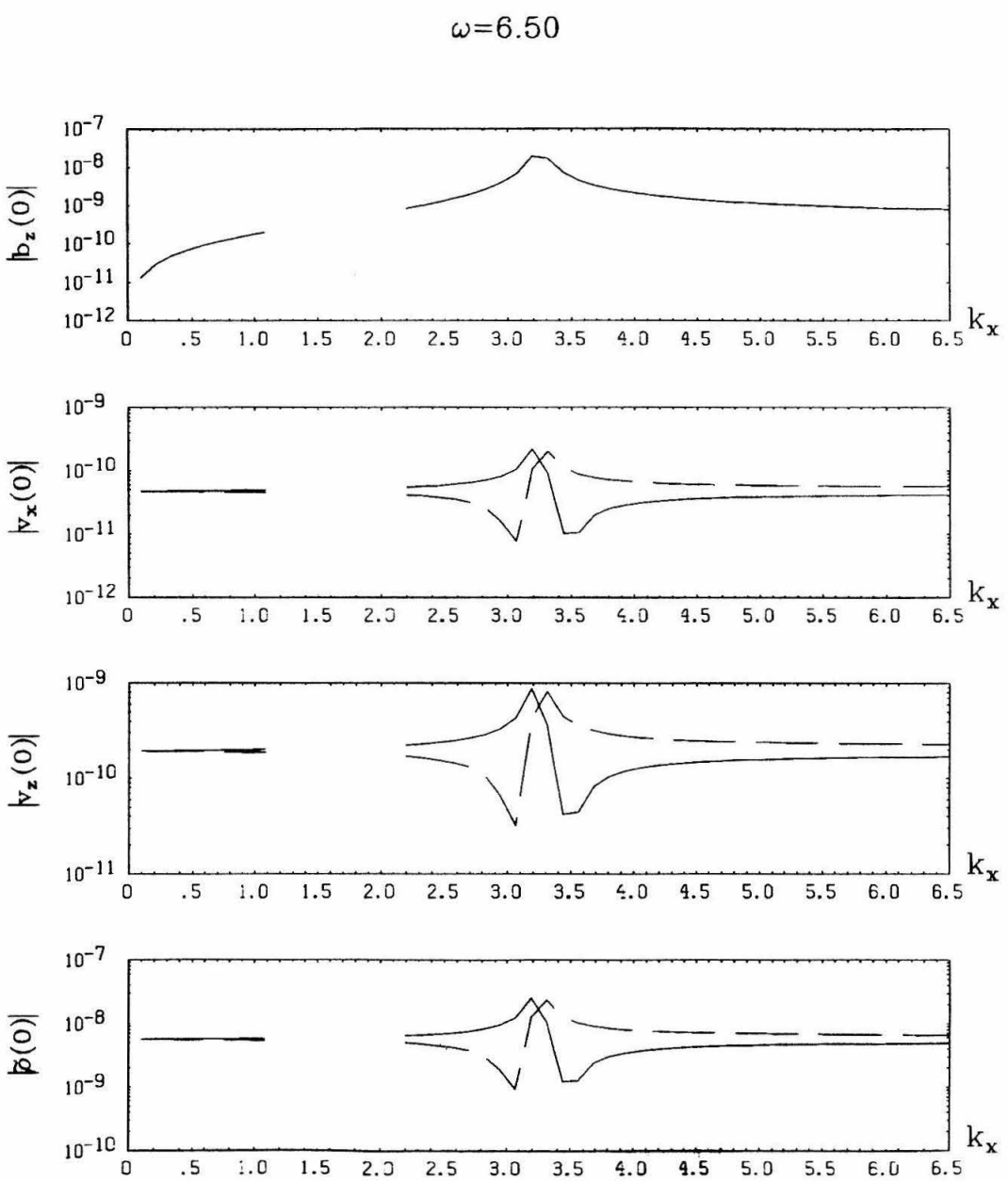

Fig. 6 (a)

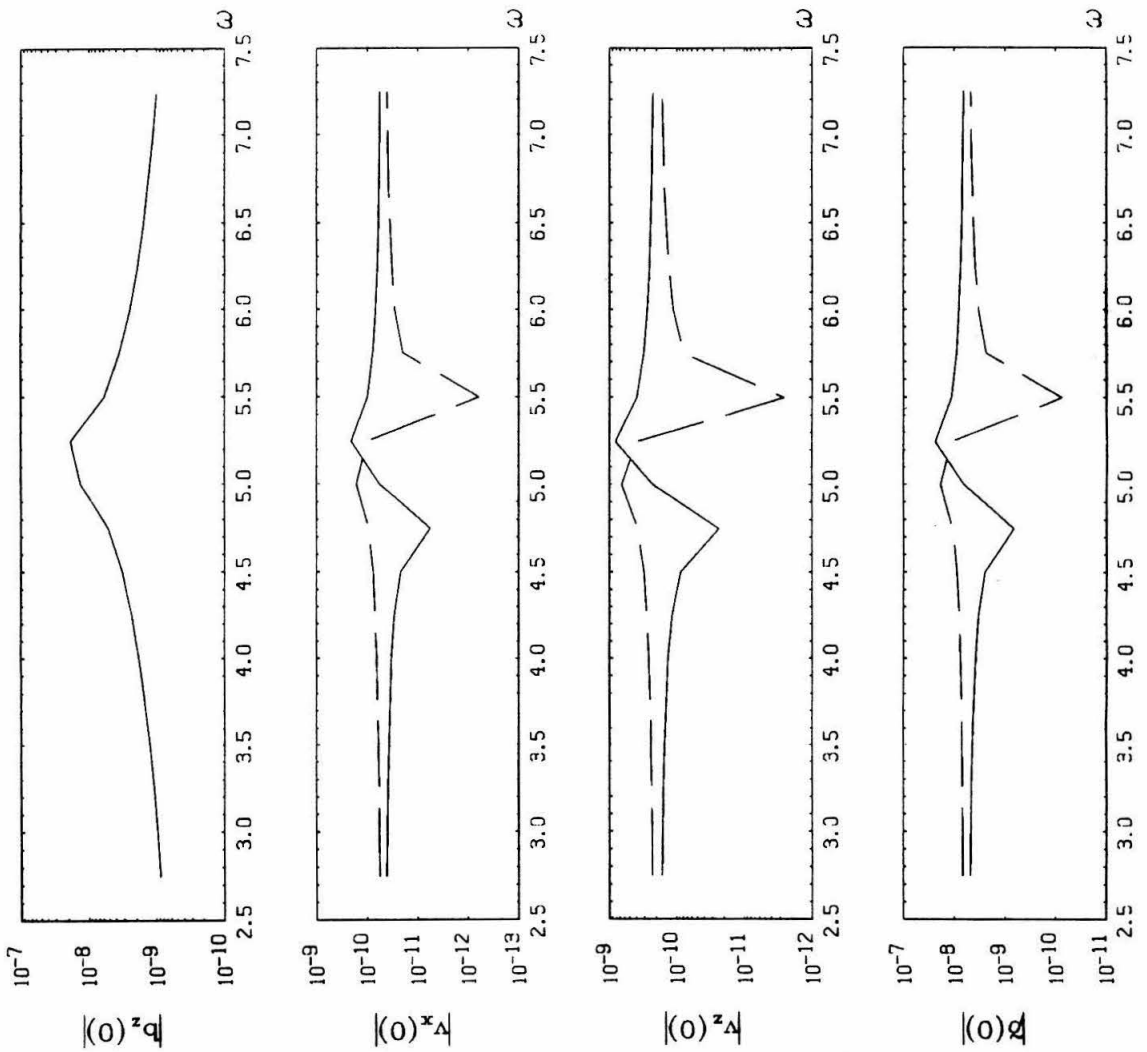

Fig. 6 (b)

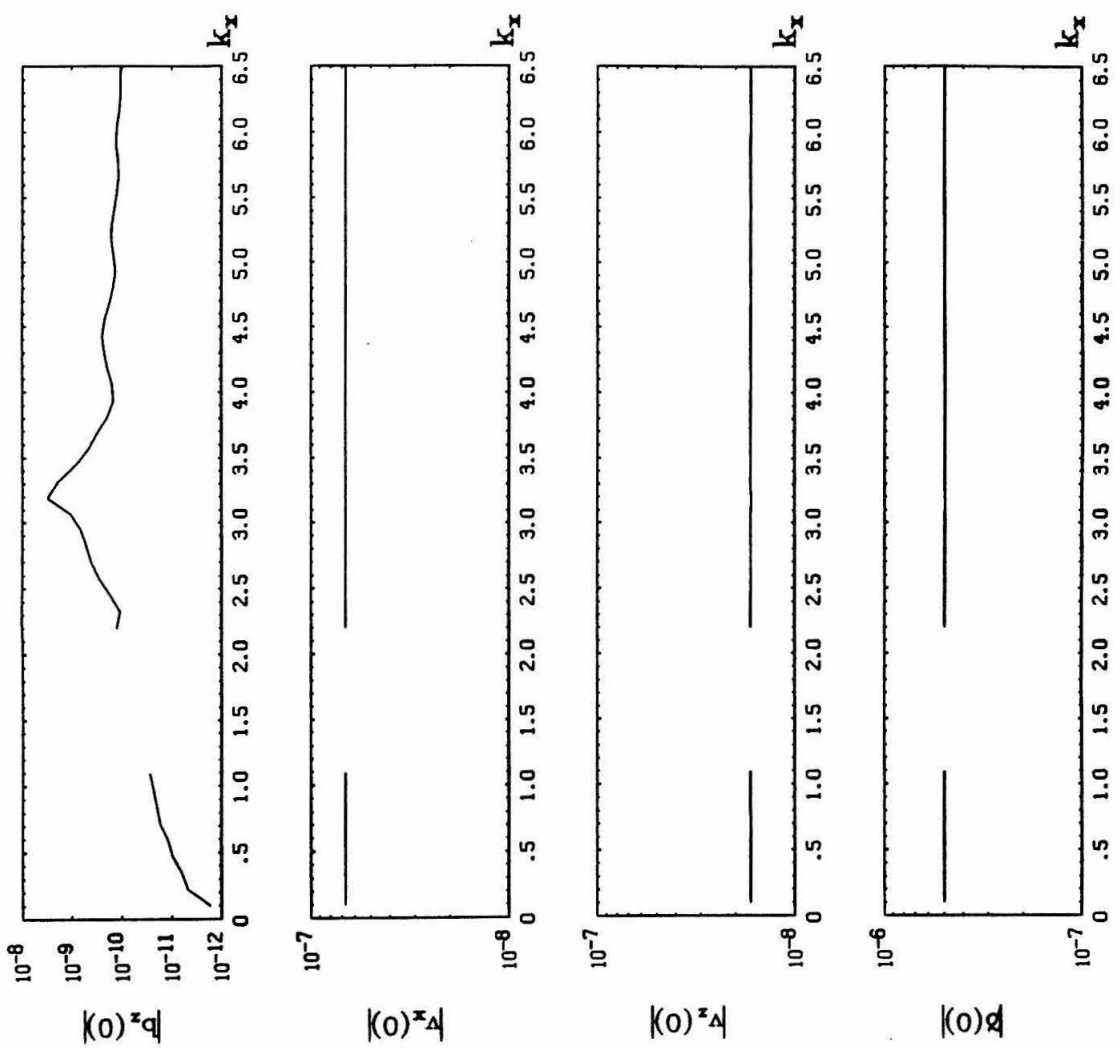
ω=6.50
$|b_z(0)|$
$|v_x(0)|$
$|v_z(0)|$
$|\theta(0)|$
k_x
0 .5 1.0 1.5 2.0 2.5 3.0 3.5 4.0 4.5 5.0 5.5 6.0 6.5
10^{-8} 10^{-9} 10^{-10} 10^{-11} 10^{-12}
10^{-7} 10^{-8}
10^{-7} 10^{-8}
10^{-6} 10^{-7}

Fig.7(a)

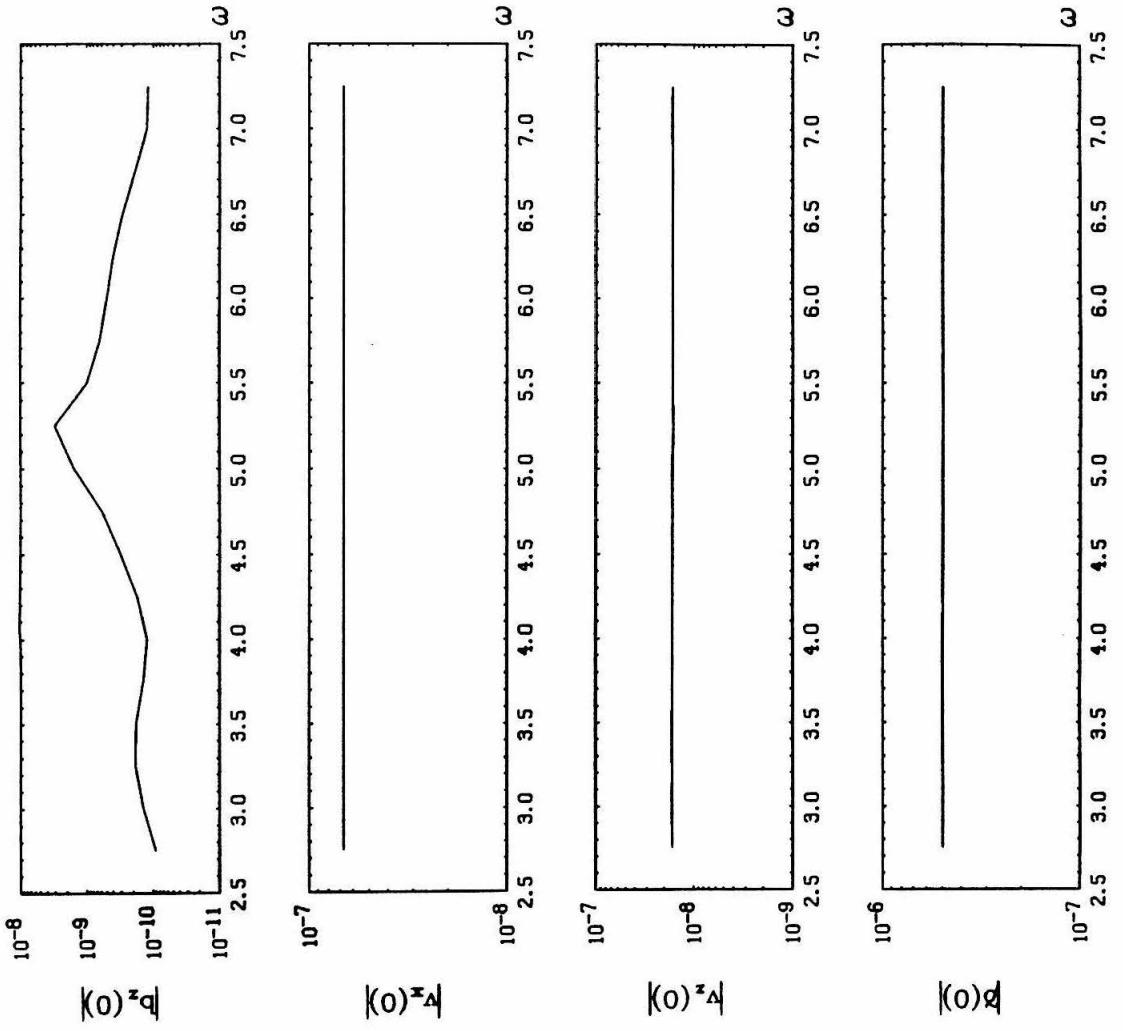

Fig.7(b)

ω=6.50

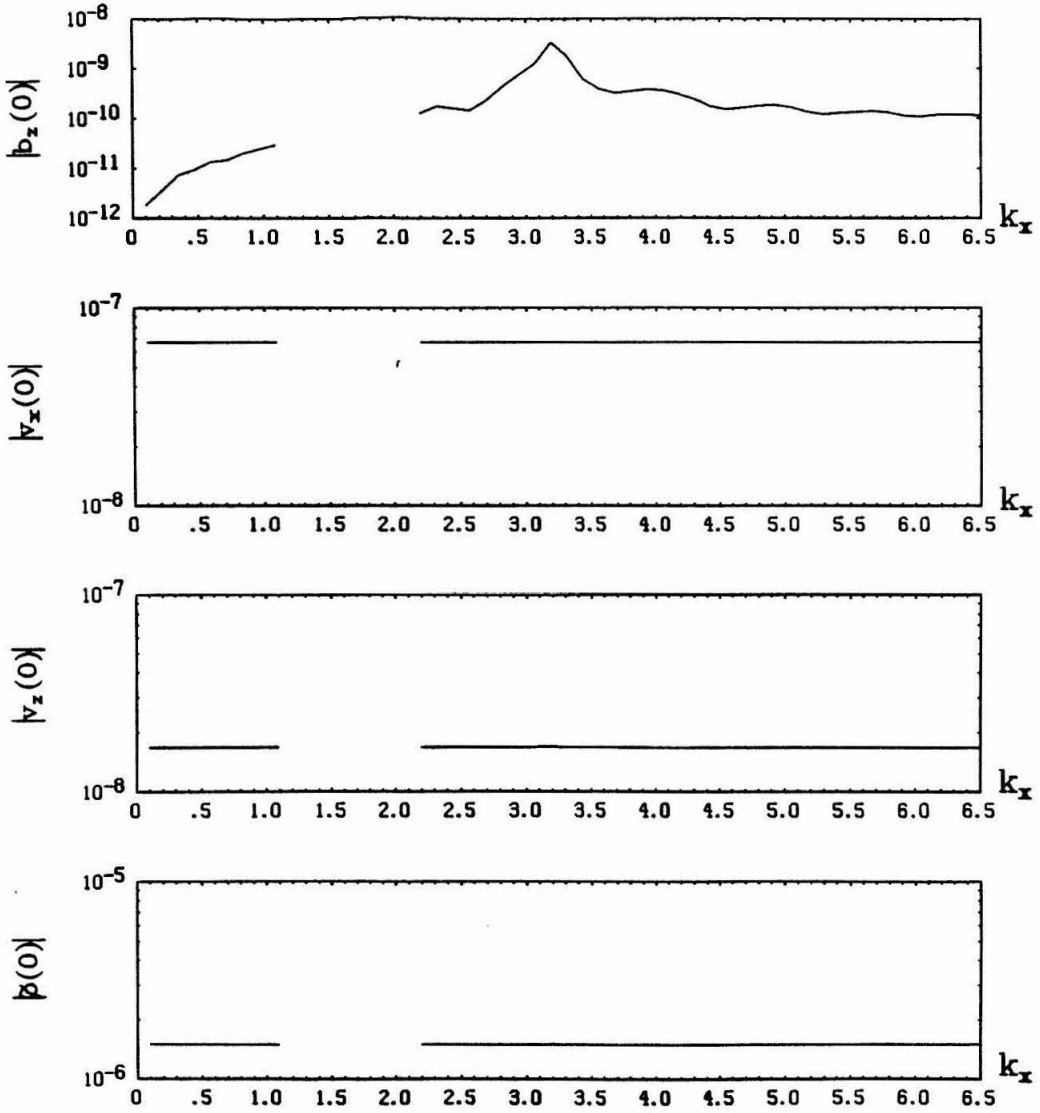

Fig.8(a)

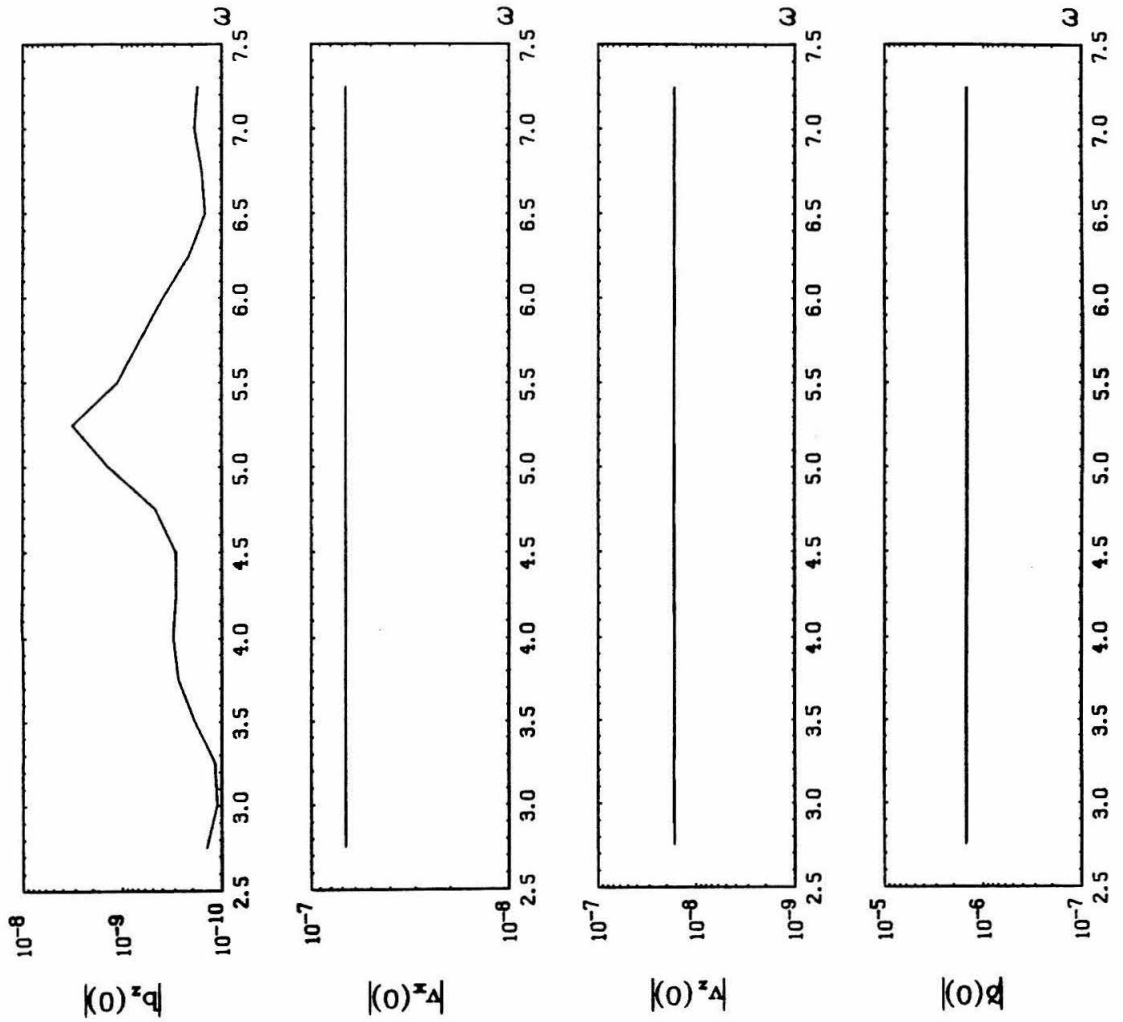

Fig.8(b)

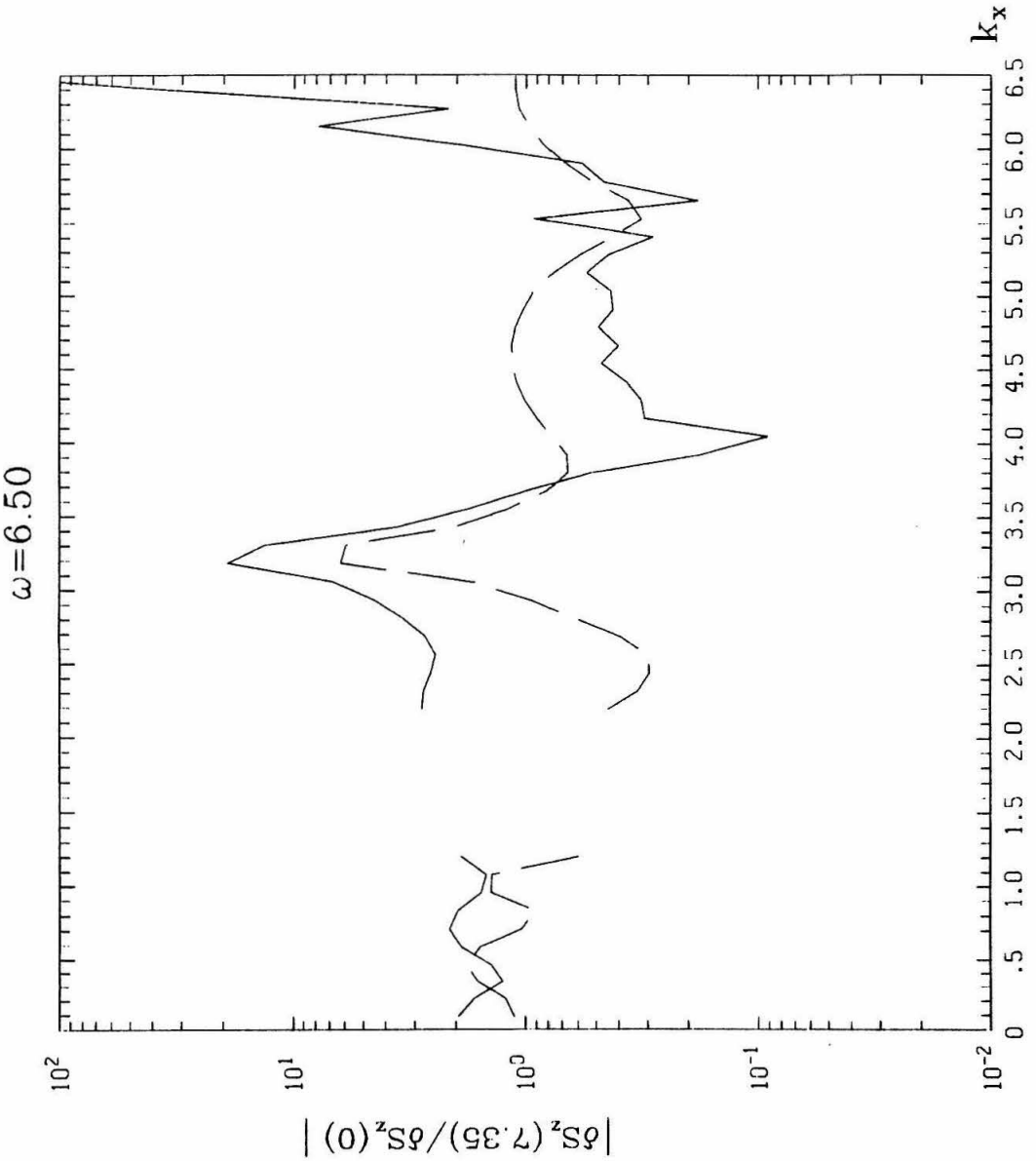
ω=6.50
$|\delta S_z(7.35)/\delta S_z(0)|$
10^2
10^1
10^0
10^{-1}
10^{-2}
0 .5 1.0 1.5 2.0 2.5 3.0 3.5 4.0 4.5 5.0 5.5 6.0 6.5
k_x

Fig. 9 (a)

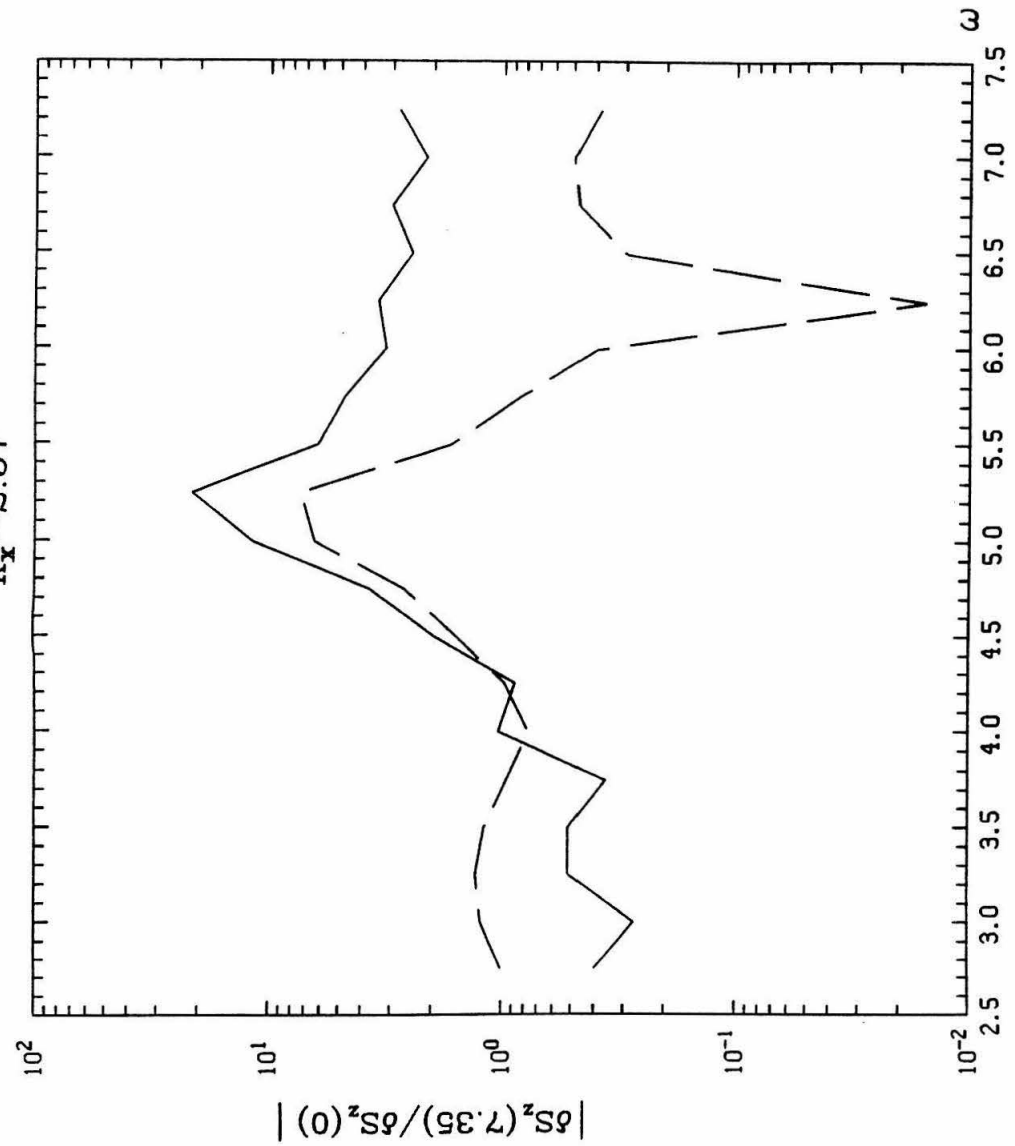
k_x=2.57
$|\delta S_z(7.35)/\delta S_z(0)|$
10^2
10^1
10^0
10^{-1}
10^{-2}
2.5
3.0
3.5
4.0
4.5
5.0
5.5
6.0
6.5
7.0
7.5
ω

Fig.9(b)

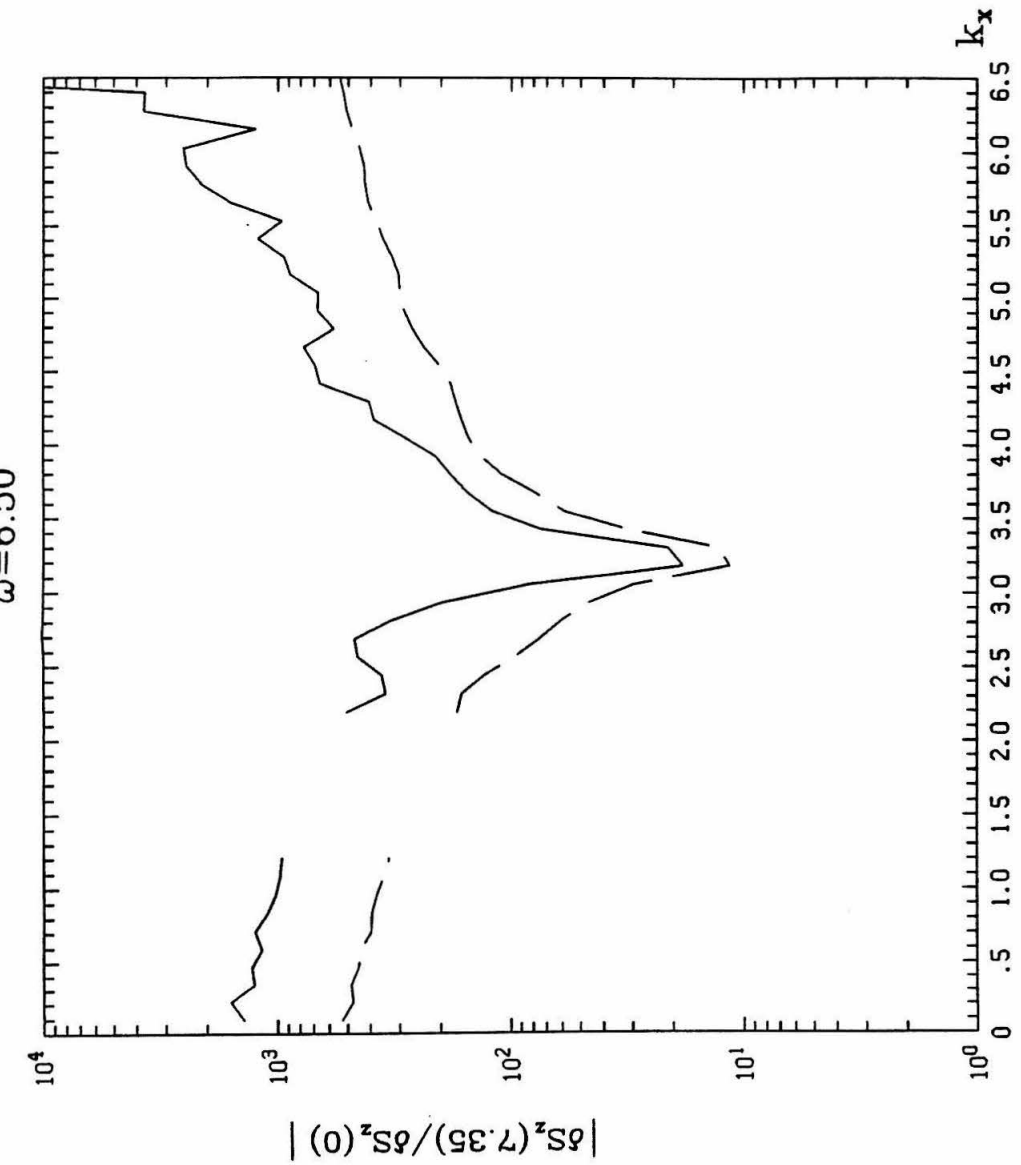
ω=6.50
$|\delta S_z(7.35)/\delta S_z(0)|$
k_x
10^4
10^3
10^2
10^1
10^0
0
.5
1.0
1.5
2.0
2.5
3.0
3.5
4.0
4.5
5.0
5.5
6.0
6.5

Fig.10(a)

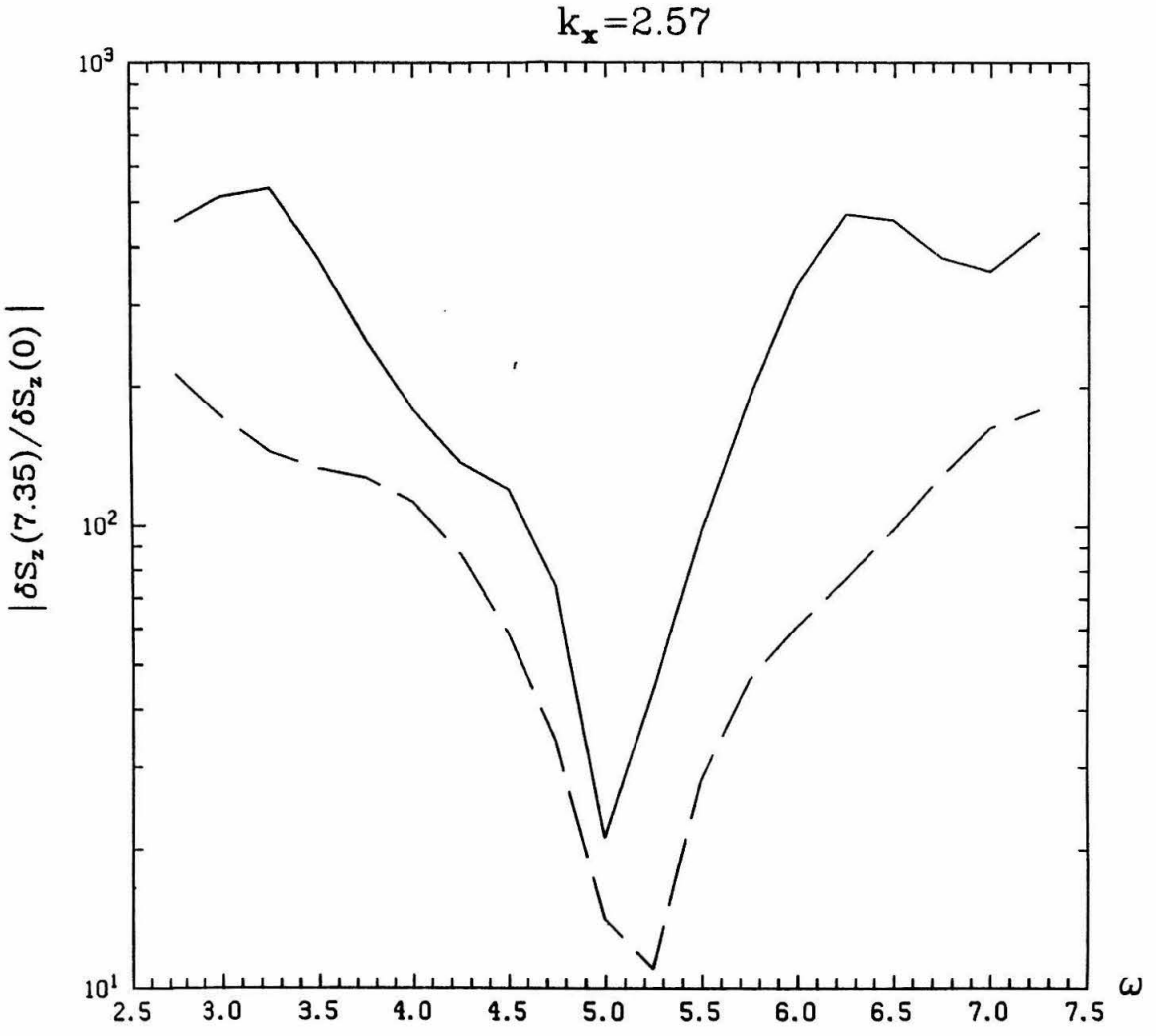
k_x=2.57
10^3
10^2
10^1
$|\delta S_z(7.35)/\delta S_z(0)|$
2.5
3.0
3.5
4.0
4.5
5.0
5.5
6.0
6.5
7.0
7.5
ω

Fig.10(b)

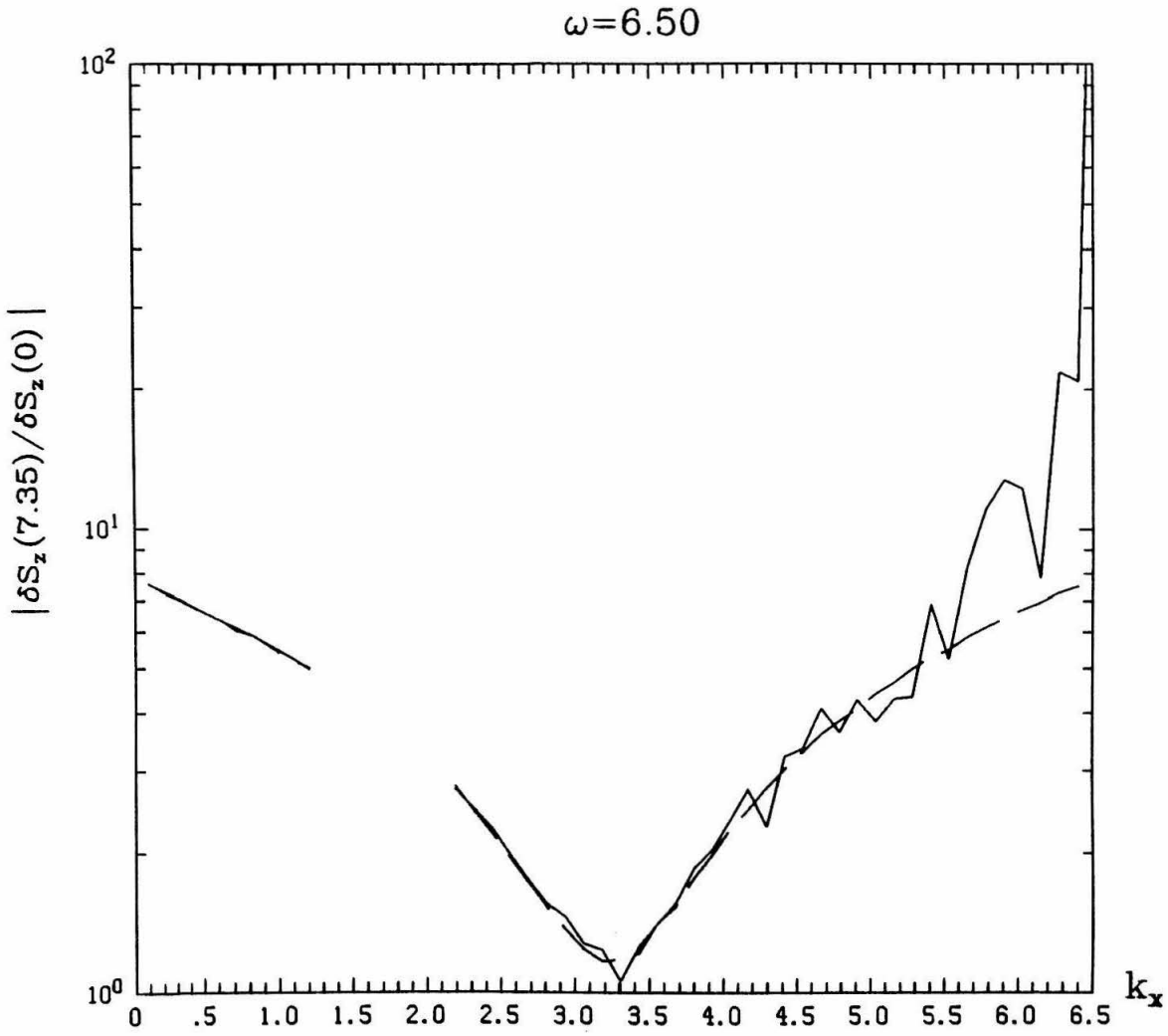
ω=6.50
10^2
10^1
10^0
$|\delta S_z(7.35)/\delta S_z(0)|$
0
.5
1.0
1.5
2.0
2.5
3.0
3.5
4.0
4.5
5.0
5.5
6.0
6.5
k_x

Fig.11(a)

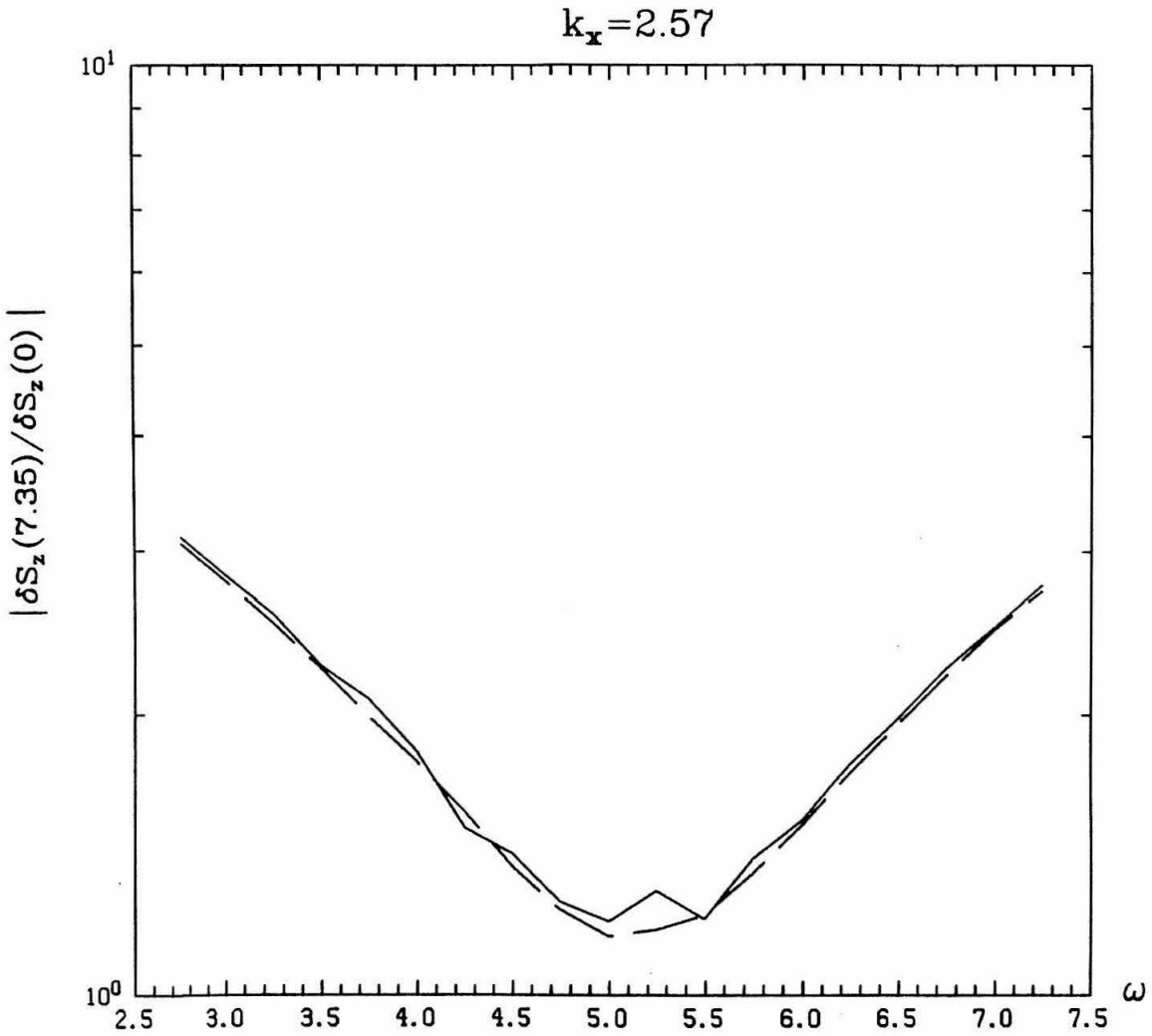
k_x=2.57
10^1
10^0
$|\delta S_z(7.35)/\delta S_z(0)|$
2.5
3.0
3.5
4.0
4.5
5.0
5.5
6.0
6.5
7.0
7.5
ω

Fig.11(b)

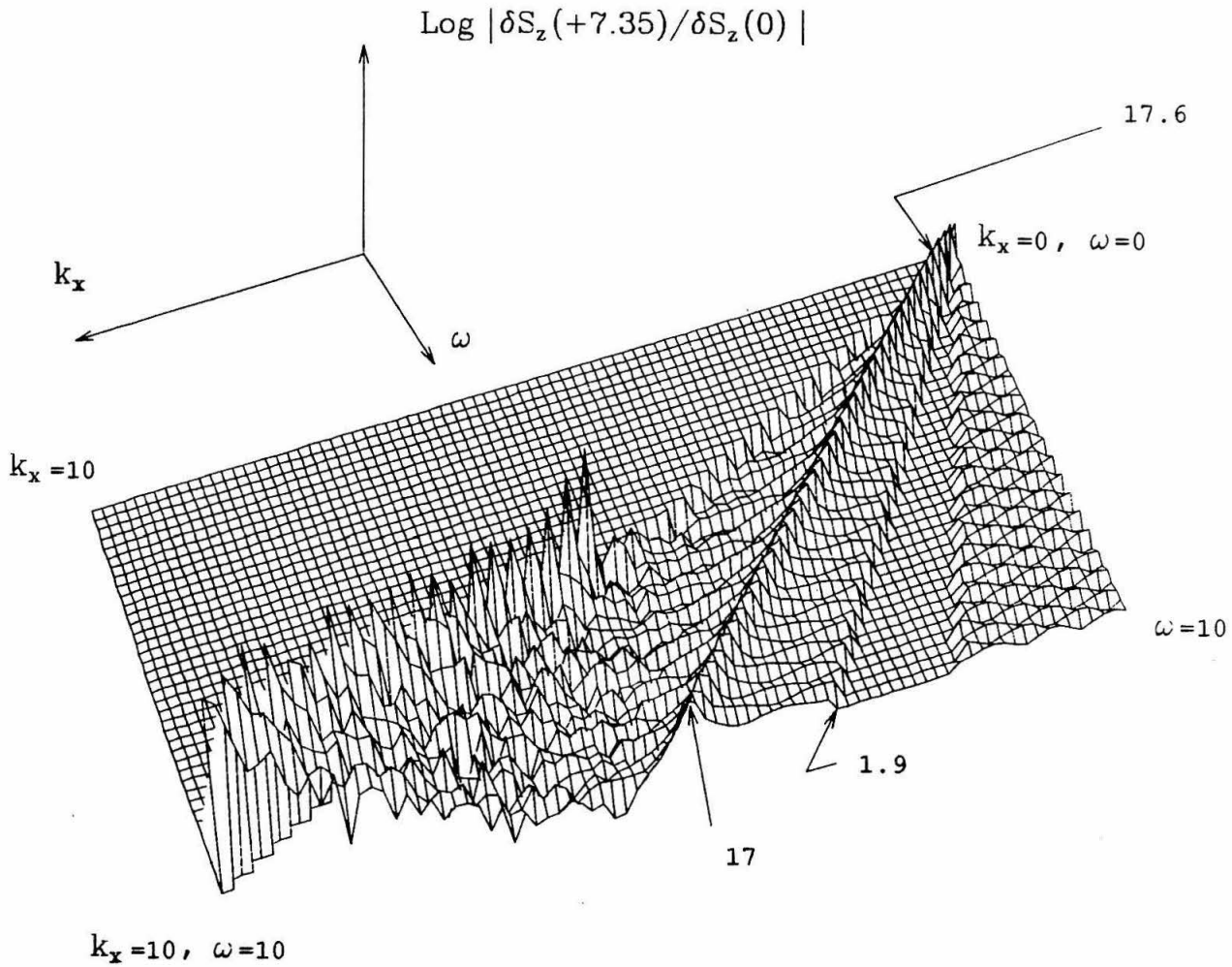

Fig. 12 (a)

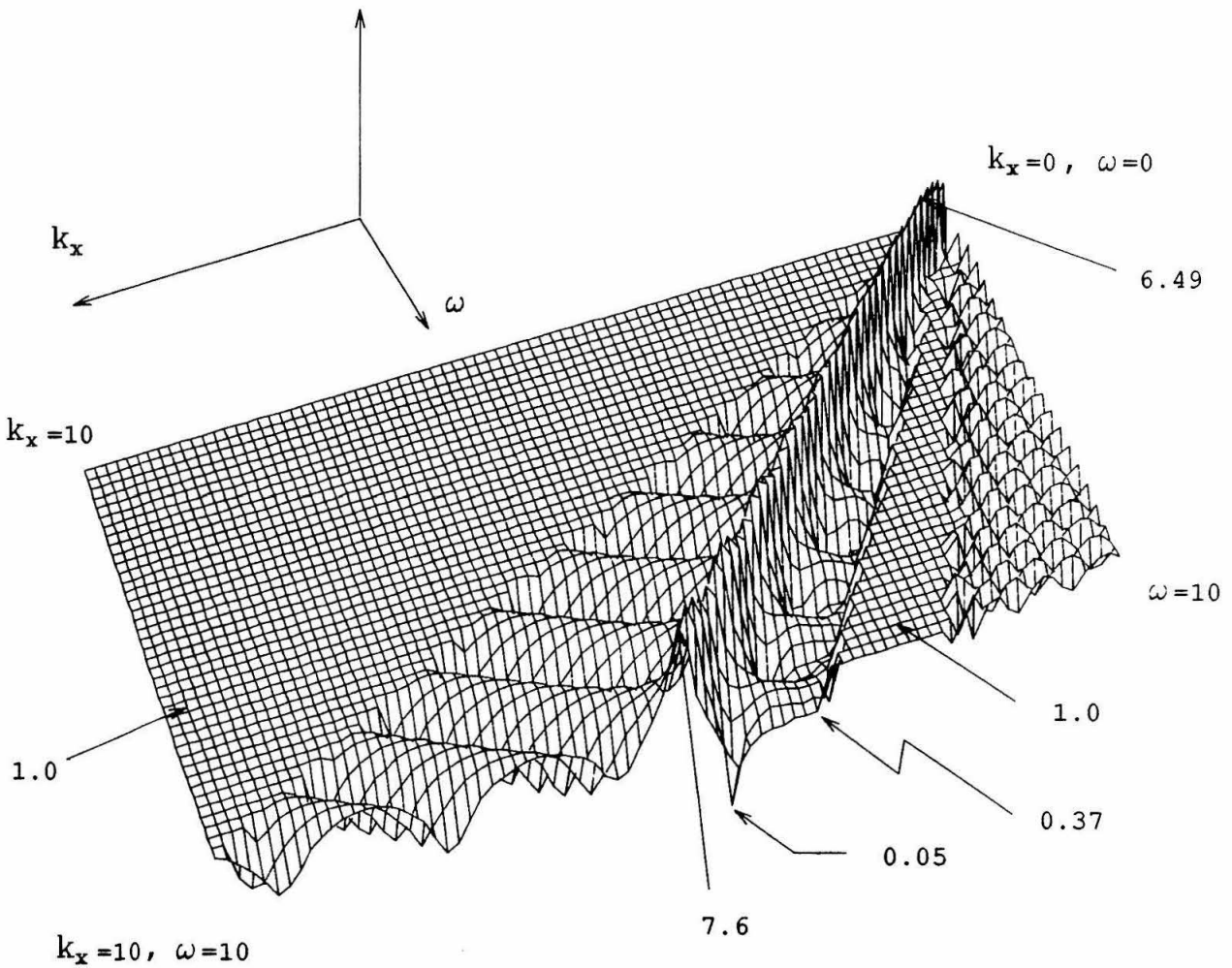
Log $|\delta S_z(-7.35)/\delta S_z(0)|$
k_x
ω
$k_x=0$, $\omega=0$
6.49
$k_x=10$
$\omega=10$
1.0
1.0
0.37
0.05
7.6
$k_x=10$, $\omega=10$

Fig. 12 (b)

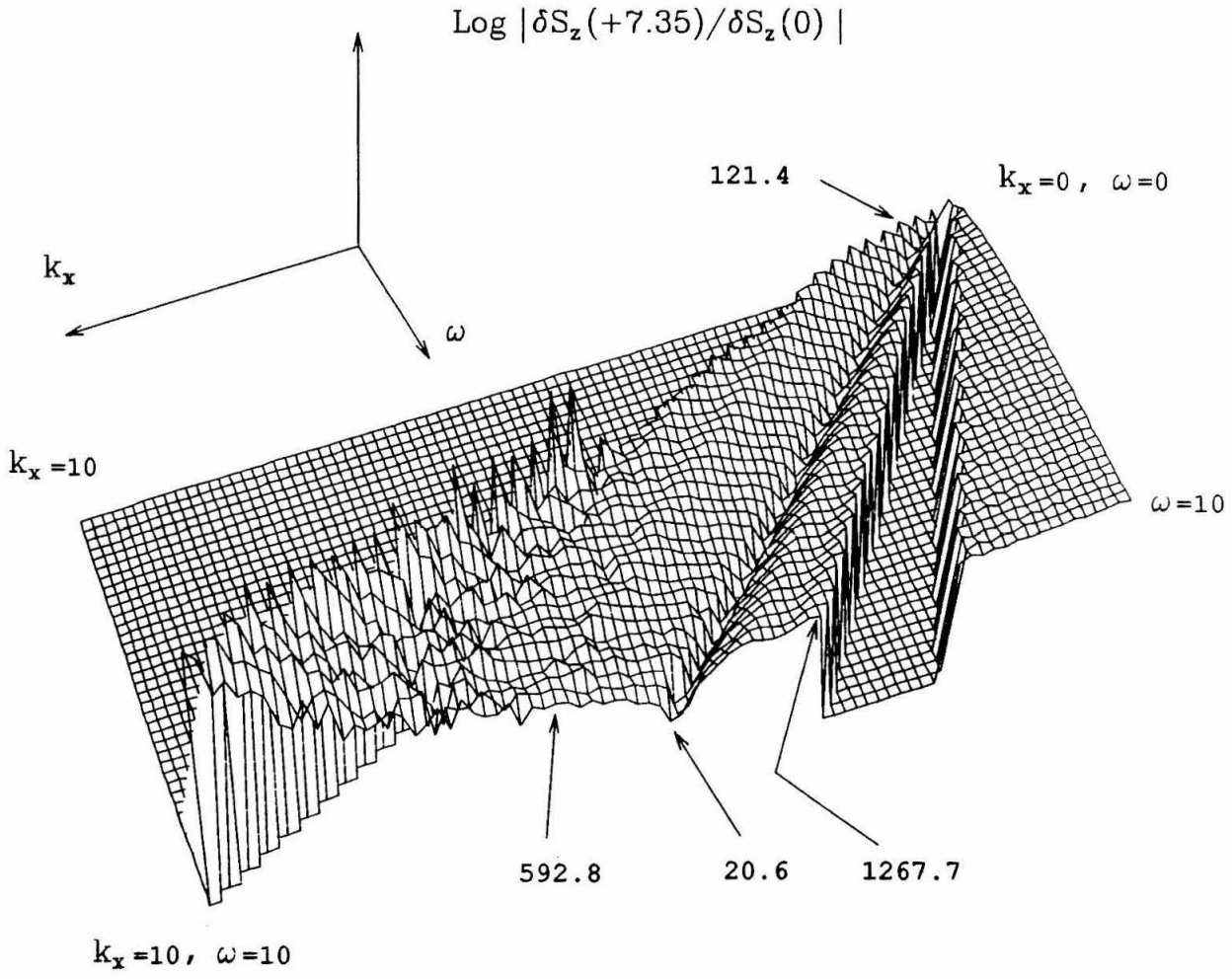
Log |δS_z(+7.35)/δS_z(0)|
121.4
k_x=0, ω=0
k_x
ω
k_x=10
ω=10
592.8
20.6
1267.7
k_x=10, ω=10

Fig. 13 (a)

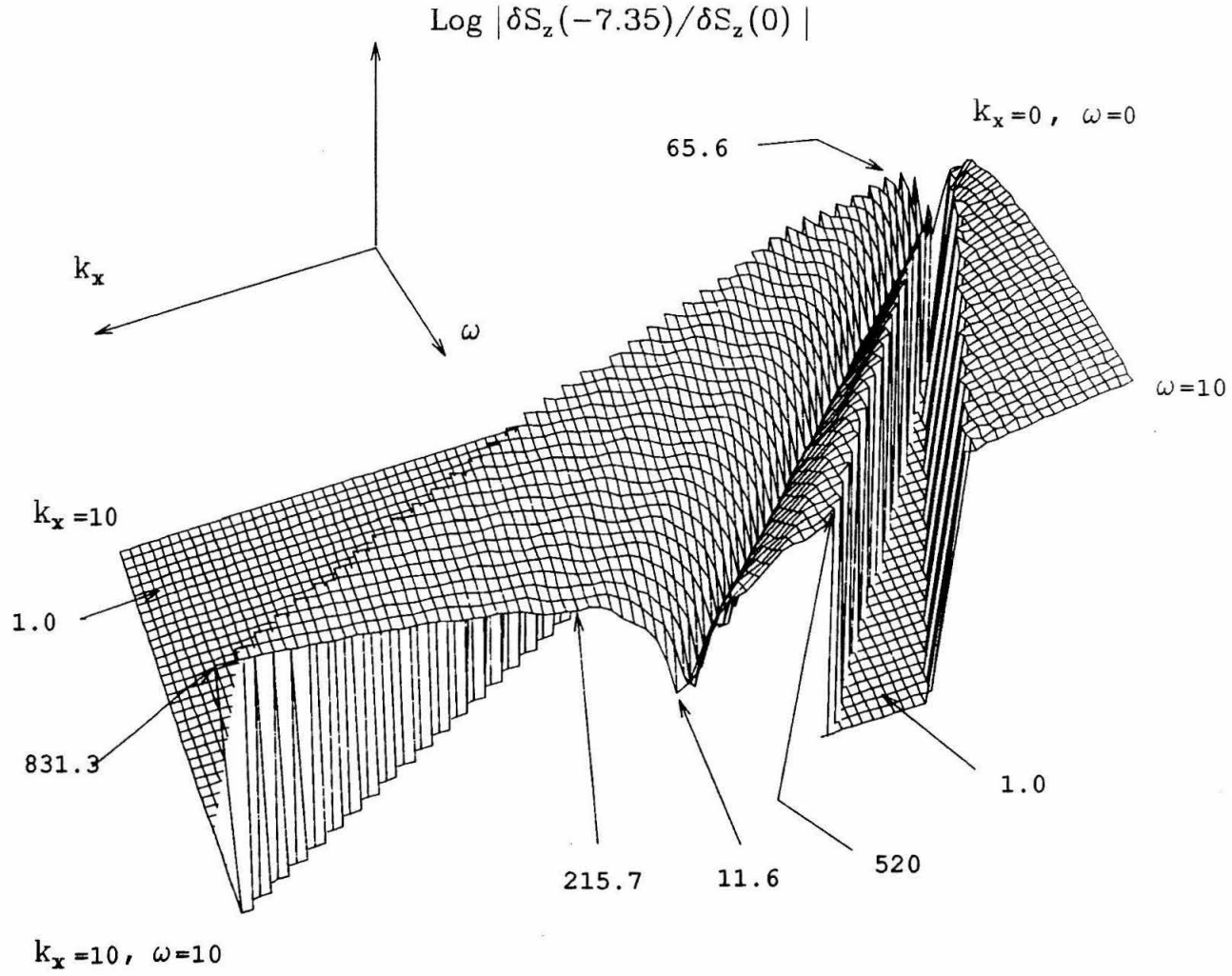
Log |δS_z(−7.35)/δS_z(0)|
k_x
ω
k_x =0, ω=0
65.6
ω=10
k_x =10
1.0
831.3
215.7
11.6
520
1.0
k_x =10, ω=10

Fig. 13 (b)

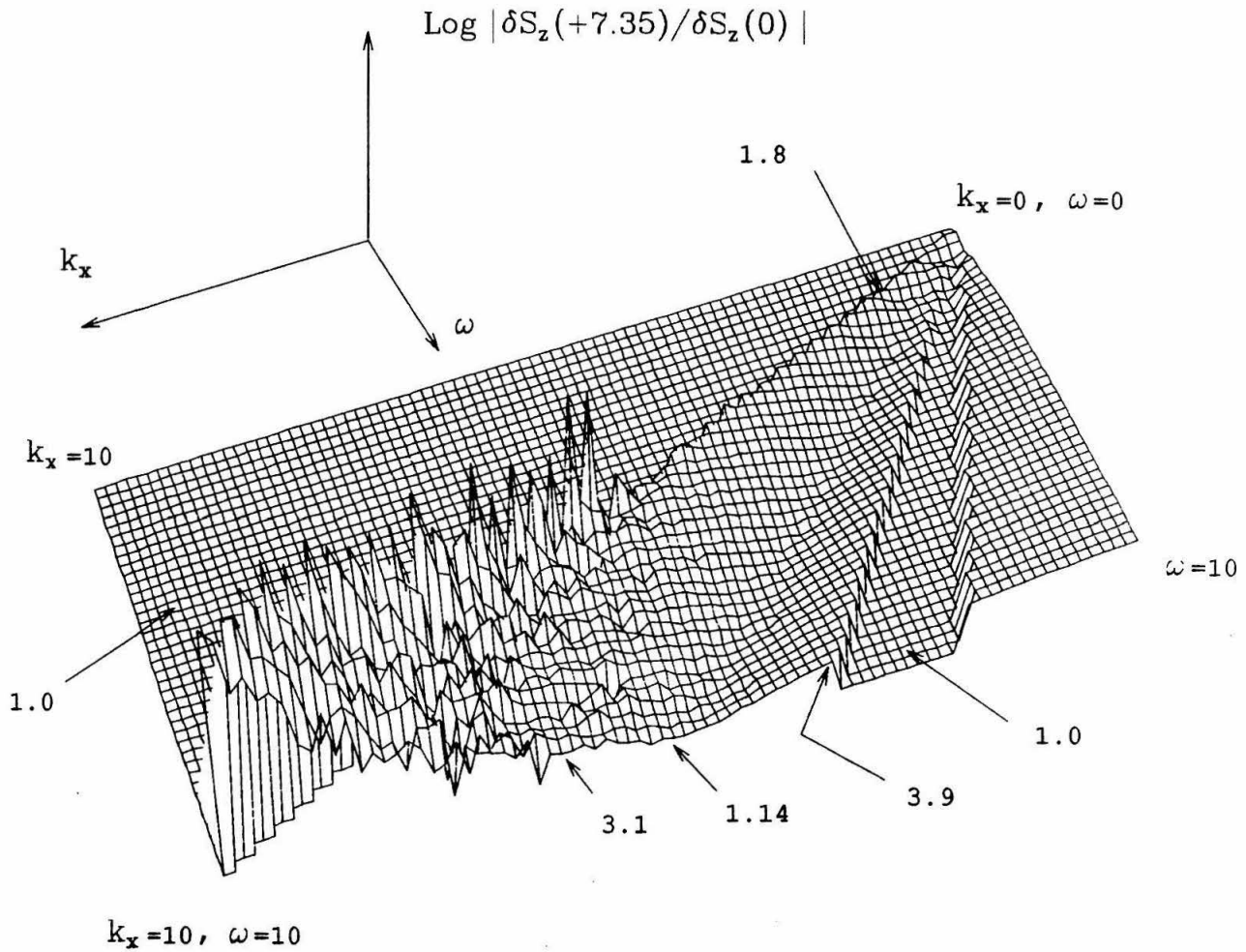

Fig. 14 (a)

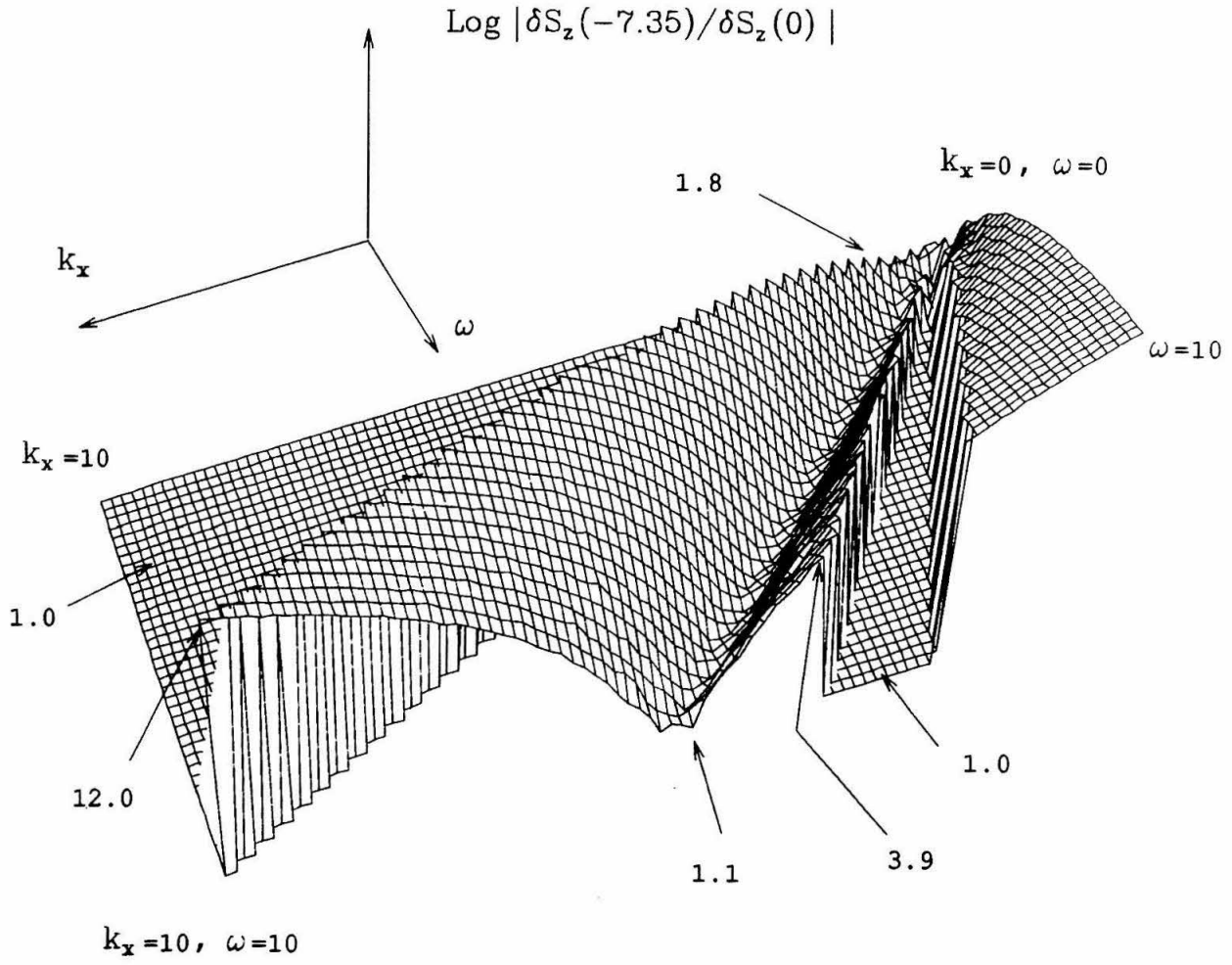

Fig. 14 (b)

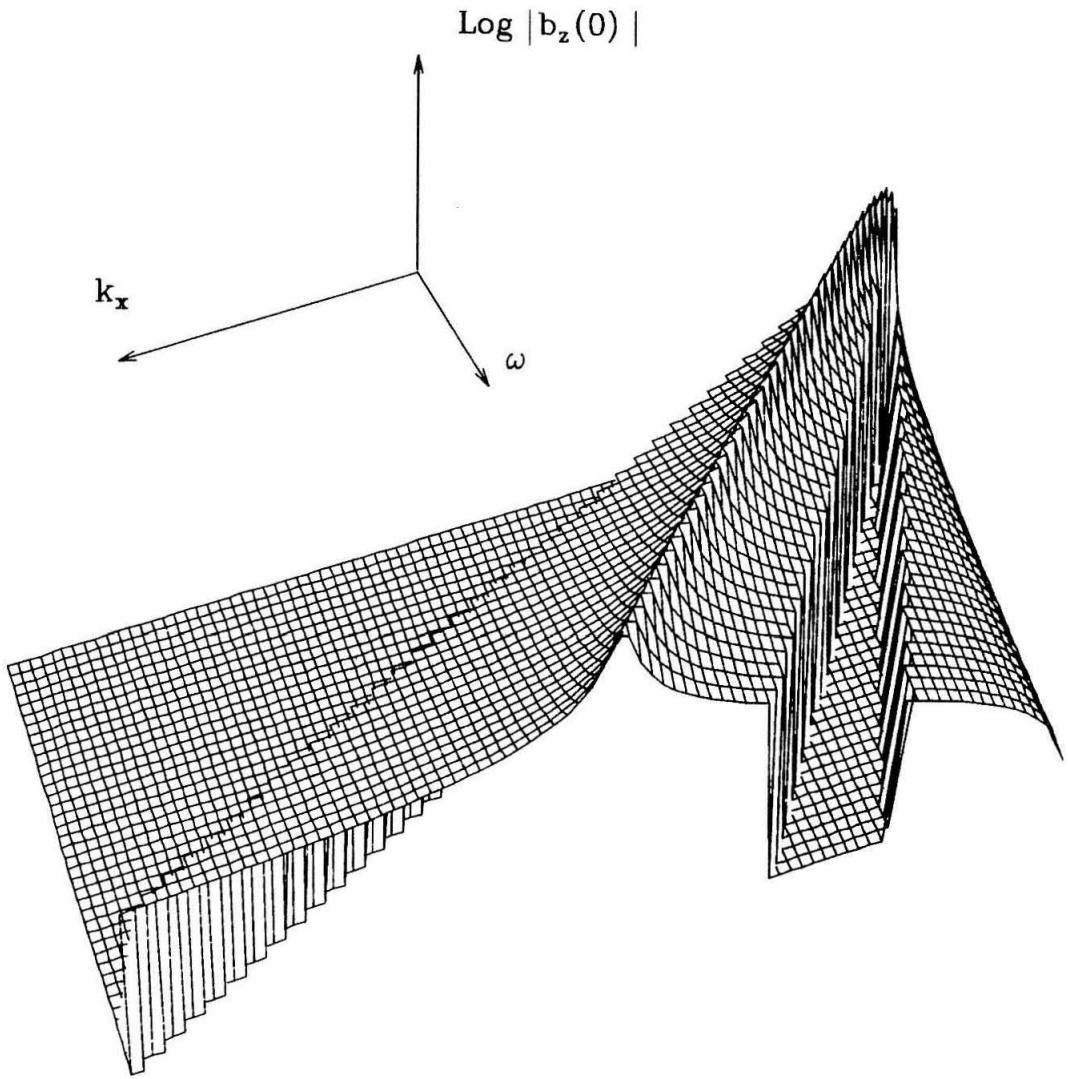

Fig. 15 (a)

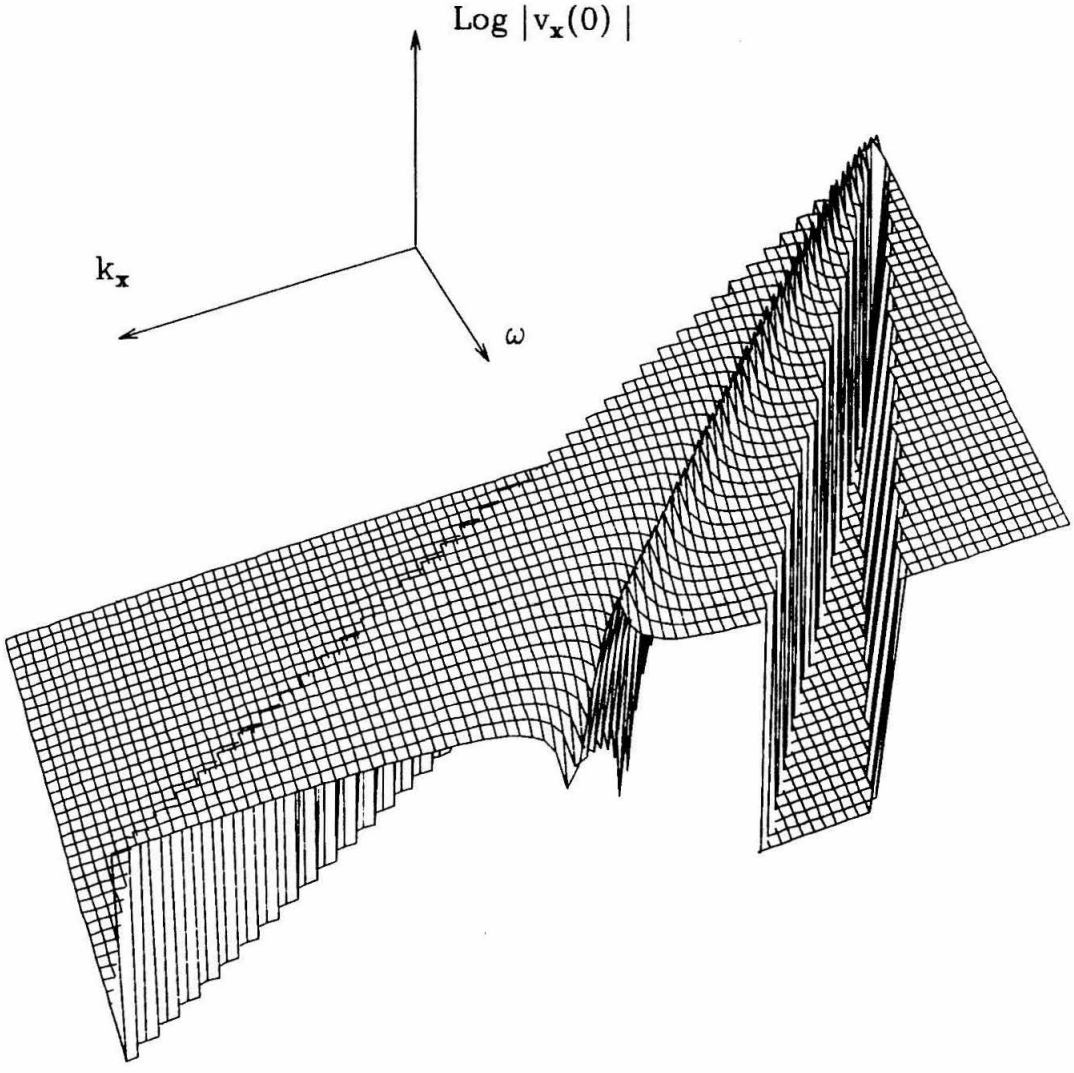

Fig. 15 (b)

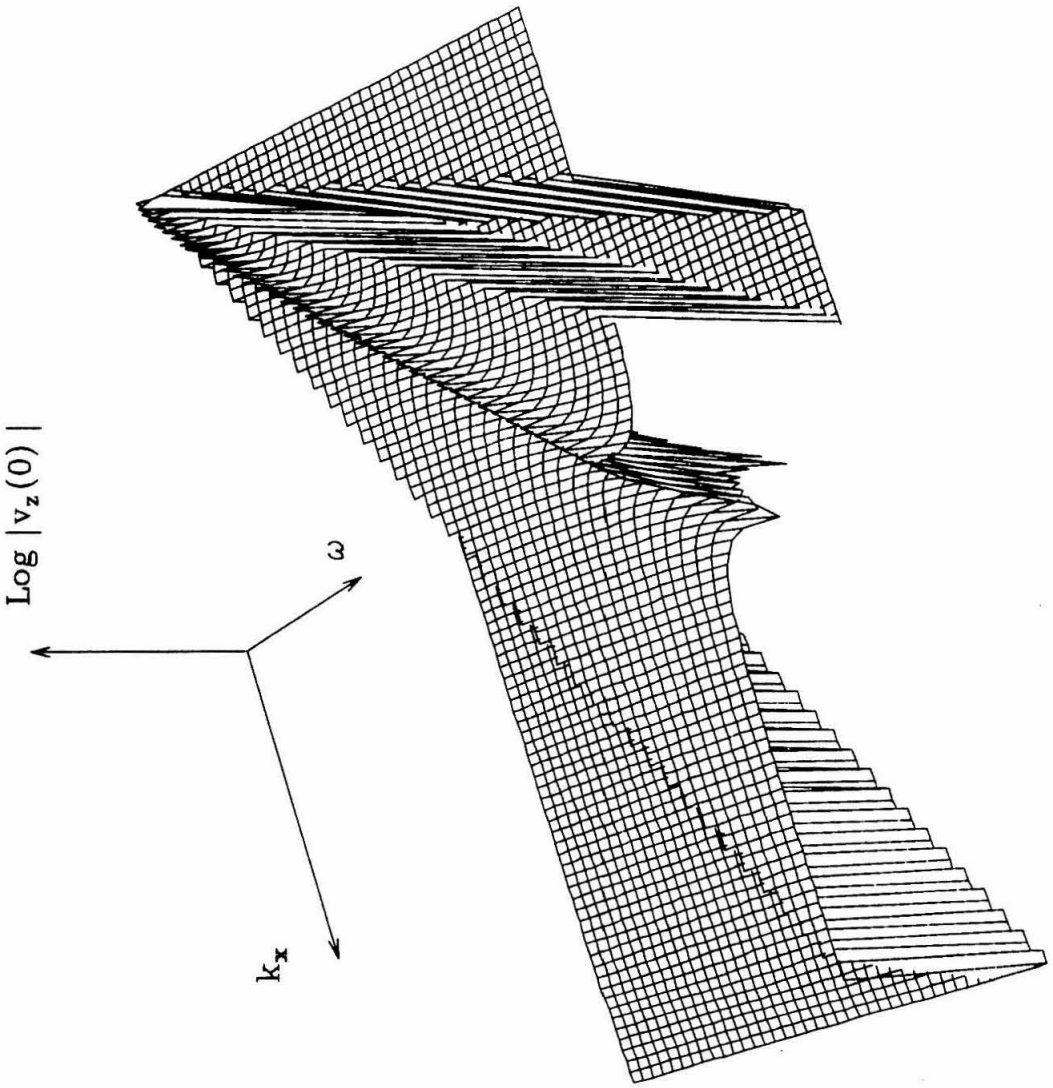

Fig. 15 (c)

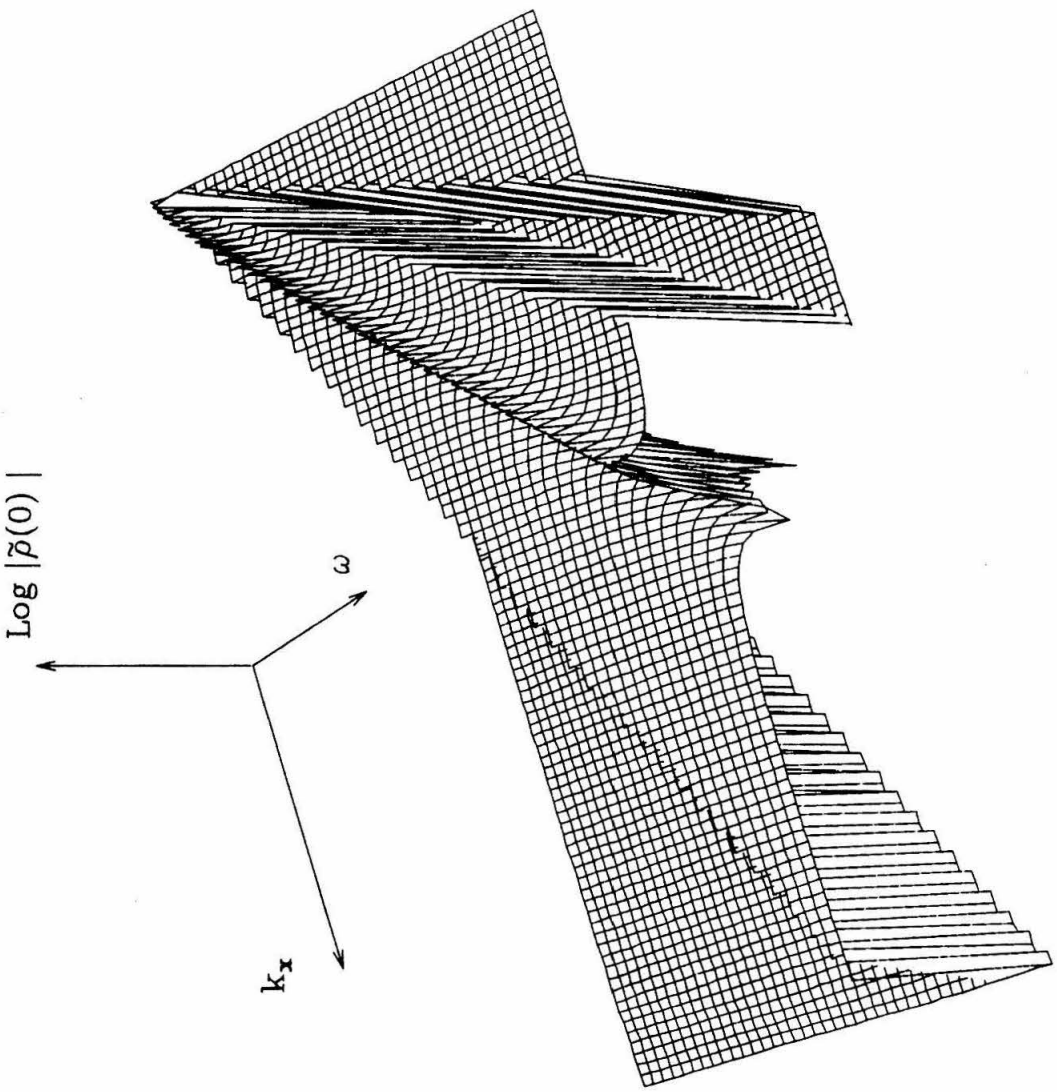

Fig. 15 (d)

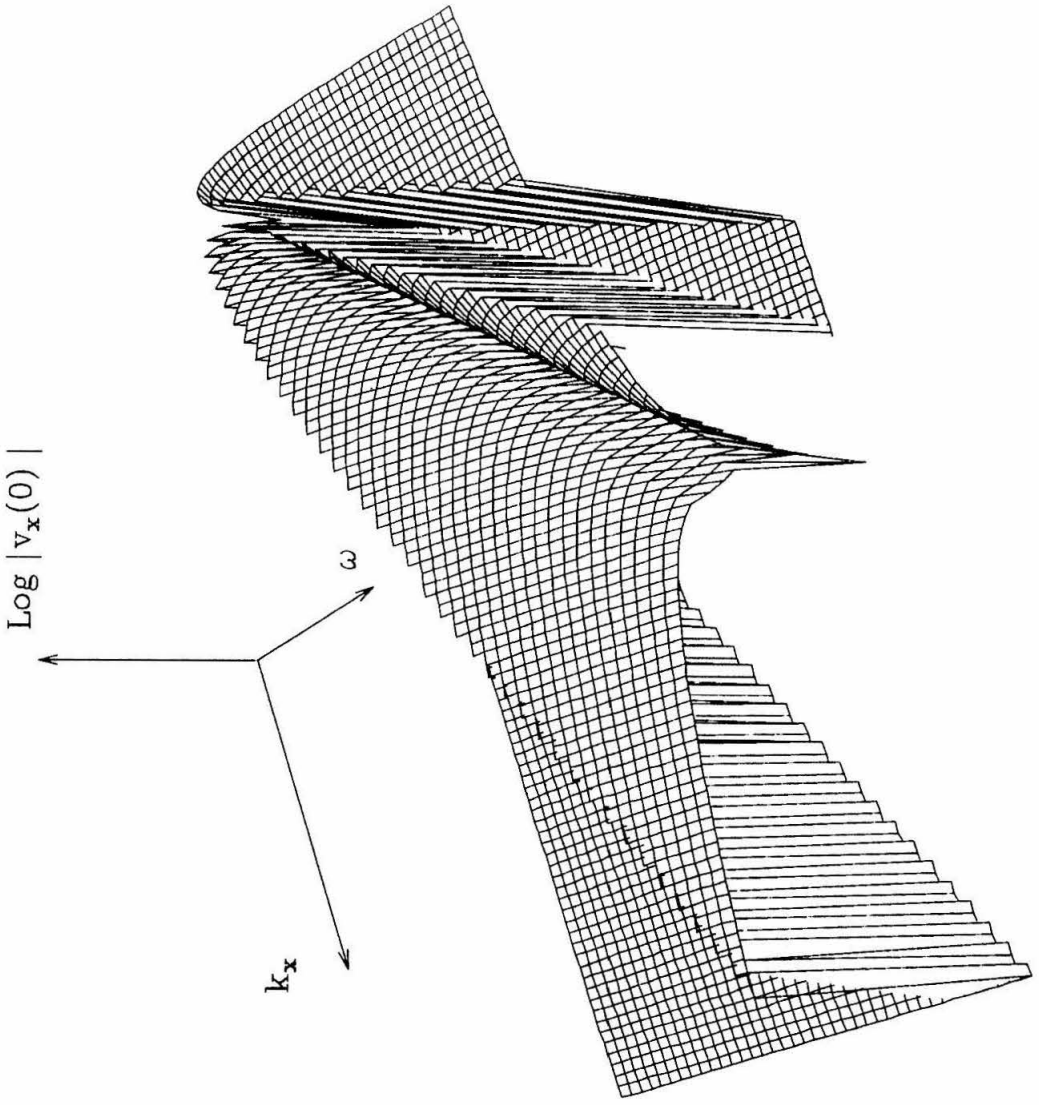

Fig. 15 (e)

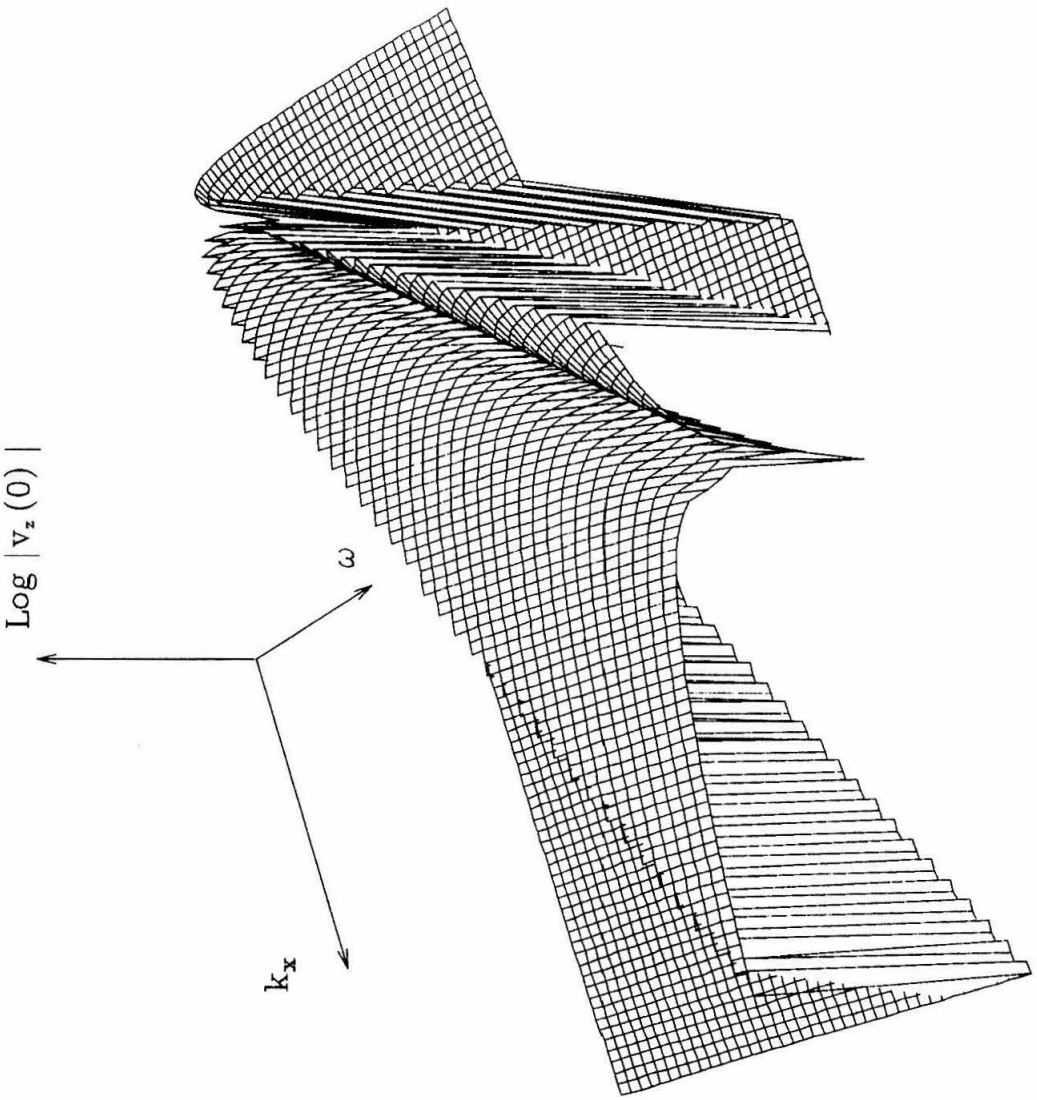

Fig. 15 (f)

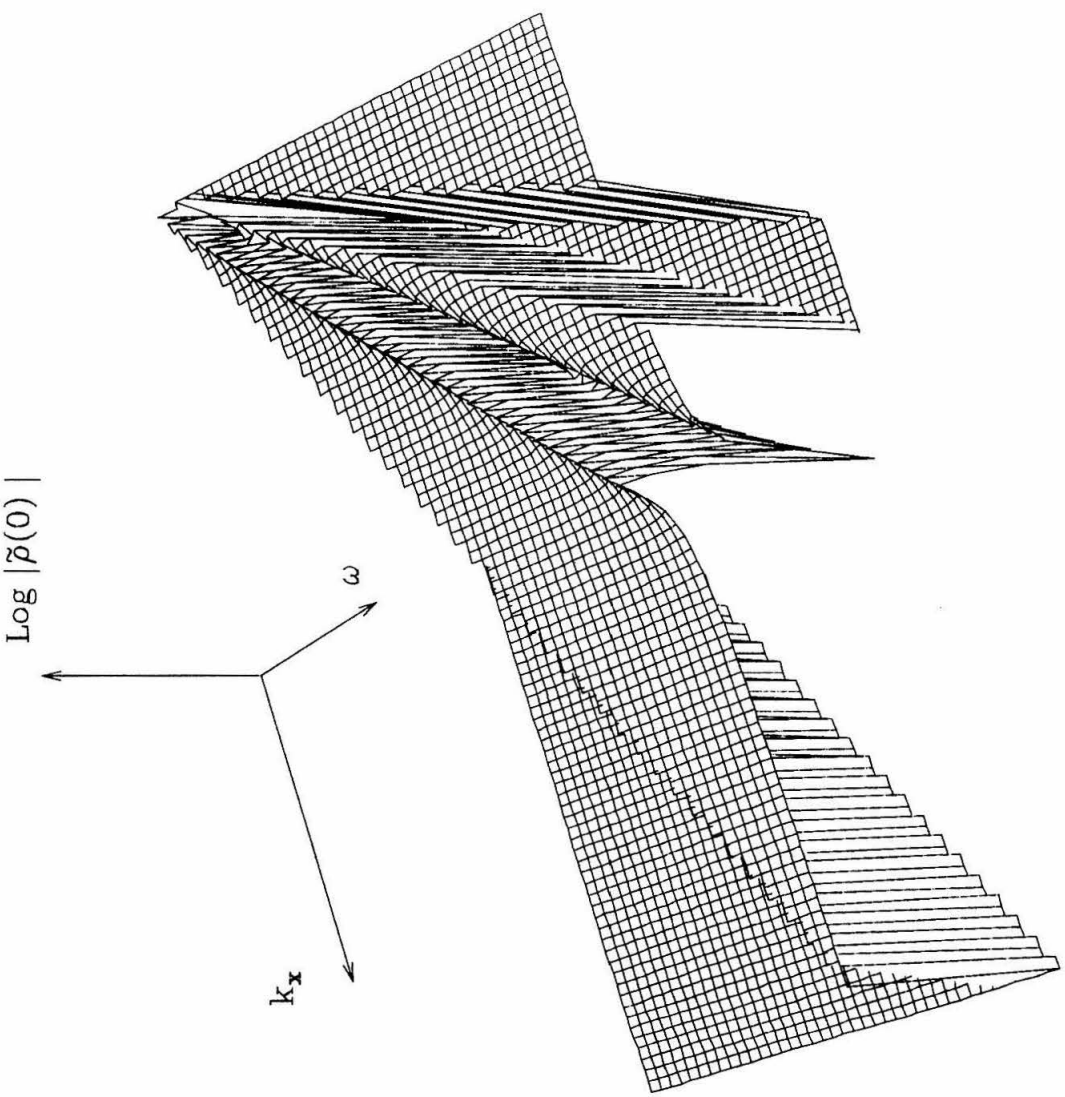

Fig. 15 (g)

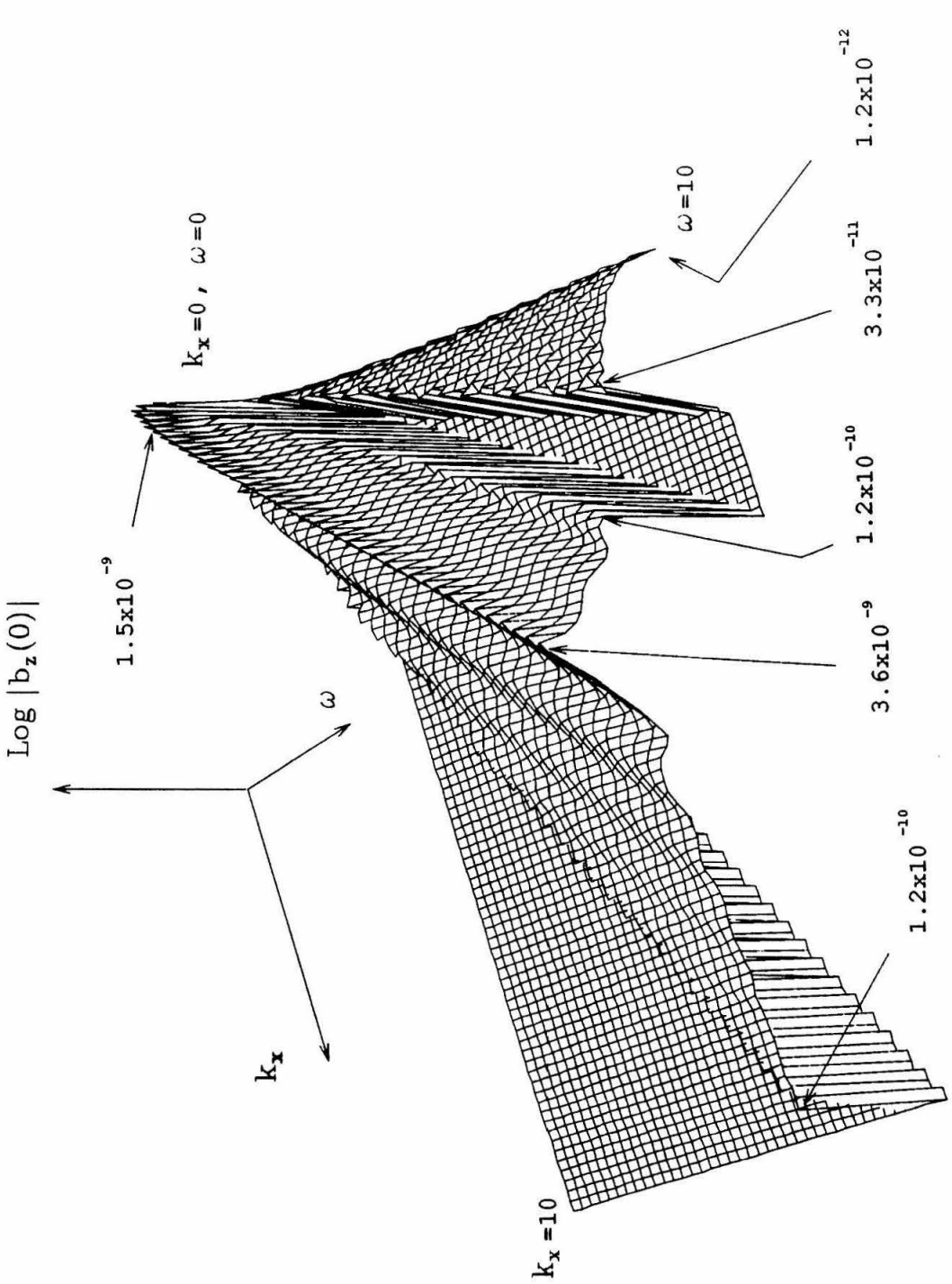
Log |b_z(0)|
1.5x10^-9
k_x=0 , ω=0
ω
k_x
k_x=10
ω=10
1.2x10^-12
3.3x10^-11
1.2x10^-10
3.6x10^-9
1.2x10^-10
k_x=10 , ω=10

Fig. 16

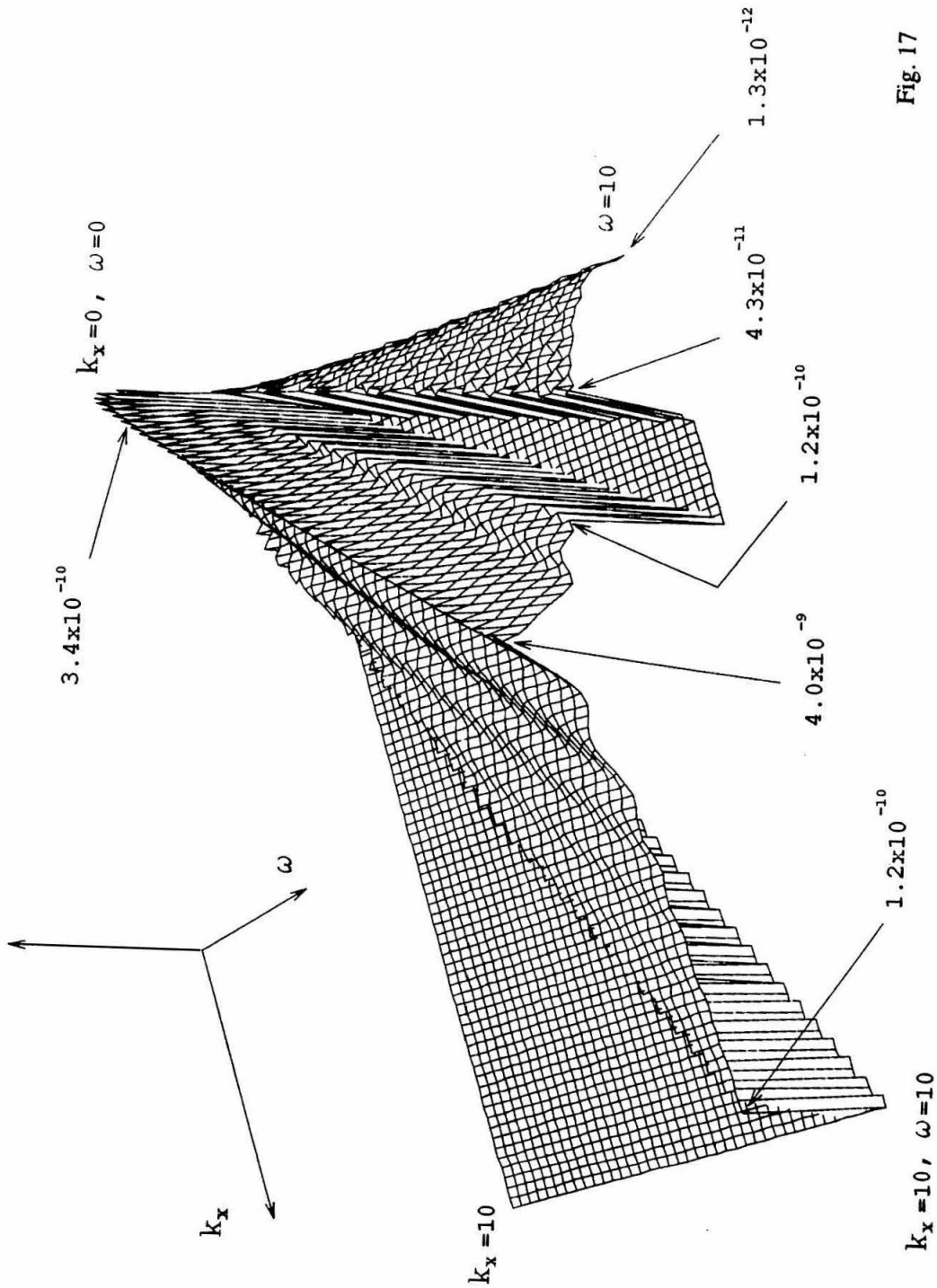
Log |b_z(0)|
ω
k_x
k_x=0 , ω=0
3.4x10^-10
ω=10
1.3x10^-12
4.3x10^-11
1.2x10^-10
4.0x10^-9
1.2x10^-10
k_x=10
k_x=10 , ω=10

Fig. 17

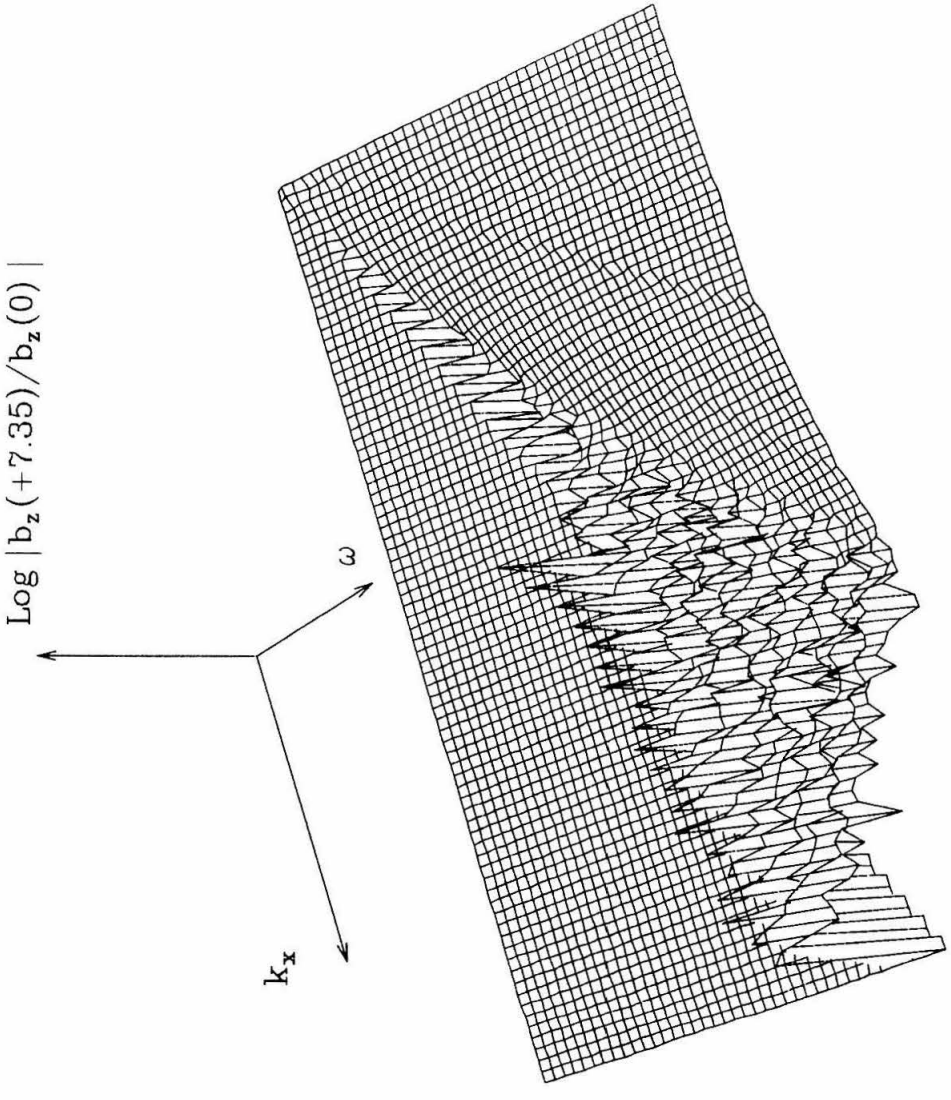

Fig. 18 (a)

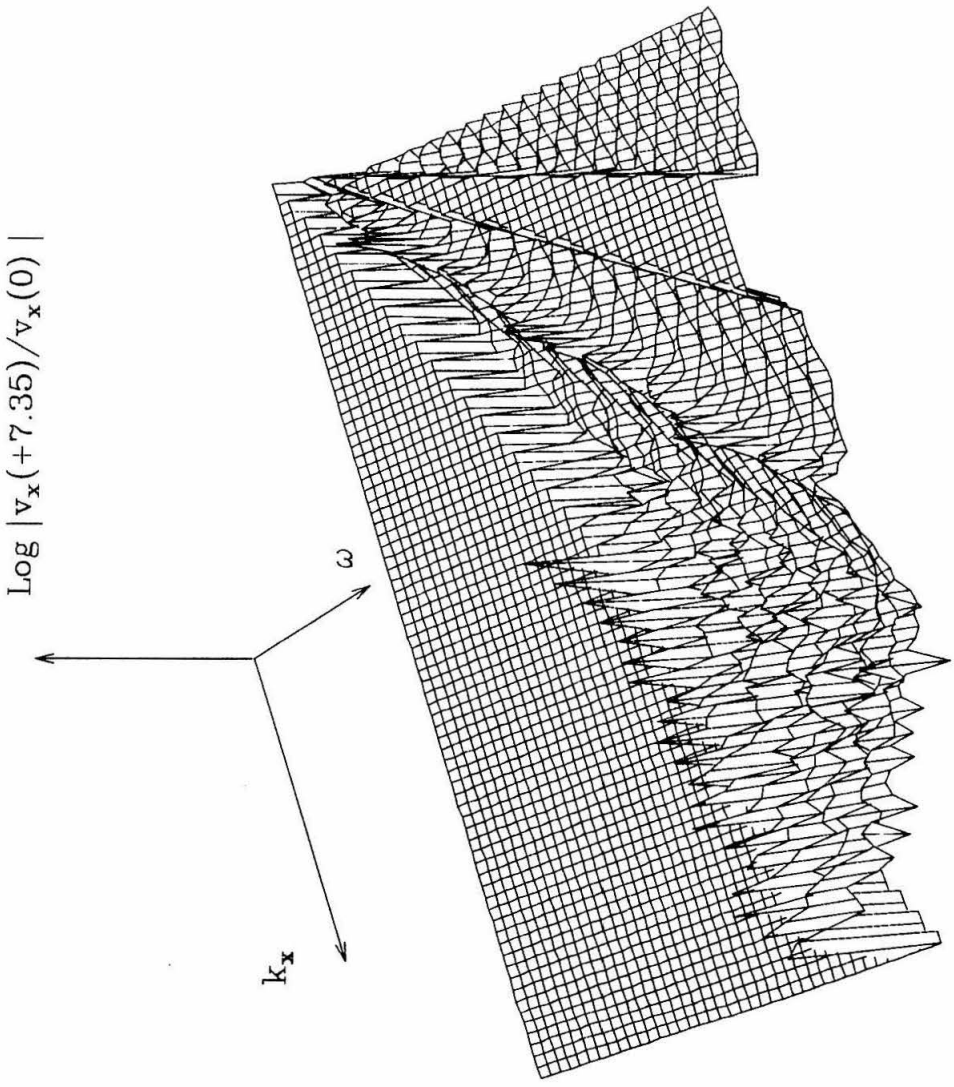

Fig. 18 (b)

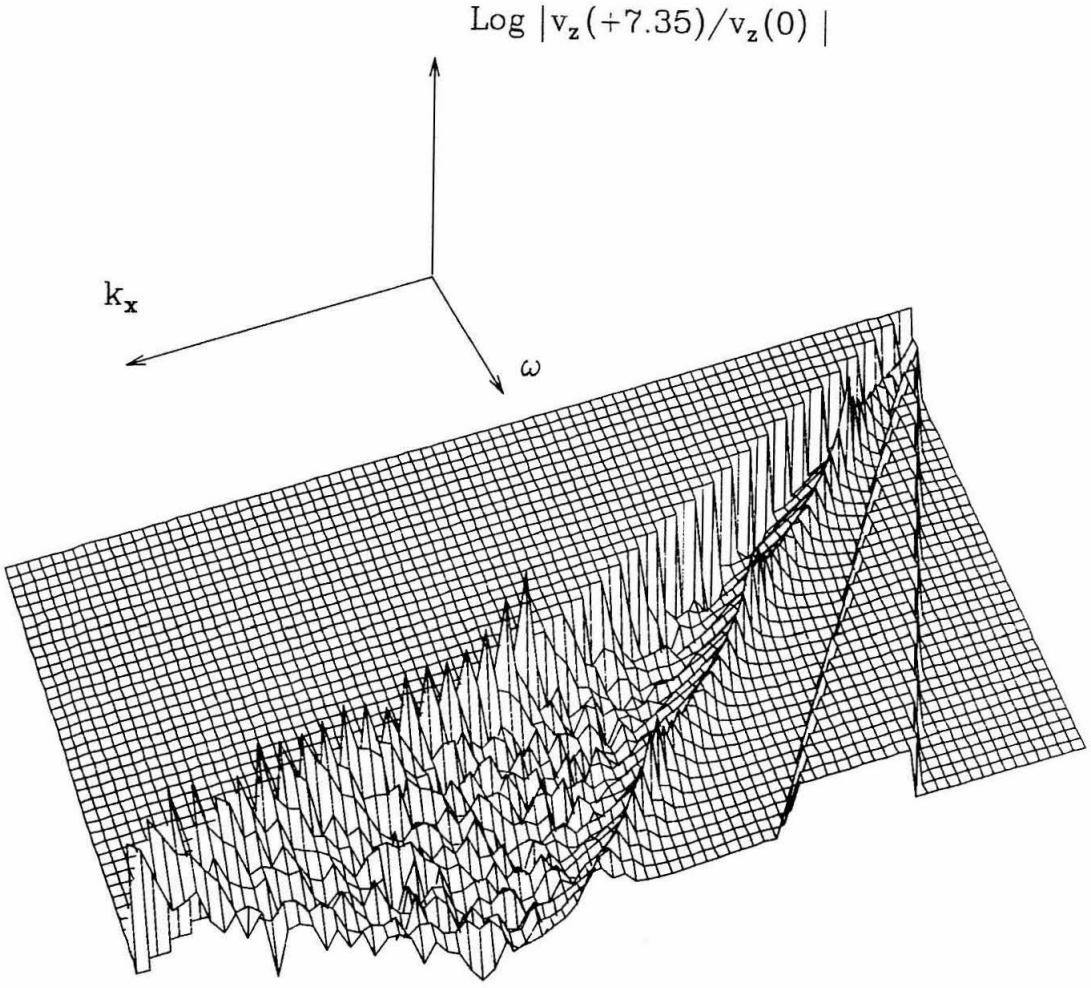

Fig. 18 (c)

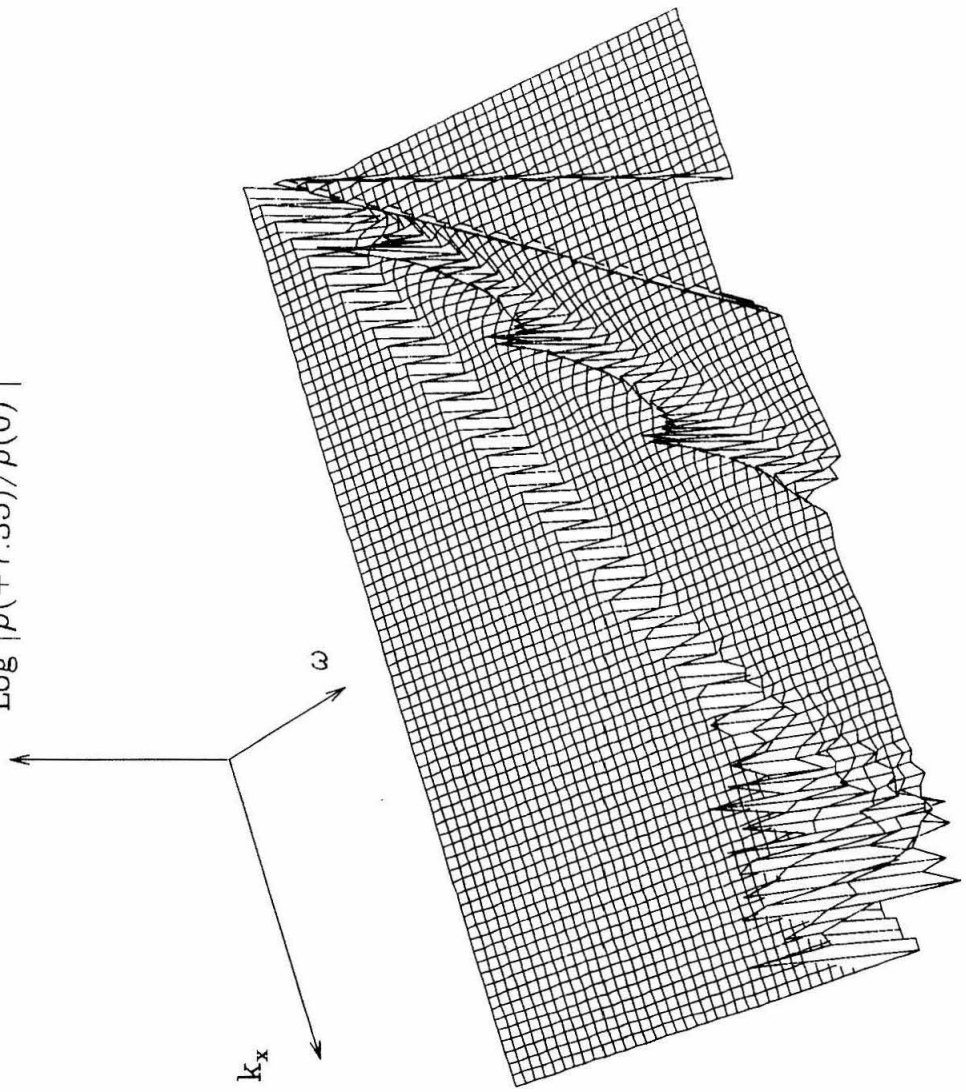

Fig. 18 (d)

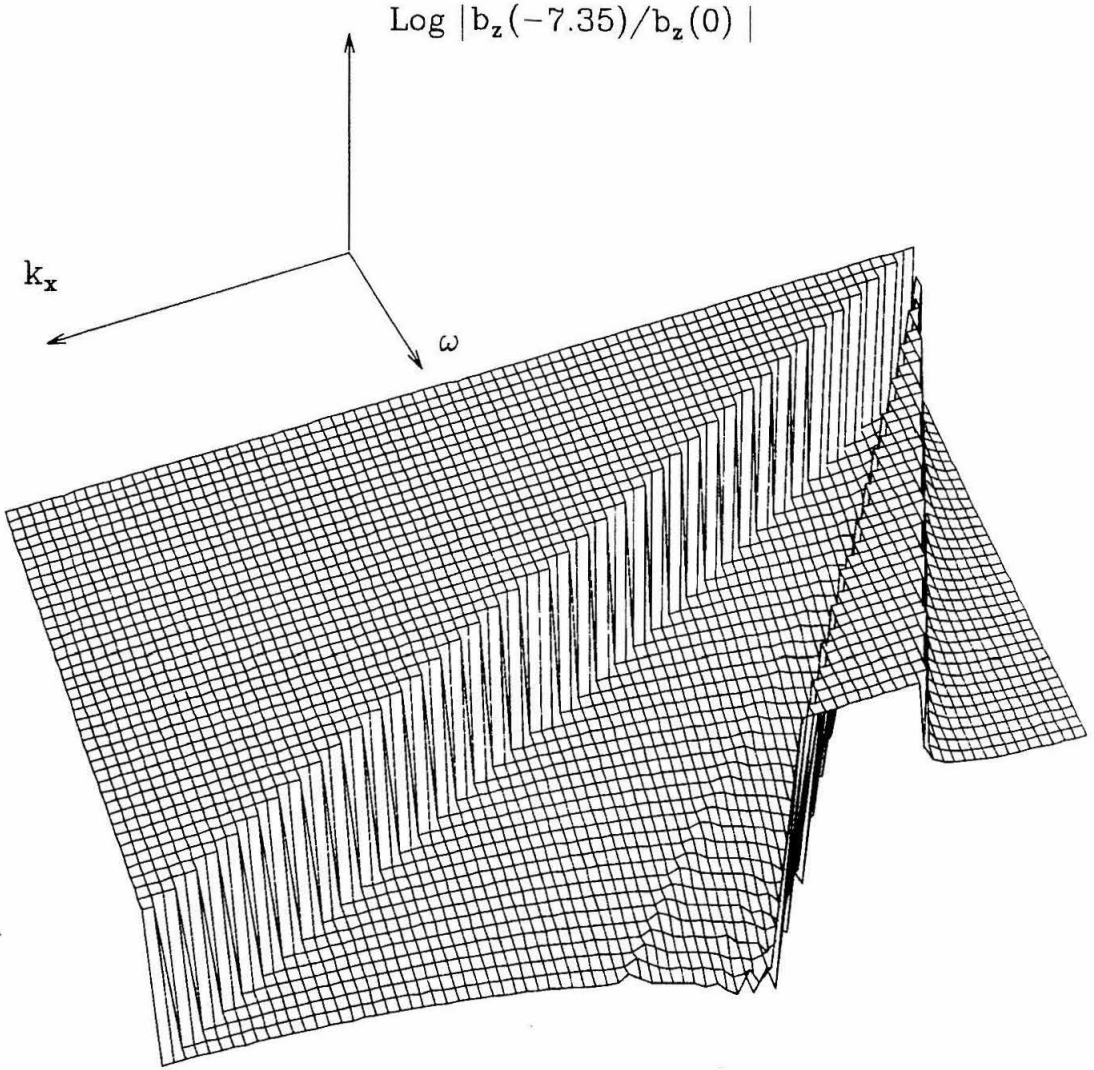

Fig. 18 (e)

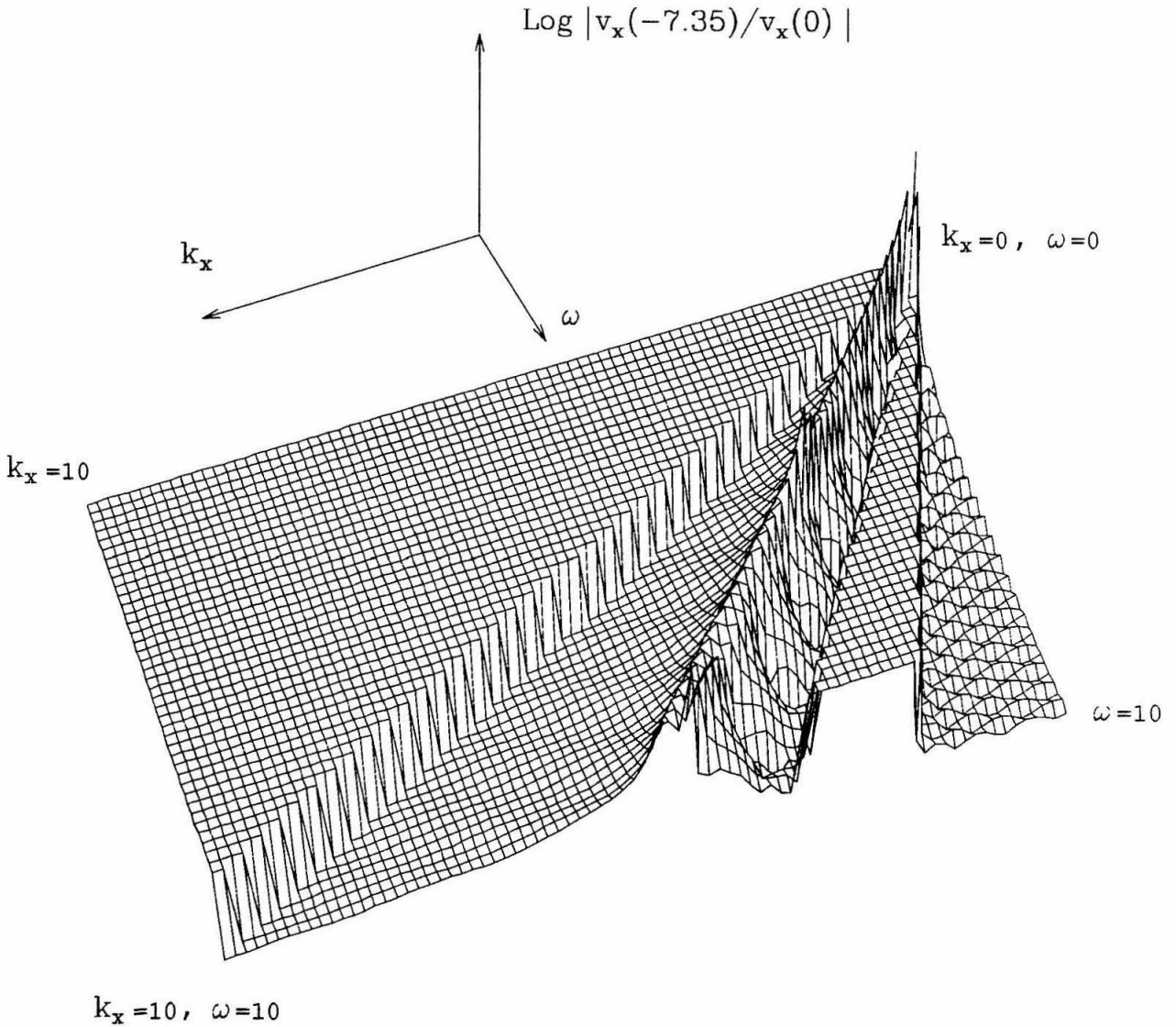

Fig. 18 (f)

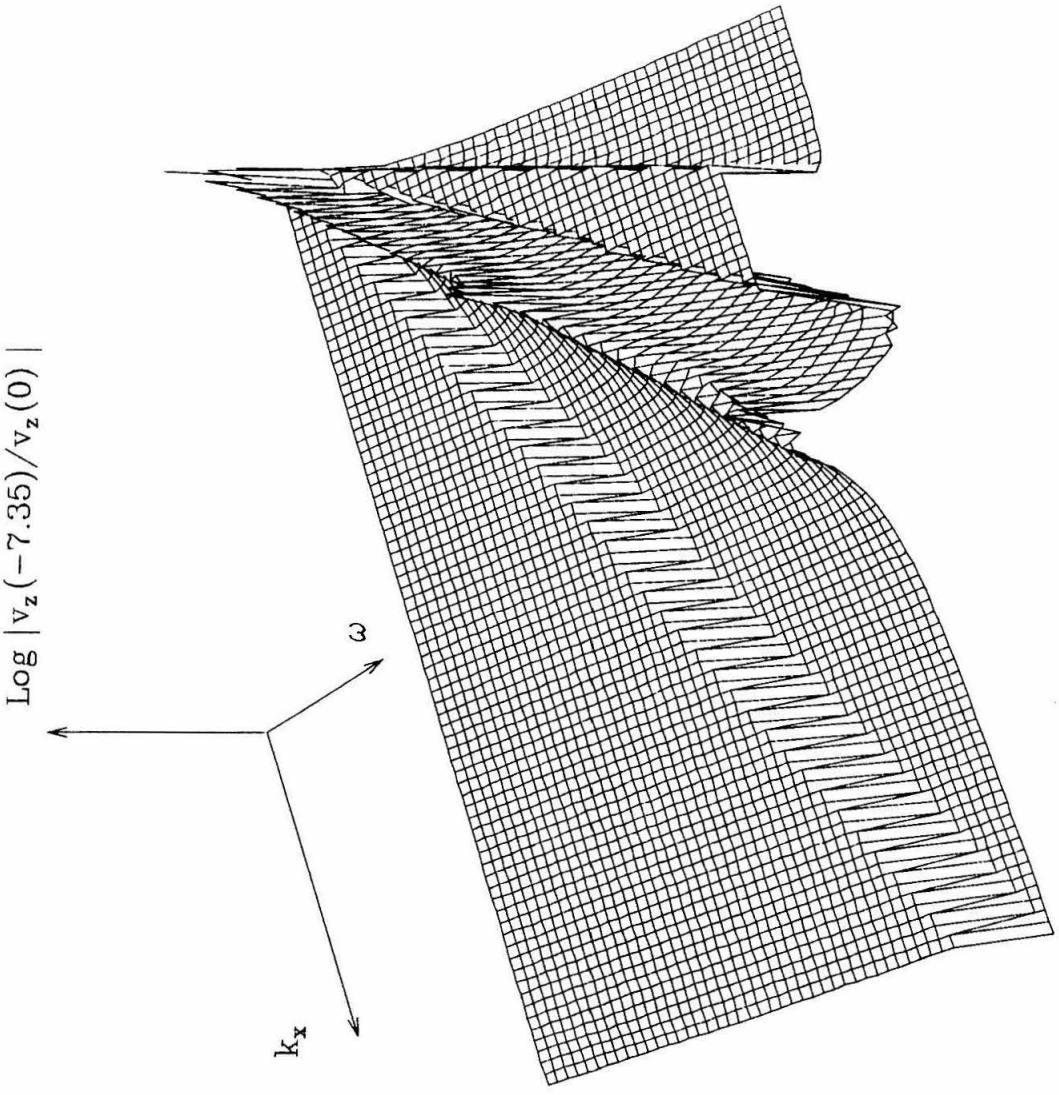

Fig. 18 (g)

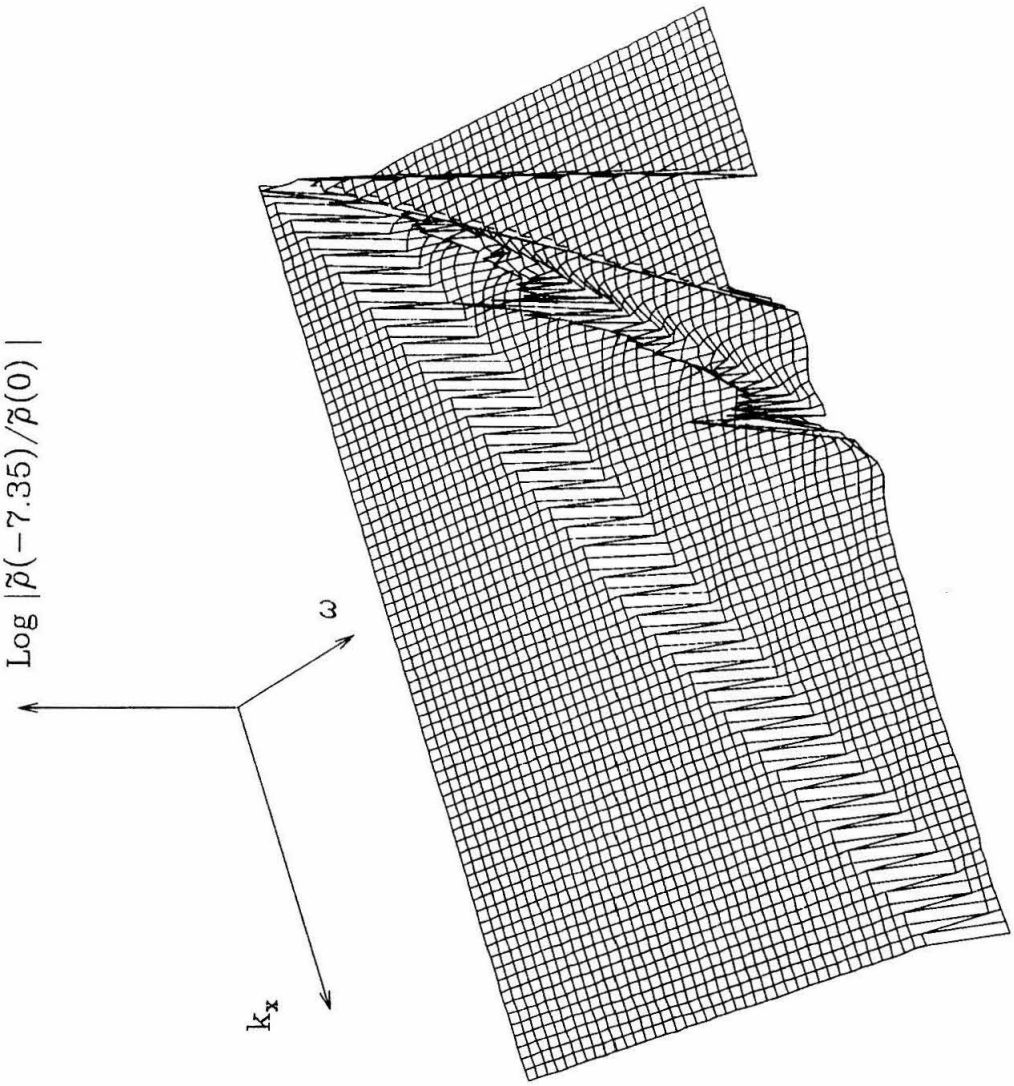

Fig. 18 (h)

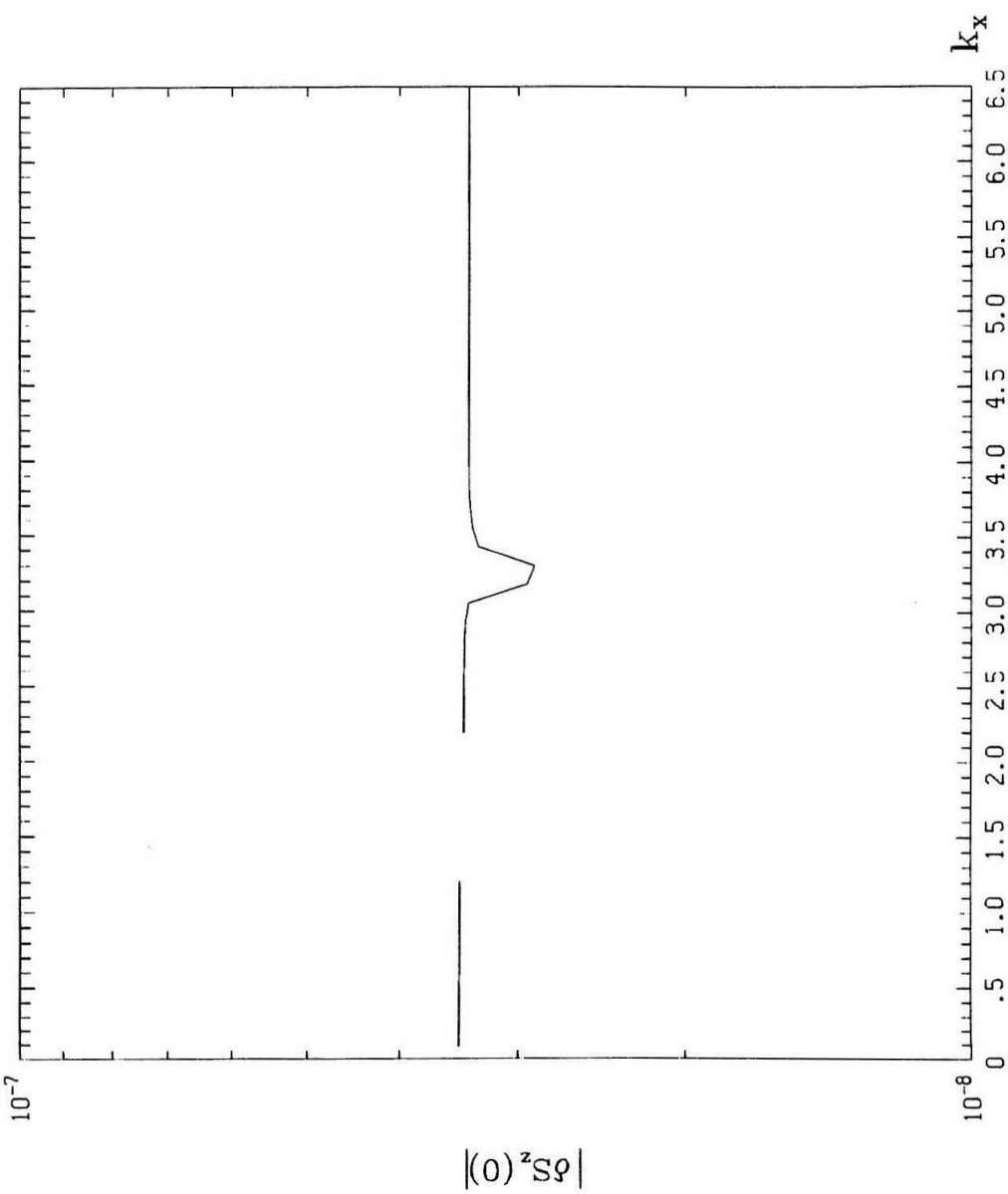
ω=6.50
$|\delta S_z(0)|$
10^{-7}
10^{-8}
0 .5 1.0 1.5 2.0 2.5 3.0 3.5 4.0 4.5 5.0 5.5 6.0 6.5
k_x

Fig. 19

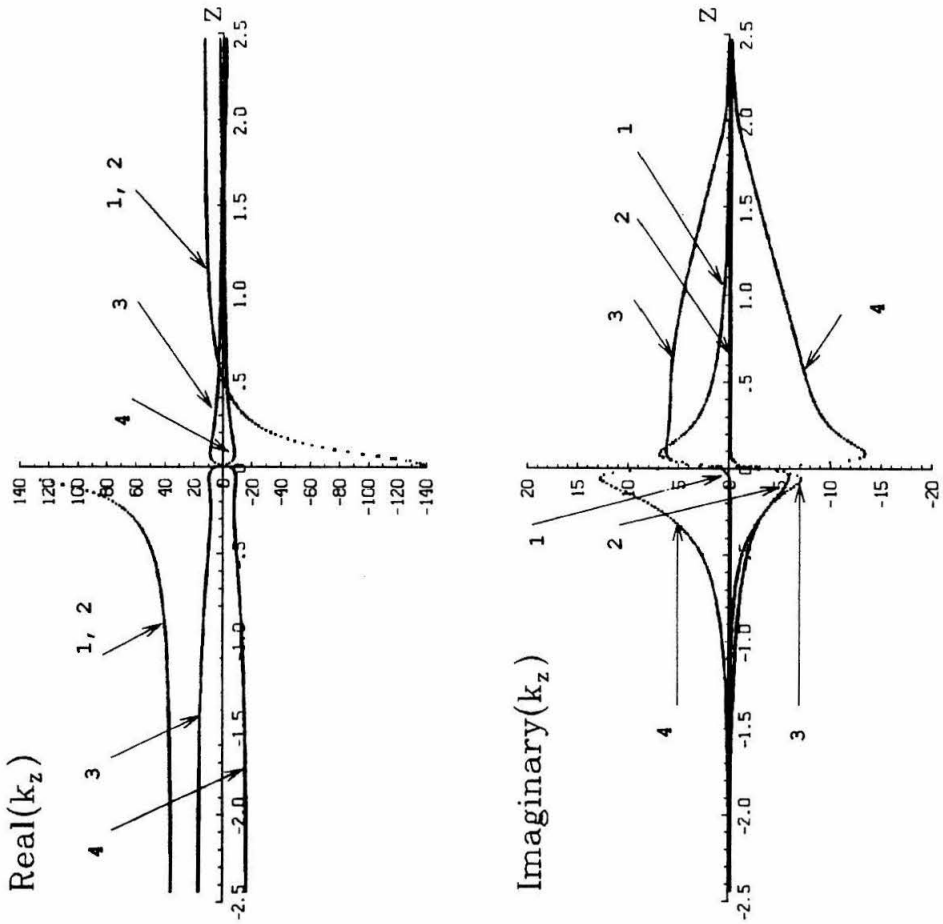

Fig. 20

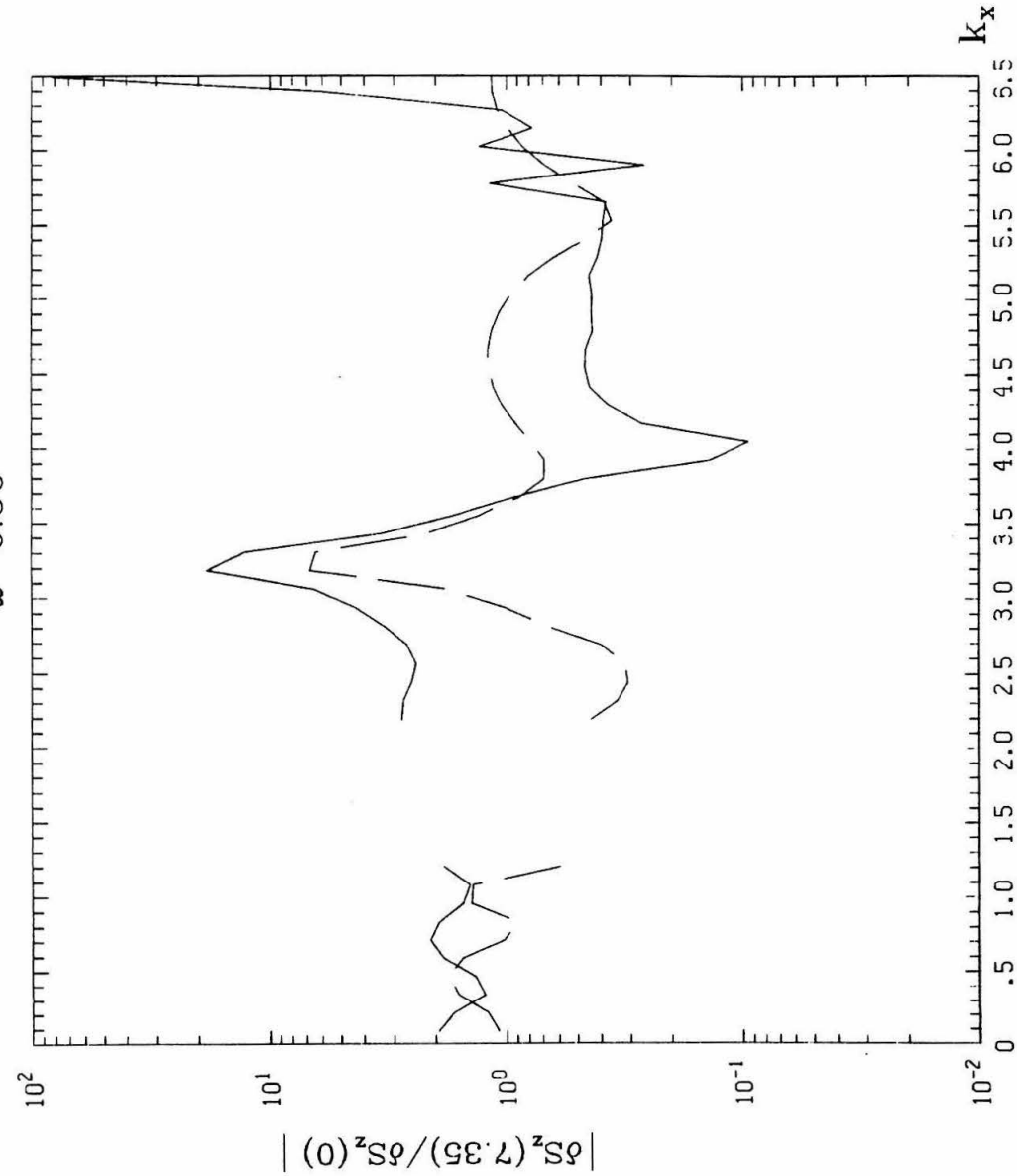
ω=6.50
$|\delta S_z(7.35)/\delta S_z(0)|$
10^2
10^1
10^0
10^{-1}
10^{-2}
0
.5
1.0
1.5
2.0
2.5
3.0
3.5
4.0
4.5
5.0
5.5
6.0
k_x

Fig. 21